Biophysical and Biochemical Determinants of Protein-Specific Polysialylation

BY

GAURANG PRAKASH BHIDE
B.Pharm., University of Mumbai, 2010

THESIS

Submitted as partial fulfillment of the requirements
for the degree of Doctor of Philosophy in Biochemistry and Molecular Genetics
in the Graduate College of the
University of Illinois at Chicago, 2017

Chicago, Illinois

Defense Committee:

Karen J. Colley, PhD	Chair and Advisor
Jack H. Kaplan, PhD	Biochemistry and Molecular Genetics
Arnon Lavie, PhD	Biochemistry and Molecular Genetics
Michael E. Caffrey, PhD	Biochemistry and Molecular Genetics
Pradip Raychaudhuri, PhD	Biochemistry and Molecular Genetics
William Walden, PhD	Microbiology and Immunology
Gerd Prehna, PhD	Microbiology and Immunology

This dissertation is dedicated to my parents, Shobhana and Prakash Bhide whose upbringing, encouragement, and motivation have been invaluable throughout.

Acknowledgements

First and foremost, I would like to thank my phenomenal mentor, Dr. Karen Colley. Without Karen's constant guidance, support, approachability, enthusiasm, and infectious energy, this work would not have been possible. Her motivation and thoroughness has made me a better researcher, presenter, writer as well as a person. I am grateful to Karen for allowing me to work on all these interesting projects that gave me an opportunity to learn a variety of techniques and become better at organization.

I would also like to thank Dr. Gerd Prehna for being my co-advisor on my biophysical project who trained me on a number of biophysical techniques and their analysis. His attention to the details, enthusiasm, and push to be perfect at these techniques has truly mattered in my training. I would like to thank Dr. Jack Kaplan for his support as the head of the department, head of my prelim committee and guidance as a committee member. I would also like to express my gratitude to Drs. Arnon Lavie, Michael Caffrey, Pradip Raychaudhuri, and William Walden for their insightful comments and suggestions. I would also like to thank Dr. Benjamin Ramirez for his help with the NMR experiments and helpful suggestions.

I am very grateful to the past members of the Colley lab, Dr. Helena Palka-Hamblin, Ninoshka Fernandes, Dr. Masaya Hane, and Dr. Matthew Thompson for creating a friendly environment in the laboratory as well as their immense help with the projects. I would like to acknowledge the kindness of Drs. Ken Kitajima and Stephen Dalton for sharing the reagents that made these studies possible.

Finally, I wish to thank my family and amazing friends, especially Dr. Aleksandar Antanasijević, Kristin Brownsword, Jean-Paul Girod, Jeremy Augustyn, Sarah Ando, and Dr. Rodolfo Gatto for their unconditional help and encouragement throughout my journey.

GPB

Author Contributions

I have performed the Isothermal Titration Calorimetry, Circular Dichroism, Size Exclusion Chromatography, analysis of the NMR spectra and NMR assignments of the NCAM FN1 domain under the guidance of Dr. Gerd Prehna. The NMR spectra were recorded in collaboration with Dr. Benjamin Ramirez. Ninoshka Fernandes generated membrane-bound NRP MAM chimeric proteins and I used these constructs to generate soluble Fc-tagged NRP MAM chimeric proteins. Ninoshka Fernandes also designed primers for NRP-2 MAM acidic patch mutants. All the ST8Sia-IV and ST8Sia-II PBR mutants were made by Dr. Deirdre Foley and Joseph Zapater. Non-autopolysialylated polyST mutants were made by Dr. Brett Close.

LIST OF TABLES

TABLE OF CONTENTS

LIST OF FIGURES

LIST OF ABBREVEATIONS

Ala	Alanine
Arg	Arginine
Asn	Asparagine
Asp	Aspartic acid
BDNF	Brain derived neurotrophic factor
CCR7	C-C chemokine receptor 7
CD	Circular Dichroism
CDG	Congenital Disorders of Glycosylation
CHO	Chinese Hamster Ovary
CMAH	Cytidine-monophospho-N-acetylneuraminic acid hydroxylase
CMAS	CMP-sialic acid synthetase
CMP	Cytidine monophosphate
CNX	Calnexin
CRT	Calreticulin
Cys	Cysteine
DMEM	Dulbecco's Modified Eagle's Medium
ECM	Extracellular matrix
EGF	Epidermal growth factor
Endo H	Endoglycosidase H
EndoN	Endoneuraminidase N
ER	Endoplasmic Reticulum
ESL-1	E-selectin ligand-1
FBS	Fetal bovine serum
FGF	Fibroblast growth factor

FGFR	Fibroblast growth factor receptor
FITC	Fluoroscein isothiocyanate
FN	Fibronectin
GAG	Glycosaminoglycan
GalNAc	N-acetylgalactosamine
GII	Glucosidase II
GlcNAc	N-acetylglucosamine
Glu	Glutamic acid
GPI	Glycosylphosphatidylinnositol
HRP	Horseradish peroxidase
HSQC	Heteronuclear Single Quantum Correlation
Ig	Immunoglobulin
IPTG	Isopropyl β-D-1-thiogalactopyranoside
ITC	Isothermal Titration Calorimetry
LacNAc	N-acetyllactosamine
LLO	Lipid-linked oligosaccharide
LTP	Long Term Potentiation
Lys	Lysine
MES	2-(N-morpholino)ethanesulfonic acid
MGAT	Mannosyl-glycoprotein-N-acetylglucosaminyltransferase
NCAM	Neural Cell Adhesion Molecule
Neu5Ac	N-acetylneuraminic acid
Neu5Gc	N-glycoylneuraminic acid
NK	Natural Killer
NMR	Nuclear Magnetic Resonance
NRP	Neuropilin

NSCLC	Non-small cell lung carcinoma
NT	Nucleotide
NTP	Nucleotide phosphate
OST	Oligosaccharyltransferase
PAGE	Polyacrylamide Gel Electrophoresis
PBR	Polybasic region
PBS	Phosphate-buffered saline
Phe	Phenylalanine
PMM	Phosphomannomutase
PNGase F	Peptide-N-glycosidase F
POFUT	Protein O-fucosyltransferase
POGLUT	Protein O-glucosyltransferase
polySia	Polysialic acid
polyST	Polysialyltransferase
POMGNT	Protein O-mannose GlcNAc-transferase
POMT	Protein O-mannosyltransferase
PSTD	Polysialyltransferase domain
RMS	Rostral migratory stream
SCLC	Small cell lung carcinoma
SDS	Sodium dodecyl sulfate
SEC	Size Exclusion Chromatography
Ser	Serine
sLe^x	Sialyl Lewis-X
SML	Sialylmotif Large
SMS	Sialylmotif Small
SMVS	Sialylmotif Very Small

SynCAM	Synaptic Cell Adhesion Molecule
TBS	Tris-buffered saline
TGN	trans-Golgi network
Thr	Threonine
TM	Transmembrane
TNFR	Tumor necrosis factor receptor
Trp	Tryptophan
TSR	Thrombospondin type repeat I
UDP	Uridine diphosphate
UGGT	UDP-glucose glycoprotein glucosyltransferase

Summary

Polysialic acid (polySia) is an oncodevelopmental glycopolymer that is unique because of its large size, negative charge, and hydrophilicity. PolySia confers these properties to the substrates on which it is found, and thus modulates their adhesion and signaling functions. The importance of polySia in development and organ physiology has been demonstrated for the nervous system and liver, and is suggested for the immune system. Specifically, polySia is essential for precursor cell migration, axon guidance in the developing and adult nervous system, and the regeneration of damaged neurons. In addition, re-expression of polySia in late stages of cancer is implicated in tumor metastasis in line with its ability to promote cell migration. Intriguingly, despite its involvement in a large number of physiological and pathological processes, polySia is found on a very limited number of cell-surface glycoproteins.

The synthesis of polySia is orchestrated by two Golgi-localized polySTs, ST8Sia-II and ST8Sia-IV. Previous work from the Colley laboratory and others has demonstrated that specific features of the underlying protein scaffold are essential for the process of polysialylation. Specifically, the FN1 domain of the major polySia carrier protein, the Neural Cell Adhesion Molecule (NCAM), is crucial for its recognition and the polysialylation of N-glycans on the adjacent Ig5 domain. A specific FN1 surface acidic patch was suggested to play a role in the initial recognition step, and this observation was complemented by the observation that the basic residues in the ST8Sia-IV polybasic region (PBR) were important for binding and polysialylation of NCAM. An X-ray crystal structure of the NCAM Ig5-FN1 domain and subsequent studies, revealed roles of Ig5, FN1 and linker sequences in the positioning of the polyST, as well as in maintaining the relationship between the two domains for optimum polysialylation.

I was interested in determining whether the NCAM FN1 acidic patch and polyST PBR residues were direct interaction partners to serve as the first step of substrate recognition for NCAM polysialylation. In Chapter III, using Isothermal Titration Calorimetry (ITC) and Nuclear Magnetic Resonance (NMR) experiments, I was able to verify the above interaction *in vitro*. $^{1}H,^{15}N$-Heteronuclear Single Quantum Correlation (HSQC) NMR experiments allowed me to map the FN1 residues perturbed

as a result of the acidic patch-PBR interaction. This analysis further refined our understanding of the mechanism of polysialylation by suggesting that binding at the acidic patch triggers a conformational change in a GGVPI loop that is adjacent to the Ig5-FN1 linker region, as well as the linker region itself. The relationship between these regions has previously been shown to be important for NCAM polysialylation. This conformational change explains a previously proposed 'restricted flexibility paradigm' in which the loop-Ig5-FN1 linker relationship is maintained, while still allowing flexibility in N-glycan placement for polysialylation.

Next, I was able to define the sequence requirements for the protein-specific O-glycan polysialylation of Neuropilin-2 (NRP-2), a VEGF and semaphorin co-receptor. My work described in Chapter IV not only demonstrated the necessity and sufficiency of the NRP-2 MAM domain and the adjacent linker region for NRP-2 polysialylation, but identified a novel mechanism of polysialylation for an analogous but weaker substrate, NRP-1. My work suggested that the polysialylation of NRP-1 in my expression system was due to its recycling to the polyST-expressing internal compartments, likely endosomes or the late Golgi. In addition, similar to the requirements for NCAM recognition and polysialylation, I was able to show the importance of a surface acidic patch on the NRP-2 MAM domain for its recognition and polysialylation by ST8Sia-IV.

In Chapter V, my work characterizing the PBR sequences in both ST8Sia-IV and ST8Sia-II has allowed me to determine the PBR sequences required for (1) the recognition of NCAM, NRP-2, and another important substrate, the Synaptic Cell Adhesion Molecule 1 (SynCAM 1), (2) the proper positioning of polySTs on the substrates for robust polysialylation, and (3) the elongation of substrate polySia chains. I propose that the polyST PBR residues are able to play these multiple roles because the acidic patches on the NCAM and NRP-2 recognition domains that are important in substrate recognition, and the growing polySia chain, are both negatively charged. Therefore, it is possible as my data suggests that specific basic residues of the polyST PBRs may sequentially interact with these acidic partners. I propose a model in which the initial protein-protein interaction between polyST and substrate, required

for the protein specificity of polysialylation, is shifted to a protein-carbohydrate interaction between the polyST and the growing polySia chain on the substrate.

Finally, I have always wondered about the significance of polyST autopolysialylation, an energy-intensive process that has been shown to be dispensable for NCAM polysialylation (7, 8). My work supports the idea that polyST autopolysialylation is self rather than cross polysialylation and that while it is not required for NCAM N-glycan polysialylation it does appear to be required for NRP-2 O-glycan polysialylation. In this dissertation, I propose how steric and charge-charge repulsion exerted by polySia chains on ST8Sia-IV could be of unique importance in the polysialylation of O-glycans.

Findings in this work have also led to the preliminary design of a polyST-substrate interaction inhibitor. It is my hope that the work presented in this dissertation contributes to a deeper understanding of the molecular mechanism of protein-specific polysialylation and that it will assist in the creation of strategies to improve or block polysialylation for therapeutic benefits.

Chapter I

Introduction

Protein glycosylation is the most abundant protein modification found in eukaryotic cells. Various mechanisms subject a number of amino acids to glycosylation- asparagines, serines, threonines (1, 2), tyrosines (3, 4), hydroxyprolines (5), tryptophans (6) and more recently, even cysteines (7–9). While some general rules may apply, glycosylation in general is not template driven. As a result, glycan structures tend to be highly complex and diverse, even on similar or the same protein molecules. This complexity is due to a number of factors including the large number of unique monosaccharides found in Nature, the cell- and tissue-specific expression of glycosyltransferases and glycosidases, glycosyltransferase competition for the same substrates in the Golgi apparatus, and differences in the linkages catalyzed by glycosyltransferases. These and other factors controlling the 'microheterogeneity' of the cellular glycome are summarized in Figure 1 (1).

Cell glycans have a variety of physiological functions including promoting the folding, solubility, and stability of proteins, serving to physically protect and maintain tissue structure by forming an extracellular matrix, acting to modulate cell surface receptor signaling by influencing receptor structure and ligand binding, regulating cell-cell adhesion, and serving as markers of 'self' to avoid autoimmunity (10, 11). Glycans are also the first point of contact for many pathogens like toxins and viruses.

The cellular glycome is very dynamic and altered glycosylation is observed during development as well as in numerous diseases including cancer, viral infections, and neurological diseases (10–12). Changes in glycosylation enzyme levels can easily achieve glycan structural variation to control and fine-tune protein function, while alterations in protein substrates may lead to a loss of function. Changes in glycosylation can also be evolutionary. For example, in order to avoid pathogen entry, the cellular

glycome keeps constantly evolving even as pathogens evolve. This 'red queen effect' achieved by the evolution of the human glycome, protects the host from pathogens (11).

Finally, over the last twenty years, it has been appreciated that protein glycosylation extends beyond the secretory pathway. Nucleocytoplasmic glycosylation events that involve the addition and removal of N-acetyl glucosamine (GlcNAc) to serines, threonines, and cysteines (7, 13, 14) on a large number of kinases, transcription factors, histones, cytoskeletal proteins, and other proteins such as RNA polymerases, are believed to be metabolically regulated as the reaction's donor, UDP-GlcNAc, serves as an important cellular metabolic sensor (15–18).

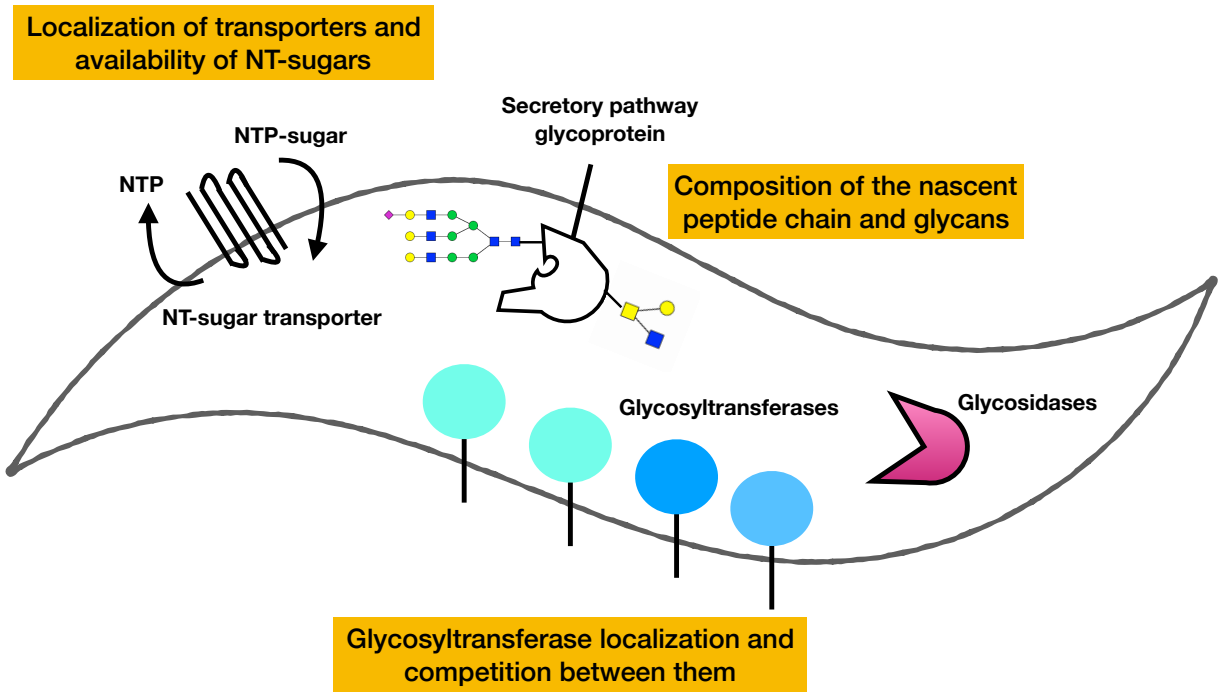

Figure 1: Glycosyltransferase expression, localization, and competition. Glycosylation of cell-surface glycoproteins is dynamic and is affected by multitude of factors including but not limited to nascent peptide composition and glycans added previously, localization and availability of nucleotide sugar donors (NTP-sugar), and the expression and localization of glycosyltransferases and glycosidases. Some of these factors are deregulated in the Congenital Disorders of Glycosylation (CDGs).

In this chapter, I will briefly discuss mechanisms of canonical N- and O-glycosylation and introduce examples of protein-specific glycan modifications. Our laboratory focuses on an unusual protein-specific glycan modification, polysialylation. I will discuss the physicochemical properties and biological roles of polysialic acid (polySia), as well as previous work characterizing mechanism of polysialylation.

A. N-glycosylation

N-glycosylation represents the most extensively studied type of glycosylation as N-glycans are found on almost all the proteins that pass through the secretory pathway. Secretory pathway proteins are proteins that reside in the Endoplasmic Reticulum (ER), Golgi apparatus, lysosomes, cell surface or extracellular space. N-glycosylation is co- as well as post-translational and commences in the ER when a $GlcNAc_2Man_9Glc_3$ structure is transferred from a dolichol phosphate lipid to asparagine residues in a polypeptide by the oligosaccharyltransferase (OST) enzyme complex (1, 2). The synthesis of the $GlcNAc_2Man_9Glc_3$ structure is initiated on the cytosolic face of the ER by phosphorylation of transmembrane lipid dolichol followed by the sequential addition of sugar residues until the structure reaches a $GlcNAc_2Man_5$ form. This dolichol-linked sugar structure is then flipped into the ER lumen where the addition of monosaccharides continues to form the final lipid linked oligosaccharide (LLO) donor, $GlcNAc_2Man_9Glc_3$-P-P-dolichol (Fig. 2) (19).

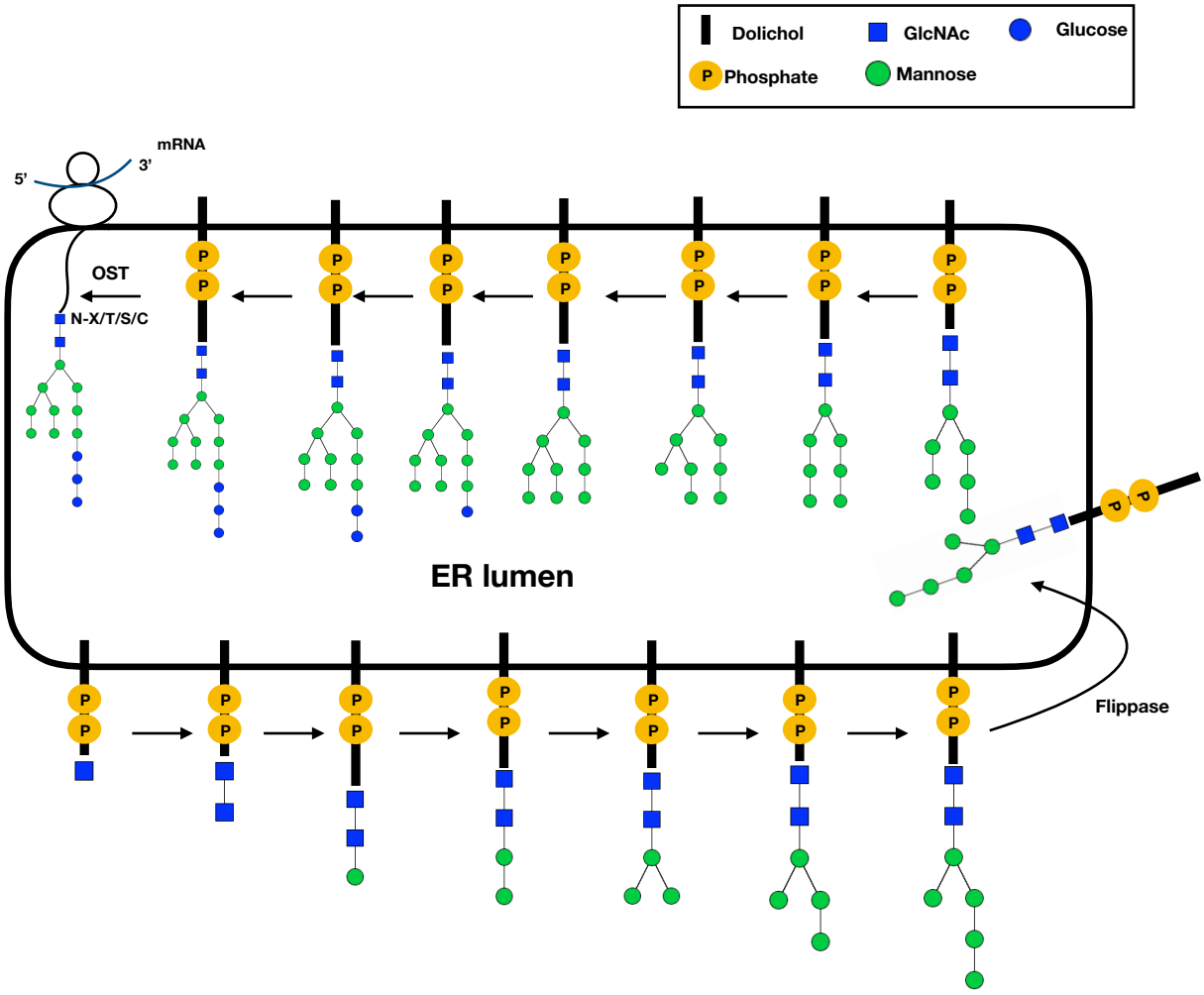

Figure 2: Synthesis of the $GlcNAc_2Man_9Glc_3$-P-P-Dolichol lipid linked oligosaccharide and transfer of the glycan onto the polypeptide. Prior to its transfer, the $GlcNAc_2Man_9Glc_3$ glycan is sequentially synthesized on dolichol phosphate (20). Addition of all of the monosaccharides is catalyzed by cytosolic and ER localized glycosyltransferases, which use UDP-GlcNAc, GDP-mannose, and UDP-glucose as donors. OST can transfer the glycan from the lipid linked oligosaccharide (LLO) to polypeptide chain co-translationally, using the OST STT3A subunit, or post-translationally using the OST STT3B subunit.

Asparagine residues that are glycosylated are found in the consensus sequence Asn-X-Thr/Ser/Cys (N-X-T/S/C) when X = any amino acid except proline (21–24). This consensus sequence represents a specific hydrogen-bonded structure wherein a hydroxyl/sulfhydryl group of Thr/Ser/Cys forms a hydrogen bond with side chain carbonyl of Asn, which is recognized by OST (22, 25). Work by Reid Gilmore and others (2, 21, 22) have demonstrated that the OST subunit STT3A is responsible for co-translational N-glycosylation, whereas the STT3B subunit is responsible for post-translational N-glycosylation. These two types of catalytic subunits modify distinct sets of proteins depending on proximity of the glycosylation site to the N- and C- termini of the protein, the location of disulfide bridges in the protein and the amino acids near the N-X-T/S/C site. Interestingly, not all the N-X-T/S/C sites are modified by OST. Generally, threonines are preferred at the +2 site followed by serines, followed by cysteines. Disulfide-forming cysteines or aspartates at the +1 site preclude N-glycosylation. Preference for threonine over serine at the +2 site is illustrated by the crystal structure of bacterial OST homolog, PglB (26).

The three glucose residues of the $Glc_3Man_9GlcNAc_2$ structure are cleaved in the ER during maturation of the glycan by α1,2-glucosidase I (GI) (glucose 1) α1,2-glucosidase II (GII) (glucose 2 and 3). The third glucose residue plays a role in protein quality control as the ER lectins, calnexin and calreticulin (CNX/CRT), bind the monoglucosylated glycan structure ($Glc_1Man_9GlcNAc_2$) (27, 28). CNX/CRT do not bind the polypeptide chain *per se;* however, they are in complex with protein disulfide isomerase A3, which aids in folding (1). Following this step, the glycopeptide is deglucosylated by GII. Protein folding is sensed by the UDP-glucose glycoprotein glucosyltransferase (UGGT), which re-adds a glucose residue only if the polypeptide chain is misfolded (28). While misfolded proteins can reenter the CNX/CRT cycle, proteins with very slow folding kinetics are subjected to mannose trimming by mannosidases and subsequent ER associated degradation (ERAD) (1, 27–29). Folded glycoproteins with $GlcNAc_2Man_8$ glycan structure after the action of ER mannosidase I, move to Golgi apparatus, where mannose trimming continues by the action of Golgi mannosidases (28).

The Golgi apparatus harbors multiple glycosyltransferases that further diversify $GlcNAc_2Man_3$ glycan structures to produce complex N-glycan structures although certain high mannose structures, as well as hybrid structures, may be observed on the cell surface (Fig. 3) (30). Glycosylation in the Golgi mostly depends on localization of glycosyltransferases and nucleotide-sugar transporters in the sub-Golgi compartments (cis, medial, trans cisternae and trans Golgi network (TGN)) (Fig. 4). Principles governing localization of the glycosyltransferases and nucleotide-sugar transporters are complex (31–33). Expression of various glycosyltransferases can also be cell-type specific and governs the types of monosaccharides added and linkages formed in the cell. Generally, the addition of GalNAc (primarily for O-glycosylation) and removal of mannose residues occurs in the cis-Golgi, GlcNAc and fucose residues are added in the medial-Golgi whereas galactose, sialic acid, and sulfate groups are added in the trans-Golgi or trans-Golgi network (TGN) (Fig. 4). Some overlap does exist between various compartments and sugars added in those compartments and this can also vary in a cell-type specific fashion and have implications for enzymes that compete for the same acceptor structure (30).

The importance of hybrid and complex glycans in mammalian development is highlighted by the finding that knocking out the GlcNAcT-I (MGAT1) enzyme, which is the gateway to the synthesis of hybrid and complex type N-glycans, leads to embryonic lethality (34). Similarly, knockout of α-mannosidase II, which cleaves two mannose residues to produce $GlcNAc_2$-Man_3 structure results in lethality around embryonic day 18.5 (35, 36). In addition, defects in N-glycosylation pathways have been implicated in multiple developmental disorders, called the Congenital Disorders of Glycosylation (CDG). Type I CDGs involve defects in the synthesis of the LLO, and a failure of OST to transfer truncated oligosaccharides to nascent proteins (hypoglycosylation), or the transfer of truncated oligosaccharides that cannot be fully processed. Type II CDGs involve defects in mannose trimming or elongation of N-glycans by Golgi enzymes (37, 38). Depending on proteins affected and glycosylation enzymes involved, CDG patients manifest multiple neurological, muscular, skeletal, endocrine, and cardiovascular defects (10, 37–39).

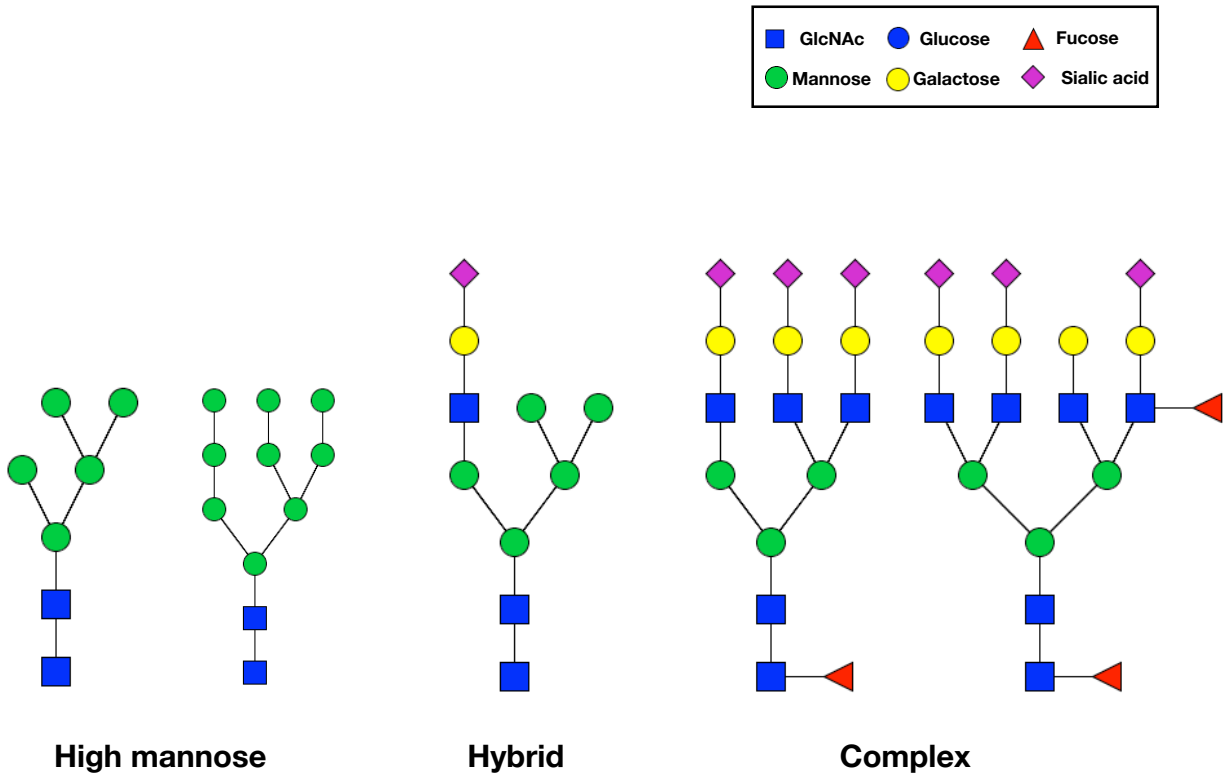

Figure 3: Examples of different types of N-glycans. Glycans that are found in the ER or undergo minimal processing in the Golgi tend to be high mannose. In hybrid structures, one of the α1,3 or α1,6 branches remains high mannose, whereas other is processed by Golgi glycosyltransferases. Glycans that are extensively modified by fucosyltransferases, various GlcNAc transferases, galactosyltransferases, and sialyltransferases are termed complex glycans.

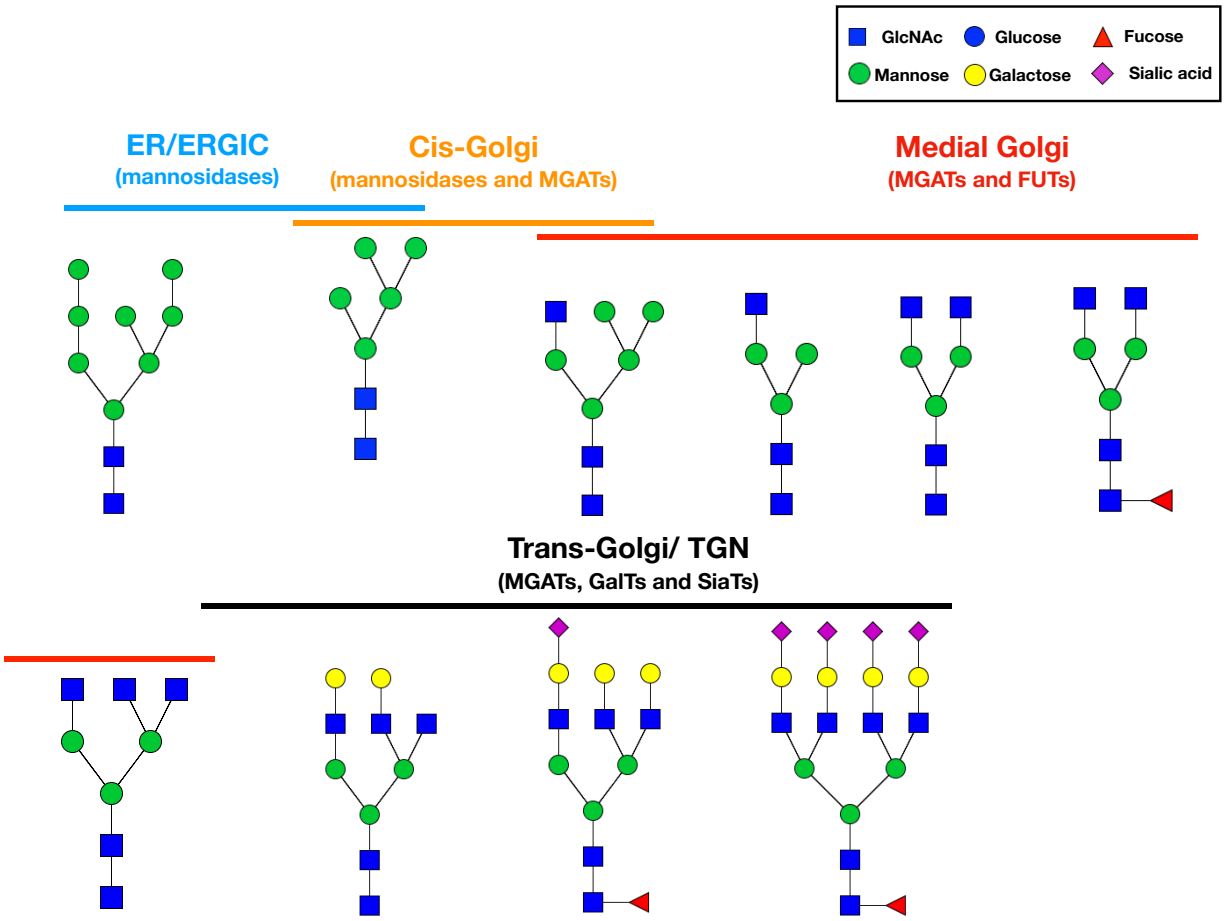

Figure 4. N-glycan modification in the Golgi. High-mannose structures that enter the Golgi are acted upon by ER and cis-Golgi mannosidases to produce $GlcNAc_2$-Man_3 structures. Mannosyl-glycoprotein-N-acetylglucosaminyl transferases (MGATs) in all the Golgi compartments sequentially add GlcNAc residues. Core fucose addition occurs in the medial Golgi whereas complex structures are made in the trans-Golgi and TGN by addition of galactose and sialic acid residues.

B. O-glycosylation

Protein O-glycosylation is even more diverse than N-glycosylation. The most commonly observed O-glycosylation of proteins, referred to as mucin-type O-glycosylation, commences in the early Golgi with addition of single GalNAc residue to Ser/Thr (40). Several other types of O-glycosylation include the biosynthesis of glycosaminoglycan (GAG) chains that begins with addition of a xylose (Fig. 5), the addition of O-fucose and O-glucose to serines or threonines in epidermal growth factor (EGF) repeats of proteins such as Notch or thrombospondin type I (TSR) repeats of proteins such as thrombospondin or the ADAMTS metalloproteinases, and the O-mannosylation of proteins such as α-dystroglycan (discussed later in section I E) (30, 41, 42). All of these unique O-glycosylation events occur in the ER and some may be subject to further elongation in the Golgi (40–42).

In humans, mucin-type O-glycosylation is initiated by 20 different UDP-GalNAc:polypeptide *N*-acetylgalactosaminyl transferases (ppGalNAcTs) (40, 43). These enzymes have tissue- and stage-specific expression patterns and are responsible for addition of the first GalNAc residue to Ser/Thr residues in proteins. These O-glycans are further extended in the Golgi apparatus to form various core structures depending on monosaccharides added to the GalNAc and their linkages (43). Eight core structures that are commonly found on O-glycosylated proteins are shown in Figure 5.

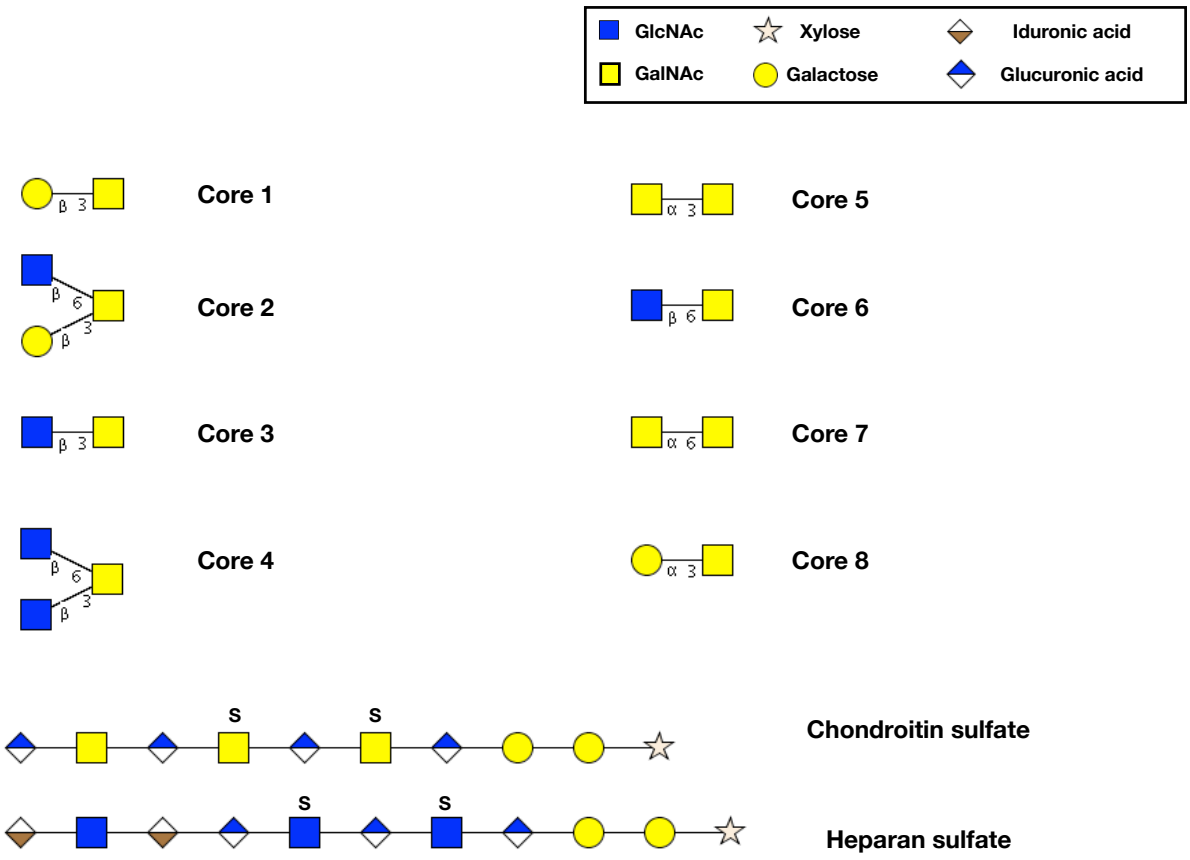

Figure 5: O-glycan core structures and glycosaminoglycans (GAGs). Most common type of O-glycosylation of secretory pathway proteins begins in the Golgi with addition of a GalNAc residue by ppGalNAcTs, which can be further extended by GlcNAc-transferases galactosyltransferases, and sialyltransferases. Common types of GAG chains include heparan sulfate and chondroitin sulfate, which are repeating units of monosaccharides shown above. GAG chains on glycoproteins or proteoglycans are also modified by sulfotransferases by Golgi that imparts negative charge (sulfate is represented by S).

Mucin-type O-glycosylation does not have a consensus polypeptide sequence (44). All but one of the ppGalNAcT enzymes have a lectin domain and a catalytic domain. A recent report has shown that two broad families exist within ppGalNAcTs. Members from the first family readily glycosylate non-glycosylated peptides but their glycosylation is enhanced by a previously added GalNAc that is 6-17 residues away from the new glycosylation site. These enzymes utilize their lectin domain to recognize previously synthesized Ser/Thr-O-GalNAc structures. Glycosylation by the members of the second family require the presence of a previously synthesized O-GalNAc for the addition of a new O-GalNAc to the -3, -1, and +1 residue relative to the previously synthesized Ser/Thr-O-GalNAc. For the second family, the catalytic domain plays a dual role of recognizing the Ser/Thr-O-GalNAc site and transferring the new O-GalNAc residue (Fig. 6) (45).

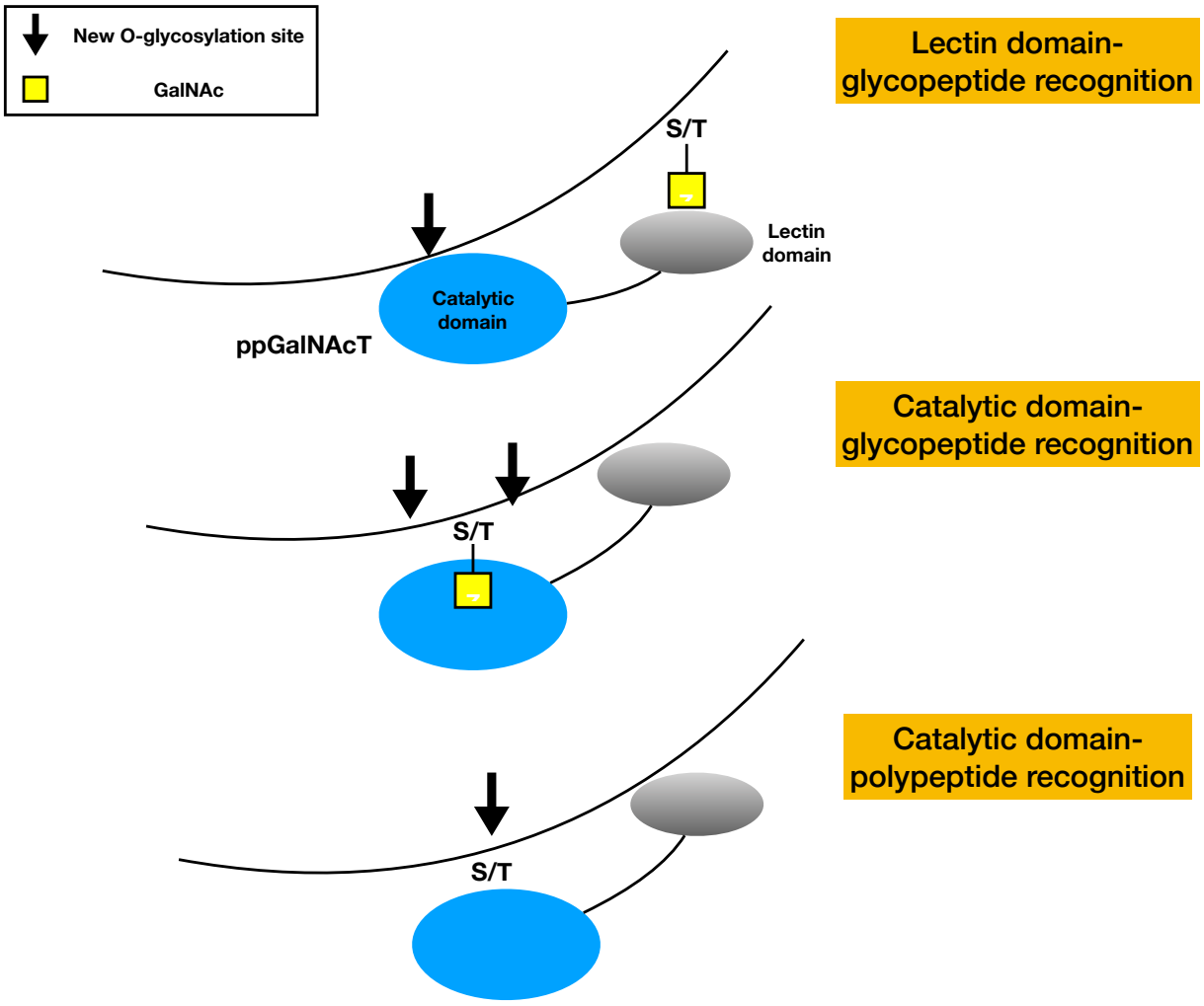

Figure 6: Proposed model of O-glycosylation by ppGalNAcTs. One family of ppGalNAcTs recognizes a glycopeptide with a previously added GalNAc residue (top two panels). The other family recognizes elements of polypeptide chain and transfers GalNAc residue on to Ser/Thr residues. This figure is adapted from Revoredo et al. (45).

Mucin-type O-glycans not only modify mucins but also numerous other cell-surface proteins such as fibroblast growth factor (FGF), Interleukin-2, and P-selectin glycoprotein ligand 1 (40, 46). These O-glycans serve to regulate stability and half-life of serum proteins, provide lubrication, are key components of the mucosal barrier, and also play a role in the extravasation of leukocytes from the blood stream in inflammation and the homing of leukocytes to the lymph nodes by serving as ligands for selectins (43, 44, 46). Knockout of the ppGalNAcTs in *Drosophila* has been shown to impact development of multiple systems including the nervous and cardiovascular systems. In fact, knockout of several ppGalNAcTs is embryonic lethal (43). For FGF23, it was shown that lack of O-glycosylation at a specific Thr residue, typically modified by Galnt3, results in excessive processing and lack of secretion leading to familial tumoral calcinosis (47). The lack of Galnt1 and hence lack of O-glycosylation during early stages of development in mice resulted in intracellular retention of basement membrane components and defects in ECM formation (48).

O-linked glycans other than mucin-type glycans have also been shown to play important roles in physiology and are implicated in various diseases. O-glycans that are synthesized in the ER aid in protein folding and quality control as exemplified by O-glucose or O-fucose on EGF repeats or O-fucose in TSR repeats. Protein O-glucosyltransferase-1 (POGLUT1), protein O=fucosyltransferase-1 (POFUT1) and protein O-fucosyltransferase-2 (POFUT2) are responsible for synthesis of these structures respectively (49, 50). O-linked fucose on Notch protein EGF repeats is crucial for Notch signaling and has been shown to serve as a surrogate amino acid to interact with its ligand, Jagged 1 (51). Knockout of POFUT1 is embryonic lethal (52). An unusual, extended O-mannose structure made by protein O-mannosyltransferases 1 and 2 (POMT1 and 2), which is found on α-dystroglycan, has been shown to be essential for mediating communication between extracellular matrix (ECM) and cytoskeleton. The O-mannose on α-dystroglycan is phosphorylated and extended by a xylose-glucuronic acid repeat polymer linked to phosphomannose by a ribitol residue. Defects in initiation and elongation of this structure have been implicated in muscular dystrophy (53, 54). Failure to modify a-dystroglycan with the proper O-

mannose glycans leads to a series of congenital muscular dystrophies. For example, a defect in either POMT1 or POMT2 genes leads to Walker Warburg syndrome, the most severe congenital muscular dystrophy (55).

GAG chains, largely found on proteins (proteoglycans), are critical structural components of the ECM. GAG chains play important roles in cellular signaling, cell growth, immune and inflammatory responses (56, 57). For example, heparan and chondroitin sulfate play a role in sequestering growth factors and regulating associated signaling events. Specifically, heparan sulfate proteoglycans are key components of the FGF receptor signaling complex (58). Heparan sulfate is also an inhibitor of proteases and plays an active role in the organization of the ECM (57)

C. Altered glycosylation in disease.

I have briefly discussed CDG pathways related to defects in N-glycosylation above. However, other types of CDGs are the result of defects in O-glycoslyation or C-mannosylation. Broadly, CDGs can also be categorized as (a) mutations in glycosyltransferases, (b) defects in synthesis of nucleotide sugar donors, (c) defects in localization of donor substrates, or (d) defects in localization of glycosyltransferases (37). For example, CDG Ia is a single point mutation in the gene for phosphomannomutase (PMM) that is key for the biosynthesis of Man-1-P, the precursor of GDP-Man. This mutation decreases enzyme activity so that the GDP-Man pool is only 10% of normal. As a result, the levels of the dolichol-P-Man precursor that is used in the ER lumen for the later stages of LLO biosynthesis are compromised, and as a result, the LLO is not fully extended (only reaches the $Man_5GlcNAc_2$ structure) and is weakly transferred by the OST leading to the hypoglycosylation of all secretory pathway proteins. As a result, individuals with this CDG exhibit psychomotor retardation, cerebral atrophy, skeletal deformations, impaired vision, cardiac and kidney disorders (38, 59–61).

Table 1. Examples of CDGs and their causes.

Type	Protein affected	Effects
Mutations in glycosyltransferases	POFUT1	Dowling-Degos disease (62)
Defects in synthesis of donors	Phosphomannomutase 2 (PMM2)	Nervous system disorders (63)
Defects in localization of donor substrates	CMP-Sia transporter (SLC35A1)	Seizures, ataxia, cardiac and renal disorders (64)
Defects in localization of glycosyltransferases	Conserved oligomeric Golgi (COG) proteins	Nervous system disorders (65)

Protein glycosylation is also dramatically altered in cancer, which manifests in altered signaling by cell surface receptors leading to changes in cell growth, metastasis, and modulation of immune response (66, 67). According to a hypothesis by Hakamori and Kannagi (68), cancer cells show glycosylation defects that can be categorized as (a) incomplete glycan synthesis and (b) neo-synthesis of cancer cell-specific glycans; the latter is mostly observed in advanced stages of cancer. Incomplete synthesis of glycans is exemplified by formation of the sialyl Tn antigen on mucin-type O-glycans, which is generally not observed in normal cells. Neo-synthesis is exemplified by higher order synthesis of polyLacNAc structures on N-glycans (67, 68). Such alterations in glycosylation are possible due to (a) dysregulated expression and localization of glycosyltransferases or glycosidases, (b) changes in the conformation of the peptide or previously added glycans, or (c) availability of sugar-nucleotide donors. Examples of some of the cancer-associated glycans are shown in Figure 7. In Table 2 below I have given some examples of glycosylation events that play a role in various aspects of cancer biology.

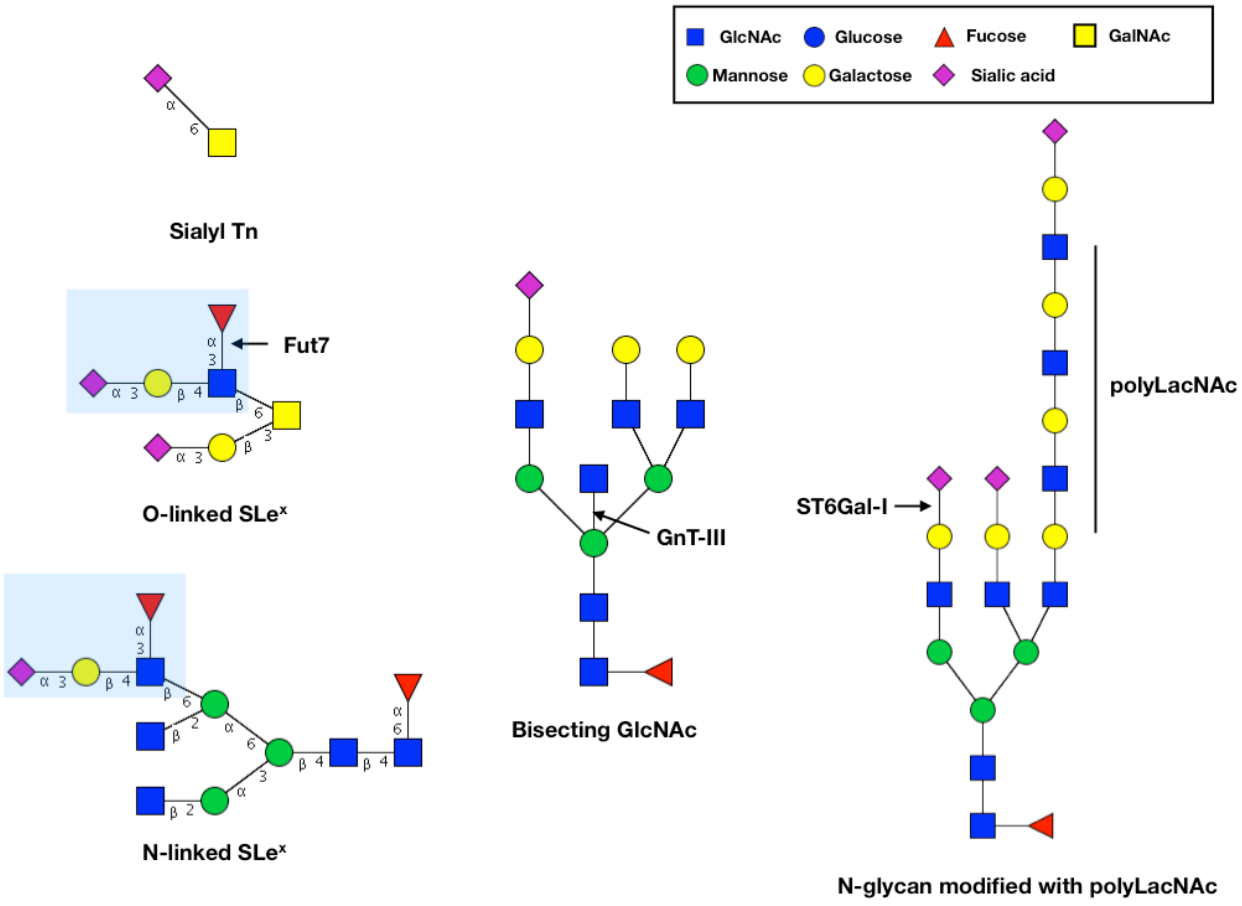

Figure 7: Glycan modifications observed in cancer. Glycan synthesis is often altered in cancer giving rise to various glycan modifications that are enriched in tumors, but not in normal tissues. These include sialyl Tn, sialyl Lewis X (marked in blue boxes), and bisecting GlcNAc and polyLacNAc structures.

Table 2. Altered glycans and their roles in cancer.

	Glycogenes implicated	Effect
Tumor initiation	CMAH	N-glycolylneuraminic acid (Neu5Gc) expression triggers inflammation and promotes hepatocellular carcinoma in the presence of anti-Neu5Gc antibodies (69)
Tumor growth	ST6Gal-I, GnT-III	Protection against growth factor withdrawal (70), increase in proliferative signaling (71).
Invasion	ST6Gal-I	Increased binding of sialylated β1 integrin to collagen I and increased migration and invasion (72)
Homing of tumor cells	FUT7, FUT8,	Increased sialyl Lewis X synthesis and resulting binding to selectins for homing of tumor cells (73)
Stemness	ST6Gal-I	Induction of stemness factors Sox9, slug (74)
Resistance to apoptosis	ST6Gal-I	Sialylation of TNFR suppresses its internalization and blocks apoptotic signaling (75)

D. Sialic acid: structure, biosynthesis and functions.

Sialic acids (Sias) are a group of about 50 diverse neuraminic acids that are ubiquitously found on cellular glycoproteins and glycolipids as terminal glycan residues (33). Sias are unique among the monosaccharides used in N- and O-glycosylation because of their net negative charge at physiological pH (33). The large diversity in Sias exists because of various modifications of the core neuraminic acid structure, e.g. acetylation (76). Commonly observed Sia structures are shown in Figure 8. Twenty different sialyltransferases orchestrate the addition of Sia to galactose (Gal), GalNAc, and other Sia residues (77). The biosynthesis of Sia begins in the glycolytic pathway from fructose-6-phosphate, which is committed to hexosamine biosynthesis pathway by fructose-6-phosphate amidotransferase. The product of this reaction, glucosamine-6-phosphate ($GlcNH_2$-6P), is then acetylated to form GlcNAc-6-phosphate. Following epimerization of GlcNAc-6-phosphate to GlcNAc-1-phosphate, it is coupled to UDP to form

UDP-GlcNAc. The bifunctional enzyme, GlcNAc 2-epimerase/ManNAc kinase (GNE), converts UDP-GlcNAc to ManNAc-6-P to channel it into Sia biosynthesis pathway. ManNAc-6-P is condensed with another glycolysis pathway intermediate, phosphoenolpyruvate, by N-acetylneuraminic acid synthase to form NeuNAc-9-P. Free N-acetyl neuraminic acid (Neu5Ac) is generated by the action of N-acetylneuraminic acid phosphatase. For reasons unclear so far, the sialyltransferase donor CMP-Sia is generated in the nucleus by CMP-sialic acid synthetase (CMAS). After its diffusion into the cytosol, it can be transported by the CMP-sialic acid transporter into the Golgi for its transfer to glycoconjugates by sialyltransferases (33, 78, 79). Defects in most of the Sia biosynthetic enzymes have been implicated in various congenital disorders of glycosylation (33, 79). Interestingly, about 2-3 million years ago, humans lost the ability to hydroxylate the 5'-acetyl group in Neu5Ac to generate Neu5Gc due to a frameshift mutation in enzyme cytidine monophospho-N-acetylneuraminic acid hydroxylase (CMAH); however, Neu5Gc is abundantly found in other mammals and some cancers (80, 81).

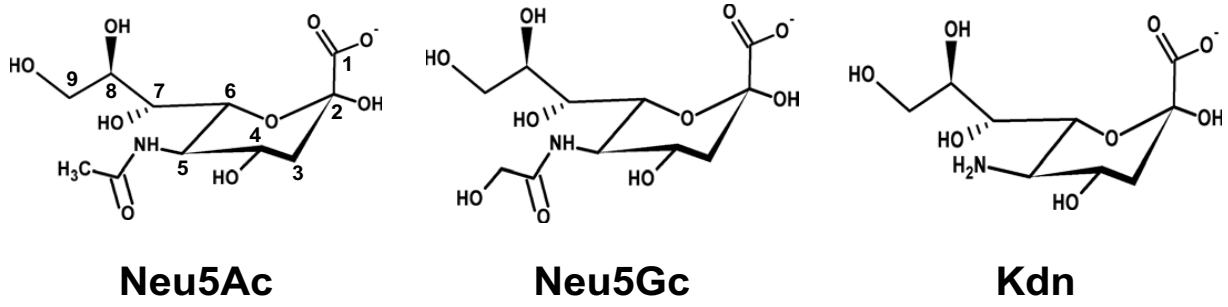

Figure 8. Common sialic acid structures. Sialic acids are 9 carbon sugars with carboxyl group at the 1 position and glycerol chain at the 6 position. This figure is adapted from (33).

As Sias are the outermost glycan residues on glycoconjugates, they play a variety of roles in normal physiology and in disease and infection. For example, numerous pathogens have evolved to exploit them as receptors for their entry into the cells. The most prominent example of one such pathogen is the influenza virus, which binds cell surface Sia using a hemagglutinin protein. Following replication of the virus in the cell, budding viruses are able to bind to cell surface Sia, but are released by virus'

neuraminidase protein that cleaves Sia (82).Physiologically, Sias play crucial roles in modulating receptor signaling, immune responses, and regulating leukocyte homing. A few examples of the role sialylation plays in modulating receptor signaling are mentioned in Table 2. Two protein families that recognize sialic acid or sialylated glyconjugates, the Siglecs and the selectins, are essential for human health and also play roles in disease processes.

A family of about 15 Sia-binding transmembrane proteins called Siglecs has evolved to bind various Sia-containing glycan structures on cells that serve as markers of 'self'. Many Siglecs intracellularly recruit signaling-active phosphatases and thus set a threshold for the immune response by establishing a crosstalk with the other B-cell receptors (83). As shown in Figure 7, sialyltransferases participate in formation of sialyl Lewis X (sLe^X) structures on leukocytes and cancer cells. These glycan structure serves as ligands for E- P- and L-selectins expressed by endothelial cells. In inflammation, the binding of sLe^X structures on leukocyte glycoproteins by E- and P-selectins, expressed on endothelial cells of inflamed tissue, mediates the initial tethering of leukocytes with the endothelium, which then leads to a rolling adhesion of leukocytes on the endothelium mediated by integrins and chemokine receptors, and ultimately extravasation of the leukocytes into the tissue (84) (Fig. 9). Knockout of the sialyltransferases, ST3Gal-IV and ST3Gal-VI, which are responsible for synthesis of sLe^X structures leads to a decrease neutrophil binding to E- and P-selectins and selectin-dependent rolling, as well as lymphocyte homing to secondary lymphoid organs (e.g., lymph nodes), a process mediated by L-selectin (85, 86).

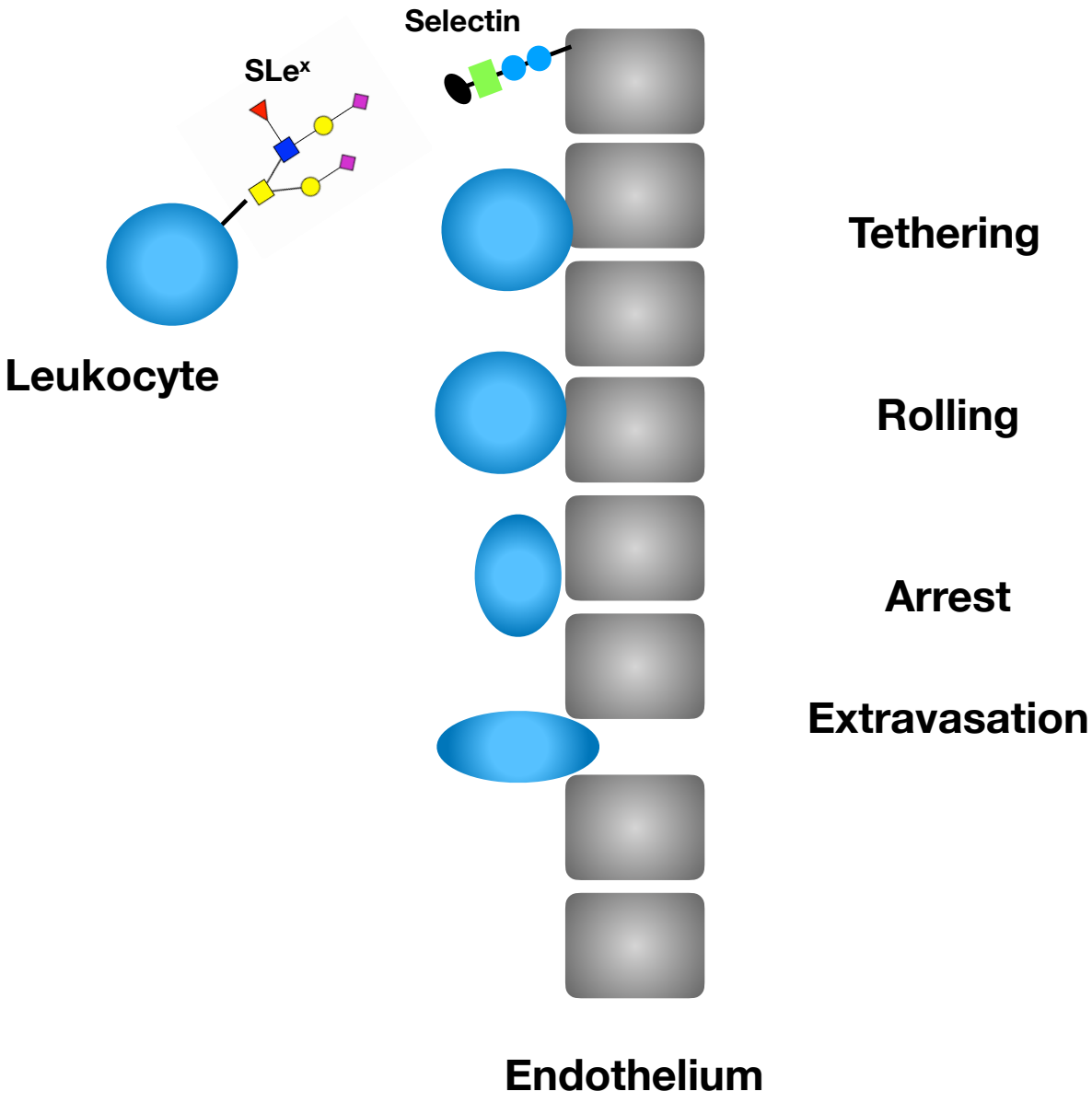

Figure 9: Sialyl Lewis X structure mediated leukocyte recruitment. In inflammatory conditions, selectin proteins on the surface of endothelial cells bind sLe^X structures on leukocytes, which then tether to the endothelium. Cells then roll on the surface of endothelium, arrest, extravasate from the blood stream into the tissue. This mechanism is also exploited by cancer cells for their metastasis.

E. Protein-specific glycosylation events

Most terminal glycosyltransferases are glycoprotein-promiscuous in that they recognize the terminal structures of acceptor glycans that are added previously to the glycoprotein. However, some glycosyltransferases or glycan modifying enzymes must first recognize specific amino acid sequences and/or protein structures before they can modify a glycan structure. These glycosylation/modification reactions are "protein-specific" and usually involve a restricted set of glycoprotein substrates.

An inaugural example of a protein-specific glycan modification comes from the modification of lysosomal enzymes N-glycans with mannose-6-phosphate that is essential for recognition of these enzymes by mannose-6-phosphate receptors in the TGN for transport to the lysosome. The biosynthesis of mannose-6-phosphate is a two-step process and the first step, catalyzed by the UDP-GlcNAc: lysosomal enzyme N-acetylglucosamine-1-phosphotransferase, is protein specific. Mutational analysis and engineering of chimeric proteins showed that two specific lysine residues on the N-terminal side of the N-glycans modified by mannose-6-phosphate are necessary and sufficient for recognition of lysosomal enzymes by this enzyme (87, 88). Similarly, the β1,4-GalNAc-transferase that produces LacdiNAc (GalNAcβ1,4GlcNAc) structures on the N-glycans of pituitary glycoprotein hormones recognizes a 19 amino acid sequence in its substrates which is necessary and sufficient for this addition (89, 90). The sulfated LacdiNAc structure is essential for the clearance of these enzymes from the circulation ensuring a pulsatile signaling cascade (91, 92).

The Haltiwanger group has extensively characterized requirements for protein O-glucosylation and O-fucosylation of EGF repeats of the Notch receptor by the protein O-glucosyltransferase (POGLUT) and protein O-fucosyltransferase (POFUT) families of glycosyltransferases. These enzymes recognize the consensus sequences C-X-X-X-X-S/T-C and C-X-S-X-P/A-C in the folded, disulfide-linked EGF repeat (41, 49, 50, 93). Similar requirements are found for the O-fucosylation of serine and threonine residues in folded, disulfide linked TSRs in thrombospondin and other TSR-containing proteins (50). Recently, it was shown that protein O-mannose GlcNAc-transferase-2 (POMGNT-2), which adds a GlcNAc residue

to the O-mannose residues on α-dystroglycan to prime it for the synthesis of its unusual, extended glycan structure also recognizes a R-X-R-X-X-I-X-X-T-P-T sequence in the polypeptide (Fig. 10) (94).

Ample evidence from our laboratory has demonstrated that modification of a select group of glycoproteins with polysialic acid (polySia), catalyzed by polysialyltransferases (polySTs), ST8Sia-II and ST8Sia-IV, is also protein-specific. I will introduce the features of protein-specific polysialylation more in depth in the remainder of this chapter, and describe my work elucidating the mechanism of protein specific polysialylation further in the subsequent chapters.

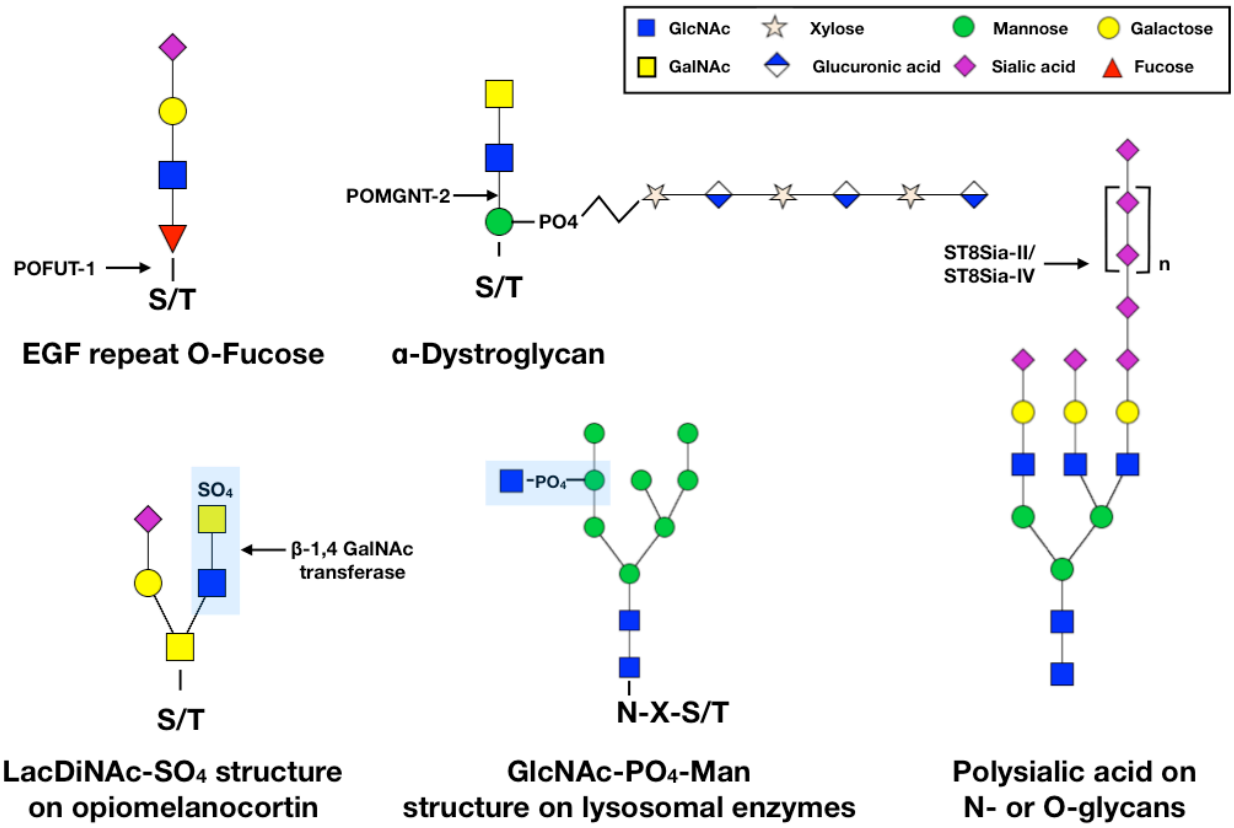

Figure 10: Examples of protein-specific glycosylation. Certain glycosyltransferases recognize features of polypeptide chain or a specific primary sequence for the synthesis of glycans with specialized functions and are only found on a limited number of proteins.

F. Polysialic acid (polySia): its structure, properties, biosynthesis, carriers and functions.

The structure and biochemical properties of polySia- PolySia is a unique carbohydrate homopolymer comprised of 8-400 α2,8 linked Sias that is added to terminal α2,3- or α2,6-linked Sia residues on N- and O-glycans (95). This large, negatively charged polymer is synthesized processively by the polySTs, ST8Sia-II and ST8Sia-IV, which are highly selective for protein scaffolds that carry the modified glycans (96). By the virtue of being a negatively charged glycopolymer, polySia binds substantial amounts of water and increases the hydrodynamic radii of the proteins it modifies, such as the Neural Cell Adhesion Molecule (NCAM), its major carrier (97). Additionally, the negative charge and large size of polySia can also lead to charge-charge repulsive effects and as well as steric hindrance (Fig. 11). As a result of these physiochemical properties, adhesion between apposing membranes (trans interactions) is significantly reduced, as observed directly by electron microscopy (98, 99). Removing cell surface polySia using a bacteriophage endoneuraminidase N (EndoN) that specifically cleaves polySia, increases the contact area between the cells (98, 99). In addition, molecular force measurements showed that polysialylation abrogates adhesion mediated by its carrier proteins, as well as that mediated by nearby non-polysialylated adhesion molecules, such as E-cadherin (100). In addition, Sato and colleagues (96) have shown that polySia is able to bind and serve as a reservoir for various neurotrophins, growth factors, and neurotransmitters, such as brain-derived neurotrophic factor (BDNF), fibroblast growth factor 2 (FGF2), and dopamine. These interactions are proposed to modulate their signaling (96, 97).

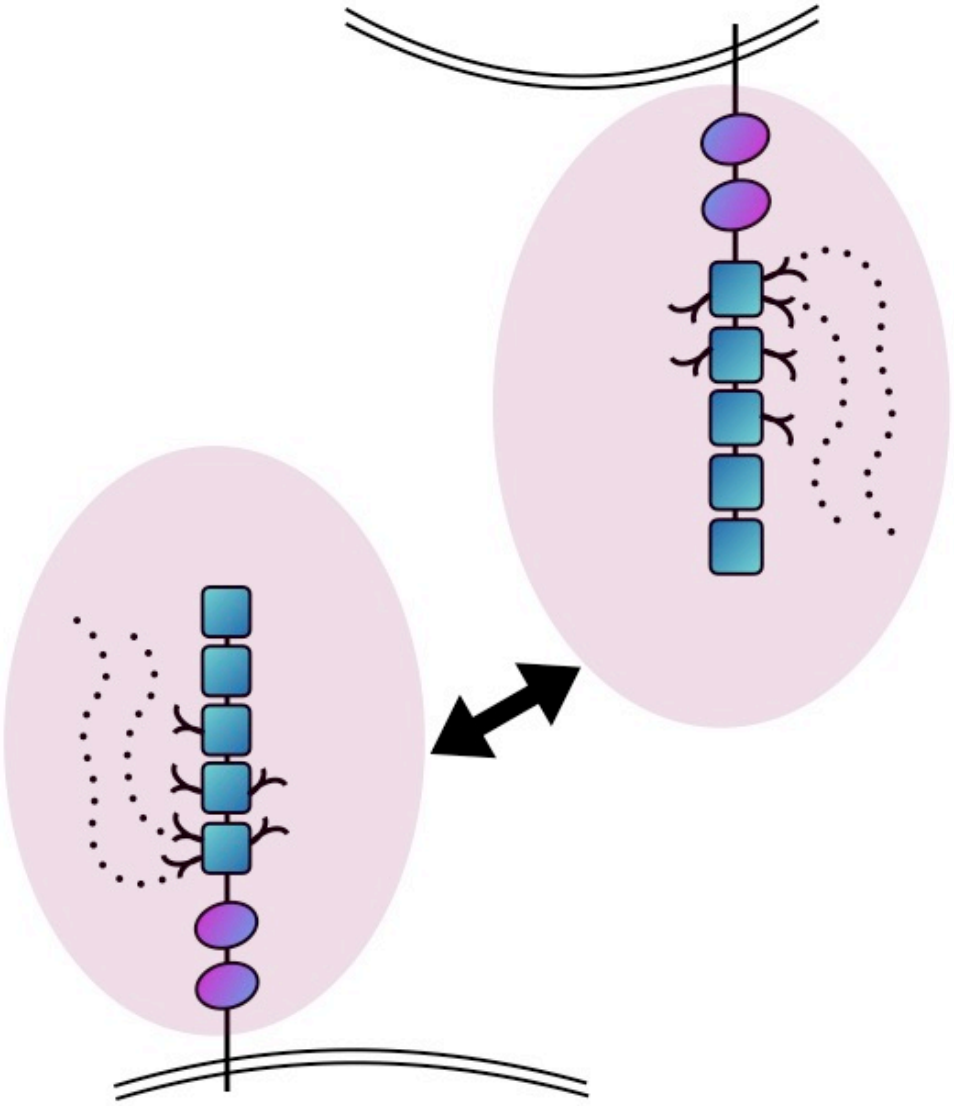

Figure 11: The impact of polySia on cell-cell adhesion. PolySia on cell-surface carrier proteins increases their hydrodynamic radius. Adhesion mediated by these proteins is affected because of entrapped water molecules that increase the hydrodynamic radii of modified proteins, as well as steric hindrance and charge-charge repulsion effects.

Non-mammalian PolySia- PolySia has been discovered on polysialoglycoproteins in Salmonidae fish eggs and on egg and sperm proteins of echinoderms such as sea urchins where it functions as a regulator of calcium concentration and promotes sperm motility, the sperm acrosome reaction, and ensures productive embyrogenesis (95, 101, 102). Intriguingly, the neuroinvasive bacteria *Neisseria meningitides* serogroups B and C decorate their capsules with α2,8- and α2,9-linked polySia. This polySia is essential for pathogenesis and allows these bacteria to evade the immune response of the mammalian host that recognizes it as "self" (96, 103).

Key players in mammalian polysialylation: the polysialyltransferases (polySTs) and their substrates - Mammalian polySia was first discovered by Jukka Finne in rat brain, which was later identified to be on NCAM (104, 105). In addition to NCAM, polySia has been found on only a limited number of proteins in mammals, as shown in Table 3. Apart from NCAM, Neuropilin-2 (NRP-2) was found to be polysialylated on mature dendritic cells as well as microglia (106, 107). PolySia on NRP-2 is believed to control chemotaxis of the mature dendritic cells and modulate their ability to activate T-lymphocytes (106, 108, 109). These groups supported the idea that NRP-2 polysialylation sequestered CCL21. Recently, Kiermaier et al. (110) showed that chemotaxis of dendritic cells to the lymph node is dependent on polySia. Chemokine CCL21 directly binds to polySia, which releases autoinhibition of CCL21 by conformational change, enabling signaling via CCR-7 receptor (110).

Polysialylated NRP-2 in microglia is shed and secreted to act as an anti-inflammatory agent in response to LPS stimulation (107). SynCAM 1 was shown to be polysialylated in NG2 glial cells as well as oligodendrocyte precursor cells (111, 112). In NG2 glial cells, it is believed to regulate interaction of NG2 cells for their inclusion into neural networks (111). On the other hand, polySia on SynCAM 1 in oligodendrocytes was shown to be downregulated during maturation to modulate synaptic contacts (112). E-selectin ligand-1 (ESL-1) was found to be polysialylated in microglia played an anti-inflammatory role similar to NRP-2 (113). In the case of CD36 scavenger receptor, only 4.6% of the total protein was shown

to be polysialylated in human milk. PolySia on these cells was postulated to be important for neonatal development and nutrition (114).

The polysialyltransferases, ST8Sia-II and ST8Sia-IV, are type-II, Golgi membrane proteins that share 59% sequence identity (115, 116). Mammalian polySTs were first cloned from rat brain and Chinese Hamster Ovary (CHO) cells (117, 118). Four regions of the polySTs, called sialylmotifs large (SML), small (SMS), very small (SMVS), and motif III are conserved with other sialyltransferases and play roles in glycan substrate and nucleotide sugar donor binding and catalysis (Fig. 12) (77, 119–121). In contrast, the polybasic region (PBR) that is involved in substrate protein-protein recognition, and the polysialyltransferase domain (PSTD) that together with the PBR may form a basic surface that stabilizes the growing polySia chain, are conserved only between the two polySTs.

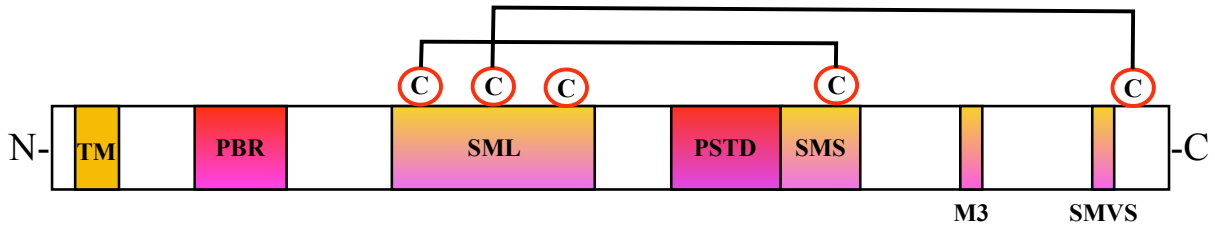

Figure 12: Schematic of the polyST domain structure showing various conserved regions of the enzymes. PolySTs are Golgi localized, type-II glycoproteins with an N-terminal cytoplasmic tail and transmembrane (TM) region followed by luminal sequences including the catalytic domain. Within the catalytic domain are sialylmotifs that are conserved among all sialyltransferases, including sialylmotifs large (SML), small (SMS), very small (SMVS), and motif 3 (M 3), and these are shown in yellow-pink. The polybasic region (PBR) and polysialyltransferase domain (PSTD) conserved only in the two polysialyltransferases are shown in red-pink. Disulfide linkages critical for folding and activity are also depicted.

Like other sialyltransferases, polySTs use CMP-Sia as a donor. Unlike other sialyltransferases that add one Sia to terminal galactose or GalNAc as acceptors, the polySTs transfer Sia in an α2,8-linkage to α2,3- or α2,6- sialylated glycans in processive fashion (95, 122). The SML region binds CMP-Sia donor whereas SMS region participates in binding of glycan acceptor as well as CMP-Sia (119, 120) (Fig. 12). Structurally, one of the two disulfide bonds in polySTs is conserved in all sialyltransferases and is crucial for folding and thus activity (123). The other disulfide bond brings C-terminal portion of polySTs in proximity to the SML region and is unique only to α2,8-sialyltransferases. Mutation of this disulfide bond results in loss of catalytic activity without misfolding the protein, suggesting that the three-dimensional structure formed as a result of this bond is critical for the polysialylation process (124).

A recent crystal structure of ST8Sia-III sheds more light on the nature of the polyST active site and catalytic mechanism. ST8Sia-III shares 59% sequence identity with ST8Sia-IV but does not polysialylate NCAM (125, 126). CMP-Sia donor binds in a pocket with its ribose and phosphate group buried. The phosphate group interacts with the side chains of His^{337} in motif III, and Asn^{167}, and Asn^{190} in SML. Intuitively, these residues are conserved across ST8Sia family. Hydroxyl groups of ribose form hydrogen bonds with side chain hydroxyl of Ser^{300} and various main chain atoms of several SMS residues. In this structure, most of the donor Sia atoms were not fully resolved. Acceptor Sia is stacked against two hydrophobic loops that are conserved in ST8Sia-II and ST8Sia-IV. N-acetyl hydrogen of the acceptor Sia interacts with the side chains of Asn^{211} and Ser^{213}. Arg^{298} in PSTD binds 7'-OH of the glycerol side chain of the acceptor Sia and is believed to be important for the proper positioning of 8'-OH for catalysis (125). A critical catalytic histidine is conserved in the SMVS of all sialyltransferases. In ST8Sia-II this is His^{346} and in ST8Sia-IV this is His^{331}. This His residue serves to deprotonate the 8'-OH of the acceptor glycan so that the new α2,8 bond can be formed with CMP in CMP-Sia acting as a leaving group (121, 127). Nearby Glu^{359} (Glu^{336} in ST8Sia-IV and Glu^{351} in ST8Sia-II) could enhance basicity of His^{354}. Mutation of these histidines to lysines renders both polySTs inactive (128). Remarkably, a large basic groove, composed of PBR and PSTD residues extends from the active site and can provide

anchoring to the growing polySia chain. Such basic groove is absent near the active sites of monosialyltransferases ST6GalI or ST8Sia-III (125, 127, 129).

Unlike other sialyltransferases, the polySTs must recognize their substrates via a protein-protein contact before polysialylating their substrates' glycans. The first evidence that polysialylation was protein specific came from Angata et al. (130) who demonstrated that free sialylated glycans or those linked to lipids or non-substrate glycoproteins could not be polysialylated by the polySTs *in vitro*. On the other hand, N-glycans attached to NCAM were readily polysialylated. (130). Analysis of the polysialylated glycans found on NCAM from cultured cells or bovine and mouse brains, showed that apart from the presence of terminal α2,3- or α2, 6-Sia, the structure of the N-glycans that are polysialylated varies considerably with respect to number of antennae and the presence or absence of core fucosylation, suggesting that the glycan structure does not mediate the protein-specificity of this process (131–134). Intriguingly, polySTs polysialylate their own N-glycans (135–137). This 'autopolysialylation' is not essential for catalytic activity as non-autopolysialylated polyST mutants in which asparagines carrying polysialylated N-glycans are mutated, polysialylate NCAM to the level of wild-type enzymes (136, 138). Intriguingly, I have recently found that while ST8Sia-IV autopolysialylation is not required for the polysialylation of N-glycans on NCAM or SynCAM 1, it does appear to be important for the polysialylation of the O-glycans of NRP-2 polysialylation (Chapter V).

Table 3. Mammalian Proteins Modified by PolySia.

Protein	Location
Neural Cell Adhesion Molecule	Nervous system and other tissues (104)
Voltage-gated sodium channel α subunit	Electric eel electroplax membranes (139) and rat brain (140)
CD-36 scavenger receptor	Human milk (114)
Neuropilin-2	Mature dendritic cells, microglia, macrophages (106, 113)
Synaptic Cell Adhesion Molecule 1 (SynCAM 1)	NG-2 glial cells (111), Oligodendrocyte precursor cells (112)
C-C chemokine receptor-7 (CCR-7)	Mature dendritic cells (110)
E-selectin ligand-1 (ESL-1)	Microglia and THP-1 macrophages (113)

The Neural Cell Adhesion Molecule (NCAM)- NCAM is the most well-characterized polyST substrate and the major carrier of polySia in the brain (134). NCAM is an type I transmembrane, immunoglobulin super-family protein, containing 5 immunoglobulin (Ig) domains and two fibronectin type III (FN) repeats. It is expressed as three isoforms-NCAM-180, NCAM-140 that are transmembrane proteins with different length cytopolasmic tails, and NCAM-120, a glycosylphosphatidylinositol (GPI)-anchored protein (Fig. 13).

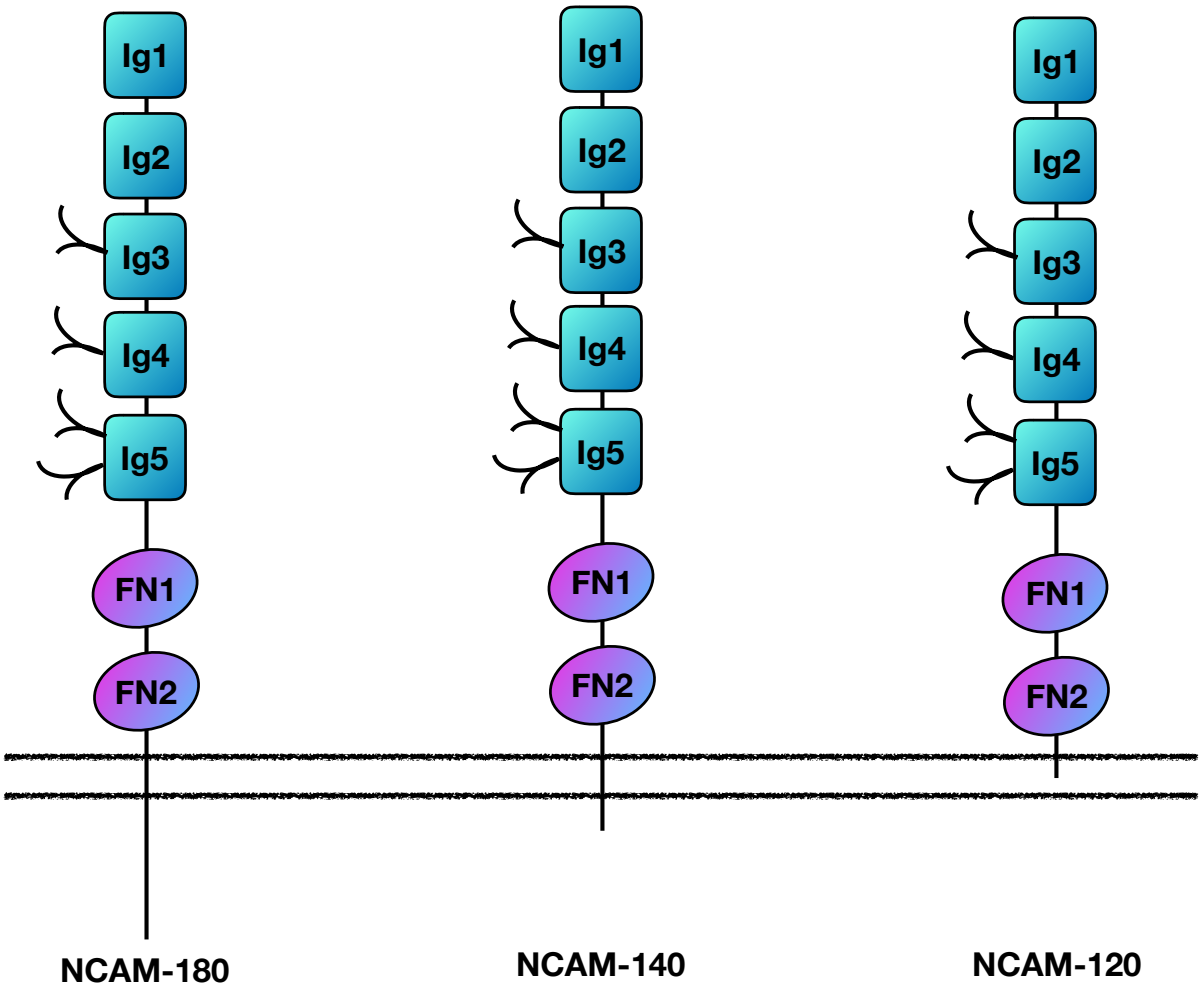

Figure 13: The three isoforms of NCAM. NCAM isoforms observed because of alternative splicing are shown. They differ from each other by the length of cytoplasmic tail and the presence of a transmembrane region (NCAM-180 and NCAM-140) or GPI anchor (NCAM 120).

The extracellular domains of NCAM have long been known to engage in homophilic and interactions with other NCAM molecules (141). However, NCAM has also been shown to engage in heterophilic interactions with various other transmembrane receptors such as fibroblast growth factor receptor 1 (FGFR1), as well as ECM components such as collagen and heparan sulfate (141–143). Several reports have implicated various NCAM Ig domains in mediating homophilic cis and trans interactions. From the analysis of various crystal structures of the NCAM Ig domains, as well as biophysical data, Elisabeth Bock's group has put forward a model in which NCAM at the cell surface exists in a cis dimer form involving interactions between Ig1 and Ig2 domains in two NCAM molecules. They propose that trans-dimeric interactions are weaker than cis-interactions and therefore, trans-homophilic NCAM interaction is believed to involve two cis-dimers with Ig2 domain of one cis-dimer interacting with Ig3 domain of the other forming tight 'zipper' like structures (Fig. 14). It is yet to be established how polySia influences formation of the NCAM cis-dimers; however, it has been hypothesized that polysialylation would block zipper formation. Furthermore, it has been proposed that the zipper structures are so dense that they may preclude formation of complexes such as NCAM-FGFR. On the other hand, polysialylated NCAM would allow for only loosely linker zippers if any, leaving room for other heterophilic interactions, such as with FGFR (141). Notably, and in contrast to the crystallography data, force measurement data suggests two different trans-binding modes for NCAM homophilic binding involving antiparallel interactions between two or all five Ig domains of opposing NCAM molecules (100).

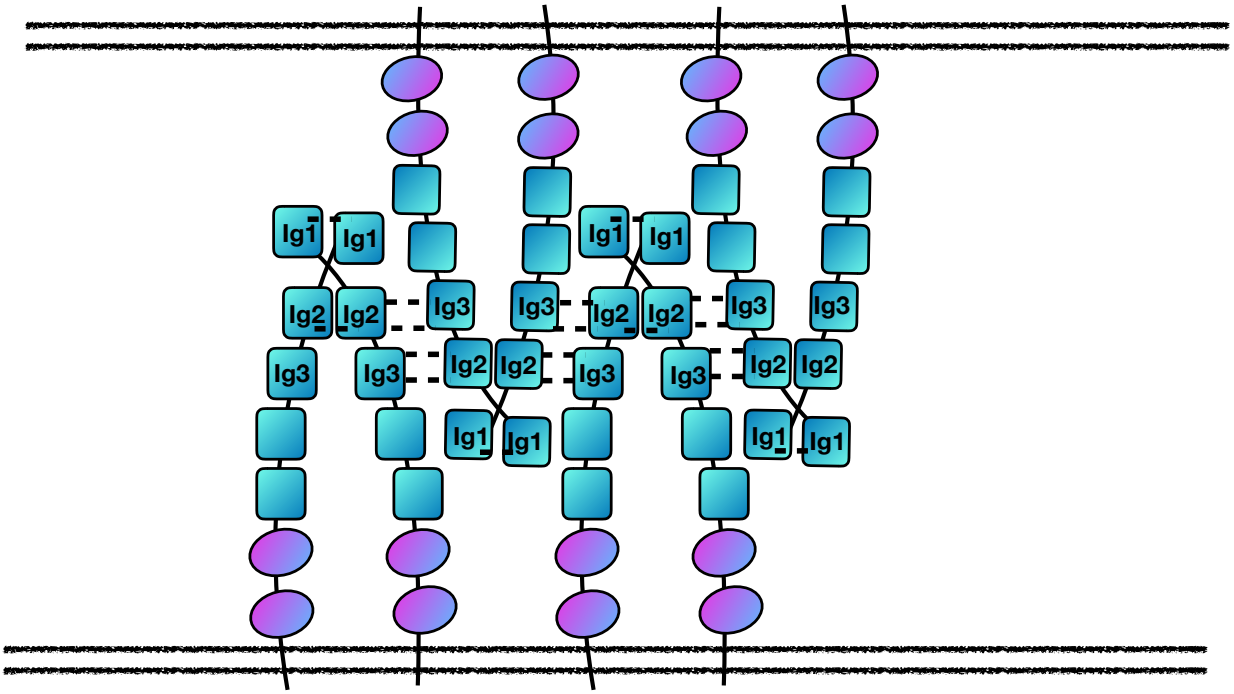

Figure 14: Zipper formation by NCAM molecules. NCAM is believed to form cis-dimers that are stabilized by interactions between Ig1 and Ig2 domains. To mediate cell-cell adhesion, the cis-dimers on one cell interact with those on the other cell. These zipper interactions are mediated by Ig2 and Ig3 domains (dashed lines) and polySia is believed to significantly disrupt this interaction.

NCAM-FGFR interaction in cis is suggested to activate FGFR to control neuritogenesis, cell growth and differentiation (reviewed in (96)). NCAM activation of FGFR has been shown to be different from FGF-mediated activation structurally, as well as functionally (144, 145). NCAM interacts with the FGFR in the Ig module 3 via sequences in its FN1 and FN2 domains (145). NCAM promotes FGFR-induced cell migration via ERK1/2 pathway while FGF promotes cell growth due to recruitment of different signaling mediators (146). In addition, NCAM results in more sustained FGFR activation than FGF alone, due to enhanced recycling of the receptor to the cell surface. While most studies support a cis NCAM-FGFR interaction, one study suggest that this interaction happens in trans (146). While effect of NCAM polysialylation on FGFR interaction has not been evaluated directly, some studies have showed that removal of polySia from NCAM activates ERK, suggesting that polySia may block NCAM-FGFR interaction and resulting signaling (147, 148). It is thought that polySia-mediated inhibition of FGFR signaling may protect cells from premature differentiation (149). Interesting studies from Sato and colleagues (150) suggest another way that polySia could impact FGFR signaling. These investigators show that the polySia can bind FGF2 directly in vitro (150). Comparison of the affinity of FGF2 for polySia and heparan sulfate that is key for FGF2 binding to FGFR, revealed that FGF2 could be transferred from polySia on NCAM to heparan sulfate associated with the FGFR, but not to the FGFR directly (150). Finally, NCAM is believed to associate with $p125^{fak}$ and $p59^{fyn}$ kinases via its intracellular sequences, possibly with the involvement of receptor protein tyrosine phosphatase RPTPα (144, 151). This interaction and activation of the FAK/Fyn signaling pathway is independent of FGFR and ERK and allows the formation of focal adhesions and polySia on NCAM was shown to block this process (152).

PolySia in development- The expression of polySTs is first observed at embryonic day 8.5 in mice. During the embryonic brain development, polySia expression attains the maximum in perinatal phase and then rapidly declines between postnatal day 10.5-13.5 although some small amount of polySia persists in specific regions of the adult brain (153, 154). This decrease in polysialylation is correlated with loss of ST8Sia-II as development proceeds. In contrast, ST8Sia-IV expression decreases only moderately in the

adult brain (155, 156). This observation indicates that ST8Sia-II is the major polyST during embryonic development, whereas ST8Sia-IV is the major polyST in adults. In addition to the developing brain, polySia expression is also observed during organogenesis of heart, kidney, pancreas, liver, respiratory and digestive tracts (140, 157–159). Expression of the two polySTs in the adult is cell-type specific and is largely observed in the areas associated with continued cell-migration and synaptic plasticity, consistent with the idea that reduced cell-cell adhesion enables migration of cells expressing polySia (160–163).

To delineate the role of NCAM and individual polySTs in development, knockout animals were generated (164–166). Mice null for either ST8Sia-II or ST8Sia-IV had normal life spans. Postnatal 1 day brains of ST8Sia-IV$^{-/-}$ mice had about ~50% of the polySia observed in wild-type mice whereas brains of ST8Sia-II$^{-/-}$ mice had only about 5% of the polySia observed in wild-type mice, indicating that ST8Sia-II can somewhat compensate for the loss ST8Sia-IV, but not vice versa (164, 165). Analysis of polySia chain length in these knockout mice, as well as mice expressing different allelic combinations of both polySTs, also revealed that ST8Sia-II is the more efficient enzyme. Strikingly, ST8Sia-IV tends to synthesize a higher amount of shorter polySia chains, implying that the concerted action of both enzymes may be required for robust synthesis of long polySia chains (133, 167). I will only be discussing phenotype of polyST double knockout mice in detail. However, Figure 15 summarizes knockout phenotypes of mice in which NCAM, ST8Sia-II, and ST8Sia-IV were individually knocked out.

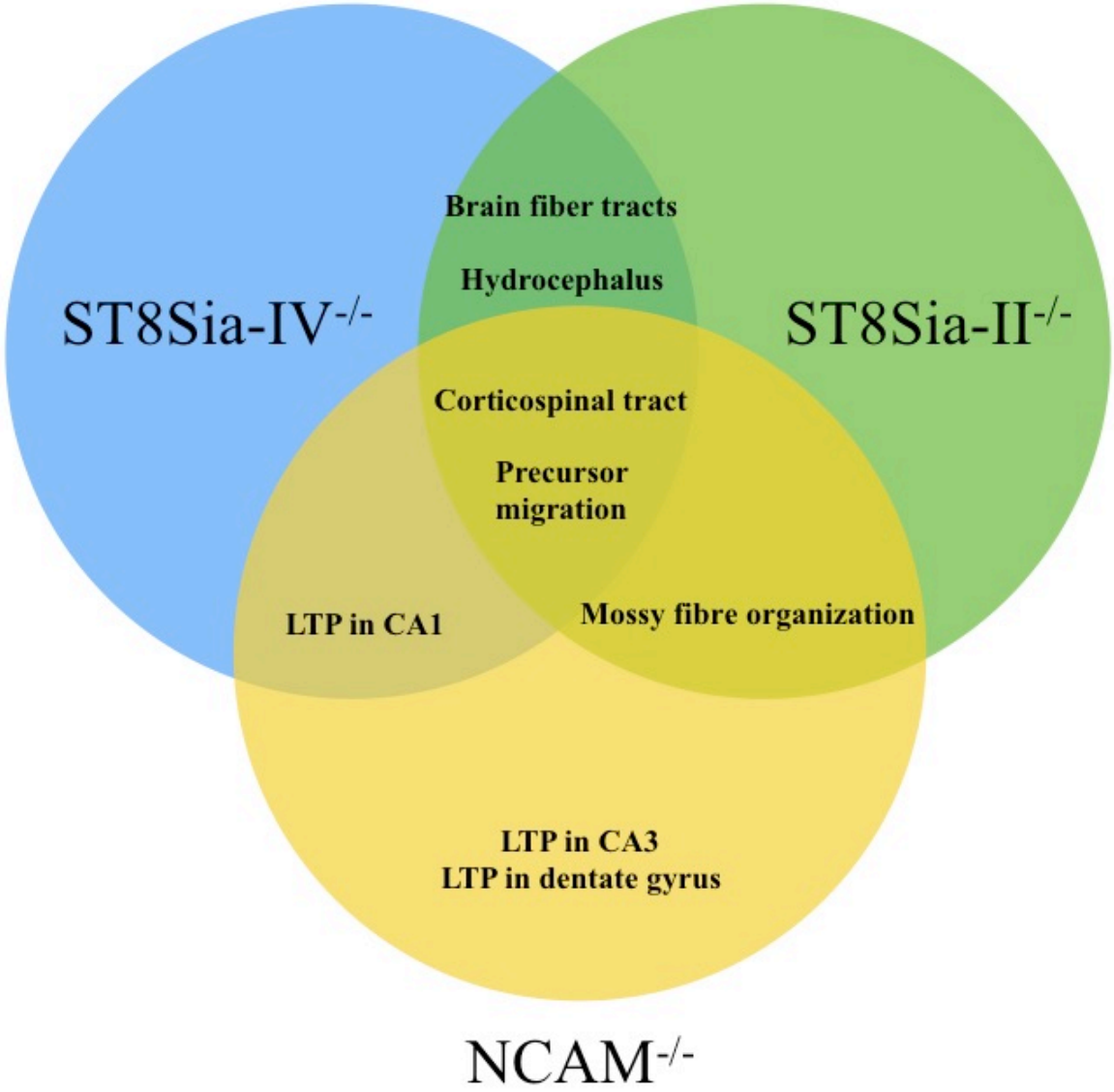

Figure 15: Summary of defects observed in NCAM$^{-/-}$, ST8Sia-II$^{-/-}$, ST8Sia-IV$^{-/-}$ as well as polyST double knockout mice. Defects represented in the area between 3 circles are defects observed in NCAM$^{-/-}$ mice as well as ST8Sia-II$^{-/-}$/ST8Sia-IV$^{-/-}$ double knockout mice and not the triple knockout mice. LTP= long-term potentiation. Defects that are specific to polyST null animals are considered gain of NCAM function due to loss of polySia (154).

ST8Sia-II/ST8Sia-IV double knockout animals had significantly smaller body size than the single knockout animals, as well as a smaller olfactory bulb, severe defects in nervous system development, and these animals died within four weeks of birth (168). PolySia-enabled migration of precursor cells occurs in the rostral migratory stream (RMS) from the subventricular zone to the olfactory bulb. In the absence of polySia, the migration of these precursor neurons is halted and they differentiate prematurely. As a result, the olfactory bulb in these knockout animals is significantly reduced in size. A similar size reduction is observed for the internal capsule and mammillothalamic tract. PolySia keeps axons from bundling together (fasciculation) to ensure branching. The loss of polySia in these animals causes increases in fasciculation and abnormal axon guidance is observed in the anterior commissure and corticospinal tract. Loss of polySia also causes aberrant lamination of mossy fibers, which provide input from various brain areas to the cerebellum. Finally, the double polyST knockout also results in hydrocephalus and mice die 4 weeks after their birth. $NCAM^{-/-}$, $ST8Sia\text{-}II^{-/-}$, $ST8Sia\text{-}IV^{-/-}$ triple knockout mice, however, did not exhibit the early death, hydrocephalus, growth retardation, and other nervous system effects observed with polyST double knockouts. However, olfactory bulb and lamination defects did persist (168). These observations suggested that many of the effects of the double polyST knockout reflect a gain of NCAM function at inappropriate times during development.

Polysialic acid in the adult animal- PolySia expression is retained in certain areas of the adult brain where synaptic plasticity and cell migration must persist. These include the olfactory bulb, the hippocampus and the hypothalamus. In the hippocampus, the presence of polySia is important for LTP, learning, and memory (97, 134). PolySia levels in the hypothalamus change in response to light exposure, and enzymatic removal of polySia deregulates photic induction, suggesting that the expression of polySia plays a role in regulating circadian rhythms (97, 169, 170). Recently, it was shown that altering polySia levels in the hypothalamus with injected EndoN, changed the balance between low-density and high-density lipoprotein levels, suggesting a role for polySia expression in cholesterol metabolism (171).

PolySia is expressed on a large number of immune cells (reviewed in Colley, Kitajima and Sato). Stamatos et al. (172) showed that polySia expression changes as mouse hematopoietic precursors differentiate along the myeloid lineage, and that polySia is also expressed on bone marrow derived neutrophils and a subset of monocytes and that its expression is decreased as these cells move to sites of inflammation. Drake and colleagues (173) showed that knocking out ST8Sia-IV led to a substantial reduction in thymocyte precursors/thymocytes and additional experiments suggest that this is due to an inability of the precursors to leave the bone marrow and travel to the thymus in order to differentiate. These investigators also demonstrated that ST8Sia-IV knockout mice exhibited increased contact hyper-sensitivity and decreased tumor killing (174). These results suggested a role for polySia in immune regulation, at least in the mouse. On the other hand, human fetal bone marrow did not possess polySia+ myeloid lineage cells like mouse bone marrow (174). However, polysialylated NCAM was found on human Natural Killer (NK) cells but not mouse NK cells, where changes in polysialylation were seen depending on activation by interleukin-2 (174).

Others have proposed that polySia-acts as an anti-inflammatory agent in the brain and in the lung. The Hildebrandt group showed that polysialylated NRP-2 in microglia and polysialylated SynCAM 1 in NG-2 glial cells moves to the cell surface upon inflammatory lipopolysaccharide (LPS) stimulation (107). Surface localized polySia in these cells is subsequently shed and is believed to serve as neuroprotective agent as treatment of soluble polySia led to attenuation of nitric oxide and proinflammatory cytokine production after LPS stimulation (113). The role of polySia in protection from inflammation was also supported by Ulm at al. (175), who showed that polysialylated NCAM is upregulated and shed in chronic obstructive pulmonary disease (COPD). Soluble polySia-NCAM was shown to reduce the cytoxicity mediated by extracellular histones that are part of neutrophil extracellular traps (NETS), likely because of its ability to bind histones directly (175, 176). The authors propose that shed polySia-NCAM may serve to protect the lung from damage during inflammation (175).

PolySia is implicated in the mammalian reproductive system. In the testis, polySia is upregulated on germ precursor cells during spermatogenesis and is believed to control progenitor differentiation by modulating their contact with the Sertoli cells (177). In females, during early pregnancy, trophoblasts in placenta express polySia, and its expression decreases in the later stages of pregnancy (178). The authors suggest that polySia may serve to regulate adhesive interactions that are necessary when mother-fetus contacts are being established for the passage of nutrients.

PolySia in tissue regeneration- Similar to pro-migratory function of polySia during development, polySia expression has been shown to be elevated in response to injury and to be important for the regenerative process. Using a mouse model of corticospinal injury, the Rutishauser group induced ST8Sia-IV expression at the injury site and demonstrated rapid recruitment of progenitor cells and the growth of axons to and across the injury site (179). Other studies by this group showed that ectopic expression of polySia stimulated axon regeneration in an injured cerebellum (180, 181) and that it could direct axons to distant sites of injury (179). Tsuchiya et al. (182) showed that polySia was necessary for proper bile duct formation and is upregulated in liver regeneration. They showed that polySia-NCAM is upregulated in ductular reaction region containing bipotential progenitor cells after severe liver injury as well as in cirrhotic livers from patients with chronic liver disease. These reports suggest therapeutic approaches targeting the polySTs (96).

PolySia in disease- With the demonstrated importance of polySia in a multitude of physiological processes in the nervous system, it may be surprising that polySia expression is altered in multiple psychiatric disorders such as schizophrenia, bipolar disorder, and autism spectrum disorder (183). Single nucleotide polymorphisms (SNPs) in the ST8Sia2 gene have been observed in these diseases and have been suggested to affect reservoir function of polySia for neurotransmitters and neurotrophins (183). Moreover, ST8Sia2 null mice exhibit a schizophrenia-like phenotype with impeded interneuron precursor migration (184). When these mice were analyzed for nervous system defects, abnormal myelination was observed. The same study demonstrated that ST8Sia-II deficiency affects oligodendrocyte differentiation

and hence, myelination. Interestingly, these effects of ST8Sia-II absence appeared to exacerbate with aging (185).

Elevated expression of PolySia is observed in a variety of cancers including small cell lung carcinoma (SCLC), non-small cell lung carcinoma (NSCLC), neuroblastoma, Wilm's tumor, medulloblastoma, medullary thyroid carcinoma, rhabdomyosarcoma, colorectal cancers and astrocytoma (reviewed in (186)). Over 65% of patients with glioma and pancreatic cancer also expressed polySia (186). In an early study involving non-small cell lung carcinoma (NSCLC) patients, only about 20% of patients expressed polySia at stage I whereas 77% of the patients in the study expressed polySia at stage IV. Most remarkably, 47% of stage IV NSCLC patients expressed polySia but not NCAM, suggesting that polySia on substrates other than NCAM, such as NRP-2 or SynCAM 1 may be of relevance in late stage cancers. Moreover, ST8Sia-II, which is not expressed in normal lung tissue was re-expressed in cancer, correlating with the stage of cancer development (187). In a study involving 236 patients, polySia expression correlated with poor prognosis showing ~40% with a less than 5-year survival rate (188). Scheidegger et al. (189) analyzed NIH H69 SCLC cell lines expressing varying amounts of polySia. PolySia-positive cells showed more growth on soft-agar and established more metastatic nodules in nude mice. Considering these observations, understanding the mechanism of polysialylation and how to inhibit it in diseases like cancer is likely to aid in development of therapeutics.

G. Mechanistic details of protein-specific polysialylation

Early experiments by Nelson et al. (190) identified NCAM Ig4, Ig5, and FN1 domains as sequences that are minimally required for the process of polysialylation. They also defined three asparagine residues within NCAM Ig5 domain as sites of polySia attachment (190). Close et al. (191) later constructed various domain deletion mutants of NCAM and determined that the Ig4 domain is dispensable for polysialylation of NCAM and that Ig5-FN1 is the minimal polysialylatable unit. The distance between the Ig5 domain and transmembrane region was also immaterial as a membrane-associated mutant containing just NCAM Ig5 and FN1 domains was polysialylated to the level of full-

length NCAM. Furthermore, membrane anchoring of NCAM was also not necessary for polysialylation. Notably, however, the FN1 domain of NCAM could not be replaced by the NCAM FN2 domain or the FN1 domain of the related L1CAM (190, 192). These observations led to the first clues about the role of the FN1 domain as a recognition and docking site for polySTs, which were later reinforced when it was determined that a NCAM ΔFN1 mutant is incapable of binding to, or being polysialylated by, ST8Sia-IV (193).

Later modeling studies and crystal structure of the FN1 domain revealed a unique acidic patch constituted by residues Asp^{520}, Glu^{521}, and Glu^{523}, and an α-helix, both of which were not present in the FN2 domain that could not replace FN1 (192, 194). Mutating the acidic residues to alanine in full-length NCAM significantly decreased NCAM polysialylation whereas mutating the same residues to arginine eliminated NCAM polysialylation (192). Replacement of the α-helix, on the other hand, did not decrease polysialylation but it shifted NCAM polysialylation from Ig5 domain N-glycans to FN1 O-glycans, suggesting that this helix may mediate proper positioning of polySTs on the NCAM FN1 domain (194).

In order to identify other important sequences within the FN1 domain, Foley et al. (195) engineered a series of NCAM-OCAM chimeric proteins. Olfactory Cell Adhesion Molecule (OCAM) shares an identical domain architecture and ~44% sequence identity with NCAM. The OCAM FN1 domain shares 37% sequence identity with the NCAM FN1 domain, its Ig5 domain has N-glycans in the same positions as that of NCAM, and yet is not polysialylated (195, 196). Remarkably, the OCAM FN1 domain was able to replace NCAM FN1 domain to allow chimera polysialylation to levels of ~50% of that of wild type NCAM (197). Why then is OCAM not polysialylated? It was postulated that sequences within the Ig5 domain may also play a role in NCAM polysialylation. Indeed, polysialylation was observed when a chimeric protein in which OCAM Ig5 domain was replaced with NCAM Ig5 domain was co-expressed with ST8Sia-IV (197). Comparison of NCAM and OCAM Ig5 sequences showed that OCAM Ig5 glycosylation sites equivalent to polysialylated asparagines in NCAM are nearby large, basic residues not found in the NCAM Ig5 domain. When these large, basic residues replaced the serine and

asparagine residues at the analogous locations in the NCAM Ig5 domain, NCAM polysialylation was abolished (197).

If the NCAM FN1 acidic patch mediates its recognition by polySTs, do polySTs have a corresponding basic region? Indeed, comparison of polyST sequences with the other mono-sialyltransferases yielded two regions that are enriched in basic residues and uniquely present in the polySTs, the polybasic region (PBR) and the polysialyltransferase domain (PSTD) (Fig. 12). Nakata et al. (198) mutated basic residues in the ST8Sia-IV PSTD region and observed decrease in NCAM polysialylation upon co-expressing these mutants with NCAM. They hypothesized that PSTD residues are crucial for tethering the growing negatively charged polySia chain. We mutated basic residues of the ST8Sia-IV PBR region and found that mutating Arg^{82} and Arg^{93} led to decrease in NCAM polysialylation. In contrast with the PSTD basic mutants, these mutations did not hamper overall catalytic activity of polySTs, as polyST autopolysialylation was still preserved. A model therefore emerged that the PBR residues are involved in interaction with NCAM whereas PSTD residues play a role in elongation of polySia chains (199). The role of PBR residues in substrate binding was further supported by the ability of a ST8Sia-IV fragment consisting of residues 1-140 to compete with the full-length ST8Sia-IV to prevent NCAM polysialylation. Moreover, when Arg^{82} and Arg^{93} were replaced with alanines in the ST8Sia-IV H331K mutant, which is catalytically inactive, it no longer competes with wild-type ST8Sia-IV for NCAM polysialylation, suggesting that these residues are critical for NCAM recognition and binding (128, 200). Taken together, these results led to the ‘two domain paradigm’ of protein-specific polysialylation where one domain (FN1 in the case of NCAM) serves as a recognition domain where polySTs dock and the other domain possesses glycans that are polysialylated (Fig. 16).

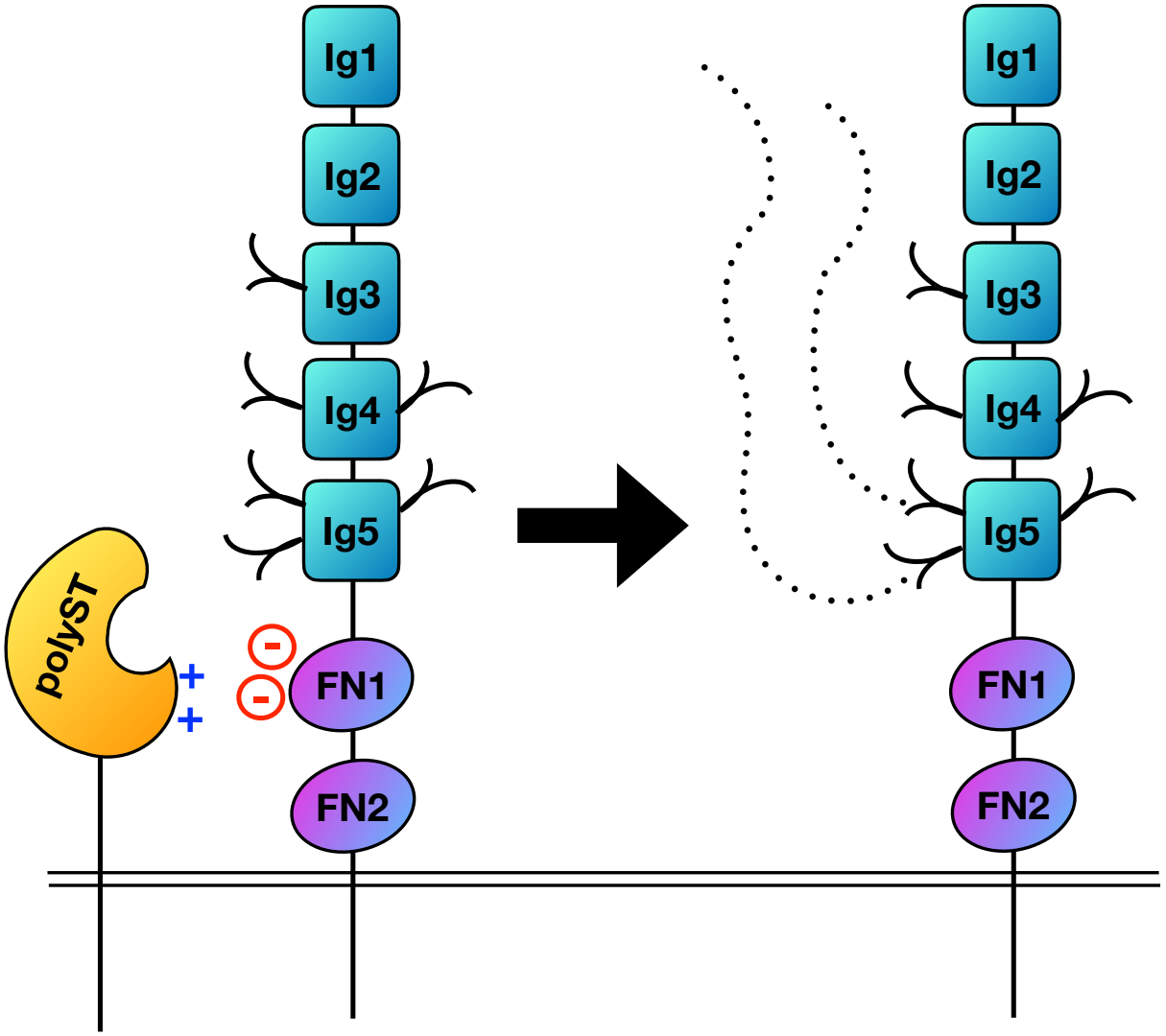

Figure 16. Model of protein specific polysialylation with NCAM as model substrate. The NCAM FN1 acidic patch interacts with basic residues of polyST PBR region. This initial interaction allows the polyST to dock onto the substrate and position itself to polysialylate glycans in the adjacent domain (Ig5).

Significance

The importance of polySia in normal developmental processes, in disease and in regeneration motivated our lab to evaluate the basic mechanism of NCAM polysialylation. My doctoral work has resulted in several key findings. First, using biophysical methods, I provided evidence that the NCAM FN1 acidic patch directly interacts with the Arg^{82} and Arg^{93} in the ST8Sia-IV PBR (Chapter III). These studies also suggested that the binding of the polyST PBR to the FN1 domain elicits a conformational change in the Ig5-FN1 linker and adjacent loop region that could be key for the polysialylation process. Second, I evaluated the requirements for NRP-2 polysialylation and found that like NCAM, NRP-2 possesses one domain that serves as a recognition domain and an adjacent region that carries the glycans that are polysialylated (Chapter IV). This established the two domain paradigm for protein-specific polysialylation. Third, in collaboration I have determined the PBR requirements for ST8Sia-IV recognition and polysialylation of NRP-2, and ST8Sia-II recognition polysialylation of NCAM and SynCAM 1 (Chapter V). In these studies, I have evaluated the mechanism of autopolysialylation and found that ST8Sia-IV autopolysialylation is required for NRP-2 polysialylation, but not for NCAM or SynCAM 1 polysialylation. I anticipate that this information and particularly that discussed in Chapter III will provide the basis for designing inhibitors of the polysialylation process that could have therapeutic applications. I will discuss my preliminary data to this end in Chapter VI.

Chapter II

Materials and Methods

(Parts of this chapter have been published in Bhide GP, Fernandes NR, Colley KJ, Sequence Requirements for Neuropilin-2 Recognition by ST8SiaIV and Polysialylation of Its *O*-Glycans, J Biol Chem, 2016, 291 (18): 9444-9457 and Bhide GP, Prehna G, Ramirez BE, Colley KJ, The Polybasic Region of Polysialyltransferase ST8Sia-IV Binds Directly to the Neural Cell Adhesion Molecule, NCAM, Biochemistry, 2017, 56 (10): 1504-1517 or will be submitted as the manuscript *Overlapping Sets of Basic Residues in the Polysialyltransferases are Required for Substrate Recognition and Polysialylation by* Bhide, G.P., Zapater, J. L., and Colley, K. J.).

Acquisition of reagents

The cDNA for full-length human NCAM140 was a gift from Dr. Nancy Kedersha (Brigham and Women's Hospital, Boston, MA). The cDNAs for full-length human SynCAM 1 and NRP-2 were obtained from Dr. Thomas Biederer (Department of Molecular Biophysics and Biochemistry, Yale University, New Haven, CT) and Dr. Nicholas Stamatos (University of Maryland School of Medicine, Baltimore, MD), respectively. The cDNAs for full-length human ST8Sia-II and ST8Sia-IV were obtained from Dr. John Lowe (Genentech, South San Francisco, CA) and Dr. Minoru Fukuda (Sanford Burnham Medical Research Institute, La Jolla, CA), respectively. pcDNA4-NCAM-Fc and pcDNA4-NRP2-Fc were kind gifts from Dr. Ken Kitajima (Nagoya University, Nagoya, Japan) and pCAG-ST8Sia-II-V5 was gifted by Dr. Stephen Dalton (University of Georgia, Athens, GA). Shiga toxin 2b (Stx2b) cDNA was a gift from Dr. Alison Weiss (University of Cincinnati, Cincinnati, OH). pET14(b)-6xHis-SUMO vector was acquired from Dr. Arnon Lavie (University of Illinois at Chicago, Chicago, IL).

Tissue culture media and reagents, including Dulbecco's modified Eagle's medium (DMEM), fetal bovine serum (FBS), and penicillin and streptomycin, Lipofectin and Lipofectamine-2000

transfection reagents, Opti-MEM I media, mouse monoclonal IgG2a anti-V5 epitope tag antibody and 4', 6'-diamidino-2- phenylindole dihydrochloride (DAPI), SuperSignal West Pico Chemiluminescence reagent were purchased from Thermo-Fisher. BioWhittaker serum- free medium was purchased from Lonza (Walkersville, MD).

Oligonucleotides were purchased from Integrated DNA Technologies (Coralville, IA) and Invitrogen (Carlsbad, CA). Restriction enzymes, T4 DNA ligase, and peptide-N-glycosidase-F (PNGase-F) were purchased from New England Biolabs (Ipswich, MA). The QuikChange™ site-directed mutagenesis kit and *Pfu* DNA polymerase were obtained from Agilent Technologies (Santa Clara, CA). In-Fusion HD cloning kit and nickel-nitrilotricetic acid (Ni-NTA) beads were obtained from Clontech Laboratories (Mountain View, CA). DNA purification kits were purchased from Qiagen (Valencia, CA) and Zymo Research (Irvine, CA).

Precision Plus Protein™ standards, Clarity™ ECL western blotting substrate and 4-15% Mini-Protean TGX Precast gels were purchased from Bio-Rad Laboratories (Hercules, CA). Protein A-Sepharose beads were obtained from GE Healthcare (Waukesha, WI). Protease inhibitors and Endoglycosidase H were purchased from Roche Applied Science (Indianapolis, IN). The anti-polySia 12F8 rat monoclonal IgM antibody was purchased from BD Biosciences (San Jose, CA). HRP conjugated anti-human IgG (H+L) was purchased from Promega (Madison, WI). Myc-tag (9B11) mouse mAb (IgG2a detecting N- or C- terminal myc tag) magnetic bead conjugates and rabbit polyclonal anti-myc antibody were purchased from Cell Signaling Technology (Danvers, MA). Anti-polySia 735 monoclonal IgG2a was purchased from Absolute Antibody Limited (Oxon, United Kingdom). Horseradish peroxidase (HRP)- and fluorescein isothiocyanate (FITC)-conjugated secondary antibodies were purchased from Jackson ImmunoResearch (West Grove, PA). Nitrocellulose membranes were obtained from Schleicher & Schuell BioScience GmbH (Dassel, Germany) and GE Healthcare. HyBlot CL® Autoradiography film was obtained from Denville Scientific (Denville, NJ).

Isopropyl β-D-1-thiogalactopyranoside (IPTG) and 2-(N-morpholino)ethanesulfonic acid (MES) were acquired from Gold Biotechnology (Olivette, MO). [^{13}C] Glucose and [^{15}N] ammonium chloride were obtained from Cambridge Isotope Laboratories (Tewksbury, MA). All other chemicals and reagents were purchased from Sigma, Fisher Scientific or VWR Scientific (Buffalo Grove, IL).

Experimental Methods

Construction of NRP-2 ΔCF and NRP-2 ΔLCF Proteins

In the pcDNA3.1/V5-His B vector, the NRP-2 cDNA sequence is flanked by HindIII and XbaI restriction sites. For the construction of the NRP-2 ΔCF construct, a unique KpnI restriction site was introduced after Cys^{592} at the beginning of the NRP-2 linker region using primer set 1 (Table 1). The NRP- 2 ΔCF portion was excised using restriction enzymes KpnI and XbaI and ligated into pcDNA3.1/V5-His B vector at these sites. To insert the signal sequence, the first 22 amino acids of NRP-2 were amplified to include a HindIII site at the N terminus and a KpnI site at the C terminus using primer set 2 (Table 1), and the amplified fragment was ligated into the pcDNA3.1 NRP-2 ΔCF vector between the HindIII and KpnI sites. For the construction of the NRP-2 ΔLCF construct, NRP-2 sequences from the MAM domain to the cytoplasmic tail were amplified with a KpnI site on the N terminus and a XbaI site on the C terminus using primer set 3 (Table 1). The pcDNA3.1 NRP-2 ΔCF vector with the inserted signal sequence was then digested with KpnI and XbaI, and the amplified NRP-2 ΔCF sequence was inserted between the signal sequence and the V5 tag.

Construction of V5-tagged NRP-1 and NRP-2 MAM Domain Swap Chimeras

To create the NRP-1 and NRP-2 chimeric proteins with their MAM domains swapped (NRP-2Δ1 and NRP-1Δ2), the NRP-2 and NRP-1 MAM domains were flanked with a unique EcoRV restriction site on the N terminus and unique NheI restriction site on the C- terminus, which were inserted by site-directed mutagenesis using primer sets 4–7, respectively. The individual domains were extracted by restriction enzyme digestion. The NRP-1 MAM domain was inserted between newly engineered EcoRV and NheI

sites in the NRP-2 cDNA to obtain the NRP-2Δ1 construct, whereas the NRP-2 MAM domain was inserted between engineered EcoRV and NheI sites in the NRP-1 cDNA to obtain the NRP-1Δ2 construct. The EcoRV and NheI restriction sites flanking the MAM domains were removed from both the chimeric mutants using primer sets 8 –11 by site-directed mutagenesis. During the removal of the restriction sites from NRP-2Δ1, a single nucleotide change at amino acid Glu^{622} introduced a stop codon, which was removed by site-directed mutagenesis using primer set 12.

Construction of Fc-tagged NRP-1, NRP-2, and Their Chimeras

I constructed NRP-1-Fc, NRP-1Δ2-Fc, and NRP-2Δ1-Fc in pcDNA4-NRP2-hFc vector. Extracellular portions of NRP-1 and the NRP-2Δ1 and NRP-1Δ2 chimeras were amplified from the full-length constructs to include a 15-bp overhang complementary to both the pcDNA4 vector on the N terminus and the human antibody Fc sequence on the C terminus using primer set 13 for NRP-1 and NRP-1Δ2 and primer set 14 for NRP-2Δ1 (Table 1). The In-Fusion homology-directed cloning kit was used according to the manufacturer's protocol to construct the Fc-tagged proteins. Briefly, the pcDNA4-hFc vector was amplified using primer set 15. The amplified vector and insert fragments were mixed. A splice consensus sequence was inserted between the NRP sequences and Fc sequence, which contains introns, to ensure splicing within the Fc portion. This sequence, ACAGGTAAGT, was inserted by site-directed mutagenesis using primer set 16 for NRP-2-Fc and NRP-2Δ1-Fc constructs and primer set 17 for the NRP-1 and NRP-1Δ2-Fc constructs.

Construction of Fc-tagged NRP-1 and NRP-2 Linker MAM (LM) Domain Chimeric Proteins

NRP-2ΔLM1 and NRP-1ΔLM2 constructs were initially made as full-length, V5-tagged constructs in pcDNA3.1/V5-His B vector. For the NRP-2ΔLM1 construct, NRP1 sequences from the linker through the cytoplasmic tail were amplified with primer set 18, which includes 15-bp overhangs complementary to the NRP2 coagulation factor 5/8 homology (F5/8)-2 region on the N terminus and to the pcDNA3.1/V5-His B, including the V5 tag, on the C terminus. For the NRP-1ΔLM2 construct, NRP2 sequences from the

linker through the cytoplasmic tail were amplified with primer set 19, which includes 15-bp overhangs complementary to the NRP1 F5/8-2 region on the N terminus and to the pcDNA3.1/V5-His B, including the V5 tag, on the C terminus. The In-Fusion homology-directed cloning kit was used according to the manufacturer's protocol to construct the chimeric proteins. The pcDNA3.1/V5-His B vector containing NRP2 sequences was amplified using primer set 20, and the same vector containing NRP1 sequences was amplified using primer set 21. An extra cytosine base was erroneously introduced during construction of the NRP-1ΔLM2 construct and was deleted by site-directed mutagenesis using primer set 22. For Fc-tagged NRP-2ΔLM1 and NRP- 1ΔLM2 constructs, ectodomains of these chimeras were amplified using primer set 23 for NRP-2ΔLM1 and primer set 24 for NRP-1ΔLM2. These primers inserted splice consensus sequence in one step and included 15-bp complementary sequences on both sides for the pcDNA4-hFc vector. The amplified pcDNA4-hFc vector, generated as described above, was then mixed with the above fragments, and the In- Fusion protocol was followed using the manufacturer's guidelines.

Construction of NRP-2 ΔMAM-Fc Construct

To remove the MAM domain from the pcDNA4-NRP-2-Fc construct, we amplified vector and NRP sequences from the Fc portion to the NRP-2 linker region and in this way eliminated the MAM sequences, using primer set 25. A primer with sequences complementary to those of the NRP-2 linker region and with a 15-bp overhang complementary to the Fc portion was used to amplify a linear fragment that was then used to regenerate the circular plasmid by homologous recombination.

Construction of SynCAM-1-Fc construct

Extracellular portion of SynCAM 1 was amplified with primers that included 15 bp overhang on each side with sequence corresponding to the pcDNA4 vector on the N-terminus and Fc fragment on the C-terminus (Table X). pcDNA4-Fc vector was amplified separately using primers indicated in Table X. The PCR amplified products were mixed and homologous recombination was carried out to create pcDNA4-SynCAM 1-Fc construct using Clontech In-Fusion HD cloning kit, according to the manufacturer's

protocol.

Construction of the 6xHis-SUMO-PBR Bacterial Expression Construct.

ST8Sia-IV residues 75−100 were amplified with the NdeI restriction site at the N-terminus and the BamHI restriction site at the C-terminus using primers 5′- CATATGTCCTCTTTGGTCCTAGAG-3′ and 5′-AAGAAT- CGCAGGTTTAAGTAGGGATCCGGCT-3′, respectively. Amplified ST8Sia-IV sequences and the vector mentioned above were digested with NdeI and BamHI restriction endonucleases and purified on an agarose gel. The insert was then ligated into the vector using T4 DNA ligase generating the 6xHis-SUMO-PBR plasmid.

Mutagenesis of various enzyme and substrate constructs

Mutagenesis reactions were carried out using the Stratagene QuikChange™ site-directed mutagenesis kit using 30 ng of the template cDNA and according to the manufacturer's protocol using primers described in Table X. Isolated clones were sequenced by the DNA Sequencing Facility of the Research Resources Center at the University of Illinois (Chicago, IL) and confirmed on SnapGene Viewer version 2.7.2 software (GSL Biotech, Chicago, IL) for accuracy.

Transfection of COS-1 Cells for Immunofluorescence Localization

COS-1 cells were maintained in DMEM with 10% FBS and 1% penicillin/streptomycin and grown in a 37 °C, 5% CO_2 incubator. They were plated on 12-mm glass coverslips in 24-well plates and incubated overnight at 37 °C. At 50–70% confluence, cells in each well were then transfected with 500 ng of NRP-1, NRP-2, chimeric protein, or deletion mutant cDNAs as well as ST8Sia-II and ST8Sia-IV mutants and 3 μl of Lipofectin in 300 ml of Opti-MEM I and incubated at 37 °C for 6 h, according to the manufacturer's protocol. After 6 h, 1 ml of DMEM, 10% FBS, 1% penicillin/streptomycin was added to each well and was kept for further incubation at 37 °C in 5% CO_2 for 20 h. COS-7 cells plated on 12 mm glass coverslips in 24-well plates were transfected at 80−90% confluence with 500 ng of V5-tagged NCAM or NCAM mutant protein expression vectors mixed with 1 μL of Lipofectamine 2000 and 150 μL of Opti-

MEM I medium per well. One milliliter of DMEM containing 10% FBS was added to each well and incubated for 24 h.

Analysis of NRP-1, NRP-2, and Chimeric Protein Localization by Indirect Immunofluorescence Microscopy

After 20 h post-transfection, COS-1 cells expressing NRP proteins were washed twice with 1 ml of phosphate-buffered saline (PBS). Cells were fixed and permeabilized with 1 ml of ice-cold methanol. Cells were again washed twice with PBS and blocked for 1 h at room temperature in 1 ml of blocking buffer (5% normal goat serum in PBS). Cells were then incubated with a 1:250 dilution of anti-V5 epitope tag antibody in blocking buffer for 2 h and then washed twice for 5 min with PBS. The cells were then incubated with a 1:100 dilution of FITC-conjugated goat anti-mouse IgG secondary antibody in blocking buffer for 45 min and washed twice with PBS for 5 min. Next, the cells were incubated with a 1:2000 dilution of DAPI in blocking buffer for 5 min in the dark and then washed twice with PBS for 5 min. After washing, coverslips were then rinsed in deionized H_2O and mounted on glass microscope slides using 20 μl of mounting medium (15% (w/v) Vinol 205 polyvinyl alcohol, 33% (w/v) glycerol, 0.1% sodium azide in PBS, pH 8.5). Cells were visualized and imaged with a Zeiss LSM 700 inverted confocal micro- scope, equipped with an AxioCam digital microscope camera using a 100X oil immersion objective at room temperature. Images were acquired using Zen software by Zeiss and processed with ImageJ software (National Institutes of Health).

Transfection of COS Cells for Immunoprecipitation and Immunoblotting

For experiments involving NRP-2, its mutants, NRP-1, and chimeric proteins, COS-1 cells or COS-7 cells were maintained in DMEM with 10% FBS and 1% penicillin/streptomycin and grown on 100-mm tissue culture plates in a 37 °C, 5% CO_2 incubator. At 80 –90% confluence, cells were transfected using 3 μg of V5- or Fc-tagged NRP cDNA and ST8Sia-IV-Myc cDNA (cloning of ST8Sia-IV cDNA into the pcDNA3.1 Myc/HisB expression was described previously (199)) and 30:l ratio of Lipofectin in 3 ml of Opti-MEM I and incubated at 37°C in a 5% CO_2 incubator, according to the manufacturer's protocol.

After a 6 h incubation, 7 ml of DMEM, 10% FBS, 1% penicillin/streptomycin was added to each plate and incubated for an additional 18 –24 h.

For experiments involving NCAM and its mutants, COS-7 cells were maintained in DMEM supplemented with 10% FBS and 1% penicillin- streptomycin in a 37 °C, 5% CO_2 incubator. Cells plated in 100 mm tissue culture plates were transfected at 80−90% confluence the next day with 5 μg each of V5-tagged NCAM and ST8Sia-IV cDNAs in 3 mL of Opti-MEM medium using 20 μL of Lipofectamine 2000 per plate, according to the manufacturer's protocol. Shortly after the addition of the DNA complexes to the cells, 7 mL of DMEM supplemented with 10% FBS was added to the cells and cells were incubated for 24 h at 37 °C and 5% CO_2.

For the experiments evaluating polysialylation of NCAM, NRP-2, SynCAM 1 by ST8Sia-II and ST8Sia-IV mutants, COS-1 cells maintained in DMEM, supplemented with 10% FBS, were plated onto 60-mm tissue culture plates and grown in a 37^{o}C, 5% CO_2 incubator until 70-80% confluent. Cells were co-transfected with 3 μg of substrate cDNA and 3 μg of wild-type or mutant polyST cDNA, using constructs shown in Table X, in 1 ml OPTI-MEM I containing 6 μl of Lipofectamine 2000 transfection reagent per tube. For autopolysialylation experiments, 6 μg of myc-tagged ST8Sia-II or ST8Sia-IV were transfected in COS-1 cells as described above.

Table 4: Vector combinations used for substrate/ polyST co-expression

Substrate construct	**Enzyme construct**
pcDNA3.1-NCAM-V5	pcDNA3.1-ST8Sia-IV-myc
pcDNA3.1-NRP-2-V5	pcDNA3.1-ST8Sia-IV-myc
pcDNA4-NCAM-Fc	pCAG-ST8Sia-II-V5
pcDNA4-SynCAM-Fc	pCAG-ST8Sia-II-V5

Cells were incubated with the transfection mixture and 3 ml of DMEM supplemented with 10% FBS was added and the cells were allowed to grow overnight in a 37^{o}C, 5% CO_2 incubator for 24 h.

Triple Transfection of COS-1 Cells with Wild-type PolyST, a Mutant PolyST, and a Substrate for competition experiments

COS-1 cells maintained in DMEM, supplemented with 10% FBS, were plated onto 60-mm tissue culture plates and grown in a 37^{o}C, 5% CO_2 incubator until 70-80% confluent. Cells were then transfected with 750 ng of V5-tagged substrate cDNA (NCAM, SynCAM 1 or NRP-2), 750 ng untagged ST8Sia-II or ST8Sia-IV cDNA, and 4.5 μg of a Myc-tagged polyST mutant cDNA (ST8Sia-IV H331K, ST8Sia-II H346K, ST8Sia-IV H331K PBR mutant, or ST8Sia-II H346K PBR mutant in pcDNA3.1 vector) in 1 ml OPTI-MEM I containing 12 μl of Lipofectamine 2000 transfection reagent. Three mL of DMEM supplemented with 10% FBS was added shortly after the addition of complexes to the cells. The cells were then grown overnight as described above.

Immunoprecipitation of V5-tagged NRP Proteins, Chimeras, and NCAM proteins

Twenty-four hours post-transfection, the cells were washed with PBS and lysed in 500 μl of immunoprecipitation buffer (50 mM Tris-HCl, pH 7.5, 150 mM NaCl, 5 mM EDTA, 0.5% Nonidet P-40, 0.1% SDS). The cells cultured in 60-mm plates were lysed in 200 μL of immunoprecipitation buffer. A 10% aliquot of the lysate was reserved and boiled (100 °C) with Laemmli sample buffer (62.5 mM Tris-HCl, pH 6.8, 25% glycerol, 2% SDS, 0.01% bromophenol blue) containing 10% β-mercaptoethanol to remove polySia and assess the relative expression of these proteins. The remaining lysate was precleared with 50 μl of protein A-Sepharose beads (50% suspension in PBS) for 1 h at 4 °C, and NRP proteins were immunoprecipitated with 2 μl (1 μl for 200 μl lysates) of anti-V5 or anti-myc epitope tag antibody overnight at 4 °C with rotation. Samples were then rotated with 50 μl of protein A-Sepharose beads for 1 h and washed four times with immunoprecipitation buffer. Samples were then resuspended in 50 μl of Laemmli sample buffer containing 10% β-mercaptoethanol, heated at 65 °C (to retain polySia) for 8 min,

and separated on a 4–15% precast polyacrylamide gel (Bio-Rad) at 110 V for 1-2 h.

Immunoprecipitation of Fc-tagged NRP Proteins

Medium containing secreted Fc-tagged proteins was harvested 22–24 h post-transfection and incubated with an 80 μl (50 μl for cells cultured in 60-mm plates) slurry of 50% protein A-Sepharose beads overnight at 4 °C. The medium was discarded, and the beads were washed four times with the immunoprecipitation buffer. Forty percent of the beads were heated to 100 °C with 32 μl (20 μl for cells cultured in 60-mm plates) of Laemmli sample buffer containing 10% β-mercaptoethanol to remove polySia and assess relative protein expression. The remaining beads were heated with 48 μl (30 μl for cells cultured in 60-mm plates) of Laemmli sample buffer containing 10% β-mercaptoethanol at 65°C for 8 min, and proteins were separated as described above.

PNGase F Treatment of Immunoprecipitated Proteins and Proteins in Cell Lysates

To remove *N*-glycans from immunoprecipitated proteins, protein A-Sepharose beads bound to the anti-V5 antibody and NRP-2 proteins were incubated with 1500 units of PNGase F in G7 buffer (New England Biolabs), 0.5% Nonidet P-40 for 3 h at 37 °C. For PNGase F treatment of cell lysates, 100 μl of cell lysate was incubated with 1500 units of PNGase F in G7 buffer, 0.5% Nonidet P-40 at 37 °C overnight.

Endoglycosidase H Treatment of Proteins in Cell Lysates

Endoglycosidase H (EndoH) digestion is used to assess whether proteins contained high-mannose N-glycans, which is a characteristic of proteins retained in the ER, that are likely misfolded. For these digesions, 100 μL of the cell lysate in immunoprecipitation buffer was mixed with 98 μL of reaction buffer (100 mM sodium citrate, pH 6, 0.075% SDS, 0.2% β-mercaptoethanol) and 0.01 units of EndoH overnight at 37 °C, as described in (137).

Immunoblot Analysis of the Expression and Polysialylation

Following SDS-PAGE, proteins were transferred to a nitrocellulose membrane at 100 V for 1 h at 4 °C.

Membranes were blocked for 1 h at room temperature in blocking buffer (5% nonfat dry milk in Tris-buffered saline, 50 mM Tris-HCl, pH 8.0, 150 mM NaCl, and 0.1% Tween 20 (TBST)). To evaluate protein polysialylation, membranes were incubated overnight at 4 °C with anti-polySia 12F8 antibody in 2% nonfat dry milk in Tris-buffered saline, pH 8.0 with dilutions indicated in Table X. After four 10-min washes, these membranes were incubated for 1 h at 4 °C with HRP- conjugated goat secondary antibodies, diluted 1:5000 in blocking buffer (Table X). The specificity of the commercially available 12F8 anti-polySia or anti-polySia 735 antibodies was confirmed by the disappearance of the immunoblot signal using endoneuraminidase N, a sialidase specific for polySia (data not shown).

To evaluate protein expression levels, membranes were incubated overnight at 4 °C with primary antibodies in blocking buffer, washed four times with TBST, for 10 min each, and then incubated for 1 h at 4 °C in 1:5000 diluted HRP-conjugated goat secondary antibodies in blocking buffer. To evaluate the expression of Fc-tagged proteins, the membranes were blocked in blocking buffer overnight and were incubated with the HRP-conjugated anti-human IgG (1:5000) in high salt TBST (500 mM NaCl, 150 mM Tris-HCl, pH 8.0, and 0.1% Tween 20) for 45 min. All membranes were washed with high salt TBST four times, each for 10 min. Immunoblots were then developed using the SuperSignal West Pico chemiluminescence kit and HyBlot CL autoradiography film. To quantify changes in polysialylation between substrates, we used ImageJ software and compared the ratio of polysialylated to loading control for each protein with the value for wild type NRP-2 set to 100%. Mean and S.D. were calculated.

Table 5: Antibodies used for immunoblotting.

Antibody	Dilution used	Blocking buffer	Secondary antibody
Anti-polySia 12F8	1:2000 for NCAM 1:1500 for NRP-2 1:500 for SynCAM 1	2% milk in TBS	Goat anti-rat IgM
Anti-polySia 735	1:1500	5% milk in TBST	Goat anti-mouse IgG
Anti-V5 mAb	1:10000	5% milk in TBST	Goat anti-mouse IgG
Anti-myc mAb	1:5000	5% milk in TBST	Goat anti-mouse IgG
Anti-myc pAb	1:1000	5% BSA in TBST	Goat anti-rabbit IgG

Pull-down Experiments to Assess NRP-2-ST8Sia-IV Binding

ST8Sia-IV-Myc and NRP-2-Fc or NRP-2 ΔMAM-Fc proteins were expressed individually in COS-7 cells using Lipofectin transfection reagent, as described above. For NRP-2-Fc- and NRP-2 ΔMAM-Fc-expressing cells, 7 ml of serum-free Bio-Whittaker™ medium was added after 6 h of transfection, and incubation was continued overnight in a 37 °C, 5% CO_2 incubator. ST8SiaIV-expressing cells were lysed in 500 l of immunoprecipitation buffer, and lysates from two 100-mm plates were combined. Lysates were then rotated overnight with anti-Myc magnetic beads at 4 °C. Medium containing NRP-2-Fc or NRP-2 ΔMAM-Fc was harvested 24 h post-transfection. A 1 ml aliquot of medium was rotated with protein A-Sepharose beads overnight at 4 °C to recover secreted proteins and assess their relative secretion/expression. These beads were washed four times with immunoprecipitation buffer and then boiled in Laemmli sample buffer containing 10% β-mercaptoethanol for 7 min prior to SDS-PAGE. To assess binding of the polyST to the NRP2 proteins, ST8Sia-IV-loaded magnetic beads were then washed with co-immunoprcipitation buffer (50 mM HEPES, 100 mM NaCl, 1% Triton X-100, pH 7.2) and were added to the serum-free medium containing NRP-2-Fc or NRP-2 ΔMAM- Fc. As a control, anti-Myc

magnetic beads were added to the medium containing NRP-2-Fc or NRP-2 ΔMAM-Fc to assess nonspecific binding. After 2 h of rotation at 4 °C, the beads were washed four times with the co-immunoprecipitation buffer. All of the samples were resuspended in Laemmli sample buffer containing 10% β-mercaptoethanol and boiled for 7 min. Proteins were separated by SDS-PAGE, and immunoblotting was performed as described above. To quantify changes in binding between NRP-2-Fc and NRP-2 ΔMAM-Fc, we used ImageJ software and compared the ratio of bound protein to secreted protein for the NRP-2 ΔMAM-Fc mutant *versus* wild-type NRP-2-Fc (normalized to 100%). Mean and S.D. were calculated.

Expression and Purification of the 6xHis-FN1, 6xHis- SUMO, and 6xHis-SUMO-PBR Proteins.

6xHis-FN1 was purified as previously described (194). Briefly, BL21(DE3) CodonPlus Escherichia coli cells expressing 6xHis-FN1 were grown in 2xYT medium at 37 °C. The culture was then induced with 1 mM IPTG at an optical density (λ = 600 nm) of 0.6−0.8 and maintained overnight at 22 °C. For isotopically labeled 6xHis-FN1, cells were grown in M9 minimal medium containing 1 g of [^{15}N] ammonium chloride and/or 5 g of [^{13}C] glucose per liter. The cells were harvested by centrifugation and lysed using Avestin Emulsiflex C5. The cleared supernatant was passed over the Ni-NTA column to bind the His-tagged protein. The column was washed with a buffer consisting of 50 mM Tris-HCl (pH 8.0), 500 mM NaCl, and 50 mM imidazole. The protein was eluted in the same buffer containing 500 mM imidazole. The protein was then dialyzed in the same buffer without the imidazole overnight at 4 °C for the ITC experiments and in a buffer containing 300 mM NaCl and 20 mM KH_2PO_4 (pH 6.6) for the NMR experiments. To obtain 6xHis-SUMO and 6xHis-SUMO-PBR, BL21(DE3) C41 E. coli cells expressing this construct were grown in 2xYT medium at 37 °C to an optical density (λ = 600 nm) of 0.8−1.0 and induced with 1 mM IPTG. The growth was continued at 37 °C for 4 h, and cells were harvested thereafter. The 6xHis- SUMO-PBR peptide was purified as described above.

Isothermal Titration Calorimetry.

Purified 6xHis-FN1, its (DEE → RRR) mutant, 6xHis-SUMO, 6xHis-SUMO-PBR, and its (R82A/R93A) mutant were dialyzed overnight at 4 °C in a buffer containing 500 mM NaCl and 50 mM Tris (pH 8). FN1 and its mutant were prepared at a concentration of 20 μM, and the PBR peptide and its mutant were concentrated to 600 μM. All the experiments were performed at 25 °C using a VP-ITC calorimeter (GE Healthcare). The final thermodynamic parameters were calculated using Origin software (GE Healthcare) using a one-site model.

NMR Spectroscopy.

$^{1}H-^{15}N$ HSQC, HNCA, HNCO, HN(CA)CO, HN(CO)CA, HNCACB, and CBCACONH spectra for FN1 backbone assignments were recorded at 25 °C on a Bruker 600 MHz DRX spectrometer equipped with a 5 mm inverse cryogenic probe. NMR spectra for HSQC titrations were recorded on a Bruker 900 MHz AVANCE spectrometer equipped with a 5 mm TCI cryogenic probe. Samples for all the NMR experiments were in a buffer containing 300 mM NaCl and 20 mM KH_2PO_4 (pH 6.6), supplemented with 10% D_2O. Backbone dihedral angles and the secondary structure of FN1 were predicted using Talos+ (201). All NMR data were processed using NMRPipe (202) and analyzed using UCSF Sparky. HSQC titrations were recorded in a 5 mm NMR tube at 1:0 (8 scans), 1:5 (32 scans), and 1:10 (64 scans) ratios of FN1 to 6xHis- SUMO-PBR and its mutant (R82A/R93A).

Circular Dichroism Spectroscopy.

Purified FN1 was prepared at a concentration of 75 μg/mL in 300 mM NaF and 20 mM KHPO (pH 6.5), and its CD spectrum was recorded in a 0.1 cm path-length cuvette on a Jasco-815 spectropolarimeter from a wavelength of 190−260 nm. The ellipticity per residue in degrees square centimeter per decimole was plotted against the wavelength to compare the secondary structures of FN1 to that of its DEE to RRR mutant.

Gel Filtration.

The 6xHis-SUMO-PBR and 6xHis-SUMO- PBR (R82A/R93A) mutant were purified and concentrated at 5 mg/mL in a buffer containing 20 mM Tris-HCl (pH 8) and 500 mM NaCl and injected into an AKTA protein purification system (GE Healthcare) connected to a Superdex 75 10/300 GL size exclusion chromatography column (GE Healthcare).

Primers used in chapter III:

Primer set	Mutant	Template	Primer Sequence
1	Isolating PBR region with NdeI on the N-terminus and BamHI on the C-terminus	ST8Sia-IV	5'- GGTCATATGTCCT-CTTTGGTCCTAGAG- 3'
			5'- AAGAATCGCAGGTTTAA-GTAGGGATCCGGCT- 3'
2	SUMO-PBR R82A	SUMO-PBR	5'-CCTCTTTGGTCCTAGAGAT-AGCGAAGAACATACTTCGTTTC-3'
			5'-GAAACGAAGTATGTTCTTCGC-TATCTCTAGGACCAAAGAGG- 3'
3	SUMO-PBR R93A	SUMO-PBR	5'-CGTTTCTTAGATGCAGAAGC-AGATGTGTCAGTGGTCAAG- 3'
			5'-CTTGACCACTGACACATCT-GCTTCTGCATCTAAGAAACG- 3'
4	$D^{520}E^{521}E^{523}$ to RRR	NCAM FN1	5'–TACTCCAGCACAGCCCAGG-TGCGTTTCGTCGCCCACGTGCCA CAGGT– 3'
			5'– ACCTGTGGCACGTGGGCGAC-GAAACTGCACCTGGGCTGTGCTG GAGTA- 3'
5	D506R	NCAM	5' –CTCTTCACCATCCATC-CGCCAGGTGGAGCCATAC– 3'
			5' – GTATGGCTCCACCTG-GCGGATGGATGGTGAAGAG– 3'
6	D520R	NCAM	5' – GCACAGCCCAGGTGCAGT-TTCGTGAACCAGAGG– 3'
			5' – CCTCTGGTTCACGAAA-

			CTGCACCTGGGCTGTGC– 3’
7	E521R	NCAM	5’ – CACAGCCCAGGTGCAGTTT-GATAGACCAGAGGCCAC– 3’
			5’ –GTGGCCTCTGGTCTAT-CAAACTGCACCTGGGCTGTG– 3’
8	E523R	NCAM	5’-CCCAGGTGCAGTTTGATG-AACCAAGGGCCACAGGTGG- 3’
			5’-CCACCTGTGGCCCTTGG-TTCATCAAACTGCACCTGGG- 3’
9	D498R	NCAM	5’-GATGGTGAAGAGGGGGTG-CGTGCTTGAACAAGGATGAA- 3’
			5’-GGAATGCCATACTTCTTCACC-AACGAATCTCCACTCAGCTTTGT ATTTGAG- 3’
10	T499A	NCAM	5’-CCTTGTTCAAGCAGAC-GCCCCCTCTTCACCATC- 3’
			5’-GATGGTGAAGAGGGGG-CGTCTGCTTGAACAAGG- 3’
11	A539S	NCAM	5’ – ATACAAAGCTGAGTGGAGA-TCAGTTGGTGAAGAAGTATG– 3’
			5’ – CATACTTCTTCACCAACT-GATCTCCACTCAGCTTTGTAT– 3’
12	A539F	NCAM	5’ – CTCAAATACAAAGCTGAGTG-GAGATTCGTTGGTGAAGAAGTAT GGCATTCC– 3’
			5’ – GGAATGCCATACTTCTTCAC-CAACGAATCTCCACTCAGCTTTG TATTTGAG– 3’
13	E543R	NCAM	5’ – ACTTGGAATGCCATACTCTT-TCACCAACTGCTCTCCACTC– 3’
			5’ – GAGTGGAGAGCAGTTGGTG-AAAGAGTATGGCATTCCAAG– 3’
14	W545A	NCAM	5’ – GAGAGCAGTTGGTGAAGAA-GTAGCGCATTCCAAGTGGTATG– 3’
			5’ – CATACCACTTGGAATGCGCT-ACTTCTTCACCAACTGCTCTC– 3’
15	W545Y	NCAM	5’ – GGCATCATACCACTTGGAAT-GATATACTTCTTCACCAACTGCT C– 3’
			5’ – GAGCAGTTGGTGAAGAAG-TATATCATTCCAAGTGGTATGAT GCC– 3’
16	S547A	NCAM	5’ – GCATCATACCACTTGGCA-TGCCATACTTCTTCACCA– 3’

			5’ – TGGTGAAGAAGTATGGCA-TGCCAAGTGGTATGATGC– 3’

Primers used in chapter IV:

No	Mutant	Template	Primer Sequence
17	NRP-2 KpnI insertion after Cys^{592}	NRP-2	5’-GAGGTGCTGGGCTGTGGTAC-CATGGACTGGACAGACTCC-3’
			5’-GGAGTCTGTCCAGTCCATG-GTACCACAGCCCAGCACCTC-3’
18	NRP-2 signal sequence amplification including HindIII and KpnI sites	NRP-2	5’-GTTAAGCTTATGGATAT-GTTTCCTCTCACCTGGG-3’
			5’-AATGGTACCGCCTCTCAC-TTGGTGTCTTGA-3’
19	MAM domain amplification with KpnI and XbaI sites	NRP-2	5’-CGGGGTACCTCGGG-ATTCAATTGCAACTTC-3’
			5’-CCTTCTAGAGCTGCCTC-GGAGCAGCACTTT-3’
20	NRP-2 EcoRV insertion between Pro^{641} & Ser^{642}	NRP-2	5’ – GCAGCTCCCTGAT-ATCTCGGGATTCAATTG – 3’
			5’ – CGTCGAGGGACTA-TAGAGCCCTAAGTTAAC – 3’
21	Nrp-2 NheI insertion between Glu^{802} & Pro^{803}	Nrp-2	5’ – GAACTGCATGGAAGCTA-GCCCCATCTCGGC – 3’
			5’ – CTTGACGTACCTTCG-ATCGGGGTAGAGCCG – 3’
22	Nrp-1 EcoRV insertion between Pro^{644} & Thr^{645}	Nrp-1	5’ – CAATCAGAGTTTCCAG-ATATCACATATGGTTTTAAC – 3’
			5’ – GTTAGTCTCAAAGGTCT-ATAGTGTATACCAAAATTG – 3’
23	Nrp-1 NheI insertion between Lys^{811} & Pro^{812}	Nrp-1	5’ – GAAGATTGTGCAAAAGC-TAGCCCAGCAGACCTG – 3’

			5’ – CTTCTAACACGTTTTC-GATCGGGTCGTCTGGAC – 3’
24	NRP-1Δ2 Remove EcoRV	NRP-1Δ2 + Restriction sites	5’ – CAATCAGAGTTTCCAT-CGGGATTCAATTG – 3’
			5’ – GTTAGTCTCAAAGG-TAGCCCTAAGTTAAC – 3’
25	NRP-1Δ2 Remove NheI	NRP-1Δ2 + Restriction sites	5’ – GAACTGCATGGAAC-CAGCAGACCTG – 3’
			5’ – CTTGACGTACCTTG-GTCGTCTGGAC – 3’
26	NRP-2Δ1 Remove EcoRV	NRP-2Δ1 + Restriction sites	5’ – GCAGCTCCCTAC-ATATGGTTTTAAC – 3’
			5’ – CGTCGAGGGATGT-ATACCAAAATTG – 3’
27	NRP-2Δ1 Remove NheI	NRP-2Δ1 + Restriction sites	5’ – GAAGATTGTGCAAAA-CCCATCTGCGC – 3’
			5’ – CTTCTAACACGTT-TTGGGTAGACGCG – 3’
28	NRP-2Δ1 (to remove stop codon inserted during MAM swap @ Glu^{622})	NRP-2Δ1	5’ – CCACCGAAGAGGAG-GCCACAGAGTG – 3’
			5’ – GGTGGCTTCTCC-TCCGGTGTCTCAC – 3’
29	Amplification of ectodomains to make NRP-Fc constructs	NRP-1 and NRP1Δ2	5’-AGACCCAAGCTGGCCATGGAGAG-GGGGCTGCCGCTCCTC-3’
			5’-AGACACCCTCCCTC-CGGGGTCTAAGGTCTTCAACACATT-3’
30	Amplification of	NRP-2Δ1	5’- GAGACCCAAGCTGGCCATG-

	ectodomains to make NRP-Fc constructs		GATATGTTTCCTCTCACCTGG-3’
			5’-AGACACCCTCCCTCCGGGATC-CAGGGTGTACAGCCAGCTC-3’
31	Amplification of pcDNA4-hFc vector for In-Fusion	pcDNA4-NRP-2-hFc	5’-GCTCTAGAGGGCCCG-CGGTTCGAAGGTA-3’
			5’-AGTCTAGAGG-GCCCGCGGTTC-3’
32	Insertion of splice consensus sequence	NRP-2-Fc & NRP-2Δ1-Fc	5’-CACCCTGGATCCCACAGG-TAAGTGGAGGGAGGGTGT-3’
			5’-ACACCCTCCCTCCACTTA-CCTGTGGGATCCAGGGTG-3’
33	Insertion of splice consensus sequence	NRP-1-Fc & NRP-1Δ2-Fc	5’-AGACCTTAGACCCCACAG-GTAAGTGGAGGGAGGGTGTC-3’
			5’-GACACCCTCCCTCCAC-TTACCTGTGGGGTCTAAGGTCT-3’
34	Amplification of NRP-1 linker region through the cytoplasmic tail for NRP-2ΔLM1 construct	NRP-1	5’-GAGGTGCTGGGCTGTGAAGT-GGAAGCCCCTACAGCTGGA-3’
			5’-CGGGCCCTCTAGAGCTGC-CTCCGAATAAGTACTCTGTG-3’
35	Amplification of NRP-2 linker region through the cytoplasmic tail for NRP-1ΔLM2 construct	NRP-2	5’-GAGCTGCTGGGCTGTGACT-GGACAGACTCCAAGCCCACG-3’
			5’- CGGGCCCTCTAGAGCTGCC-TCGGAGCAGCACTTTTGGT-3’.
36	Amplification of NRP-2 sequences except the linker region through the cytoplasmic tail sequences in pcDNA3.1/V5-His B vector	NRP-2	5’-ACAGCCCAGCACC-TCCAGCCGCATCCCA-3’
			5’-GCTCTAGAGGGCCC-GCGGTTCGAAGGTA-3’
37	Amplification of NRP-1 sequences except the linker region through the cytoplasmic tail in pcDNA3.1/V5-His B vector	NRP-1	5’-ACAGCCCAGCAGCT-CCATTCT-GAGCCCCA-3’
			5’-GCTCTAGAGGGCCC-GCGGTTCGAAGGTA-3’

38	Deletion of extra cytosine base erroneously introduced	NRP-1ΔLM2	5'-GACAACCACCCCCT-ACCCCACCGAAG-3'
			5'-CTTCGGTGGGGTAG-GGGGTGGTTGTC-3'
39	Amplification of ectodomains to make NRP-Fc constructs	NRP-2ΔLM1	5'- GAGACCCAAGCTGGCCAT-GGATATGTTTCCTCTCACCTGG-3'
			5'-GACACCCTCCCTCCACTTA-CCTGTGGGGTCTAAGGTCT-3'
40	Amplification of ectodomains to make NRP-Fc constructs	NRP-1ΔLM2	5'-AGACCCAAGCTGGCCATG-GAGAGGGGGCTGCCGCTCCTC-3'
			5'-ACACCCTCCCTCCAC-TTACCTGTGGGATCCAGGGTG-3'
41	Inverse PCR of NRP-2-Fc to eliminate MAM domain	NRP-2-Fc	5'-CCTCCACTTACCTGTAGGGAG-CTGCAAATCTTTGTCATCCTCA-3'
			5'-GGAGGGAGGGTG-TCTGCTGGAA-3'
42	NRP-2 E652A	NRP-2-Fc	5' – CTTCGATTTCCTCG-CGGAGCCCTGTGG – 3'
			5' – GAAGCTAAAGGAG-CGCCTCGGGACACC – 3'
43	NRP-2 E653A	NRP-2-Fc	5' – CGATTTCCTCGAGG-CGCCCTGTGGTTGG – 3'
			5' – GCTAAAGGAGCTC-CGCGGGACACCAACC– 3'
44	NRP-2 E652A/ E653A	NRP-2-Fc	5' – CTTCGATTTCGCGG-CGCCCTGTGGTTGG – 3'
			5' – GAAGCTAAAGCGC-CGCGGGACACCAACC – 3'
45	NRP-2 D683A	NRP-2-Fc	5' – GACGTTTCCAGAT-GCCAGGAATTTCTTGCG – 3'
			5' – CTGCAAAGGTCTA-CGGTCCTTAAAGAACGC – 3'

Primers used in Chapter V

Primer set	Mutant	Template	Primer Sequence
46	R87A	ST8Sia-II	5’- GCCTCGTCCAAATGCGCACA-TAACCAGACGCTC - 3’
			5’-GAGCGTCTGGTTATGTGC-GCATTTGGACGAGGC-3’
47	R95A	ST8Sia-II	5’- CAGACGCTCTCTCTGGC-GATCAGGAAGCAGATT - 3’
			5’- AATCTGCTTCCTGATCG-CCAGAGAGAGCGTCTG - 3’
48	R97A	ST8Sia-II	5’- CTCTCTCTGAGGATCGCG-AAGCAGATTTTAAAG - 3’
			5’- CTTTAAAATCTGCTTCGCGA-TCCTCAGAGAGAG - 3’
49	K98A	ST8Sia-II	5’– CTGAGGATCAGGGCGCAG-ATTTTAAAGTTC – 3’
			5’– GAACTTTAAAATCTGC-GCCCTGATCCTCAG - 3’
50	K102A	ST8Sia-II	5’ – AGGAAGCAGATTTTAGC-GTTCTTGGATGCTGAA – 3’
			5’ – TTCAGCATCCAAGAACGC-TAAAATCTGCTTCCT – 3’
51	K108A	ST8Sia-II	5’ – CTTGGATGCTGAAGCGG-ACATTTCTGTC – 3’
			5’ – GACAGAAATGTCCGCTTC-AGCATCCAAG – 3’
52	K114A	ST8Sia-II	5’ GACATTTCTGTCCTAGCG-GGAACCCTGAAGCCT – 3’
			5’ – AGGCTTCAGGGTTCCCGCT-AGGACAGAAATGTC – 3’
53	K118A	ST8Sia-II	5’- CTAAAGGGAACCCTGGC-GCCTGGAGATATTATT - 3’
			5’- AATAATATCTCCAGGCG-CCAGGGTTCCCTTTAG - 3’
54			5’- CCAATGCAAGCCCTAAGAG-AATGCCATTAG - 3’

	H331K	ST8Sia-IV and its PBR mutants	5’- CTAATGGCATTCTCTTA-GGGCTTGCATTGG - 3’
55	H346K	ST8Sia-II and its PBR mutants	5’- CAGGCCAGCCCGAAGA-CCATGCCCTTG - 3’
			5’- CAAGGGCATGGTCTTCGG-GCTGGCCTG - 3’

CHAPTER III

Biophysical characterization of the NCAM FN1-ST8Sia-IV PBR interaction interface

(Parts of this chapter have been published in Bhide GP, Prehna G, Ramirez BE, Colley KJ, The Polybasic Region of Polysialyltransferase ST8Sia-IV Binds Directly to the Neural Cell Adhesion Molecule, NCAM, Biochemistry, 2017, 56 (10): 1504-1517).

Introduction

Previous work in the laboratory has defined the sequences in NCAM FN1 and ST8Sia-IV critical for NCAM recognition and polysialylation. The NCAM FN1 domain is essential for the polysialylation of the N-glycans in the adjacent Ig5 domain, and mutating acidic residues Asp^{520}, Glu^{521}, and Glu^{523} in the NCAM FN1 domain simultaneously to arginine abolishes NCAM polysialylation (192). Co-immunoprecipitation experiments showed that this triple mutation also reduced binding of ST8Sia-IV to NCAM (193). On the polyST side, NCAM polysialylation by ST8Sia-IV is nearly abolished when Arg^{82} and Arg^{93} in the ST8Sia-IV PBR are mutated to alanine (199). A catalytically inactive mutant of ST8Sia-IV, H331K, serves as competitive inhibitor of NCAM polysialylation by wild-type ST8Sia-IV. However, when Arg^{82} and Arg^{93} were mutated to alanine in this mutant, it loses its ability to compete (200). These data suggest that Arg^{82} and Arg^{93} are essential for ST8Sia-IV recognition of and binding to NCAM. It was therefore tempting to speculate that the NCAM acidic patch and ST8Sia-IV basic residues bind each other, and that this interaction constitutes the initial recognition step for NCAM protein-specific polysialylation.

In order to determine whether NCAM FN1 domain and ST8Sia-IV PBR basic residues bind each other directly, biophysical characterization of ST8Sia-IV was necessary. Purification of ST8Sia-IV in a quantity and purity sufficient for biophysical studies has proven difficult precluding the crystallization of ST8Sia-IV (discussed in (127)). However, the ST8Sia-IV structure has been modeled on the X-ray crystal

structure of the α2,8-sialyltransferase, ST8Sia-III (125), using Phyre2 server (203). I therefore decided to evaluate the interaction between a recombinant 6xHis-SUMO tagged ST8Sia-IV PBR peptide (SUMO-PBR), comprised of ST8Sia-IV residues 75-100, and a recombinant NCAM FN1 domain using Isothermal Titration Calorimetry (ITC) and Heteronuclear Single Quantum Correlation (HSQC) Nuclear Magnetic Resonance (NMR) spectroscopy. These techniques allowed me to demonstrate a direct interaction between the NCAM FN1 domain and the SUMO-PBR peptide that is dependent upon Arg^{82} and Arg^{93} in the ST8Sia-IV PBR and Asp^{520}, Glu^{521}, and Glu^{523} in the NCAM FN1 domain. Other data suggest that binding of the ST8Sia-IV PBR to the acidic patch induces a conformational change that translates to a loop adjacent to the Ig5-FN1 linker region, and this in turn influences the polysialylation of N-glycans in the Ig5 domain.

Results

A. SUMO-PBR peptide binds the NCAM FN1 acidic patch directly and specifically.

Given the difficulties in obtaining purified ST8Sia-IV, I decided to use isolated PBR region to probe the requirements for NCAM FN1 recognition. We first obtained a commercially synthesized PBR peptide, consisting of ST8Sia-IV residues 71-105. The peptide had very limited solubility in physiological buffers, possibly due to its high hydrophobicity (15/35 amino acids are hydrophobic). I therefore decided to employ a 6xHis-SUMO tagged version of PBR peptide that contained residues 75-100 of ST8Sia-IV reasoning that the residues 71-74 and 101-105 play little to no role in NCAM polysialylation, as suggested by previous work (199) (Fig. 17A). Eliminating these residues reduced the hydrophobicity of the peptide, improved its solubility and enabled its purification from *E.coli* cell lysates. To serve as an experimental control, I expressed the 6xHis-SUMO tag itself and purified it. The 6xHis tagged NCAM FN1 domain was also purified from *E.coli* cells as described previously (194).

In order to determine whether the two proteins are capable of binding each other, I performed ITC experiments, which analyze binding of the two proteins in solution and also yields the thermodynamic and stoichiometric parameters of binding (Fig. 17B). I titrated concentrated SUMO-PBR

peptide, or the SUMO tag alone as a control, into the dilute FN1 domain at a 30:1 ratio. After subtracting the background heats from the SUMO control, I observed a 1:1 stoichiometry of binding (N= 1.060 ± 0.0698) and a K_d of 10 μM (10.88 ± 2.46 μM) for FN1 and the SUMO-PBR peptide using a one-site binding model. The interaction was enthalpy as well as entropy driven as implied by an ΔH value of approximately -1 kcal/mol and an ΔS value of 19.39 cal K^{-1} mol^{-1}, respectively. The entropic contribution to the binding suggests that hydrophobic residues in PBR peptide also contribute to the interaction. The stretch of ST8Sia-IV PBR selected for this analysis possesses about 10 hydrophobic residues (Fig. 17A). It is plausible that acidic patch-PBR binding results in displacement of water molecules from the hydrophobic regions of the PBR, thereby increasing entropy. Alternatively, a change in local disorder secondary to binding may have resulted in this entropy change (204).

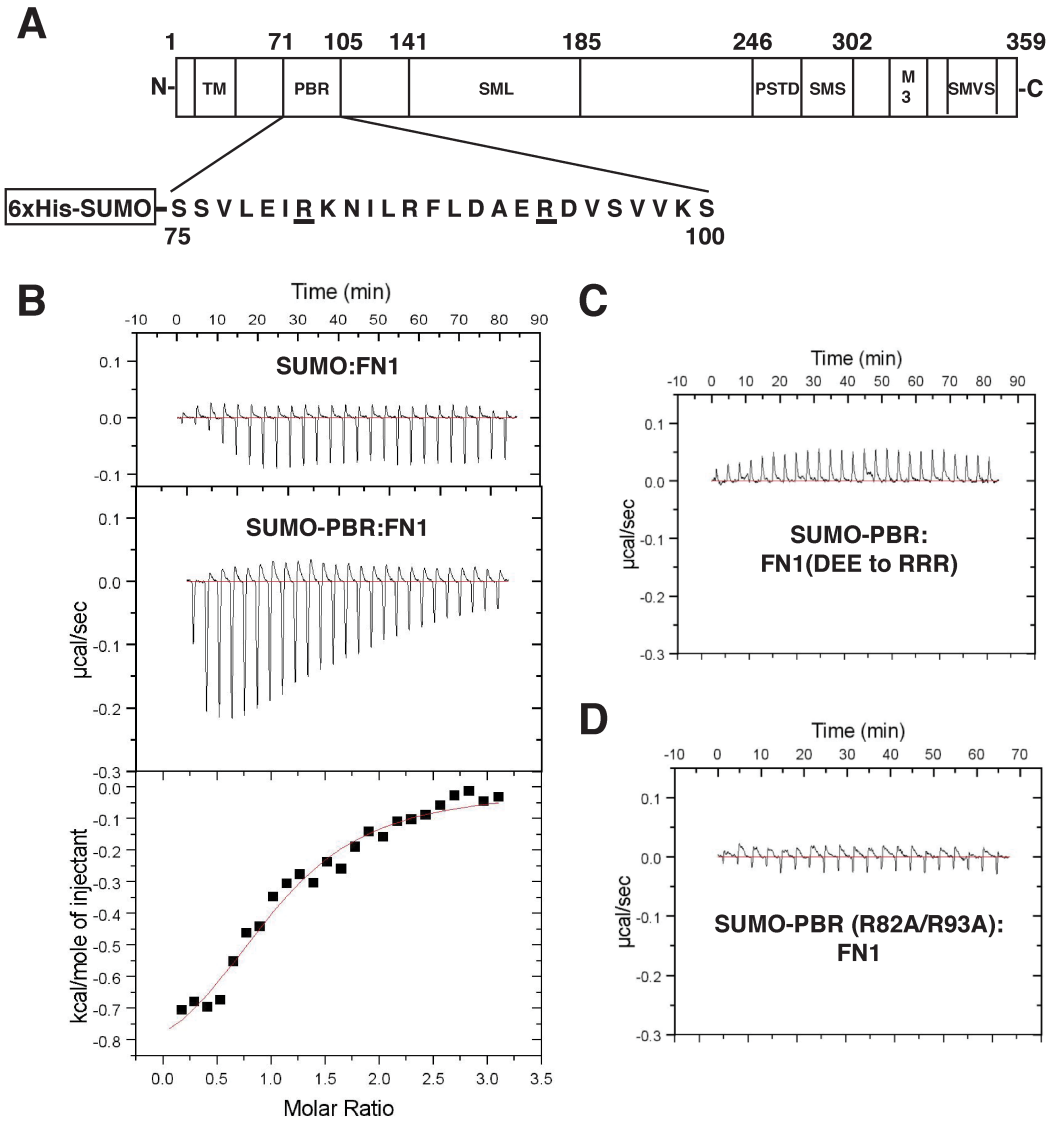
A
1
71
105
141
185
246
302
359
N-
TM
PBR
SML
PSTD
SMS
M 3
SMVS
-C
6xHis-SUMO
S S V L E I R K N I L R F L D A E R D V S V V K S
75
100
B
Time (min)
SUMO:FN1
SUMO-PBR:FN1
µcal/sec
kcal/mole of injectant
Molar Ratio
C
Time (min)
µcal/sec
SUMO-PBR:
FN1(DEE to RRR)
D
Time (min)
µcal/sec
SUMO-PBR (R82A/R93A):
FN1

Figure 17: Isothermal titration calorimetry analysis of NCAM FN1 and SUMO-PBR. (A) Schematic of ST8Sia-IV showing its various regions. Sialylmotifs large (SML), small (SMS), very small (SMVS), and motif 3 (M3) are marked. PBR and PSTD regions are unique to the polySTs. The sequence of PBR region is shown with key residues, Arg^{82} and Arg^{93}, underlined. (B) Heat exchanges resulting from titration of 600 μM SUMO-PBR with 20 μM FN1 (bottom panel). Heat exchanges resulting from titration of 600 μM SUMO, used as a control with 20 μM of FN1 is shown in top panel. (C) The FN1 DEE to RRR mutation abolishes binding between FN1 and SUMO-PBR. (D) Mutating Arg^{82} and Arg^{93} in SUMO-PBR eliminates binding to FN1.

To ascertain the specificity of this interaction, we purified the SUMO-PBR with the R82A/R93A mutations and the NCAM FN1 domain with the DEE to RRR acidic patch mutations (Asp^{520}, Glu^{521}, Glu^{523} to arginines) that abolish polysialylation of full-length NCAM (199). When the above mutants were titrated with their wild-type interaction partners, we observed little to no heat exchanges indicating that the FN1 acidic patch residues bind the Arg^{82}/Arg^{93} basic residues in the PBR portion of the SUMO-PBR peptide directly (Fig. 17 C and D). Using Circular Dichroism (CD) and Size-Exclusion Chromatography, we confirmed that the mutants assume a similar secondary structure to that of their wild-type counterparts and therefore, loss of binding was not due to misfolding of these proteins (Fig. 18).

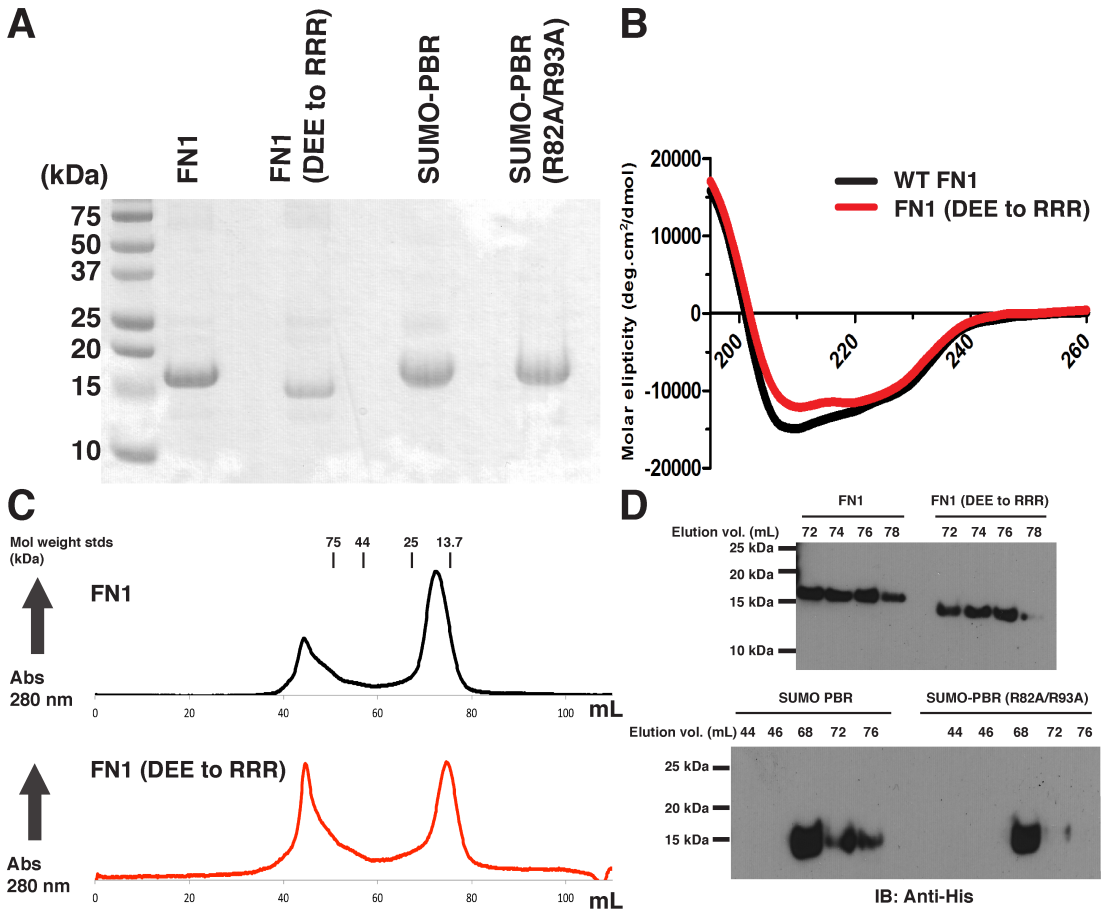

Figure 18: Purification of FN1 and SUMO-PBR and respective mutants. (A) Purified FN1, FN1 (DEE to RRR), SUMO-PBR, and SUMO-PBR (R82A/R93A) were analyzed on 15% polyacrylamide gel using SDS-PAGE and Coomassie brilliant blue staining. (B) The circular dichroism spectra recorded for purified FN1 and the FN1 DEE to RRR mutant at pH 8. (C) The Size Exclusion Chromatography (SEC) profile of FN1 (black) and FN1 (DEE to RRR) (red). Molecular weight standards include conalbumin (75 kDa), ovalbumin (44 kDa), chymotrypsinogen A (25 kDa), and RNAse A (13.7 kDa). (D) Anti-His tag immunoblots of elution fractions from the SEC of FN1 and FN1 (DEE to RRR) (top panel) and of SUMO-PBR and SUMO-PBR (R82A/R93A) (bottom panel). The SEC chromatograms for the SUMO-PBR proteins are not shown because the SUMO-PBR peptide and its mutant lack tryptophan residues and the resulting absorbance (280 nm) signals are very weak. For all proteins, only monomeric species were used in the ITC and NMR experiments.

B. HSQC-NMR experiments reveal the ST8Sia-IV PBR-FN1 interaction surface.

The ITC experiments above gave a strong indication that the NCAM FN1 acidic patch and ST8Sia-IV PBR basic residues interact with each other, as mutating acidic patch and Arg^{82}/Arg^{93} residues in respective interaction partners eliminated binding. However, other residues in the FN1 domain could be involved in the interaction, and to address this possibility we used HSQC NMR to map the "footprint" of the PBR peptide on the FN1 domain in solution. Our laboratory has previously reported the X-ray crystal structure of the NCAM FN1 domain (194), and we first obtained chemical shift assignments using standard heteronuclear experiments for the FN1 domain labeled with ^{13}C and ^{15}N (Fig. 19). Next, we performed HSQC NMR titrations using the ^{15}N labeled FN1 domain with increasing amounts of unlabeled SUMO-PBR peptide (Fig. 20A). As a control, we performed the same titrations using the SUMO-PBR (R82A/R93A) mutant that does not bind the FN1 domain. For the sake of clarity, only the 1:10 titration point is shown in Figure 20. When we overlaid the spectra for SUMO-PBR and FN1 titrations at various ratios, we observed dose-dependent chemical shift perturbations for several residues in the spectra (Fig. 20A and C). In contrast, little change was observed with SUMO-PBR (R82A/R93A) mutant (Fig. 20B). Interacting proteins appear to be in fast exchange as only one peak is observed for the perturbed residues at each ratio.

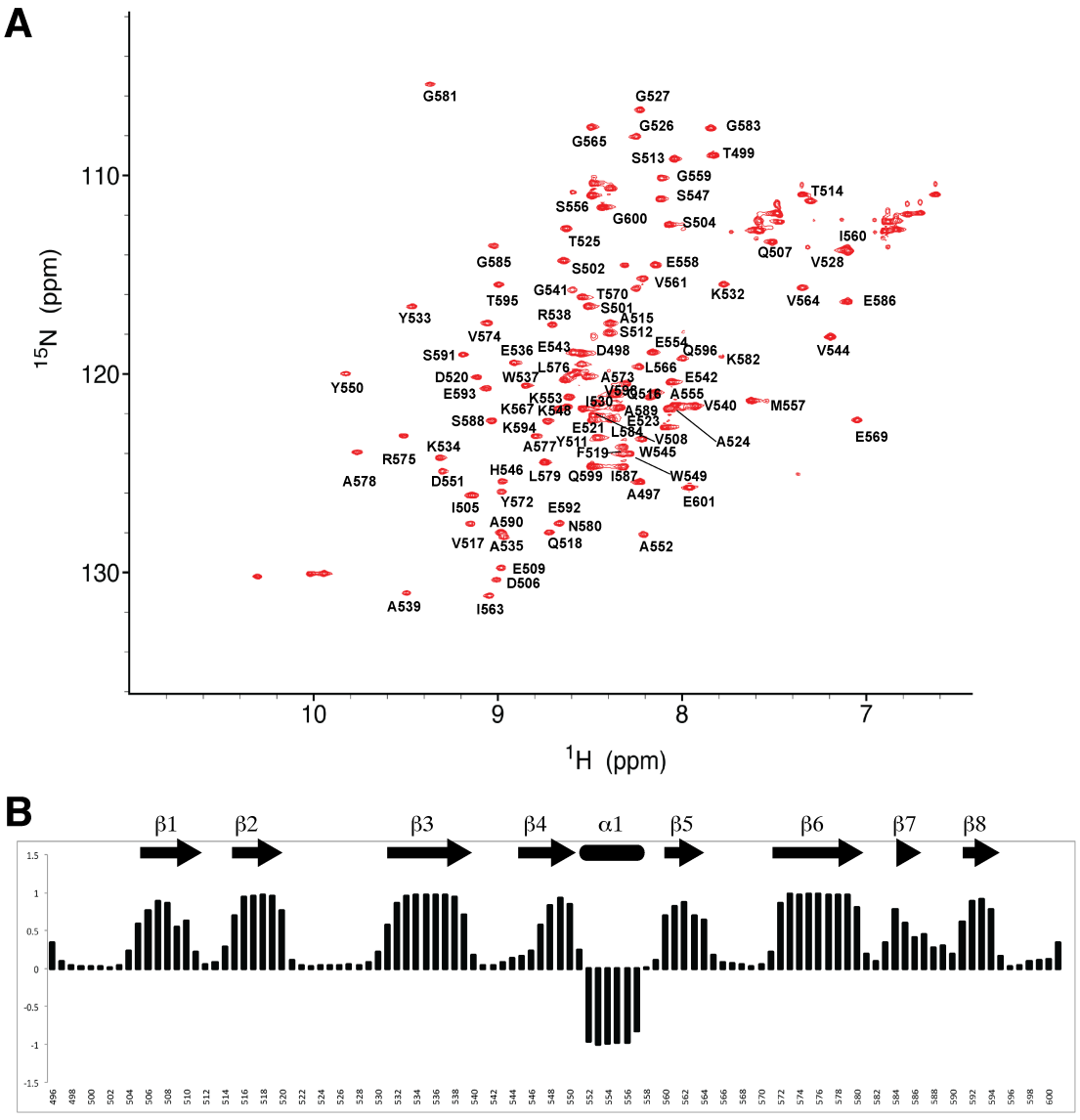

Figure 19: The NCAM FN1 ^{1}H-^{15}N HSQC spectrum and residue assignments. (A) ^{1}H-^{15}N HSQC spectrum recorded for isotopically labeled FN1 at pH 6.6 and 25°C. Backbone assignments were performed using CBCACONH, HNCACB, HNCA, HNCO, HN(CO)CA, and HN(CA)CO experiments. The overall assignments are 99% complete with 93% N, 99% CO, 98% CA, 98% CB, and 99% HN of the FN1 backbone assigned. (B) Using the Talos+ program, the secondary structure of FN1 was calculated from chemical shifts (201). The full chemical shift list can be accessed using BMRB accession code 26929.

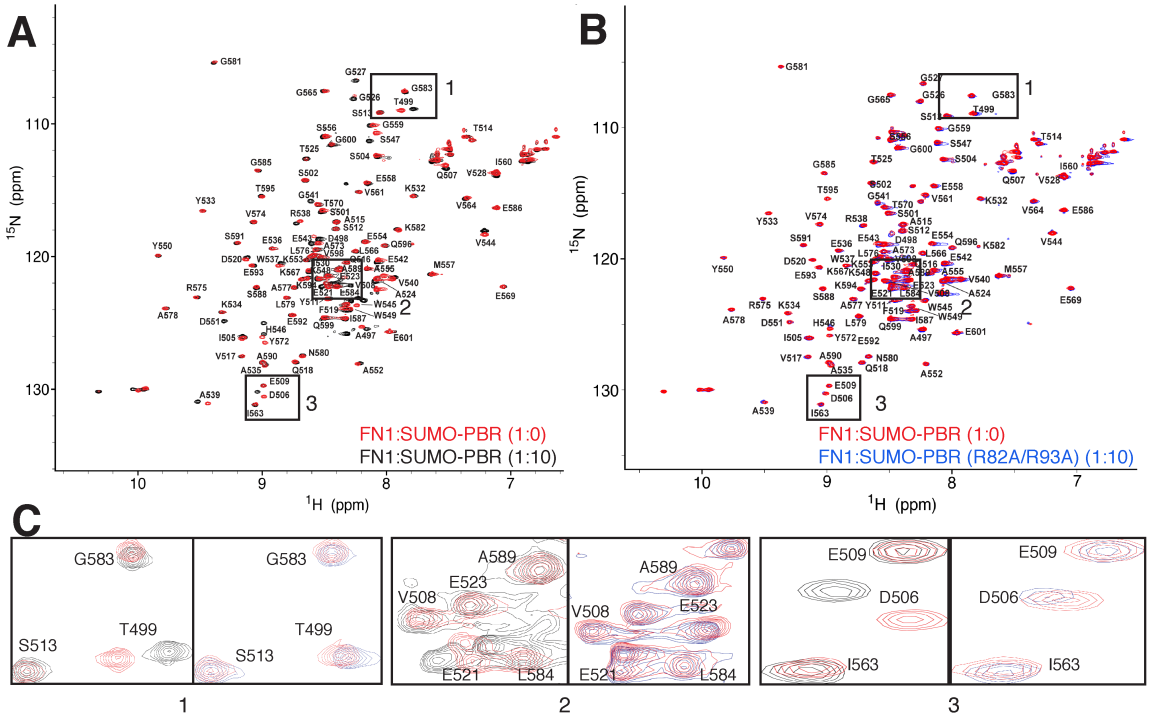

Figure 20: ^{1}H-^{15}N HSQC spectra for titration of ^{15}N- FN1 domain with SUMO and SUMO-PBR peptide. (A) Overlay of ^{1}H-^{15}N HSQC spectra of ^{15}N-FN1 (red) and after addition of unlabeled SUMO-PBR peptide at a 1:10 concentration ratio (black). (B) Overlay of ^{1}H-^{15}N HSQC spectra of ^{15}N-FN1 (red) and after addition of unlabeled SUMO peptide at a 1:10 concentration ratio (blue), used as a control. (C) Chemical shift perturbations observed for selected interacting residues Thr^{499} (box 1), Glu^{521} (box 2), and Asp^{506} (box 3) are magnified with spectra from panel A on the left and panel B on the right.

In order to identify NCAM FN1 residues which interact with the SUMO-PBR peptide or undergo conformational change as a secondary effect of binding, we calculated combined shift difference (CSD) values for each residue as $[(\text{proton shifts})^2 + (\text{nitrogen shifts}/6.51)^2]^{0.5}$ (205). CSD values obtained from the control experiment were then subtracted from the experimental values, and plotted as shown in Figure 21. The average CSD value for all the residues was calculated and indicated on the graph as a horizontal line, and residues causing perturbations above this threshold value were identified (Figure 21). These residues were then mapped to crystal structure of FN1 domain (PDB 2HAZ) (194) and were color-coded by function. Residues that showed significant chemical shift perturbations included acidic patch residues, Asp^{520} (D520) and Glu^{521} (E521) that were previously characterized (192). As shown in Figure 20 C (box 2), Glu^{523} (E523), which belongs to the same surface acidic patch in accordance with surface electrostatics and experimental evidence ((192) and see below), was also expected to be involved in SUMO-PBR-FN1 interaction; however, due to residue overlap in ^{1}H-^{15}N HSQC spectrum, we were not able to definitively conclude whether Glu^{523} exhibits any chemical shift difference. Additionally, Asp^{506} (D506) and Asp^{498} (D498) also display chemical shift perturbations (Fig. 21 C). Asp^{506} is adjacent to the previously characterized acidic patch residues; whereas, Asp^{498} is found in Ig5-FN1 linker region (Fig. 22). However, these residues constitute the same electrostatic surface, based on the map of FN1 domain generated using the Adaptive Poisson-Boltzmann Solver (APBS) server (206) (Fig. 21B).

In addition to Asp^{498}, other residues in the Ig5-FN1 linker region, namely, Gln^{496}, Ala^{497}, and Thr^{499} also show chemical shift differences upon addition of the SUMO-PBR peptide (Fig. 21A). The Ig5-FN1 linker region in NCAM is flanked by ^{526}GGVPI^{530} and ^{580}NGKG^{583} loops (207) (Fig. 23). Mutating these loops to alanine or glycine residues eliminated NCAM polysialylation (193). Interatomic distances in the crystal structure of NCAM Ig5-FN1 domain indicated that the backbone carbonyl oxygen of Asp^{498} forms a hydrogen bond with the amide side chain of Asn^{580} in the ^{580}NGKG^{583} loop, whereas main chain amide group of Asp^{498} forms a hydrogen bond with main chain carbonyl of Gly^{526} in the ^{526}GGVPI^{530} loop (Fig. 22 B and C). Interestingly, in our ^{1}H-^{15}N HSQC analysis, we observe slight perturbations in Gly^{526}

as well as neighboring Gly^{527} indicating direct binding of SUMO-PBR at the $^{526}GGVPI^{530}$ loop or a relayed conformational change upon binding at the acidic patch which is in proximity (Fig. 22A).

In addition, our NMR analysis revealed a potential PBR interaction surface, consisting of residues Trp^{537}-Ser^{547}. These residues are located in a large loop between β3 and β4 strands of the FN1 domain, found on a face opposite to the acidic patch. Previous structural or mutagenesis studies have not implicated any of the above residues in interaction with the ST8Sia-IV (Fig. 21 A and B). It is plausible that our peptide wraps around FN1 domain to bind the β3-β4 loop residues in extended conformation. However, this binding mode is not compatible with previous docking studies performed using Ig5-FN1 domain crystal structure and a model of ST8Sia-IV, based on the crystal structure of ST8Sia-III (125).

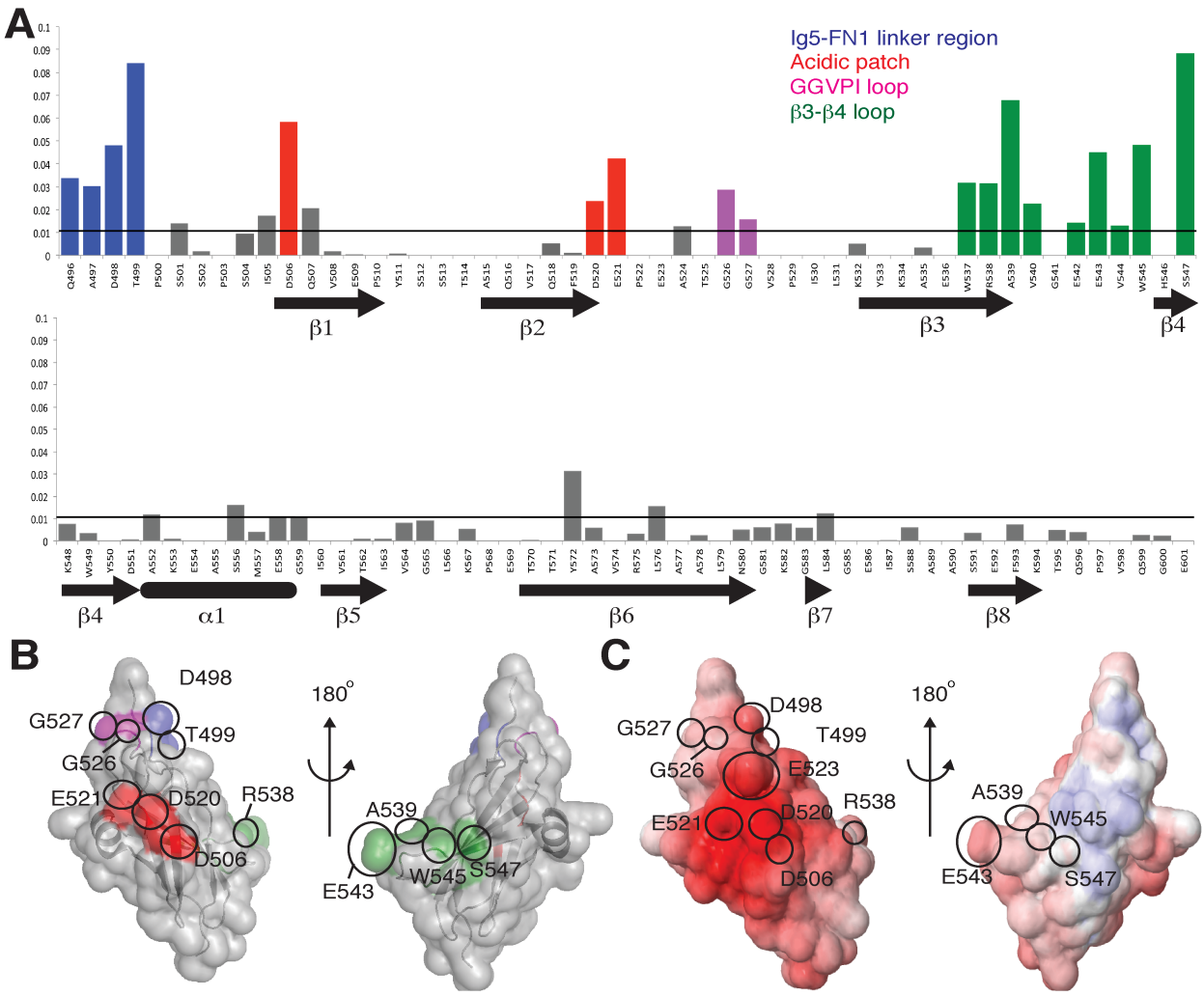
A
Ig5-FN1 linker region
Acidic patch
GGVPI loop
β3-β4 loop
β1
β2
β3
β4
β4
α1
β5
β6
β7
β8
B
D498
G527
T499
G526
E521
D520
R538
D506
180°
A539
E543
W545
S547
C
D498
G527
T499
G526
E523
E521
D520
R538
D506
180°
A539
W545
E543
S547

Figure 21: NCAM FN1 residues impacted by ST8Sia-IV PBR peptide binding. (A) Residues displaying specific and significant NMR chemical shift perturbations upon addition of the SUMO-PBR peptide. After subtracting the combined shift difference (CSD) values for FN1-SUMO-PBR (R82A/R93A) titration, CSD values for the FN1−SUMO-PBR interaction were plotted and the data are presented as two bar graphs representing the N-terminal (top) and C-terminal (bottom) residues of the FN1 domain. (B) The FN1 residues most perturbed by SUMO-PBR interaction are mapped onto the crystal structure of the FN1 domain (PDB entry 2HAZ) (194). (C) Electrostatic surface potential map of NCAM FN1 calculated using the Adaptive Poisson−Boltzmann Solver (APBS) (206). For both panels B and C, two views of the NCAM FN1 domain structure are shown rotated by 180°.

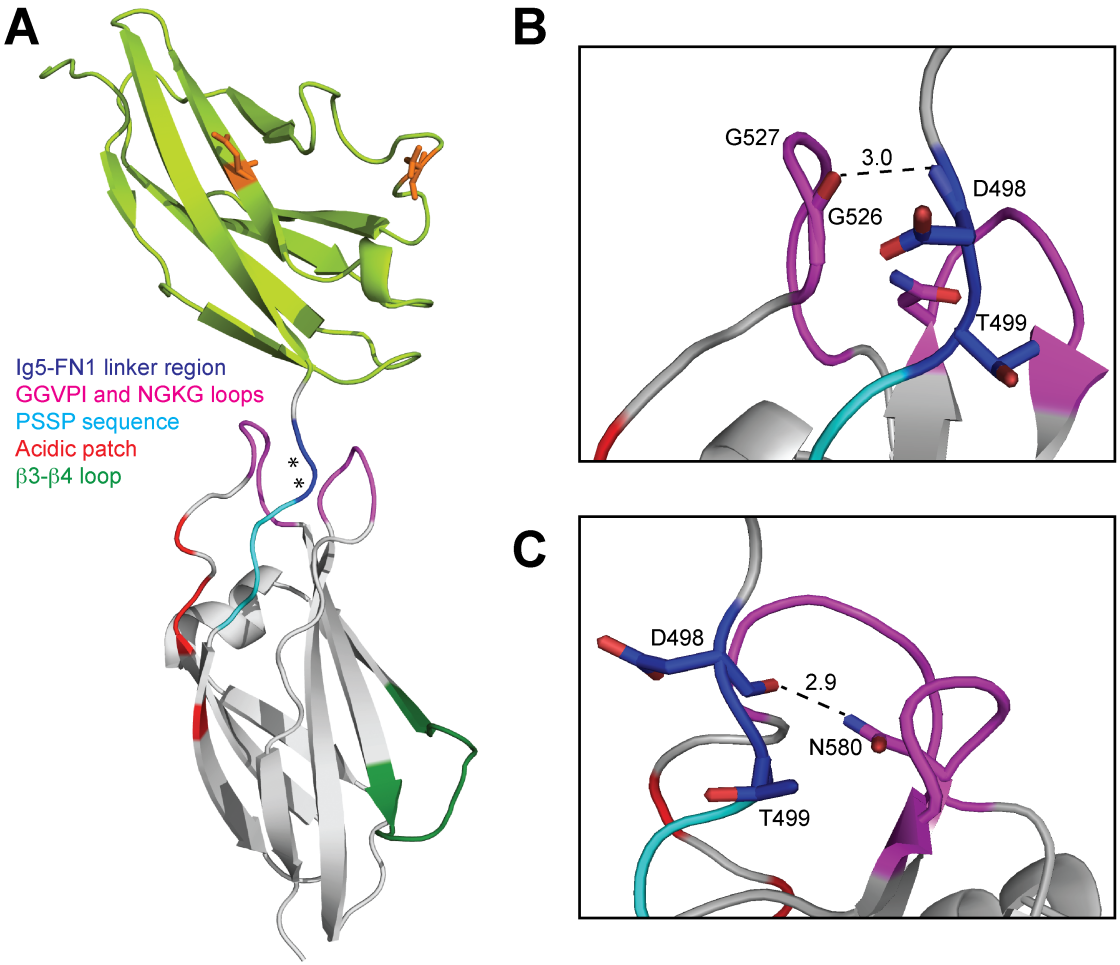
A
Ig5-FN1 linker region
GGVPI and NGKG loops
PSSP sequence
Acidic patch
β3-β4 loop
B
G527
3.0
D498
G526
T499
C
D498
2.9
N580
T499

Figure 22. NCAM Ig5−FN1 structure and interactions between the linker region and FN1 GGVPI and NGKG loops. (A) Crystal structure of the NCAM Ig5−FN1 linker region (PDB entry 3MTR) (207). Asparagine residues in the Ig5 domain bearing N-glycans that are polysialylated are colored orange. The Ig5−FN1 linker region, including Gln^{496}, Ala^{497}, Asp^{498}, and Thr^{499}, is colored dark blue with asterisks indicating the positions of Asp^{498} and Thr^{499}. The PSSP sequence, colored cyan, is a part of the same unstructured segment that comprises the linker region. The GGVPI and NGKG loops flanking and stabilizing the linker region are colored magenta. The acidic patch that includes Asp^{506}, Asp^{520}, Glu^{521}, and Glu^{523} is colored red. The β3−β4 loop that connects strands leading to a unique FN1 α-helix and the GGVPI loop and acidic patch is colored green. (B) Predicted hydrogen bond formed between the main chain amide group of Asp^{498} in the linker region and the main chain carbonyl of Gly^{526} in the GGVPI loop. (C) Predicted hydrogen bond formed between the side chain amide group of Asn^{580} in the NGKG loop and the main chain carbonyl of Asp^{498} in the linker region. This figure is adapted from ref (193).

C. Impact of various FN1 acidic surface residues on NCAM polysialylation by ST8Sia-IV.

In section IV B, I identified several NCAM FN1 acidic patch residues that are impacted upon addition of SUMO-PBR. These include previously characterized Asp^{520} and Glu^{521} as well as Asp^{498} and Asp^{506}, which were identified by our NMR analysis. Dr. Shalu Mendiratta previously mutated Asp^{520}, Glu^{521}, and Glu^{523} simultaneously to arginines and observed loss of NCAM polysialylation (192). In order to assess contribution of Asp^{498} and Asp^{506} relative to Asp^{520}, Glu^{521}, and Glu^{523}, I mutated these residues individually to arginines in V5-tagged full-length NCAM and co-expressed the mutants in COS-7 cells with ST8Sia-IV. After immunoprecipitation, I assessed their relative polysialylation using anti-polySia antibody. Relative expression of mutants was determined as described earlier. Mutating Asp^{506} (D506R) decreased NCAM polysialylation to 61 ± 9% (S.D.) of that of wild type NCAM, whereas D498R mutation essentially abolished NCAM polysialylation (4 ± 5% (S.D.) of that of wild type NCAM) (Fig. 23A). Of the previously identified acidic residues, replacing Glu^{521} (E521R) and Glu^{523} (E523R) had maximum impact with decreases in polysialylation to 19 ± 6% (S.D.) and 12 ± 7% (S.D.) of that of wild type NCAM, respectively (Fig. 23A). This loss of polysialylation was not due to misfolding because these mutant proteins were localized to the Golgi and cell surface similar to wild type NCAM (Fig. 24). Proper localization of E521R and E523R was confirmed previously (192).

D. The Ig5-FN1 linker region plays a role in NCAM polysialylation.

Ig5-FN1 linker region residues in the recombinant FN1 domain protein are preceded by 6xHis tag and thrombin cleavage site. All four linker region residues in this protein, Gln^{496}, Ala^{497}, Asp^{498}, and Thr^{499}, displayed chemical shift differences upon addition of the SUMO-PBR peptide (Fig. 21). I have demonstrated the importance of Asp^{498} in the earlier section. For comparison, I mutated Thr^{499} to alanine along side Asp^{498} and co-expressed it with ST8Sia-IV. I found that this mutation resulted in a decrease in polysialylation to 39 ± 24% (S.D.) of that of wild type NCAM (Fig. 23B). Results of indirect immunofluorescence confocal microscopy revealed that the T499A mutant was also localized to the Golgi apparatus and cell surface and hence, the observed loss of polysialylation was not due to misfolding and ER retention (Fig. 24).

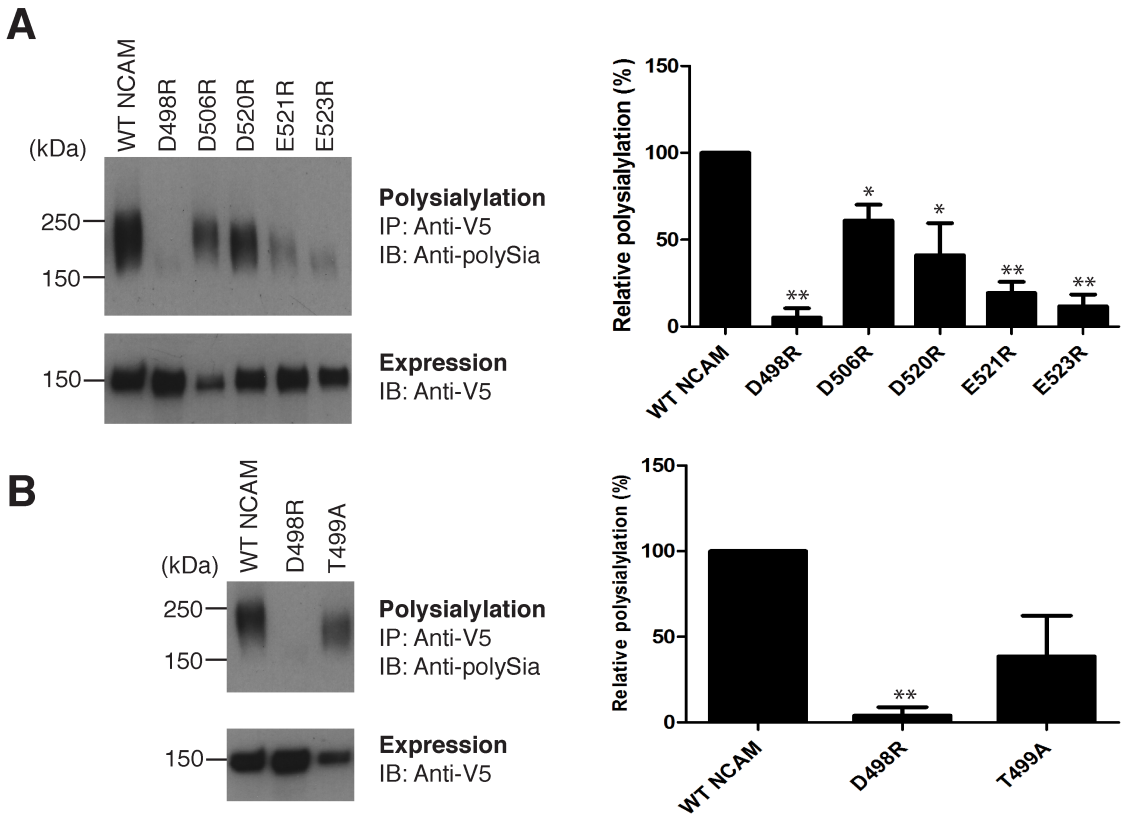
A
WT NCAM
D498R
D506R
D520R
E521R
E523R
(kDa)
250
150
Polysialylation
IP: Anti-V5
IB: Anti-polySia
150
Expression
IB: Anti-V5
Relative polysialylation (%)
150
100
50
0
*
*
**
**
**
WT NCAM
D498R
D506R
D520R
E521R
E523R
B
WT NCAM
D498R
T499A
(kDa)
250
150
Polysialylation
IP: Anti-V5
IB: Anti-polySia
150
Expression
IB: Anti-V5
Relative polysialylation (%)
150
100
50
0
**
WT NCAM
D498R
T499A

Figure 23: The effect of acidic patch and linker mutations on NCAM polysialylation. V5-tagged NCAM mutants were co-expressed with ST8Sia-IV in COS-7 cells. After immunoprecipitation with an anti-V5 antibody, their polysialylation was assessed by immunoblotting using an anti-polySia antibody. An aliquot of cell lysate was boiled in Laemmli sample buffer to remove polySia and immunoblotted with anti-V5 antibody to assess protein expression. (A) Polysialylation (top) and expression (bottom) of NCAM mutants with replacements of known and potential acidic patch residues. The adjacent bar graph shows statistics resulting from three different experiments. (B) Polysialylation (top) and expression (bottom) of NCAM mutants with replacements of two Ig5−-FN1 linker residues. The adjacent bar graphs show statistics from three different experiments. Quantification of the experimental results in panels A and B was performed as described in Materials and Methods with error bars representing the standard deviation (S.D.). Statistical analysis was performed with respect to wild-type NCAM, which is normalized to 100%, using unpaired Student's t tests, where *,$0.01 < p < 0.05$, **,$0.001 < p < 0.01$, and ***,$0.0001 < p < 0.001$. The p value for T499A is 0.06.

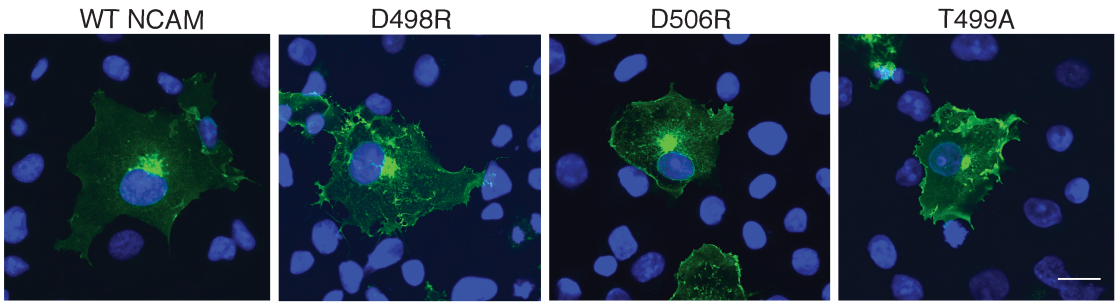

Figure 24. Immunofluorescence localization of mutants of NMR-identified FN1 acidic residues and Ig5-FN1 linker region residues. V5-tagged NCAM mutants were expressed in COS-7 cells and localized by indirect immunofluorescence microscopy using a mouse anti-V5 antibody and a FITC-conjugated goat anti-mouse IgG antibody. DAPI is used to stain the cell nucleus. Bar = 20 μm.

E. NCAM FN1 β3-β4 loop residues and NCAM polysialylation.

FN1 residues that showed significant chemical perturbations when titrated with SUMO-PBR peptide in ^{1}H-^{15}N HSQC NMR experiments included not only surface acidic residues and Ig5-FN1 linker residues but also a large stretch of residues from Trp^{537}-Ser^{547} that are in a loop region between β3 and β4 strands of the FN1 domain (Fig. 21). In order to evaluate whether these residues play a role in NCAM polysialylation, I mutated some of these residues in full-length NCAM. Of the residues tested, only mutation of Ala^{539} and Trp^{545} impacted NCAM polysialylation depending on the amino acid replacement. When Trp^{545} was replaced with alanine (W545A), it reduced NCAM polysialylation to 33 ± 13% (S.D.) that of wild type NCAM. Likewise, when Ala^{539} is replaced with serine (A539S), it reduced NCAM polysialylation to 41 ± 9% (S.D.) that of wild type NCAM (Fig. 25). Analyzing intracellular localization of these mutants revealed that the loss of polysialylation was not due to misfolding or mislocalization, as shown in Figure 26. Conversely, when Ala^{539} and Trp^{545} were replaced with phenylalanine (A539F) and tyrosine (W545Y), respectively, NCAM polysialylation was barely affected (77 ± 5% (S.D.) for A539F and 91 ± 18% (S.D.) for W545Y).

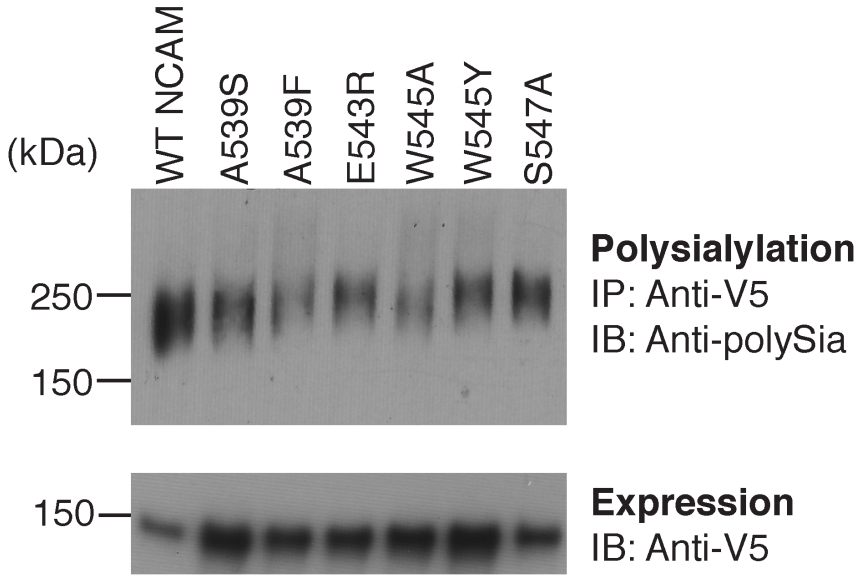
(kDa)
WT NCAM
A539S
A539F
E543R
W545A
W545Y
S547A
250
150
Polysialylation
IP: Anti-V5
IB: Anti-polySia
150
Expression
IB: Anti-V5

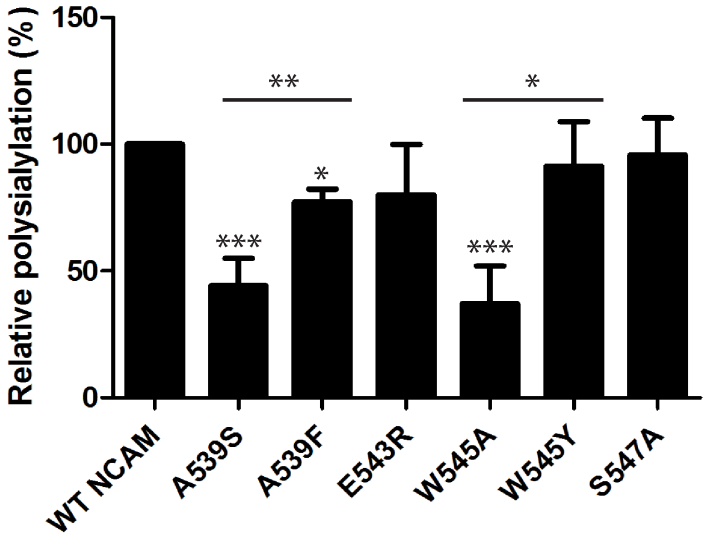
Relative polysialylation (%)
150
100
50
0
**
*
***
*
***
WT NCAM
A539S
A539F
E543R
W545A
W545Y
S547A

Figure 25: Impact of mutating residues in the FN1 β3−β4 loop on NCAM polysialylation. V5- tagged β3−β4 loop mutants of NCAM were expressed in COS-7 cells with ST8Sia-IV. Their effect on polysialylation relative to wild-type NCAM was evaluated by immunoblotting with anti-polySia antibody after immunoprecipitating with anti-V5 antibody (top panel). Expression of mutants was assessed by immunoblotting a boiled aliquot of cell lysate with an anti-V5 antibody (bottom panel). The adjacent bar graph shows statistics resulting from three different experiments. Quantification of the experimental results was performed as described in Materials and Methods with error bars representing the SD. Statistical analysis with respect to wild-type NCAM, which is normalized to 100%, was performed using unpaired Student's t tests, where *,$0.01 < p < 0.05$, **,$0.001 < p < 0.01$, and ***,$0.0001 < p < 0.001$. Pair-wise comparisons between specific proteins are indicated by a line above the compared bars in the graph.

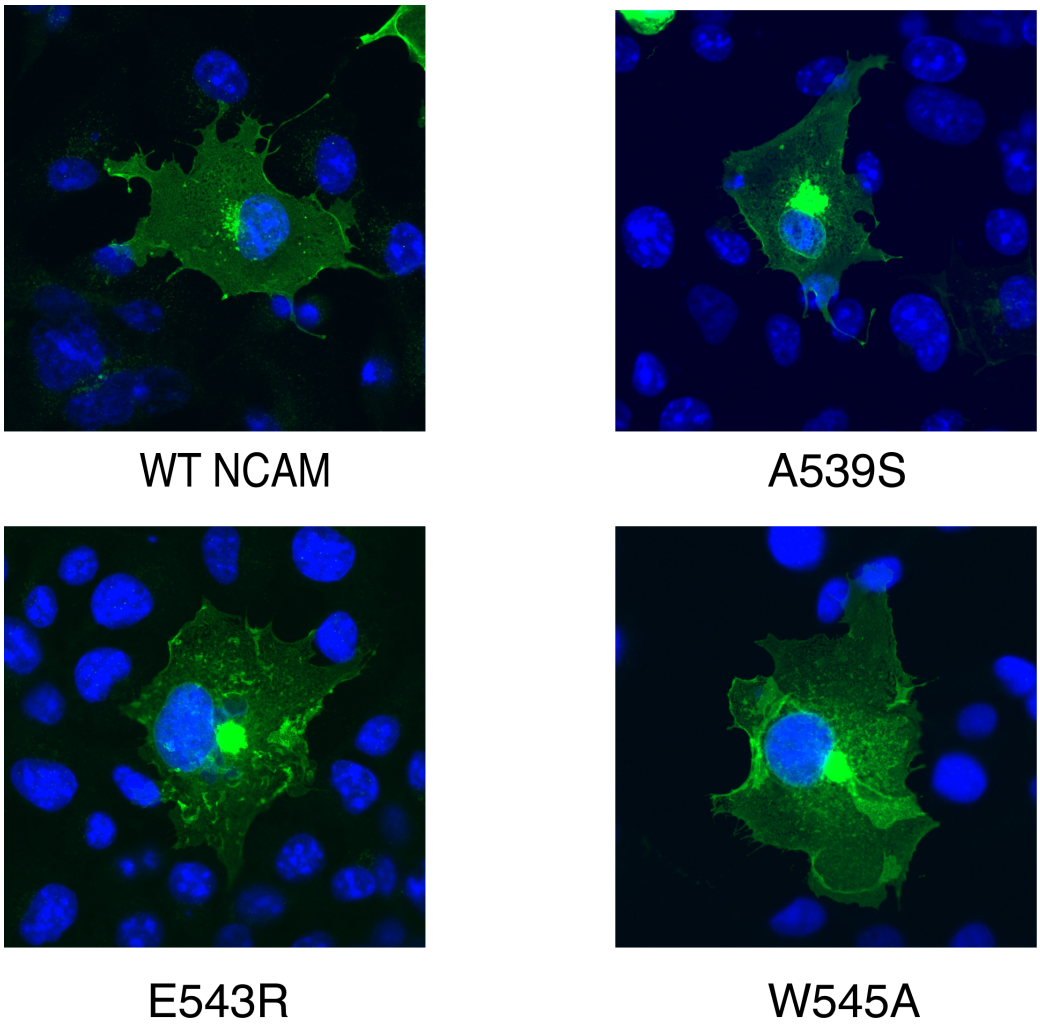

Figure 26: Intracellular localization of NCAM FN1 domain β3−β4 loop mutants. V5-tagged NCAM mutants were expressed in COS-7 cells and their localization was determined by indirect immunofluorescence confocal microscopy using an anti-V5 antibody and a FITC goat anti-mouse IgG antibody (green). Nuclei were stained with DAPI (blue). Bar = 20 μM

Notably, some of the β3-β4 loop residues are conserved between FN1 and FN2 domains of NCAM (Fig. 27). I therefore wondered whether these residues play a role in maintaining structural integrity of FN1 domain.

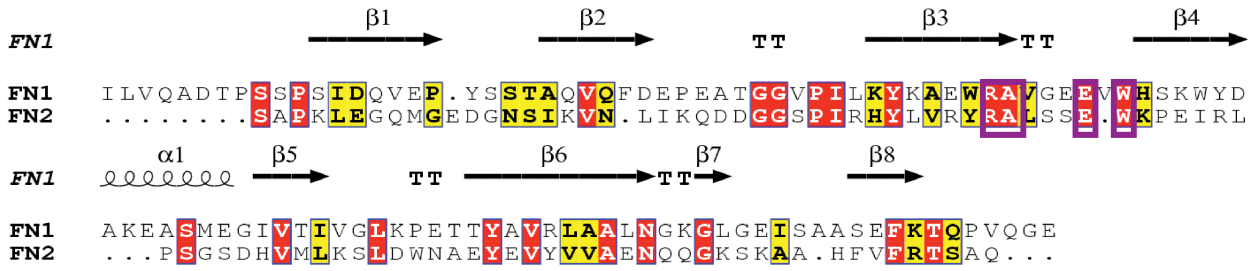

Figure 27: Conservation of the primary sequence between the NCAM FN1 and FN2 domains generated using the ESPript server (208). Conserved residues in the β3−β4 loop are are colored red and similar residues yellow, and purple boxes mark the β3−β4 loop residues conserved between the NCAM FN1 and NCAM FN2 domains.

In the crystal structure of the FN1 domain, it was apparent that the several β3−β4 loop residues that are also conserved between FN1 and FN2 domains might be involved in packing interactions (Fig. 28). For instance, the aliphatic chain of Arg^{538} appears to be stacked against indole ring of Trp^{545}. One can also envision that the benzene ring of phenylalanine as a replacement for Ala^{539} might exhibit stacking interactions with benzene ring of Tyr^{572}. Notably, in our ^{1}H-^{15}N HSQC analysis, Tyr^{572} shows chemical perturbations to some extent upon addition of the SUMO-PBR peptide (Fig. 21). Hence, it is likely that residues in the β3−β4 loop provide conformational stability to the FN domains. Importantly, the β3 and β4 strands directly link acidic patch and GGVPI loop to FN1 α-helix, which has previously been shown to be important for proper positioning of ST8Sia-IV on to the FN1 domain (194). Hence, perturbations in this loop could translate to changes in any of these elements leading to alterations in NCAM polysialylation.

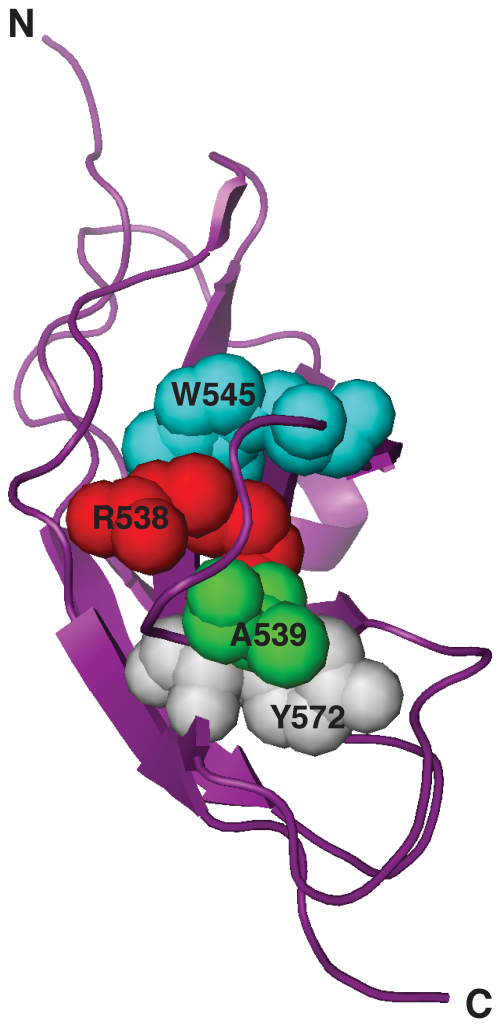

Figure 28: The X-ray crystal structure of the NCAM FN1 domain (PDB 2HAZ) (194) **showing packing interactions between residues of the β3−β4 loop.** Trp^{545} is depicted in cyan, Arg^{538} is depicted in red, Ala^{539} is depicted in green, and Tyr^{572} is depicted in gray.

DISCUSSION

In this chapter, I have described my work demonstrating that the ST8Sia-IV PBR and NCAM FN1 domain are direct interaction partners using ITC and NMR spectroscopy. Furthermore, HSQC NMR analysis allowed us to map the entire footprint of the PBR peptide on the FN1 domain. Among the residues that undergo chemical shift perturbation upon addition of the PBR peptide include not only the FN1 acidic patch residues, but also residues in the Ig5-FN1 linker region and in the adjacent GGVPI loop, as well as those in a distal loop between the β3 and β4 strands on a face opposite of that on which the acidic patch is found. This data, in the context of previous observations made in the laboratory, suggests that binding of PBR at the acidic patch induces a conformational change that translates from the GGVPI loop to the Ig5-FN1 linker region which influences the polysialylation of N-glycans in the Ig5 domain.

Our laboratory has provided ample evidence for the importance of the NCAM FN1 acidic patch and ST8Sia-IV PBR in substrate polysialylation. However, work described in this chapter demonstrates for the first time that the FN1 acidic patch and polyST PBR region directly bind each other, defining this step as the initial recognition event for the process of NCAM protein-specific polysialylation. I envision the FN1 acidic patch as a docking site for the polyST that allows it to subsequently interact with other elements in the Ig5-FN1 tandem in order to properly polysialylate glycans in the Ig5 domain.

Mutating Asp^{520}, Glu^{521}, and Glu^{523} in NCAM FN1 domain simultaneously to alanines reduces NCAM polysialylation, while mutation to arginines eliminates NCAM polysialylation (192). However, mutating the acidic patch residues to arginines or alanines reduces binding of ST8Sia-IV only by ~35% (193). One possibility is that Asp^{498} or Asp^{506} that align with the acidic patch might partially mediate binding. On the other hand, Asp^{498} may be more important for the structural stability of the linker region, considering the detrimental effect of altering the composition or length of this region on NCAM polysialylation (193, 195). Another possibility is that interactions of the polySTs with the Ig5 domain may be important. Indeed, analysis of NCAM-OCAM chimeric proteins suggested that secondary interactions between ST8Sia-IV and the Ig5 domain may stabilize the enzyme-substrate interaction (193,

197).

The importance of "permissive" Ig5 sequences first became apparent when Dr. Matthew Thompson analyzed an NCAM-OCAM chimera. The Olfactory Cell Adhesion Molecule (OCAM) is a protein that has the same domain structure as NCAM and even N-glycans in the Ig5 domain that are identically positioned to those in the Ig5 domain of NCAM, but it is not polysialylated. The FN1 domain of OCAM allows for some recognition of an NCAM-OCAM chimera in which the OCAM FN1 domain replaces that of NCAM. This chimera is polysialylated albeit to a lower extent than the wild type protein. Conversely, the Ig5 domain of OCAM actively blocks polysialylation of a chimera in which it replaces the Ig5 domain of NCAM. Comparison of NCAM and OCAM Ig5 sequences identified large basic residues adjacent to the N-glycans in OCAM Ig5 domain hindered access and N-glycan polysialylation (197). Therefore, one possibility is that any changes in the Ig5-FN1 linker region, GGVPI or NGKG loops that stabilize this linker might impede NCAM binding by ST8Sia-IV if they misalign the Ig5 and FN1 domain and eliminate secondary Ig5 binding. However, earlier work demonstrated that the Ig5 interactions alone in a ΔFN1 mutant are not sufficient for NCAM binding or polysialylation, making it unlikely that they can fully explain the residual binding of the acidic patch mutants. It may be that the residual binding in the absence of polysialylation can be explained by a non-specific and non-productive binding of ST8Sia-IV to NCAM where no polysialylation occurs. Based on my results that show that mutating the acidic patch residues eliminates FN1-PBR binding, it is likely that this non-specific binding involves regions outside the NCAM FN1 domain and the ST8Sia-IV PBR.

The importance of the Ig5-FN1 linker region in maintaining the relationship between the two domains for optimum polysialylation first became apparent when it was observed that insertion of three amino acids to the linker region abrogates NCAM polysialylation (195). This relationship is not only important because of the presence of polySia carrying glycans in the Ig5 domain but also because Ig5 domain bears sequences that provide a secondary interaction with ST8Sia-IV and play a role in proper positioning of the glycans. My ^{1}H-^{15}N HSQC analysis revealed that PBR binding also alters chemical

environment of Gly^{526} and Gly^{527} in the GGVPI loop and all four Ig5-FN1 linker region residues present in the FN1 domain (Gln^{496}, Ala^{497}, Asp^{498}, and Thr^{499}). This raises two possibilities. The first possibility is that binding at the acidic patch relays a conformational change to the linker region via the GGVPI loop that is connected to the acidic patch by only a few residues. As shown in Figure 22B, Gly^{526} of the GGVPI loop forms a hydrogen bond with Asp^{498} of the linker region and thus, it can be envisioned that a conformational change may be translated from the GGVPI loop to the linker region. The second possibility is that the PBR peptide binds the acidic patch as well as the GGVPI loop and this alters conformation of the linker region. This is unlikely since the previous results in the laboratory have shown that the GGVPI loop does not mediate binding to ST8Sia-IV (193). On the other hand, the Ig5-FN1 linker region is connected to the linker region by a stretch of amino acids that contains a Pro^{500}-Ser^{501}-Ser^{502}-Pro^{503} sequence, which has been implicated in binding to the ST8Sia-IV, as well as NCAM polysialylation (193). Interestingly, the serine residues in this sequence are dispensable for polysialylation (193). Because ^{1}H-^{15}N HSQC experiments cannot discern perturbations in proline residues, we cannot conclude involvement of the prolines in the $^{500}PSSP^{503}$ sequence in binding to the PBR peptide and/or relaying a conformational change to the linker region.

These observations might suggest a highly rigid relationship between NCAM Ig5 and FN1 domains for polysialylation. However, when additional N-glycosylation sites were engineered in NCAM FN1 domains at various sites, it became evident that some flexibility in the placement of N-glycans is tolerated (207). Remarkably, engineered N-glycans that were on the same face as that of the two glycosylation sites that are typically polysialylated, were more highly polysialylated. The laboratory therefore proposed an idea of restricted flexibility wherein the Ig5 domain does not have complete rotational freedom but can move closer or farther away from the FN1 domain (207). According to my results, the GGVPI loop also undergoes a conformational change upon PBR peptide binding and this translates to the Ig5-FN1 linker region. This might reflect a restricted freedom in this region and explain why certain engineered glycans sites in Ig5 could be polysialylated. It is interesting to note that the

GGVPI and NGKG loops are conserved in the OCAM FN1 domain; however they are farther apart from the linker region (196).

In addition to chemical shift perturbations in the acidic patch, GGVPI loop, and the Ig5-FN1 linker region, we were surprised to observe perturbations in a distal loop between β3 and β4 strands of the FN1 domain. Mutational analysis of select residues in this loop revealed that NCAM polysialylation is affected depending on choice of amino acid (Fig. 25) suggesting that the residues of this loop are involved in positioning of various elements within the FN1 domain and stabilize the domain structure by forming packing interactions (Fig. 28). Indeed, the β3 and β4 strands connect the FN1 α-helix with the GGVPI loop and in turn, the acidic patch. The α-helix has been previously suggested to play a role in the proper positioning of ST8Sia-IV on the FN1 domain. Mutating it to two threonine residues shifts NCAM polysialylation from NCAM Ig5 N-glycans to FN1 O-glycans (194) but it does not alter binding of ST8Sia-IV to NCAM (193). This observation is confirmed by our ^{1}H-^{15}N HSQC results, as we do not observe any perturbations in the α-helix residues; however, mutating β3-β4 loop residues may affect positioning of ST8Sia-IV and therefore polysialylation. Changes in chemical environment of the β3-β4 loop residues could however be due to a translated conformational change or to induction of local disorder upon binding of the PBR peptide at the acidic patch. It is plausible that the β3-β4 loop serves as a binding site for the 6xHis-SUMO tag; however, using a two-site binding model to interpret my ITC data generated large error values relative to the one-site binding model we have used in our analysis for curve fitting. Another possibility is that the β3-β4 loop mediates a weak dimer effect. However, The FN1 domain is predominantly a monomer in solution, as my SEC data reflects (Fig. 18).

Volkers et al (125) have reported a crystal structure of the α2,8-sialyltransferase, ST8Sia-III (PDB 5BO9). Using this structure, they then modeled ST8Sia-IV, which shares 36% sequence identity, and also performed docking studies using the crystal structure of Ig5-FN1 tandem (PDB 3MTR) (125, 207). According to their model, Glu^{521} in the FN1 domain interacts with Arg^{93} in the ST8Sia-IV PBR

region whereas Glu^{523} interacts with the basic residues in the PSTD. The PSTD is next to the small sialylmotif SMS and mutations in PSTD basic residues have been shown to reduce NCAM polysialylation (198, 199) Moreover, Nakata et al. (198) postulated that PSTD basic residues form a basic surface that anchors the growing polySia chain. In support of this hypothesis, the Volkers model suggests that the PBR and PSTD regions together form a basic surface that provides an interaction interface for the negatively charged polySia chain growing on substrates (125). Indeed, our immunoblotting analysis using an anti-polySia antibody shows that when Glu^{523} is mutated to arginine, polysialylated NCAM migrates at a lower molecular mass (Fig.23). However, as mentioned above, Glu^{523} is found in a crowded region of the ^{1}H-^{15}N HSQC spectrum so I could not definitively conclude its involvement in the interaction with the PBR peptide.

Given the restricted physiological expression of polySia normal tissues, and its overexpression in pathological conditions, such as cancer, the polyST-substrate recognition interface is an attractive target for the inhibition of polysialylation in diseases such as cancer. My findings reported in this chapter may be exploited for the design competitive inhibitors of the polysialylation process. Attempts I have made in order to design and deliver PBR peptide to the polySia expressing cells are described in chapter VI.

CHAPTER IV

Elucidating the Requirements for NRP-2 Polysialylation Establishes a Two Domain Paradigm for Protein–Specific Polysialylation.

(Parts of this chapter have been published in Bhide GP, Fernandes NR, Colley KJ, Sequence Requirements for Neuropilin-2 Recognition by ST8SiaIV and Polysialylation of Its *O*-Glycans, J Biol Chem, 2016, 291 (18): 9444-9457).

Introduction:

Neuropilin-1 and -2 (NRPs) are type I glycoproteins that associate with various cell surface signaling receptors, such as TGFβ receptor, VEGF receptor and plexins. NRPs are mostly believed to be incapable of signaling independently owing to their short cytoplasmic tails. However, NRPs modulate signaling of their coreceptors by participating in ligand binding as well as by altering their intracellular trafficking (209, 210). The importance of NRPs in development is demonstrated by their knockout phenotypes. The NRP-1 knockout in mice is embryonic lethal and is characterized by severe cardiovascular and neuronal defects (211, 212). The NRP-2 knockout phenotype is relatively mild. These mice are viable but show defects in axon guidance and lymphatic system development (213, 214). Members of the chemorepulsive semaphorin 3A family, via their interaction with NRPs, have been shown to mediate growth cone collapse (212, 215), and this axis is also crucial for the formation of cranial and spinal nerve projections (216). VEGFs can signal via VEGF receptors without NRPs; however, NRPs enhance chemotaxis and migration during angiogenesis in response to VEGF stimulation (217). Various semaphorin and VEGF family ligands have a complex pattern of NRP specificity. For example, VEGF-A165 binds to both NRPs; however, VEGF-A145 binds exclusively to NRP-2 (210, 218). Overall, NRP-1

binds a larger variety of ligands, partially explaining the severity of its knockout phenotype.

NRPs have two CUB (Complement binding factors c1s/c1r, Uegf, Bmp1 (bone morphogenic protein)) domains, two FV/VIII (coagulation Factor V/VIII homology) domains and a MAM (Meprin-A5 antigen-μ tyrosine phosphatase) domain (210). The CUB domains are important for binding to semaphorins (215, 219), whereas the FV/VIII domains are involved in binding to VEGF as well as heparin (220–222). I have established the role of the MAM domain as polyST recognition domain for NRP-2 polysialylation (223), however others' work suggest that it also plays a role in dimerization. Using co-immunoprecipitation experiments, Nakamura et al. (215) suggested that the MAM domain mediates NRP dimerization. However, an X-ray crystal structure by Appleton et al. (221) suggests that the CUB domains may be important for dimerization. However, using dynamic light scattering experiments, Appleton et al. have shown that the soluble NRP constructs containing MAM domains and CUB domains are not dimerized (221). Heparin has also been implicated in NRP dimerization via FV/VIII domains (222). More recent studies using the purified NRP-1 MAM domain also preclude dimerization via the MAM domain (224). Finally, the cytoplasmic tails of NRPs, albeit short, have been shown to govern their intracellular trafficking along with their co-receptors (225).

NRPs are upregulated in various cancers including non-small cell lung carcinoma (NSCLC), neuroblastoma, glioma, astrocytoma, colorectal, pancreatic, and breast cancers where they promote survival, migration, and proliferation (reviewed in (209, 210, 226, 227). Interestingly, many of these cancers also express elevated levels of polySia (186). The direct link between polySia and NRP expression in cancers is yet to be established; however Tanaka et al have reported that a large number of stage IV NSCLCs are NCAM-negative and polySia-positive (187).

NRP-2 was first found to be polysialylated by ST8Sia-IV in mature dendritic cells (mDCs). In this report, polySia on NRP-2 was shown to impede T-cell activation by the mDCs (106). PolySia on NRP-2 binds the chemokine CCL21 and drives the chemotaxis of mDCs toward lymph nodes by

promoting the CCL21-CCR7 interaction (108, 109). However, it was recently shown that CCR7 receptor itself is polysialylated raising questions about the role of polysialylated NRP-2 in chemotaxis (110). Other cell types that express polysialylated NRP-2 are THP-1 macrophages (228) and microglia (107). Interestingly, polysialylated NRP-2 is localized to the Golgi in microglia. Upon stimulation with lipopolysaccharide, this pool translocates to the cell surface. Remarkably, production of nitric oxide was lower in microglial cells expressing polySia suggesting a role of polysialylated NRP-2 in amelioration of inflammation (107).

Rollenhagen et al. (229) reported that NRP-2 is polysialylated on core-1 as well as core-2 O-glycans in the linker region between the MAM domain and FV/VIII domains. Using mutational analysis, they showed that at least four different threonine residues in this region carry most of the polySia (229). Notably, in this linker region NRP-1 is modified by a heparan sulfate or chondroitin sulfate glycosaminoglycan (GAG) chain (230), which sequesters VEGF and modulates VEGF signaling depending on the composition of the GAG chain. The presence of this GAG chain has also been shown to enhance migration of vascular smooth muscle cells in response to Platelet Derived Growth Factor (PDGF) (231). It is therefore plausible that polySia in NRP-2 linker region may play a similar role in chemotaxis by acting as a reservoir for VEGF and modulating VEGF signaling.

Our laboratory has demonstrated that specific elements within the NCAM FN1 domain govern polysialylation of N-glycans on the adjacent Ig5 domain, as shown in Figure 29 (191, 193). I therefore hypothesized that the MAM domain of NRP-2 serves as a recognition domain for polysialylation of O-glycans in the FV/VIII-MAM linker region by ST8Sia-IV. In this chapter, I describe my work to investigate the basis of NRP-2 recognition and polysialylation by ST8Sia-IV and also discuss NRP-1 as a potential polyST substrate.

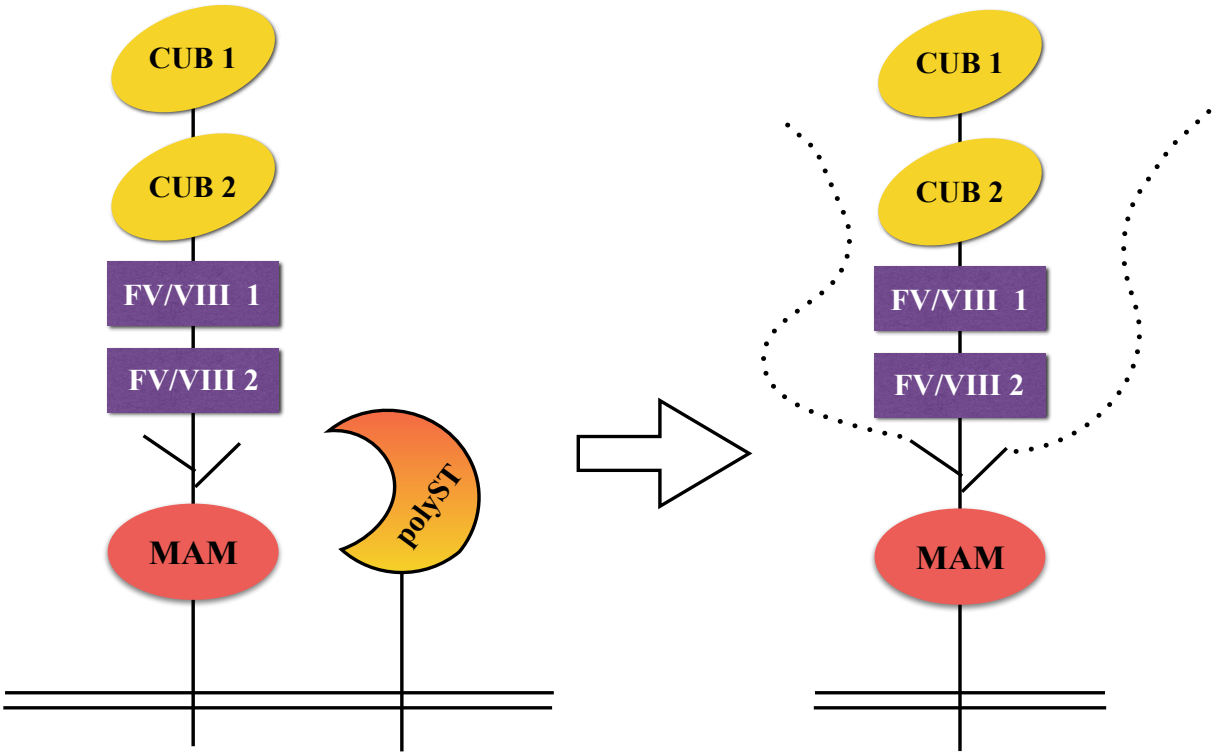

Figure 29: Working model for the polysialylation of NRP-2. PolySTs recognize and dock at the MAM domain to polysialylate O-glycans (represented by dashes) in the FV/VIII-MAM linker region.

RESULTS:

A. The NRP-2 MAM-linker tandem is sufficient for polysialylation.

In order to determine the minimum unit required for NRP-2 polysialylation by ST8Sia-IV, I first made V5-tagged domain deletion mutants of NRP-2, shown in Figure 30.

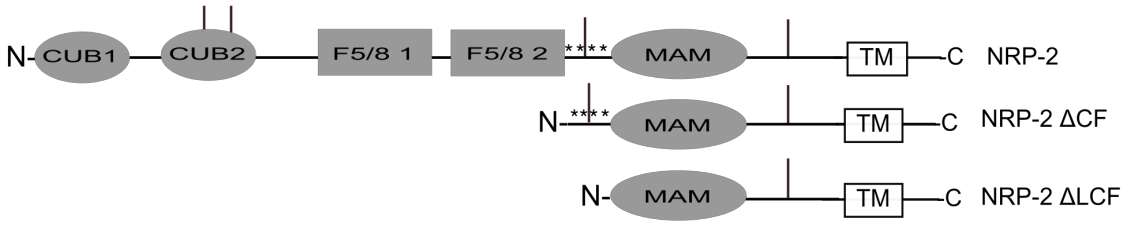

Figure 30: Schematic representation of domain deletion mutants of NRP-2. Asterisks represent locations of O-glycans and dashes represent locations of N-glycans.

The intracellular localization and folding of these mutants was assessed by inverted confocal microscopy using an anti-V5 antibody and FITC-conjugated goat anti-mouse antibody. Wild type NRP-2 and NRP2 ΔCF were localized to Golgi and the plasma membrane, as expected for secretory pathway proteins trafficking to the plasma membrane. NRP2 ΔLCF exhibited a reticular staining pattern suggesting that this protein was localized in the ER and possibly misfolded, potentially due to loss of an N-glycan in the linker region between the MAM and FV/VIII domains. This protein still retains an N-glycan in the stem region between transmembrane region and MAM domain (Figs. 30 and 31).

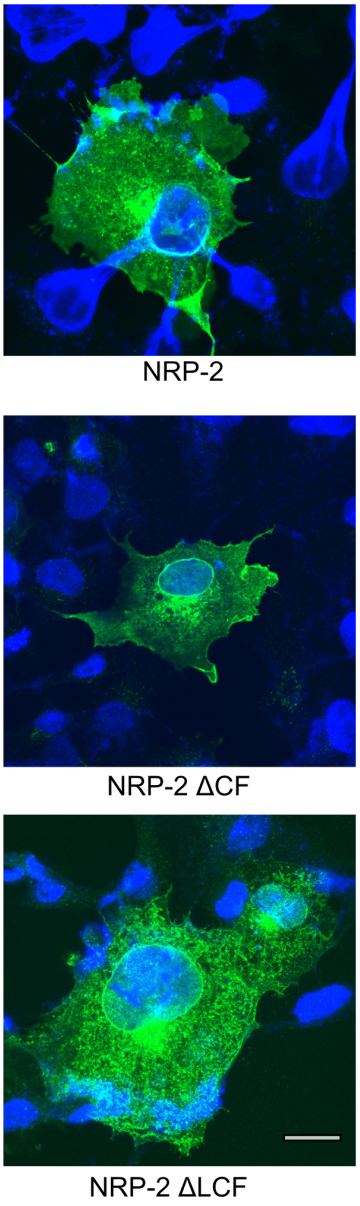

Figure 31: Intracellular localization of NRP-2 domain deletion mutants. V5-tagged NRP-2 and its domain deletion mutants were expressed in COS-1 cells and their localization was determined using an anti-V5 tag antibody and a FITC goat anti-mouse antibody (green). Nuclei were stained with DAPI (blue). Cells were visualized using a Zeiss LSM 700 inverted confocal micro- scope, equipped with an AxioCam digital microscope camera using a 100X oil immersion objective at room temperature. Bar = 20 μM.

In order to confirm ER localization of the NRP2 ΔLCF protein, I immunoprecipitated it from COS-1 cell lysates using an anti-V5 antibody and digested it with endoglycosidase H (Endo H). This enzyme cleaves high-mannose type N-glycans, which are mostly found in the ER as processing by the Golgi N-acetylglucosaminyltransferase I (GlcNAcT-1) renders N-glycans insensitive to Endo H digestion (REF). Upon treating with Endo H, NRP-2 ΔLCF migrated at a lower molecular weight on an SDS-PAGE gel, suggesting that it carries high mannose glycans and is likely to be ER localized (Figure 32).

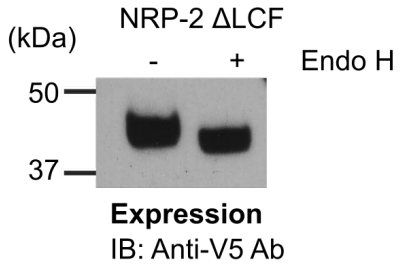

Figure 32: Endoglycosidase H digestion of NRP-2 ΔLCF protein N-glycans. NRP-2 ΔLCF was expressed in COS-1 cells and 50% of the lysate was treated with Endo H for 2 h at 37°C. The molecular mass of the treated and untreated protein was assessed by reducing and denaturing SDS-PAGE and immunoblotting with an anti-V5 antibody.

Next, these V5-tagged proteins were coexpressed with myc-tagged ST8Sia-IV in COS-1 cells, immunoprecipitated with the anti-V5 tag antibody, and immunoblotted with the 12F8 anti-polySia antibody to assess their polysialylation. A small aliquot of the lysate was boiled with Laemmli sample buffer containing 10% BME to remove polySia, and immunoblotted with the anti-V5 tag antibody to evaluate protein expression levels. I observed that the NRP-2 ΔCF protein was capable of being polysialylated, albeit to a slightly lesser extent than the wild type protein. The NRP-2 ΔLCF protein was not polysialylated, as expected (Fig 33A). However, its lack of polysialylation could be due to either the absence of the linker region or its ER localization (Figs. 30 and 32). Domain deletions may redirect the polyST to polysialylate glycans not polysialylated on the wild type protein, as observed in the case of NCAM7. In this case, when the NCAM Ig5 domain and therefore N-glycans that typically carry polySia were deleted, and surprisingly FN1 domain O-glycan polysialylation was observed (191). We evaluated this possibility for the NRP-2 ΔCF protein by treating the immunoprecipitated protein with PNGase-F to remove N-glycans. Polysialylation was unaffected verifying that the NRP-2 ΔCF protein was polysialylated on O-glycans like NRP-2.

What could cause the lower polysialylation of NRP-2 ΔCF protein? The FV/VIII-2-MAM linker region could be structurally destabilized due to absence of N-terminal domains and its glycosylation compromised. In line with this idea, the NRP-2 ΔCF protein migrated as a doublet, suggesting that the two bands in the doublet represented different glycoforms. I therefore performed PNGase-F digestion on the immunoprecipitated NRP-2 ΔCF protein (detected with anti-V5 antibody). This treatment reduced the molecular mass of the upper band but not the lower band, indicating that the upper band contained N-glycans, and the lower band lacked any N-glycans suggesting a compromised glycosylation (Figs. 33B and 33C). This suggested that the lower band could also lack the O-glycans necessary for polysialylation, explaining at least in part, the reduced polysialylation of the NRP-2 ΔCF protein.

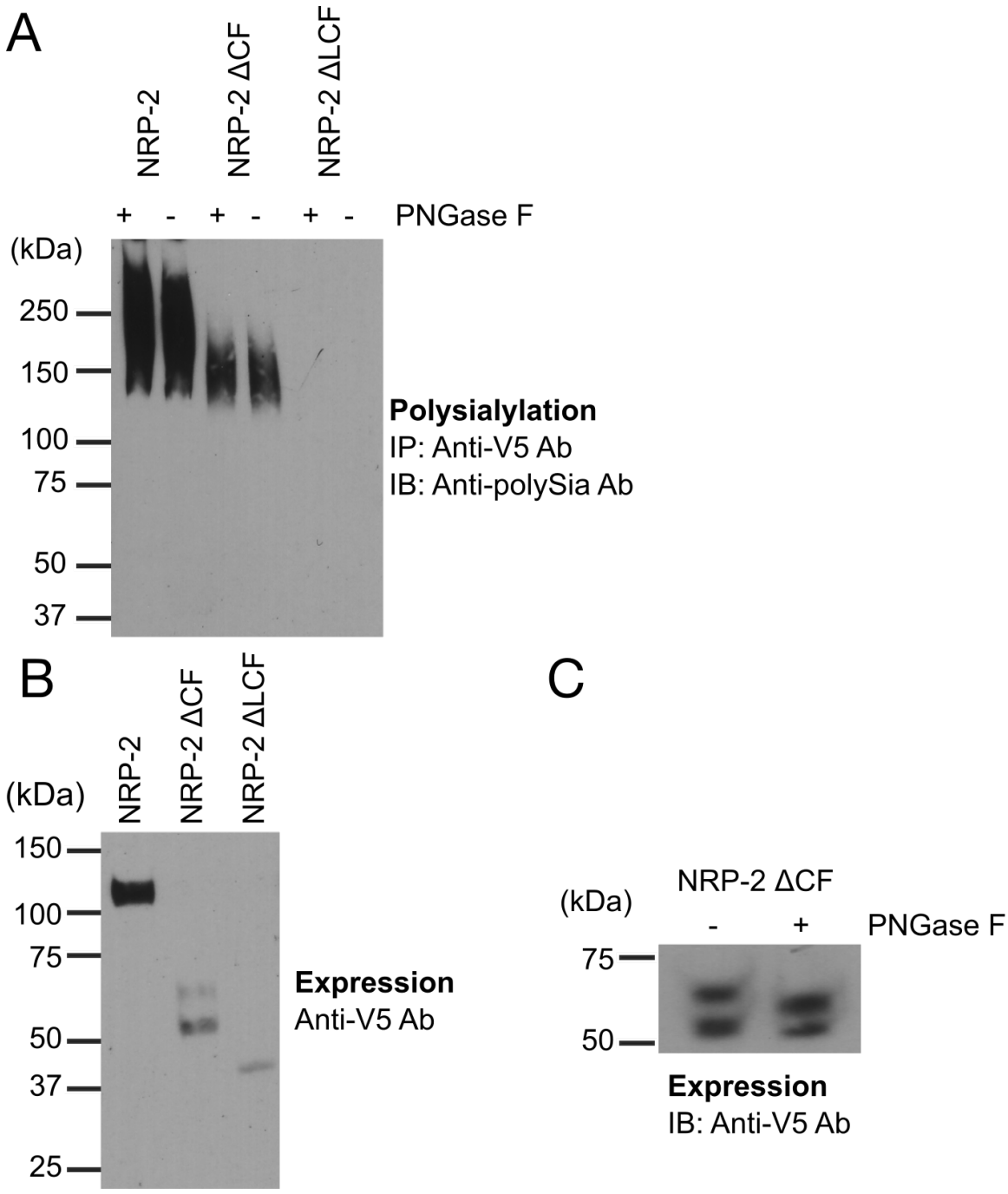
A
NRP-2
NRP-2 ΔCF
NRP-2 ΔLCF
+ - + - + - PNGase F
(kDa)
250
150
100
75
50
37
Polysialylation
IP: Anti-V5 Ab
IB: Anti-polySia Ab
B
NRP-2
NRP-2 ΔCF
NRP-2 ΔLCF
(kDa)
150
100
75
50
37
25
Expression
Anti-V5 Ab
C
NRP-2 ΔCF
(kDa)
- + PNGase F
75
50
Expression
IB: Anti-V5 Ab

Figure 33: Polysialylation and glycosylation analysis of NRP-2 domain deletion mutants. V5-tagged wild-type NRP-2 and its domain deletion mutants were co-expressed with myc-tagged ST8Sia-IV in COS-1 cells. A, Immunoprecipitated proteins were divided in two portions and one portion was treated with PNGase-F overnight at 37°C. Both portions were subjected to SDS PAGE and then immunobloted with an anti-polySia antibody. B, Relative expression levels of these proteins were determined by boiling an aliquot of lysate in Laemmli sample buffer and immunoblotting with an anti-V5 antibody. C, The NRP-2 ΔCF protein was expressed in COS-1 cells and a half the lysate was treated with PNGase-F at 37°C overnight. The molecular mass of the treated and untreated proteins was assessed by SDS-PAGE and immunoblotting with an anti-V5 antibody.

B. Replacing the NRP-2 MAM domain with the NRP-1 MAM domain results in lower levels of polysialylation.

The NRP-2 MAM domain and the linker region are sufficient for polysialylation but does MAM domain hold a key to protein specific polysialylation? In other words, can the analogous NRP-1 MAM domain replace NRP-2 MAM domain for the process of polysialylation? To determine this we replaced MAM domain of NRP-2 with that of NRP-1 to create the NRP-2Δ1 chimera and replaced the MAM domain of NRP-1 with that of NRP-2 to create NRP-1Δ2 chimera (Figure 34). At the time this experiment was performed, I expected that the NRP-1 MAM domain would not replace the NRP-2 MAM domain to support polysialylation, because the polysialylation of NRP-1 had not been previously reported.

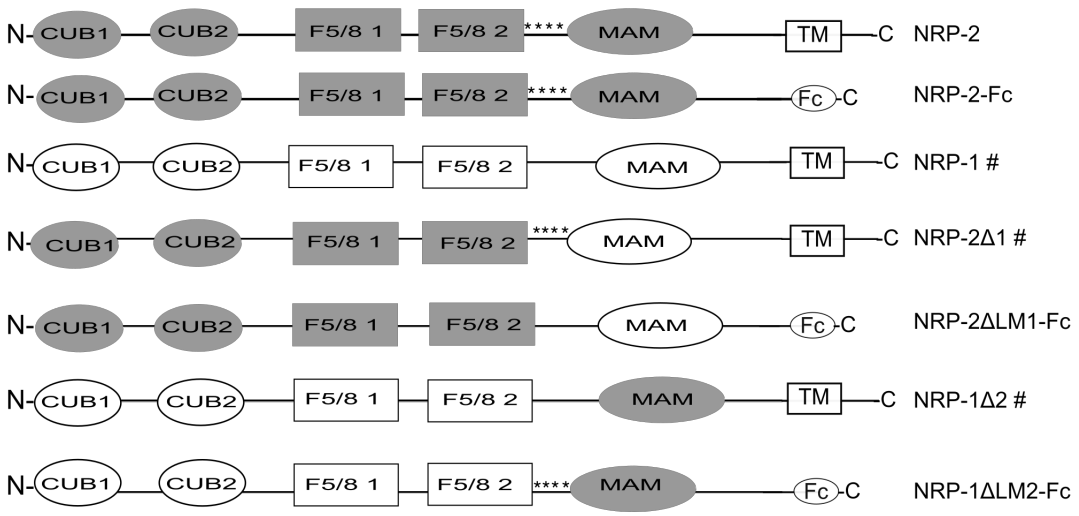

Figure 34: Schematic representation of NRP MAM domain chimeric proteins. Asterisks represent O-glycan sites that have been shown to be polysialylated in vivo (229). Proteins that were used in this study in membrane bound and soluble Fc forms are marked with a #.

V5-tagged NRP-1, NRP-2, NRP-2Δ1, and NRP-1Δ2 were coexpressed with ST8Sia-IV-myc in COS-1 cells. Proteins were immunoprecipitated with an anti-V5 tag antibody and their polysialylation evaluated by immunoblotting with an anti-polySia antibody. Indeed, replacing NRP-2 MAM domain with that of NRP-1 reduced its polysialylation significantly to 18 ± 11% (S.D.) of wild type levels. However, to our surprise, NRP-1 was also polysialylated by ST8Sia-IV, and this had never been reported previously. Taking expression levels into account, NRP-1 polysialylation was 47 ± 9% (S.D.) that of NRP-2. Finally, swapping the NRP-1 MAM domain with the NRP-2 MAM domain led to an approximately 30% increase in its polysialylation (to 77 ± 22% (S.D.) of NRP-2) (Fig. 35).

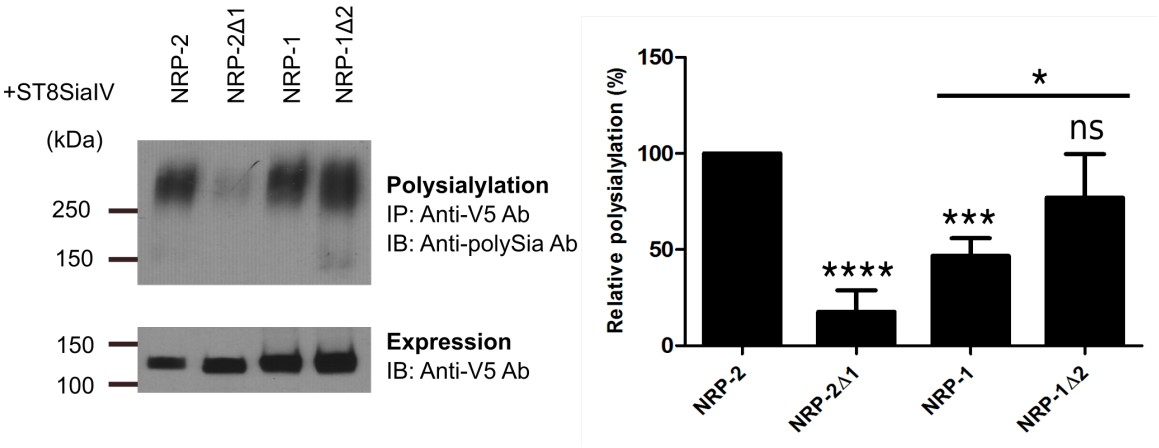

Figure 35: Polysialylation of NRP MAM domain chimeras. NRP-1, NRP-2 and the NRP chimeric proteins were expressed in COS-1 cells with ST8Sia-IV-myc and their polysialylation was assessed immunoblotting with anti-polySia antibody after immunoprecipitation (top left panel). Prior to immunoprecipitation, an aliquot of cell lysate was boiled and immunoblotted with anti-V5 antibody to evaluate the protein expression level (bottom left panel). The right panel shows quantification of relative polysialylation in comparison to wild type NRP-2, which is normalized to 100%. Statistics were performed on 5 different experiments with error bars representing S.D. values. Statistical analysis was performed using unpaired Student's t-test, where *$0.01<p<0.05$; ***, $0.0001<p<0.001$; ****, $p<0.0001$; *ns*, $p>0.05$. Pair-wise comparisons between specific proteins are indicated by a line above the compared bars in the graph.

Differences in polysialylation of the chimeric proteins could also be influenced by differences in their intracellular localization and trafficking. To assess these variables, I expressed the chimeric proteins in COS-1 cells and after permeabilizing and fixing the cells, stained the proteins using anti-V5 antibody and FITC-conjugated goat anti-mouse secondary antibody and localized them using inverted confocal microscopy (Fig. 36).

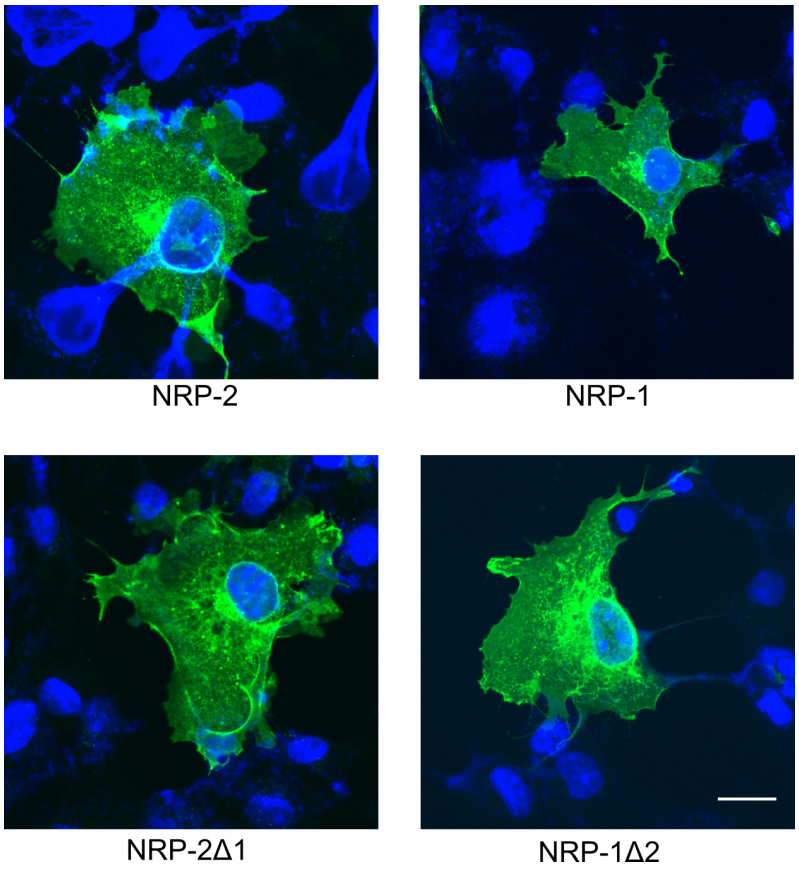

Figure 36: Intracellular localization of NRP MAM domain chimeric proteins. V5-tagged NRP MAM chimeric proteins were expressed in COS-1 cells. Cells were fixed and permeabilized using -20°C methanol and their localization was determined using an anti-V5 antibody and FITC-goat anti-mouse antibody (green). Nuclei were stained with DAPI (blue). Bar = 20 μM

As expected for overexpressed secretory pathway proteins, NRP-2 and NRP-1 were localized primarily to the Golgi and cell-surface; however the NRP-2Δ1 and NRP-1Δ2 showed increased reticular staining in addition to Golgi and cell-surface staining, suggesting that these proteins may take longer to fold or to traffic to the cell surface. As a result, it is possible that the chimeric proteins are capable of achieving higher polysialylation levels than observed in this expression system.

C. Intracellular trafficking plays a role in the polysialylation of NRPs.

The polysialylation of NRP-1 was an unexpected result, as mere overexpression of polySTs in cells does not lead to polysialylation of non-substrate glycoproteins. For instance, upon overexpression of polySTs in COS-1 cells, the only polysialylated proteins identified were the autopolysialylated polySTs (137). Furthermore, co-expression of cell-surface glycoproteins such as human chorionic gonadotropin or CD4 with ST8Sia-IV did not lead to their polysialylation (Dr. Brett Close and Gaurang Bhide, unpublished results). NRP-1 has a Ser-Glu-Ala (SEA) sequence at the C-terminus that engages with PDZ domain of GIPC/synectin, which links it in turn to the cytoskeletal motor myosin VI (232). GIPC/Synectin has been shown to play an active role in endocytosis and membrane trafficking (233). The importance of the NRP-1 SEA sequence was highlighted in endothelial cells where it was shown to be involved in association with Rab-11 positive recycling endosomes and to alter the intracellular fate of VEGFR-2 by preventing its lysosomal degradation upon VEGF stimulation (225). Differences in cytoplasmic tail sequences of the NRPs leads to their association with different Rab compartments and to different intracellular fates (234). The importance of NRP cytoplasmic sequences in their trafficking is further suggested by the data from Bae et al. (235) that shows stabilization of NRP-2, but degradation of NRP-1, in hypoxic conditions.

These differences in trafficking led me to ask whether the polysialylation of NRP-1 might be the result of its repeated recycling from the cell surface to ST8Sia-IV positive compartments like the trans Golgi and TGN. So despite weaker recognition by ST8Sia-IV, NPR-1 may be polysialylated due to repeated encounters with ST8Sia-IV. To explore this possibility, I generated soluble forms of NRP-1,

NRP-2 and the NRP chimeric proteins by replacing their transmembrane regions and cytoplasmic tails with an antibody Fc fragment. This allowed these proteins a single pass through the secretory pathway prior to their secretion into the extracellular space, and excluded the possibility that NRP-1 would be recycled from the cell surface. The secretion of these proteins from the cell will also indicate that these proteins are properly folded.

Soluble NRP-1, NRP-2, NRP-1Δ2 and NRP-2Δ1 were coexpressed with ST8Sia-IV in COS-1 cells. Fc-tagged proteins were recovered from the cell medium using protein A-Sepharose beads and their polysialylation assessed by immunoblotting with an anti-polySia antibody. A portion of the protein A-Sepharose beads was boiled with Laemelli sample buffer and immunblotted with HRP-conjugated anti-human IgG to obtain the relative expression levels of the proteins. I observed that the polysialylation of NRP-2Δ1-Fc was 38 ± 13% (S.D.) that of NRP-2-Fc polysialylation. Interestingly, NRP-1-Fc polysialylation was virtually undetectable, in stark contrast to the membrane-bound form (see Fig. 37). However, replacing its MAM domain with that of NRP-2 in the NRP-1Δ2-Fc protein, led to a significant increase in its polysialylation to 51 ± 11% (S.D.) of that observed for NRP-2-Fc, suggesting that the NRP-2 MAM domain contains sequences required for optimum recognition by ST8Sia-IV (Fig. 37).

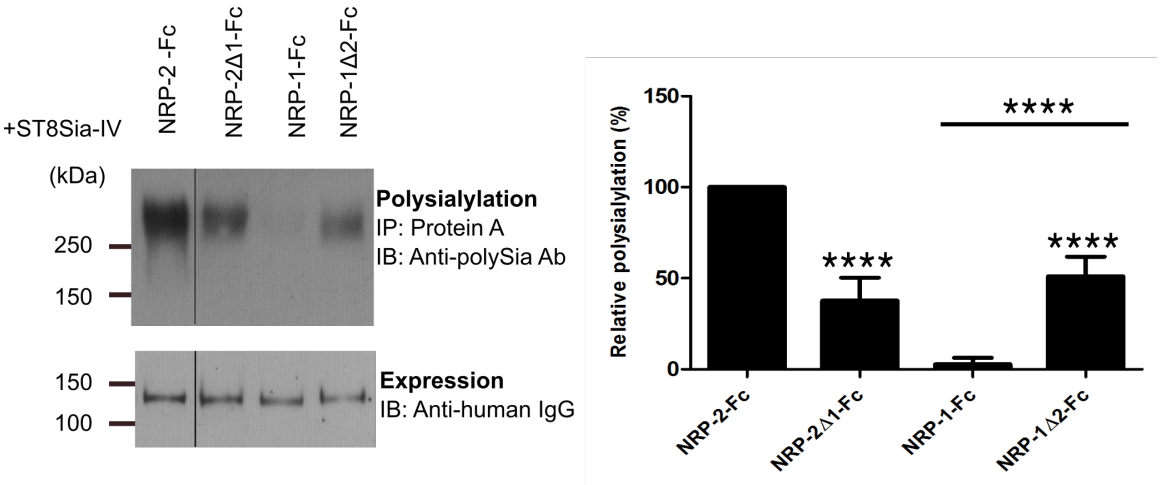

Figure 37: Polysialylation of soluble NRP MAM chimeras. Soluble, Fc-tagged NRP-2, NRP-1 and NRP MAM chimeras were co-expressed with ST8Sia-IV-myc in COS-1 cells and were recovered from cell medium using protein A-Sepharose beads. Their polysialylation was assessed by immunoblotting with an anti-polySia antibody (top left panel). Ten percent of the protein bound beads was boiled and immunoblotted with HRP-conjugated anti-human IgG to evaluate protein expression levels (bottom left panel). The *line* separating NRP-2-Fc and NRP-2Δ1-Fc reflects the removal of an extraneous lane so that the chimera and NRP-2-Fc can be more directly compared. The right panel shows quantification from 7 different experiments with error bars representing S.D. values. Statistical analysis was performed with respect to wild type NRP-2, which is normalized to 100%, using an unpaired Student's t-test, where ****, $p < 0.0001$.

D. The NRP-2 MAM domain-linker region tandem are necessary and sufficient for polysialylation by ST8Sia-IV.

As shown in Figure 37, the MAM domain of NRP-2 promotes polysialylation of NRP-1Δ2 that possesses NRP-1 linker region. However, it doesn't bring polysialylation of this chimera back to the level of full-length NRP-2, suggesting that sequences beyond MAM domain, likely the O-glycan containing linker region, might be essential for optimum polysialylation. To test this idea, I swapped the MAM domains as well as linker regions of NRPs the LM chimeras (NRP-2ΔLM1-Fc and NRP-1ΔLM2-Fc in Figure 34). These constructs were then coexpressed with ST8Sia-IV in COS-1 cells, precipitated from the cell medium using protein A-Sepharose and their polysialylation was compared with Fc-tagged wild type proteins as well as NRP-2Δ1 and NRP-1Δ2 by immunoblotting (Fig. 38). Remarkably, replacing the NRP-2 linker region and MAM sequences with those in NRP1 (NRP-2ΔLM1) led to near-complete loss of polysialylation (8 ± 9% (S.D.) of wild type NRP-2). On the other hand, replacing the NRP-1 linker region and MAM sequences with those in NRP-2 (NRP-1ΔLM2), brought polysialylation of the chimera up to the level of NRP-2 (98 ± 25% (S.D.) of wild type NRP-2) (Fig. 38). These results and those previously obtained for NCAM polysialylation establish a two-domain paradigm for protein-specific polysialylation.

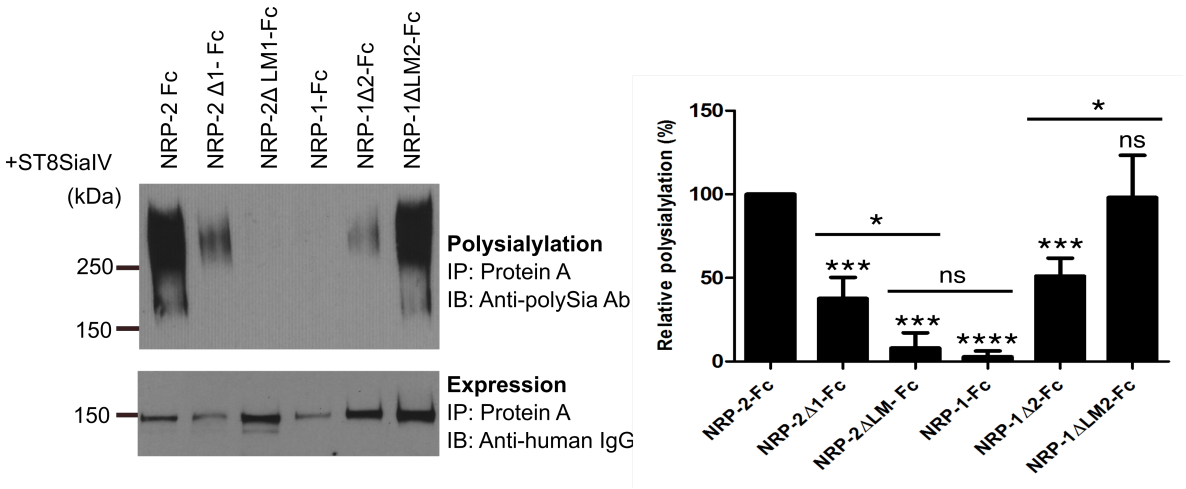

Figure 38: Polysialylation of NRP linker-MAM (LM) chimeras. Fc-tagged NRP-2, NRP-1 and NRP chimeric proteins were expressed with ST8Sia-IV-myc in COS-1 cells and their polysialylation was assessed by immunoblotting with an anti-polySia antibody after precipitating with protein A-Sepharose beads (left panel). A portion of beads were boiled Laemmli sample buffer and immunoblotted with HRP-conjugated anti-human IgG antibody to evaluate the expression levels of the chimeric proteins (bottom left panel). The right panel shows quantification from 4 different experiments with error bars representing S.D. values. Statistical analysis was performed with respect to wild type NRP-2, which is normalized to 100%, using an unpaired Student's t-test, where *, $0.01< p< 0.05$; ***, $0.0001< p< 0.001$; ****, $p <0.0001$; *ns*, $p>0.05$. Pair-wise comparisons between specific proteins are indicated by a line above the compared bars in the graph.

E. The NRP-2 MAM domain mediates recognition by ST8Sia-IV.

As shown in Figure 38, replacing NRP-1-Fc MAM domain with NRP-2 MAM domain allowed for polysialylation of the chimera (NRP-1Δ2-Fc), even in the presence of the NRP-1 linker region. This suggests that MAM domain is crucial for recognition by ST8Sia-IV. Our laboratory has previously shown that protein-specific polysialylation of NCAM involves a direct recognition event between ST8Sia-IV and the NCAM FN1 domain (193). Here I ask whether the initial recognition event between ST8Sia-IV and the NRP-2 MAM domain drives NRP-2 polysialylation.

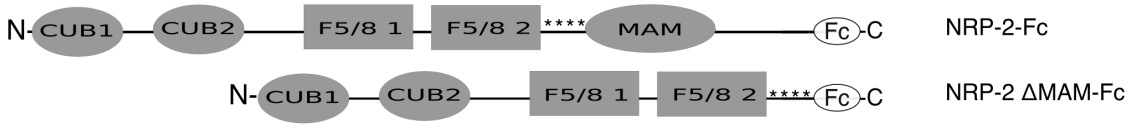

Figure 39: Schematic representation of the Fc-tagged NRP-2 ΔMAM mutant. Asterisks represent O-glycan sites that have been shown to be polysialylated in vivo (229).

To address this question, I created an Fc-tagged NRP-2 ΔMAM construct (Fig. 39). To determine whether NRP-2 ΔMAM can be polysialylated, I expressed this protein with ST8Sia-IV in COS-7 cells and precipitated it from the cell medium to compare its polysialylation to wild type NRP-2 by immunoblotting. As expected, this mutant is not polysialylated (Fig. 40A). Next, to determine whether NRP-2 MAM domain mediates binding to ST8Sia-IV, I performed pull-down experiments. I individually expressed ST8Sia-IV-myc and NRP-2 ΔMAM-Fc in COS-7 cells, and immobilized ST8Sia-IV on magnetic beads coupled to an anti-myc antibody. I incubated the ST8Sia-IV-bound magnetic beads with cell medium containing secreted NRP-2-Fc or NRP-2 ΔMAM-Fc proteins. Following an incubation step, I recovered the magnetic beads and immunoblotted for the Fc tag to evaluate whether the NRP proteins co-immunoprecipitated with ST8Sia-IV-myc. I observed that deletion of MAM domain resulted in significantly less binding to ST8Sia-IV-myc (17 ± 14% (S.D.) of wild type NRP-2-Fc), indicating that MAM domain is required for NRP-2 interaction with ST8Sia-IV (Fig. 40B).

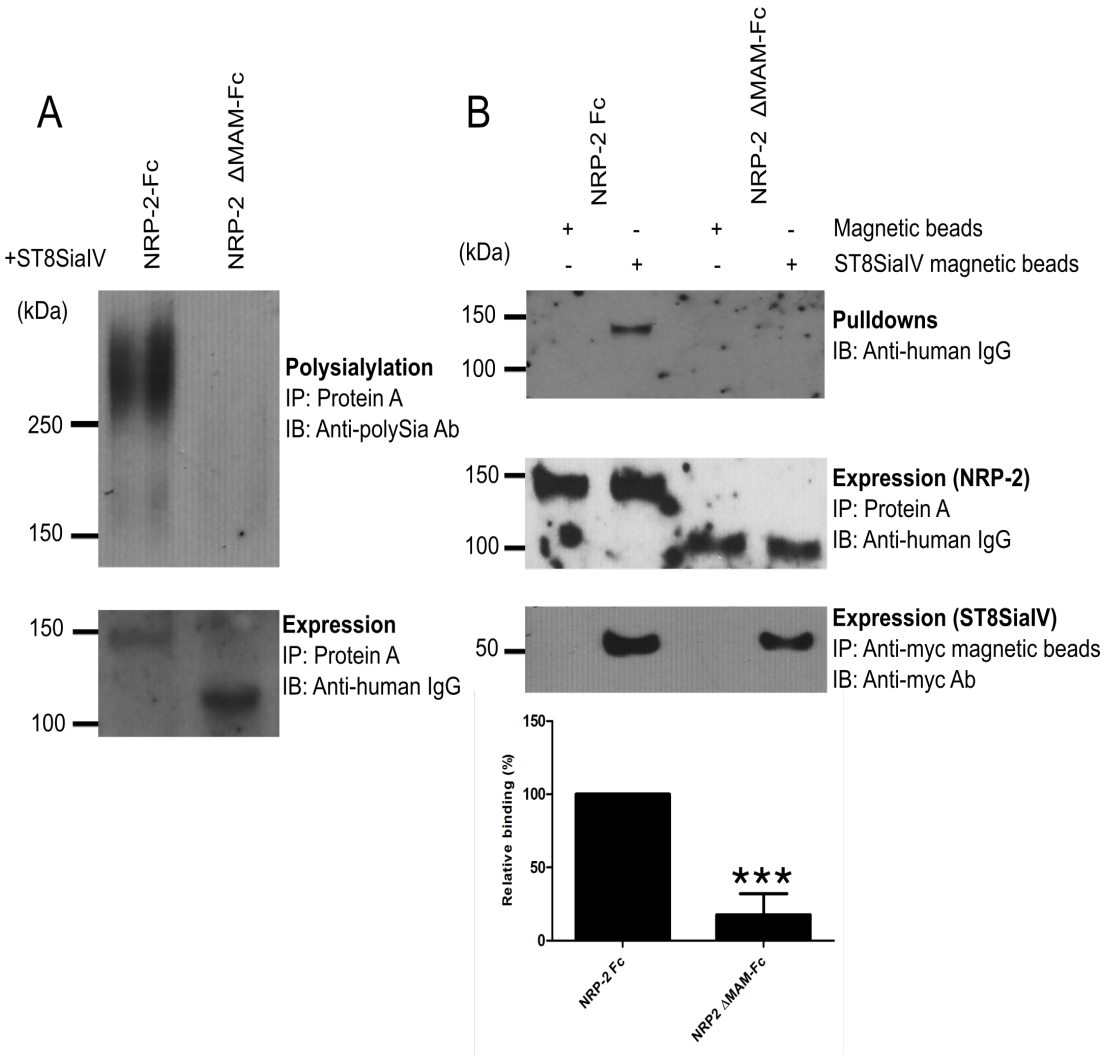
A
NRP-2-Fc
NRP-2 ΔMAM-Fc
+ST8SiaIV
(kDa)
250
150
Polysialylation
IP: Protein A
IB: Anti-polySia Ab
150
100
Expression
IP: Protein A
IB: Anti-human IgG
B
NRP-2 Fc
NRP-2 ΔMAM-Fc
+ - + - Magnetic beads
- + - + ST8SiaIV magnetic beads
(kDa)
150
100
Pulldowns
IB: Anti-human IgG
150
100
Expression (NRP-2)
IP: Protein A
IB: Anti-human IgG
50
Expression (ST8SiaIV)
IP: Anti-myc magnetic beads
IB: Anti-myc Ab
Relative binding (%)
150
100
50
0
***
NRP-2 Fc
NRP2 ΔMAM-Fc

Figure 40: The NRP-2 MAM domain is essential for recognition as well as polysialylation by ST8Sia-IV. (A) Co-expression of NRP-2-Fc and NRP-2 ΔMAM-Fc proteins with ST8Sia-IV-myc in COS-7 cells shows that deletion of the MAM domain results in complete loss of polysialylation. (B) ST8Sia-IV, NRP-2-Fc, and NRP-2 ΔMAM-Fc were individually expressed in COS-7 cells cultured in serum-free medium. Anti-myc magnetic beads were loaded with ST8Sia-IV-myc, cell media containing either NRP-2-Fc or NRP-2 ΔMAM-Fc were incubated with either anti-myc magnetic beads (control) or ST8SiaIV-bound anti-myc magnetic beads. Proteins bound to the magnetic beads were released and immunoblotted with HRP-linked anti-human IgG to determine the proportion of NRP-2-Fc or NRP-2 ΔMAM-Fc bound to ST8SiaIV-myc (*top*). An aliquot from the medium was incubated with protein A-Sepharose and was immunoblotted with HRP-linked anti-human IgG to assess the relative expression levels of NRP-2-Fc and NRP-2 ΔMAM-Fc (*middle*). The amount of ST8Sia-IV in complex with the NRP-2-Fc proteins was determined by immunoblotting these complexes with the anti-myc antibody (*bottom*). Quantification of the experimental results was performed as described under "Methods and Materials" with data from 3 different experiments and error bars representing S.D. Statistical analysis was performed with respect to wild type NRP-2, which is normalized to 100%, using an unpaired Student's *t* test, where ***, $0.0001<p<0.001$.

F. Glu^{652} and Glu^{653} in the NRP-2 MAM domain are important for polysialylation of NRP-2.

Previous work from our laboratory has characterized importance of an acidic patch in the NCAM FN1 domain for polyST recognition and polysialylation. When Asp^{520}, Glu^{521}, and Glu^{523} in this domain are mutated to arginines, NCAM polysialylation is abolished (192). In my work, I have demonstrated that the FN1 acidic patch directly binds ST8Sia-IV PBR (discussed in Chapter IV) (236). I therefore wondered whether NRP-2 MAM domain has similar acidic residues that might serve as a ST8Sia-IV recognition element. I modeled the NRP-2 MAM domain on the crystal structure of the meprin-A MAM domain (PDB 4GWN) using Swiss-Model (237–241) (Figure 41). Interestingly, I observed two residues, Glu^{652} and Glu^{653}, that formed an exposed surface patch similar to Asp^{520}, Glu^{521}, and Glu^{523} in the NCAM FN1 domain (PDB 2HAZ) (207). Notably, other acidic residues were rather scattered across the surface of the MAM domain. The exposed nature of these residues was later corroborated using a crystal structure of the NRP-1 MAM domain from Yelland et al. (224) to model the NRP-2 MAM domain.

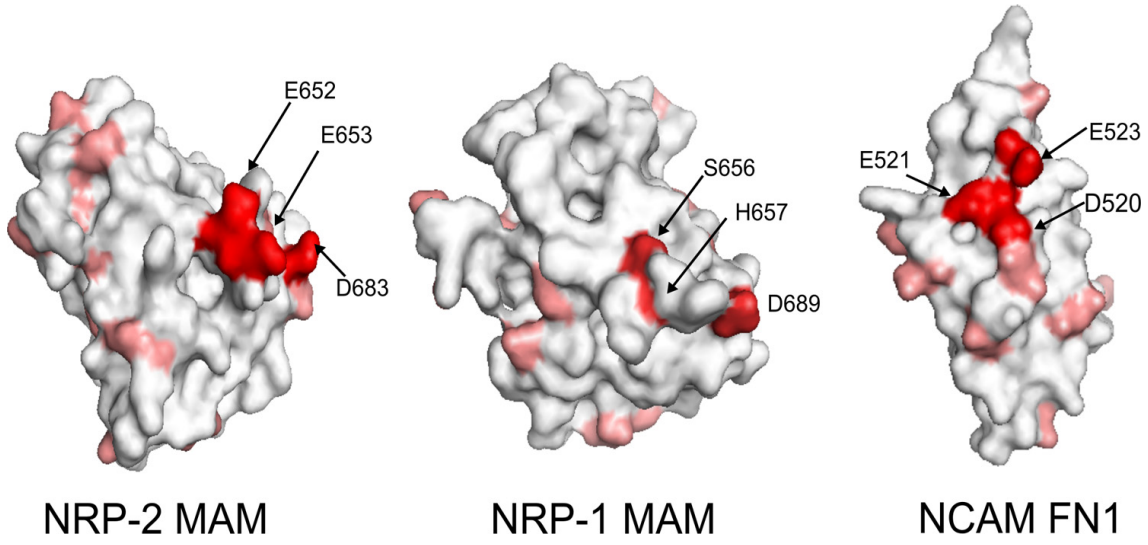

Figure 41: The distribution of acidic residues on structural models of the NRP-1 and NRP-2 MAM domains and the X-ray structure of the NCAM FN1 domain. The structure of the NRP MAM domains was modeled on the meprin A MAM domain structure (Protein Data Bank entry 4GWN (237)) using the SWISS-MODEL homology modeling server (238–241). Root-mean-square-deviation (RMSD) for the model of the NRP-1 MAM domain was 0.103 with sequence identity of 32.5%, whereas RMSD for the model of the NRP-2 was 0.184 with sequence identity of 26.3%. Analysis of these models reveals two adjacent acidic residues, Glu^{652} (E652) and Glu^{653} (E653), on the surface of the NRP-2 MAM domain (*left*), which are not present on the surface of the NRP-1 MAM domain (*right*). Instead, Ser^{656} (S656) and His^{657} (H657) in the linear sequence of NRP-1 replace Glu^{652} and Glu^{653} in NRP-2. A similar acidic patch in the NCAM FN1 domain (Protein Data Bank entry 2HAZ (207)) was shown to be critical for the polysialylation of NCAM (Asp^{520}, Glu^{521}, Glu^{523}).

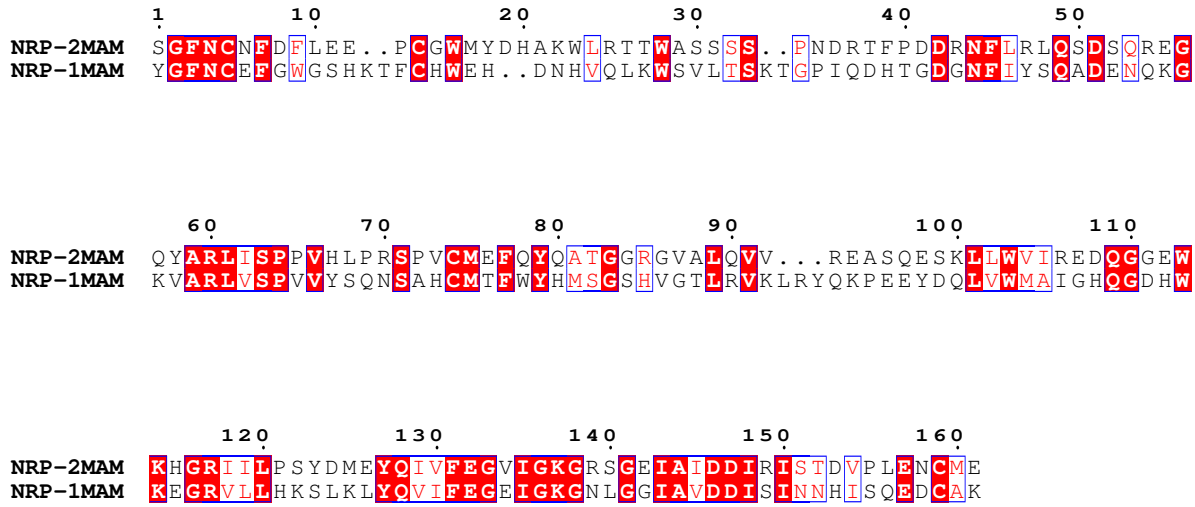

Figure 42: Sequence alignment of NRP MAM domains. Amino acid sequence of the NRP MAM domains were aligned using ESPRIPT server (208). Residues boxed in red represent conserved residues, whereas the ones boxed in blue represent similar residues.

I mutated Glu^{652} and Glu^{653} in NRP-2-Fc. As a control, I also mutated Asp^{683}, which is conserved in the NRP-1 sequence as Asp^{689} (Figs. 41 and 42). I coexpressed these mutants with ST8Sia-IV-myc in COS-1 cells. They were then precipitated from the medium using protein A-Sepharose beads and differences in their polysialylation were evaluated by immunoblotting with an anti-polySia antibody. A portion of precipitated beads was boiled in Laemmli sample buffer to remove polySia and subjected to immunoblotting to obtain relative expression levels of these acidic patch mutants. Secretion of these mutants into the condition medium to the level of wild type NRP-2 indicates that these mutants are properly folded (Fig. 43). Mutating Glu^{652} and Glu^{653} to alanines reduced polysialylation of NRP-2-Fc to 59 ± 20% (S.D.) and to 39 ± 16% (S.D.) that of NRP-2-Fc, respectively. The NRP-2 E652A/E653A double mutant further decreased polysialylation of NRP-2 to 15 ± 11% (S.D.) of that of NRP-2-Fc, whereas the D683A mutant had no significant impact on NRP-2 polysialylation (Fig. 43). These results suggest that Glu^{652} and Glu^{653} are critical for recognition by ST8Sia-IV and polysialylation of NRP-2.

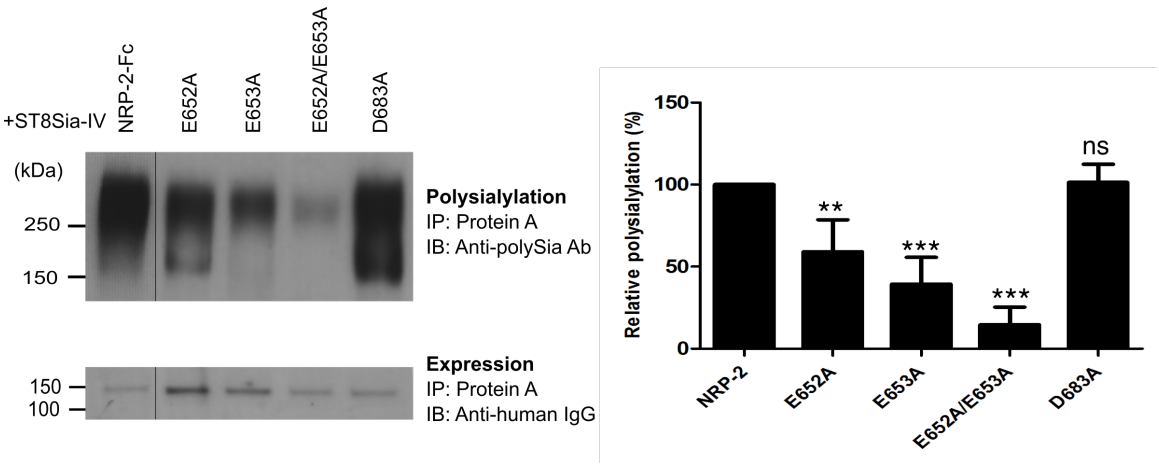

Figure 43: Glu^{652} and Glu^{653} are critical for NRP-2 polysialylation. MAM domain surface residues, Glu^{652} and Glu^{653} were mutated to alanines in NRP-2-Fc. Asp^{683} was also mutated to alanine as a control. These mutants were expressed in COS-1 cells with ST8Sia-IV-myc and their polysialylation was assessed by immunoblotting with anti-polySia antibody following precipitation from cell medium with protein A-Sepharose beads. Relative expression levels were obtained by boiling an aliquot of protein A-Sepharose beads and immunoblotting with an HRP-linked anti-human IgG. The line separating NRP-2-Fc and the E652A mutant reflects the removal of an extraneous lane so that the mutants and NRP-2-Fc can be more directly compared. Quantification of the experimental results was performed as described under "Materials and Methods" with data from four different experiments with error bars representing S.D. Statistical analysis was performed with respect to wild type NRP-2-Fc, which is normalized to 100%, using unpaired Student's t tests, where **, $0.001 < p < 0.01$; ***, $0.0001 < p < 0.001$; *ns*, $p > 0.05$.

DISCUSSION

In this chapter, I have described my work delineating the requirements for the recognition and polysialylation of NRP-2 by ST8Sia-IV. Using chimeric proteins and mutational analysis, I have identified the NRP-2 MAM domain as a primary recognition element for the initial protein-protein interaction between NRP-2 and ST8Sia-IV. Importantly, an acidic patch constituted by Glu^{652} and Glu^{653} on the surface of the MAM domain is critical, as their mutation of these residues to alanines substantially reduces NRP-2 polysialylation. However, my results also suggest that features of the FV/VIII-MAM linker region might also be important for robust polysialylation. These results reinforce the model for protein-specific polysialylation put forth by our laboratory based on observations made with NCAM as substrate, and also provide insights into previously unstudied variables that affect protein polysialylation such as intracellular trafficking.

Based on observations made with NCAM as polyST substrate, our laboratory hypothesized that polysialylation is unusual as a glycosylation process owing to a requirement for polyST recognition of specific substrate sequences prior to glycosylation of a substrate's glycans (193, 236). Deletion of the NCAM FN1 domain leads to lack of recognition by ST8Sia-IV, and polysialylation of N-glycans in the adjacent Ig5 domain is abolished as a result (192, 193). My results establish importance of NRP-2 MAM domain as polyST recognition and binding domain for polysialylation of O-glycans in the adjacent linker region (Fig. 40), affirming the above hypothesis, and suggesting a two-domain paradigm for polysialylation. In this paradigm, one domain serves as the polyST recognition site and the adjacent domain (or region) carries the glycans that are polysialylated.

A subtle revision of the simple two-domain paradigm for protein-specific polysialylation emerged when the polysialylation of NCAM-OCAM domain swap chimeras was evaluated by the laboratory. OCAM is not a polyST substrate; however, its FN1 domain allowed for polysialylation of an NCAM-OCAM chimera, although to a lesser extent compared to wild-type NCAM (193). In contrast, the Ig5 domain of OCAM blocked polysialylation when it was swapped into the NCAM sequence. Further

evidence for the importance of Ig5 sequences in polysialylation came from the observation that OCAM Ig5 contained large, basic residues nearby the polysialylated N-glycans in the Ig5 domain. When analogous residues in the NCAM Ig5 domain were replaced with these large, basic residues, NCAM polysialylation was eliminated. This suggested that sequences in the Ig5 domain may provide a secondary polyST interaction site (197). Similarly, the NRP-2 MAM domain enables polysialylation of NRP-1 (NRP-1Δ2, Figs. 37 and 38), but is not sufficient to support polysialylation of this chimera to the level of wild-type NRP-2. However, a NRP-1 chimera possessing both the NRP-2 MAM domain and linker region is polysialylated to the same level as wild type NRP-2 (NRP-1ΔLM2, Figure 38). These results together with the very different lengths of this linker region in NRP-1 (49 residues) and NRP-2 (62 residues) suggest that certain features of the NRP-2 linker, such as the spacing of the O-glycan acceptors from the MAM domain, clustering of O-glycan acceptors, as Rollenhagen et al (229) have suggested, and/or specific sequences within the linker region that allow a secondary, stabilizing interaction with ST8Sia-IV, may promote its higher level of polysialylation. The requirement for O-glycan clustering may play a role, as serine/threonine O-glycosylation sites in NRP-1 are rather scattered as compared to these sites in NRP-2 (Fig. 44). Moreover, the glycosylation status of NRP-1 linker region has not been reported thus far, except for Ser^{612}, which carries a GAG chain. GAG chains are negatively charged, similar to polySia, but are synthesized prior to polySia in the ER by the GAG biosynthesis enzymes, EXT1 and EXT2 (230). It therefore seems plausible that the presence of the GAG chain might block polysialylation in physiological settings. In this case, mutation of this Ser residue should enhance NRP-1 polysialylation. I compared polysialylation of NRP-1 with its S612A mutant and there were no significant differences in polysialylation. Synthesis of GAG chain in COS-1 cells; however, was evident by upward shift in molecular mass on the SDS-PAGE gel for wild type NRP-1 but not the S612A mutant (data not shown).

NRP-2 linker: ^{593}DWTDSKPTVKTLGPTVKSEETTTPYPTEEEATECGENCSFEDDKDLQLP^{641}

NRP-1 linker: ^{584}EVEAPTAGPTTPNGNLVDECDDDQANCHSGTGDDFQLTGGTTVLATEKPTVIDSTIQSEFPT^{684}
+

Figure 44: Comparison of NRP-2 and NRP-1 linker region sequences. Polysialylated O-glycans in NRP-2 are underlined. Ser^{612} in NRP-1 linker region, that gets modified with heparan sulfate/chondroitin sulfate GAG chains is marked with + sign.

Similar to the NCAM FN1 domain, where a surface acidic patch formed by the residues Asp^{520}, Glu^{521}, Glu^{523} is important for NCAM polysialylation (192, 194, 236), Glu^{652} and Glu^{653} on the surface of the MAM domain are important for NRP-2 polysialylation (Figs. 41 and 43). Nevertheless, residual polysialylation is still observed even after mutating both of these residues to alanines indicating that other residues in the vicinity might still play a minor role in this process. Attempts to determine whether Glu^{652} and Glu^{653} are required for ST8Sia-IV binding using pull-down assays were inconclusive, likely due to non-specific binding of ST8Sia-IV on the surface of the MAM domain. This was not surprising since previous work by Matthew Thompson in the laboratory showed that mutating the three key acidic residues in the NCAM FN1 domain to arginines eliminated polysialylation, but only reduced binding to ST8Sia-IV by 30-40% (193). In the latter case, non-specific and non-productive binding was suggested. In addition, the NCAM FN1 and MAM domains are structurally very different. The FN1 domain is fibronectin type III repeat domain, whereas the MAM domain is β jelly-roll fold. The MAM domain is larger (18 kDa vs 11 kDa for NCAM FN1) and consequently, has more acidic residues (24 vs 16 for NCAM FN1), potentially increasing the possibility for non-productive enzyme binding.

The observation that membrane-bound NRP-1 can be polysialylated in cells overexpressing of ST8Sia-IV was surprising (Fig. 35). Previous literature showed that NRP-1 is in fact a receptor undergoing recycling endocytosis (225). Evidence for the endocytosis of cell-surface receptors to TGN or trans-Golgi, where sialyltransferases including polySTs reside, originally came from Duncan and Kornfeld (242) who showed that unsialylated mannose-6-phosphate receptors recycle from the plasma membrane to internal compartments and in the process get resialylated. Endocytic recycling of NRP-1 is a function of specific cytoplasmic sequences that are not found in NRP-2. The C-terminal SEA sequence in the NRP-1 cytoplasmic tail binds GIPC-synectin that links it to the endocytic machinery (232). NRP-2 undergoes endocytosis as well; however, Okon et al. (234) showed that NRP-1 and NRP-2 show a different distribution in Rab-positive compartments, implying that their intracellular trafficking differs significantly.

To eliminate the potential effects of recycling to ST8Sia-IV expressing compartments, I constructed Fc-tagged soluble NRPs. The lack of polysialylation of NRP-1-Fc suggested that cytoplasmic sequences and the trafficking mediated by these sequences likely plays a role in the polysialylation of this protein in this experimental system. I attempted to delete cytoplasmic SEA sequence in membrane bound NRP-1, which resulted in a decrease in, but not elimination of, polysialylation. This could suggest that other cytoplasmic sequences play a role in the recycling process. On the other hand, the Fc tag did not have any impact *per se* on polysialylation, as a soluble NRP-1 construct lacking the transmembrane region and cytoplasmic tail fused to a V5-tag also exhibited a reduced polysialylation (Fig. 45). In sum, although polysialylated NRP-1 has not been reported *in vivo,* I believe that under pathological conditions such as cancer, where NRP-1 and polySTs are both overexpressed, the possibility that NRP-1 may be polysialylated cannot be excluded.

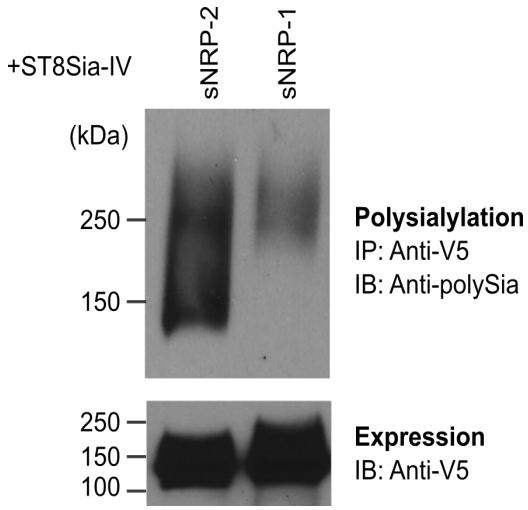

Figure 45: Soluble NRP-1 devoid of the Fc tag shows a significant reduction in polysialylation. V5-tagged soluble NRPs (sNRPs) that lacked cytoplasmic tail and transmembrane regions were co-expressed with ST8Sia-IV in COS-1 cells. V5 tagged proteins were recovered from the cell media using an anti-V5 antibody and protein A-Sepharose bead, s and their polysialylation was assessed using an anti-polySia antibody.

Finally, I have made several attempts to define the physiological parameters of NRP-2 polysialylation. In these efforts, I have transfected NCAM and NRP-2 in various cancer cell lines (A549 lung adenocarcinoma, SW2 small cell lung carcinoma, and MCF-7 breast cancer cells) that endogenously express polySTs. Surprisingly, endogenous polySTs in all of the above cell lines polysialylated NCAM, but not NRP-2. On the other hand, when ST8Sia-IV was co-expressed with NRP-2 in these cell lines, NRP-2 polysialylation was detected, indicating that NRP-2 polysialylation might necessitate higher levels of ST8Sia-IV than NCAM polysialylation. To determine whether NRP-2 is a weaker substrate for ST8Sia-IV, binding studies with purified MAM domain and ST8Sia-IV PBR region might prove informative, as would in vitro polysialylation studies to determine relative Km values.

Another possibility is that ST8Sia-IV prefers the N-glycans in NCAM to the O-glycans in NRP-2. To address this possibility, I mutated the first threonine residue (Thr^{613}) in O-glycan cluster in the NRP-2 FV/VIII-MAM linker region to asparagine. This generated an N-glycosylation consensus site $^{613}NTT^{615}$ in the same region where polysialylated O-glycans reside (NRP-2 T613N). This construct was expressed in A549 cells that express endogenous ST8Sia-IV and in COS-1 cells with exogenous ST8Sia-IV. Its polysialylation was not detected in A-549 cells. When coexpressed with ST8Sia-IV in COS-1 cells, PNGase-F treatment to remove N-glycans demonstrated no change in polysialylation, implying that even this construct was O-polysialylated (data not shown). I have, however, not assessed whether the intended N-glycan was indeed synthesized.

In summary, these results define the requirements for NRP-2 recognition and polysialylation by ST8Sia-IV and suggest the possibility that NRP-1 may also be polysialylated in situations, like cancer, where ST8Sia-IV is highly expressed. Further studies will be required to determine the precise NRP-2 MAM-ST8Sia-IV interaction interface, the role of polySia in NRP-2 co-receptor interactions and related signaling events, and whether NRP-1 is polysialylated in vivo in normal tissues or in disease.

CHAPTER V

Overlapping sequences within the polybasic region of the polysialyltransferases are required for recognition of NCAM, NRP-2, and SynCAM 1.

(Parts of this chapter will be submitted as the manuscript *Overlapping Sets of Basic Residues in the Polysialyltransferases are Required for Substrate Recognition and Polysialylation by* Bhide, G.P., Zapater, J. L., and Colley, K. J.)

Introduction

Most glycosyltransferases recognize specific glycan structures as substrates prior to monosaccharide transfer. PolySTs are unique because they do not modify all sialylated glycan structures and instead rely on the recognition of protein sequences of select glycoprotein substrates (33). Earlier studies in the laboratory performed on NCAM, and my work on NRP-2 described in Chapter III, has revealed specific protein sequences in these glycoproteins that are crucial for their polysialylation (33, 243). Chimeric enzymes made by Angata et al. (126) gave early insights into sequences required for NCAM recognition and polysialylation. Sequences in the polySTs were replaced with analogous sequences from ST8Sia-III. ST8Sia-III is an α2,8-oligosialyltransferase that transfers sialic acid residues to glycoprotein and glycolipid acceptors in vitro (244), but cannot polysialylate NCAM (130). While analysis of enzyme deletion mutants identified ST8Sia-IV amino acids 62-356 as the catalytic region, replacement studies led investigators to postulate that amino acids 62-127 and possibly 194-267, are important for NCAM recognition, because replacement of these sequences reduced NCAM polysialylation but not autopolysialylation (126).

Surface exposed acidic residues in the NCAM FN1 or NRP-2 MAM domain are involved in the initial recognition step leading to polysialylation (192, 193, 223, 236). Consequently, it was hypothesized

that basic residues in polySTs might be important for interacting with the substrate acidic residues. Troy and colleagues (198) mutated basic residues within ST8Sia-IV polysialyltransferase domain (PSTD), that is constituted of amino acids from 246 to 277 (Fig. 45). Mutating most of these residues hampered NCAM polysialylation. However, Deirdre Foley in the lab later found out that these mutants also impacted autopolysialylation suggesting that these mutants affected overall enzymatic activity and not NCAM polysialylation *per se* (199). The exact reason behind these effects are unknown, however, as the PSTD residues are in close proximity to the catalytically important SMS region, mutating residues in the PSTD may have induced changes in local structure leading to compromised activity. On the other hand, simultaneously mutating Arg^{82} and Arg^{93} in the polybasic region (PBR) region to alanines eliminated NCAM polysialylation without significantly reducing autopolysialylation or misfolding the enzyme (199). The Arg^{82} mutation, reduced NRP-2 polysialylation but the Arg^{93} mutation did not (200). This suggests that polysialylation of different substrates might necessitate interaction with different PBR residues, which is conceivable considering differences in the known recognition domains.

Later work showed that a truncated ST8Sia-IV fragment consisting of residues 1-140 that contains the PBR, but not PSTD, can act as a competitive inhibitor of NCAM polysialylation. However, a fragment consisting of residues 1-71 that lacks the PBR cannot. Moreover, a catalytically dead mutant of ST8Sia-IV (H331K), which acts as competitive inhibitor of polysialylation, loses its ability to compete for NCAM polysialylation if Arg^{82} and Arg^{93} are replaced by alanines, suggesting the importance of these residues for NCAM recognition (200). Finally, in Chapter III, I demonstrated that Arg^{82} and Arg^{93} are essential for the direct binding of the ST8Sia-IV PBR peptide to the NCAM FN1 domain (236). As the polySTs are 59% identical and their PBRs are very similar (Fig. 46), we hypothesized that similar residues in the ST8Sia-II and ST8Sia-IV PBRs will be critical for NCAM polysialylation and that NRP-2 polysialylation by ST8Sia-IV and SynCAM 1 polysialylation by ST8Sia-II may require additional or even different PBR residues.

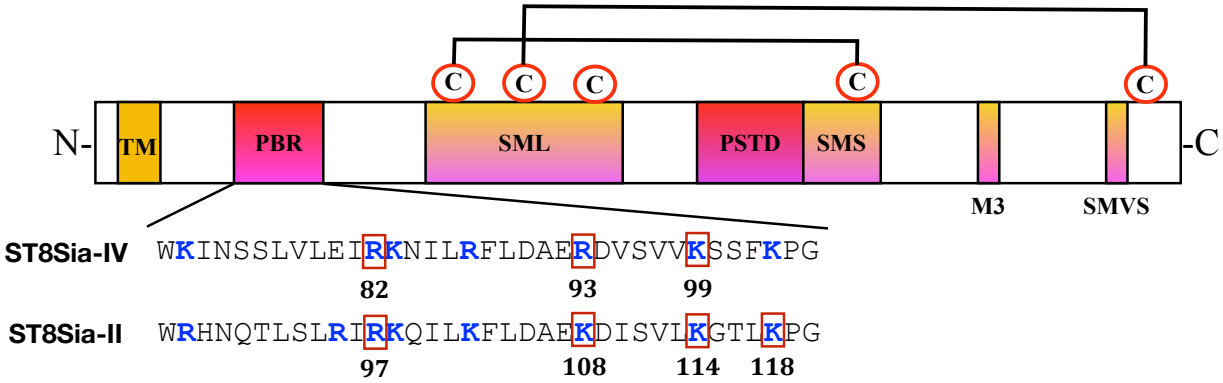

Figure 46. A comparison of ST8Sia-IV and ST8Sia-II PBR regions. Sialylmotifs conserved between sialyltransferases are shown as large (SML), small (SMS), very small (SMVS) and M3 are marked along with the polybasic region (PBR) and polysialyltransferase domain (PSTD), which are unique to polySTs are shown in red. The polyST PBR sequences are shown with the basic residues are highlighted in blue and residues involved in polysialylation of various substrates in this study are boxed in red.

In this chapter, I describe my work that expands our understanding of the role that the polyST PBR plays in substrate recognition by identifying specific residues in the PBR domains of ST8Sia-IV and ST8Sia-II involved in the recognition of NCAM, NRP-2 and SynCAM 1. In addition, I evaluate the role of PBR residues in enzyme autopolysialylation and the importance of this auto-modification for substrate polysialylation.

RESULTS

A. Overlapping sets of PBR basic residues affect NCAM and NRP-2 polysialylation by ST8Sia-IV.

In order to compare the ST8Sia-IV and ST8Sia-II PBR basic residues involved in NCAM, NRP-2 and SynCAM 1 polysialylation, we replaced these residues with alanines. If a specific polyST PBR basic residue is critical for the polysialylation of a substrate, then when that residue is mutated to alanine we expect a decrease or elimination in the ability of that mutant polyST to polysialylate the substrate. However, as the proper localization of the polySTs in the Golgi is necessary for their ability to polysialylate co-expressed substrates, we examined all ST8Sia-II and ST8Sia-IV PBR alanine mutants for proper localization by individually expressing each protein in COS-1 cells and staining the cells with an anti- antibody as detailed in Chapter II. Co-localization of these mutants with the Golgi marker GM130 confirmed their localization to the Golgi (data not shown).

To determine the significance of specific ST8Sia-IV PBR basic residues for NCAM and NRP-2 polysialylation, we co-expressed myc-tagged wild-type and PBR mutant ST8Sia-IV proteins with V5-tagged substrates in COS-1 cells. Substrates were immunoprecipitated from cell lysates and the level of substrate polysialylation was assessed by immunoblotting with the 12F8 anti-polySia antibody (Figs. 47 and 48). Relative levels of NCAM or NRP-2 expression (Figs. 47 and 48, *middle panels*) as well as overall polyST expression levels (Figs. 47 and 48, *bottom panels*) were evaluated by immunoblotting a small aliquot of lysate with anti-V5 and anti-myc antibodies, respectively. The relative amount of substrate polysialylation observed in the presence of each polyST PBR mutant was quantified using NIH ImageJ and indicated as a percentage of wild-type polyST polysialylation of NCAM or NRP-2.

The effect of ST8Sia-IV PBR basic residues in NCAM polysialylation has been formerly reported by Deirdre Foley and Joseph Zapater in the lab (199, 200). To make a direct comparison between NCAM and NRP-2 requirements using a newer anti-polySia antibody (12F8), I again performed this experiment. NCAM polysialylation was greatly reduced in the presence of ST8Sia-IV proteins containing the R82A and R93A mutations to 51 +/- 15% (S.D.) and 20 +/- 14% (S.D.) of that seen with the wild type enzyme (Fig. 47, *bottom panel*). While smaller reductions in NCAM polysialylation are seen with other ST8Sia-IV PBR mutants, Arg^{82} and Arg^{93} are the most critical ST8Sia-IV PBR basic residues for NCAM polysialylation. This result matches my ITC results in the previous chapter that demonstrated that Arg^{82} and Arg^{93} are the key PBR residues for NCAM FN1 recognition (236). Notably, the anti-polySia 12F8 antibody detects polysialylated NCAM of a lower molecular mass when Arg^{93} in ST8Sia-IV is mutated to alanine. This suggests that this mutant enzyme may have a defect in the elongation of polySia chains in addition to weaker substrate recognition.

When NRP-2 polysialylation by ST8Sia-IV PBR mutants was evaluated, we found that replacing Arg^{82} or Lys^{99} significantly reduced NRP-2 polysialylation to 6 +/- 0.6% (S.D.) and 4 +/- 4% (S.D.) of that seen with wild type enzyme, respectively (Fig. 48, *top panel*). Arg^{87} also decreases polysialylation to a lesser extent (65 +/- 2% (S.D.)). These results suggest that differences within polyST recognition domains in the substrates might necessitate interaction with different PBR residues for substrate polysialylation.

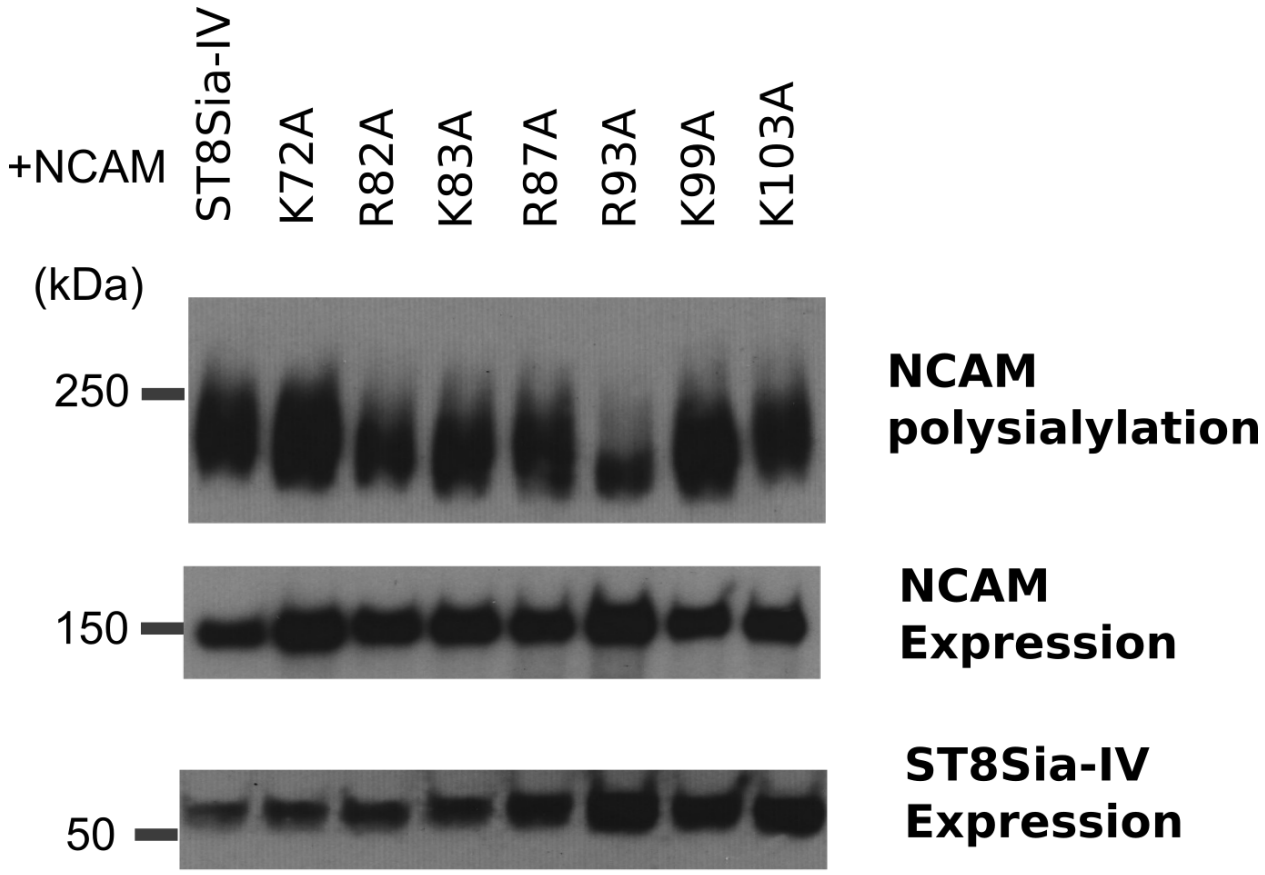
+NCAM
ST8Sia-IV
K72A
R82A
K83A
R87A
R93A
K99A
K103A
(kDa)
250
150
50
NCAM polysialylation
NCAM Expression
ST8Sia-IV Expression

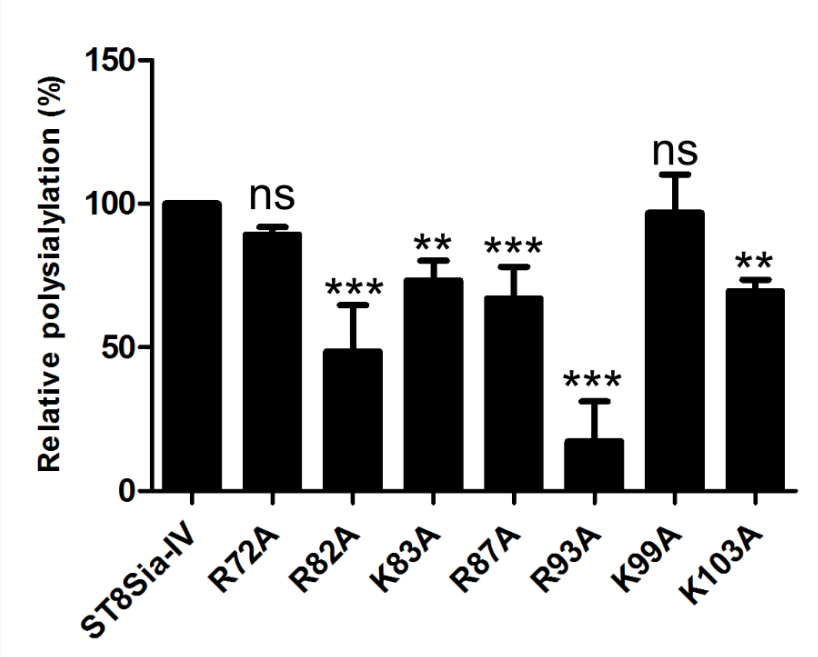
Relative polysialylation (%)
150
100
50
0
ns
***
**
***
***
ns
**
ST8Sia-IV
R72A
R82A
K83A
R87A
R93A
K99A
K103A

Figure 47: Effect of mutating the ST8Sia-IV PBR basic residues on NCAM polysialylation. myc-tagged ST8Sia-IV PBR mutants were co-expressed with NCAM-V5 and polysialylation of NCAM by these mutants was assessed using an anti-polySia antibody immunoprecipitation of the NCAM proteins using an anti-V5 tag antibody. For each sample, an aliquot of cell lysate was boiled with Laemmli sample buffer to remove polySia and immunoblotted with anti-V5 or anti-myc antibodies to determine the relative expression levels of NCAM and the ST8Sia-IV mutants, respectively. Quantification of the experimental results was performed as described under "Materials and Methods" with data from four different experiments and with error bars representing S.D. Data was reported as % polysialylation with respect to NCAM polysialylation by wild type ST8Sia-IV, which is normalized to 100%. Statistical analysis was performed using a one-way ANOVA test with a Dunnett's post-hoc test, where **, $0.001<p<0.01$; ***, $0.0001<p<0.001$; *ns*, $p>0.05$.

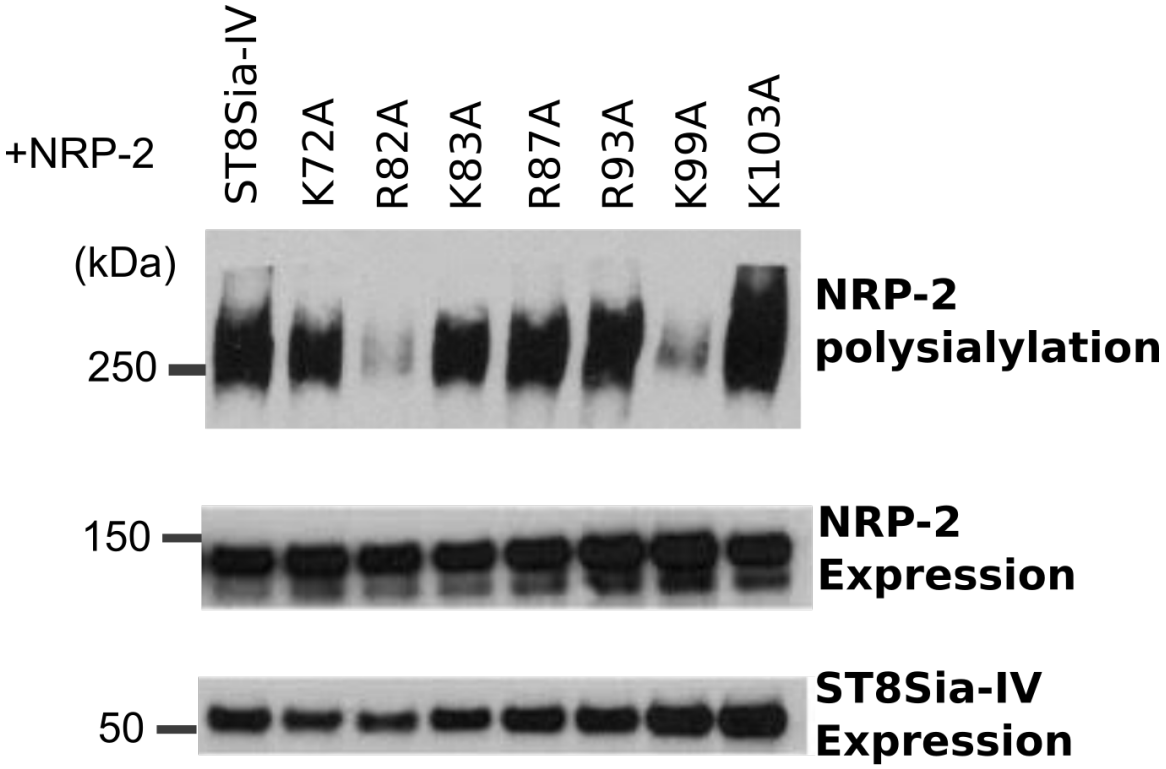
+NRP-2
ST8Sia-IV
K72A
R82A
K83A
R87A
R93A
K99A
K103A
(kDa)
250
150
50
NRP-2
polysialylation
NRP-2
Expression
ST8Sia-IV
Expression

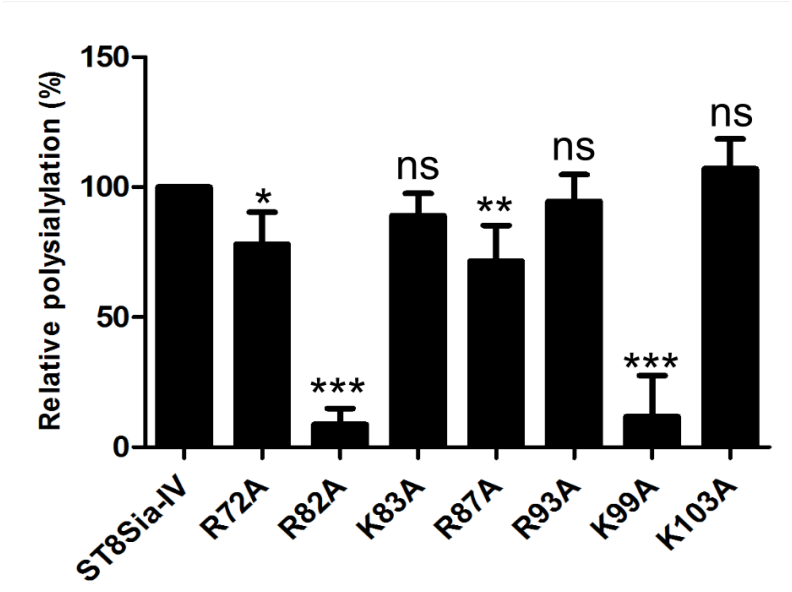
Relative polysialylation (%)
150
100
50
0
*
***
ns
**
ns
***
ns
ST8Sia-IV
R72A
R82A
K83A
R87A
R93A
K99A
K103A

Figure 48: The effect of mutating ST8Sia-IV PBR basic residues on NRP-2 polysialylation. Myc-tagged ST8Sia-IV PBR mutants were expressed with NRP-2-V5. After immunoprecipitating NRP-2 with an anti-V5 antibody, the extent of polySia synthesized by various mutants was evaluated by immunoblotting using an anti-polySia antibody. For each sample, an aliquot of cell lysate was boiled with Laemmli sample buffer to remove polySia and immunoblotted with anti-V5 or anti-myc antibodies to determine the relative expression levels of NRP-2 and the ST8Sia-IV mutants, respectively. Quantification of the experimental results was performed as described under "Materials and Methods" with data from four different experiments with error bars representing S.D. Data was reported as % polysialylation with respect to NRP-2 polysialylation by wild type ST8Sia-IV, which is normalized to 100%. Statistical analysis was performed using a one-way ANOVA test with a Dunnett's post-hoc test, where *, $0.01<p<0.05$; **, $0.001<p<0.01$; ***, $0.0001<p<0.001$; *ns*, $p>0.05$. The data in the top panel of this figure was obtained by Joseph Zapater.

.

B. The role of ST8Sia-IV PBR basic residues in NCAM and NRP-2 recognition.

Based on the earlier observation that the full-length catalytically inactive ST8Sia-IV H331K protein is able to compete with wild-type ST8Sia-II and block NCAM polysialylation (200), I proceeded to determine whether specific PBR residues participate in NCAM recognition. If a specific polyST PBR basic residue is critical for substrate recognition and subsequent polysialylation, then mutating that residue in ST8Sia-IV H331K would reduce the ability of this catalytically inactive enzyme to compete with wild-type enzyme and block substrate polysialylation. Each arginine and lysine residue in the ST8Sia-IV H331K PBR was mutated individually to alanine, and as before, we examined the cellular localization of each mutant protein. All the mutants co-localized with GM130 Golgi marker, indicating that the mutants were correctly folded and in their desired intracellular compartment (data not shown).

Next, I expressed V5-tagged NCAM or NRP-2 with an untagged active ST8Sia-IV and a myc-tagged inactive ST8Sia-IV PBR mutant in COS-1 cells at a ratio of 1:1:6 (substrate: wild-type ST8Sia-IV: ST8Sia-IV competitor) (Fig. 49). V5-tagged substrates were immunoprecipitated from cell lysates with an anti-V5 antibody, and their polysialylation was assessed by immunoblotting with the 12F8 anti-polySia antibody (Figs. 49 and 50, *upper panels*). Relative levels of NCAM or NRP-2 expression (Figs. 50 and 51, *middle panels*), as well as competitor enzyme expression (Figs. 50 and 51, *bottom panels*), were evaluated by immunoblotting a small sample of cell lysate with anti-V5 and anti-myc antibodies, respectively. Relative substrate polysialylation observed in the presence of ST8Sia-IV H331K and its PBR mutants was quantified and reported as fold recovery from competition with ST8Sia-IV H331K.

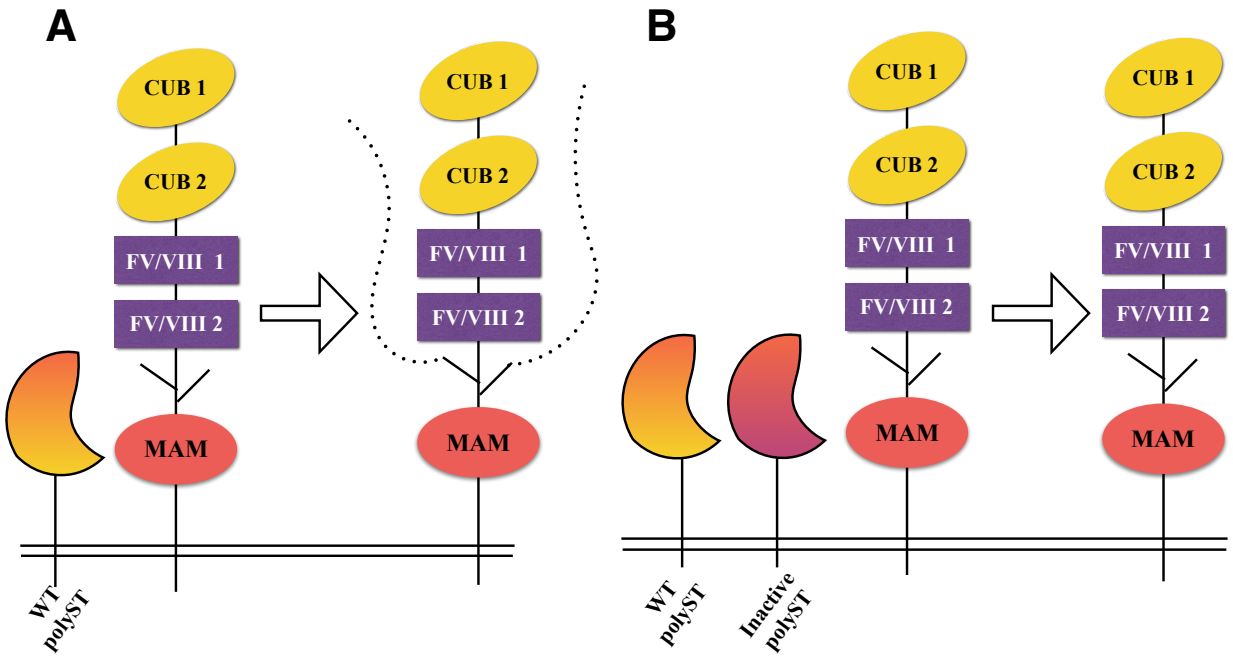

Figure 49: Design of competition experiments. A, Interaction of the wild-type (WT) polyST (shown in orange) results in polysialylation of the substrate (NRP-2 is shown here as an example). B, Inactive polyST, which serves as competitive inhibitor of WT enzyme for binding to the substrate is shown in red. If a particular residue is crucial for binding to the substrate, it will not be capable of exhibiting competition, allowing wild-type polyST to polysialylate the substrate.

In my analysis of these competition experiments, I observed that the R82A and R93A mutations that significantly impacted NCAM polysialylation also led the ST8Sia-IV H331K protein to lose ability to compete with the wild type enzyme. The end result is a recovery of NCAM polysialylation by 2.94 ± 0.45 fold (S.D.) and 2.51 ± 0.3 fold (S.D.), respectively (Fig. 50). This observation is in accordance with my data demonstrating importance of these residues in direct interaction between isolated PBR region and recombinant NCAM FN1 domain (236), described in Chapter III. Other PBR mutants, such as K83A and R87A that show a modest reduction in NCAM polysialylation (Fig. 47, 72% and 74% of that observed with wild-type ST8Sia-IV, respectively), exhibit varying losses of competition and recoveries of polysialylation. The R87A mutant exhibits a 1.46 ± 0.3 fold (S.D.) recovery of polysialylation, commensurate with the modest reduction in polysialylation observed when this mutation is made in the wild type enzyme. In contrast, the K83A mutant shows a surprisingly large recovery of polysialylation (2.58 ± 0.57 fold (S.D.)) that is similar to what is observed for the R82A and R93A mutants that dramatically impact polysialylation (Fig. 47, *top panel*).

Results of competition experiments for NRP-2 supported the importance of Arg^{82}, but not Lys^{99}, in NRP-2 recognition. When Arg^{82} was replaced by alanine in the ST8Sia-IV H331K protein, a substantial loss of competition and recovery of polysialylation was observed (4.37 ± 0.83 fold (S.D.). In contrast, replacing Lys^{99} with alanine in the ST8Sia-IV H331K protein lead to a significantly smaller loss of competition and recovery of polysialylation (1.91 ± 0.68 fold (S.D.), even though this mutation in the wild type enzyme nearly eliminated NRP-2 polysialylation. In comparison, R87A, which shows intermediate reduction in NRP-2 polysialylation (72 ± 14% (S.D.)) and unexpectedly, K83A, which shows no reduction in NRP-2 polysialylation (Fig. 48), exhibit much larger recoveries from competition (3.61 ± 0.68 fold (S.D.) and 2.73 ± 0.58 fold (S.D.), respectively) than the K99A mutant (Fig. 51, *top panel*). I will address why I think that certain PBR residues that play little or only moderate roles in substrate polysialylation (Lys^{83} for both NCAM and NRP-2 and Arg^{87} for NRP-2), appear to play a more substantial role in substrate recognition in the Discussion section of this chapter. Below, I link the effects

I see for the K99A mutant in the polysialylation of NRP-2 to its importance for ST8Sia-IV autopolysialylation.

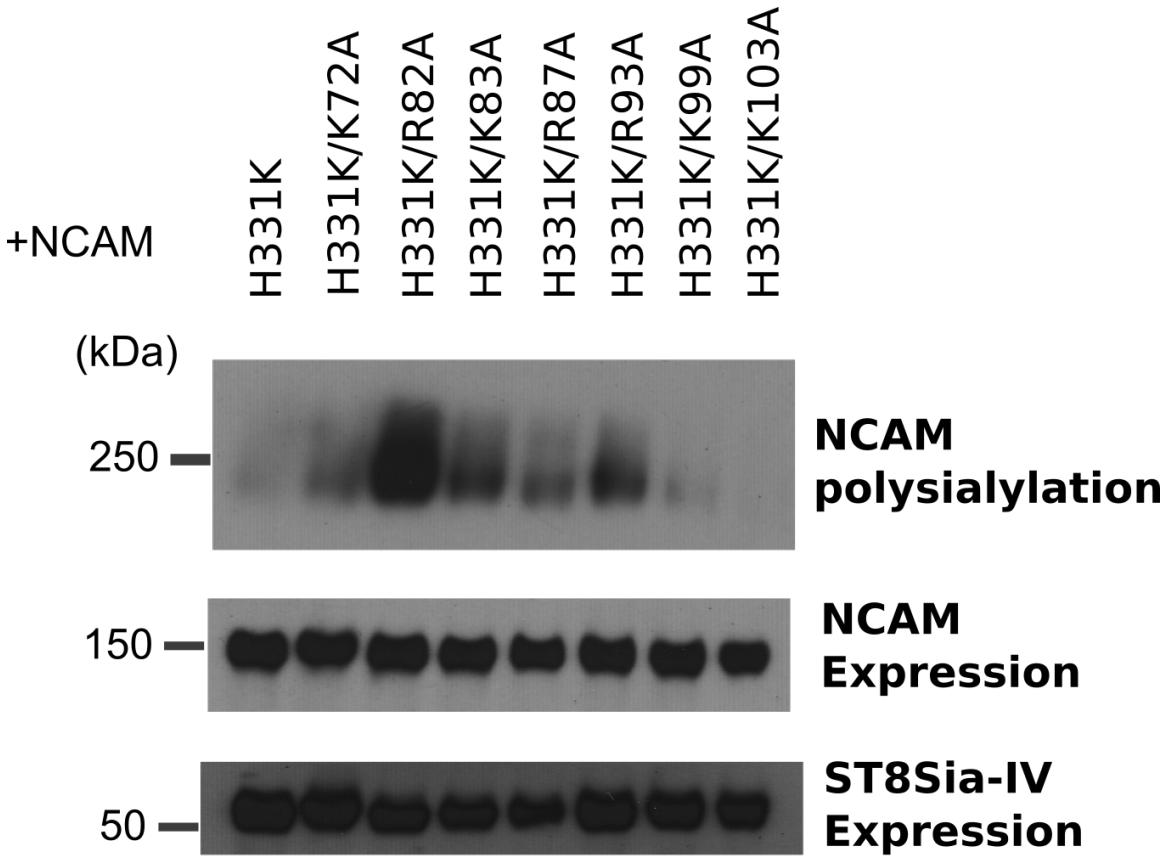
+NCAM
H331K
H331K/K72A
H331K/R82A
H331K/K83A
H331K/R87A
H331K/R93A
H331K/K99A
H331K/K103A
(kDa)
250
150
50
NCAM polysialylation
NCAM Expression
ST8Sia-IV Expression

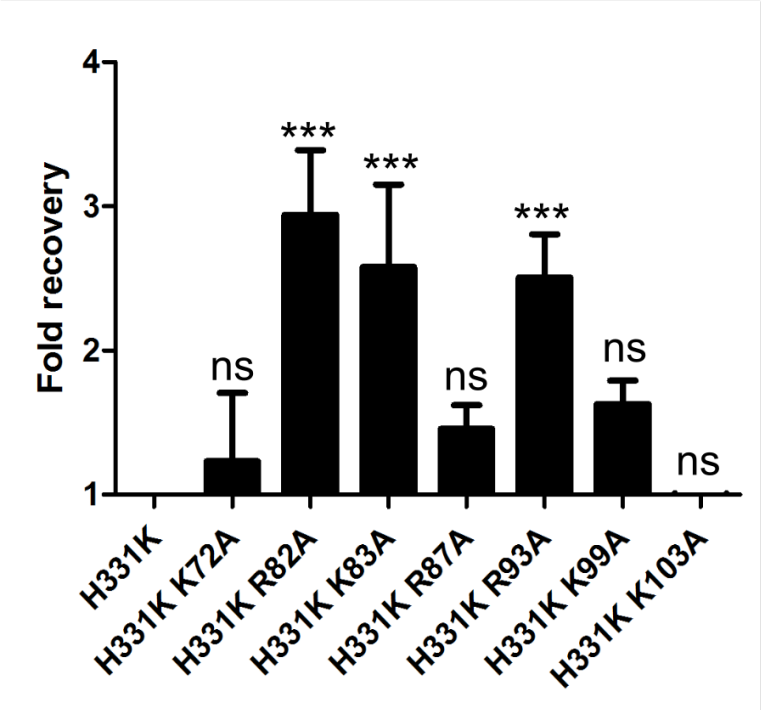
Fold recovery
4
3
2
1
***
***
***
ns
ns
ns
ns
H331K
H331K K72A
H331K R82A
H331K K83A
H331K R87A
H331K R93A
H331K K99A
H331K K103A

Figure 50: Competition experiments demonstrate the importance of ST8Sia-IV PBR Arg^{82} and Arg^{93} in NCAM recognition. NCAM-V5, untagged wild-type ST8Sia-IV, and myc-tagged H331K ST8Sia-IV PBR mutants were co-expressed at a 1:1:6 ratio in COS-1 cells. NCAM was precipitated using an anti-V5 antibody and its polysialylation was assessed by immunoblotting with an anti-polySia antibody. A portion of cell lysate was boiled in Laemmli sample buffer to remove polySia and immunoblotted with anti-V5 and anti-myc antibodies to determine relative expression levels of NCAM and the ST8Sia-IV mutants. Quantification of the experimental results was performed as described under "Materials and Methods" with data from four different experiments and with error bars representing S.D. Data was reported as fold recovery with respect to the polysialylation of NCAM with wild type ST8Sia-IV in the presence of H331K ST8Sia-IV as a competitor, which is normalized to 1. Statistical analysis was performed using a one-way ANOVA test with a Dunnett's post-hoc test where ***, $0.0001<p<0.001$; *ns*, $p>0.05$.

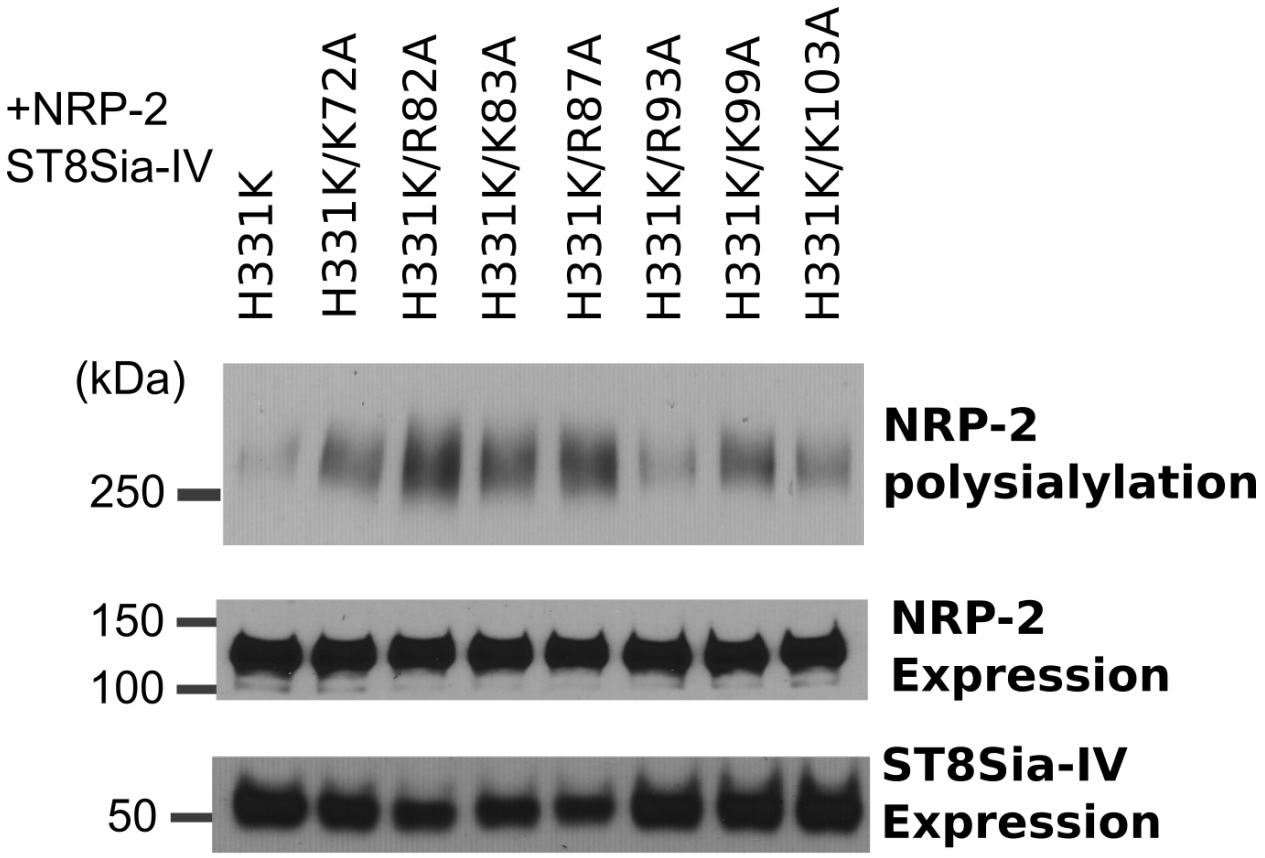
+NRP-2
ST8Sia-IV
H331K
H331K/K72A
H331K/R82A
H331K/K83A
H331K/R87A
H331K/R93A
H331K/K99A
H331K/K103A
(kDa)
250
150
100
50
NRP-2
polysialylation
NRP-2
Expression
ST8Sia-IV
Expression

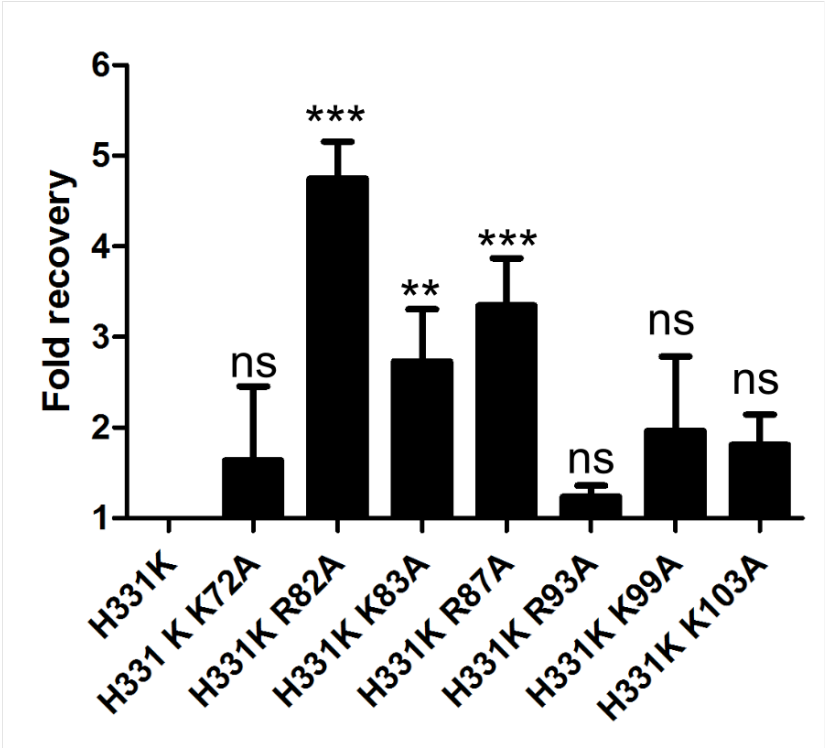
Fold recovery
6
5
4
3
2
1
***
ns
**
***
ns
ns
ns
H331K
H331 K K72A
H331K R82A
H331K K83A
H331K R87A
H331K R93A
H331K K99A
H331K K103A

Figure 51: Competition experiments identify Arg^{82} as a key residue for recognition of NRP-2 by ST8Sia-IV with lesser contributions by other residues. NRP-2-V5, untagged wild-type ST8Sia-IV, and myc-tagged H331K ST8Sia-IV PBR mutants were co-expressed at a 1:1:6 ratio in COS-1 cells. NCAM was precipitated using anti-V5 antibody and its polysialylation was assessed by immunoblotting with anti-polySia antibody. A portion of cell lysate was boiled in Laemmli sample buffer to remove polySia and immunoblotted with anti-V5 and anti-myc antibodies to determine relative expression levels of NRP-2 and the H331K ST8Sia-IV PBR mutants. Quantification of the experimental results was performed as described under "Materials and Methods" with data from three different experiments and with error bars representing S.D. Data was reported as fold recovery with respect to the polysialylation of NRP-2 with wild type ST8Sia-IV in the presence of H331K ST8Sia-IV as a competitor, which is normalized to 1. Statistical analysis was performed using a one-way ANOVA test with a Dunnett's post-hoc test, where **, $0.001<p<0.01$; ***, $0.0001<p<0.001$; *ns*, $p>0.05$.

C. Replacing Arg^{82} and Lys^{99} reduces ST8Sia-IV autopolysialylation.

It was surprising to observe that the K99A mutant substantially reduced polysialylation of NRP-2, yet did not reduce competition exhibited by H331K ST8Sia-IV. This indicated that Lys^{99} may not participate in recognition of NRP-2 by ST8Sia-IV. I considered other scenarios in which a particular residue can affect polysialylation without being involved in substrate binding. First, replacing a particular residue could affect the overall catalytic activity of the enzyme. This is ruled out in this case by the observation that the ST8Sia-IV K99A mutation does not alter its ability to polysialylate NCAM (see Fig. 47). Second, replacing a particular residue may not impact substrate recognition and the initiation of polysialylation, but could hamper the elongation of polySia chains, thus precluding recognition by an anti-polySia antibody with a minimum chain length requirement. A model of ST8Sia-IV based on the crystal structure of ST8Sia-III shows that the PBR and PSTD regions fold together to create a basic surface that could engage and anchor the negatively charged polySia chain as it elongates (125). It is therefore possible that replacing Lys^{99} with alanine disrupts the structure or charge of this basic surface and polySia chain elongation. Third, another possibility is that replacing a particular polyST PBR residue impacts enzyme autopolysialylation and this in turn alters NRP-2 polysialylation. Why do I evoke this possibility when previous results showed that ST8Sia-IV autopolysialylation is not required for NCAM polysialylation (138)? Evaluating the ST8Sia-IV structure modeled on the structure of ST8Sia-III (PDB 5BO9) (125), we observe that the two sites of ST8Sia-IV polysialylation, Asn^{74} and Asn^{119}, are within or nearby the PBR region, respectively (Fig. 52).

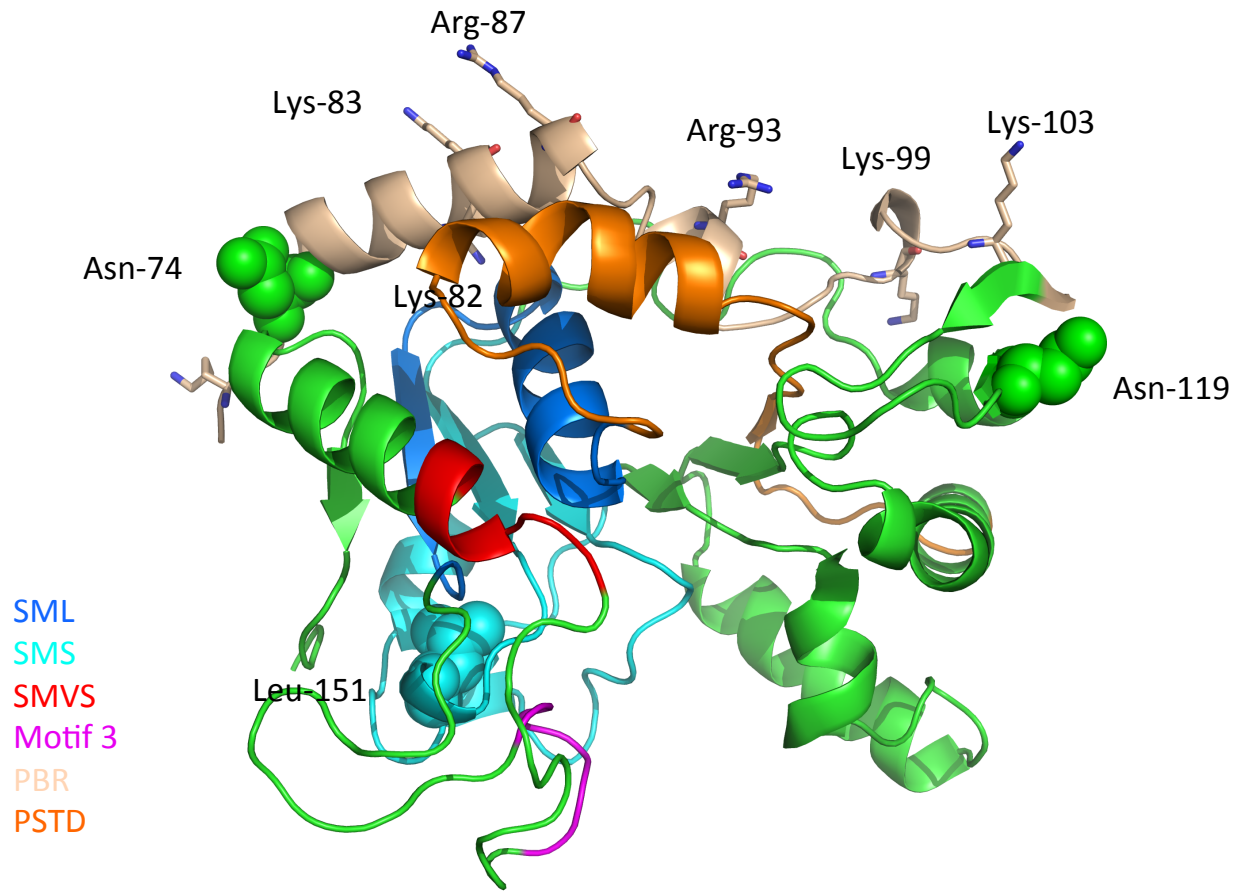

Figure 52: A model of ST8Sia-IV based on the X-ray crystal structure of ST8Sia-III (PDB 5BO6) (125). The PBR region is depicted in orange and the PSTD is depicted in wheat. Sialylmotifs are depicted in cyan (SML), marine (SMS), red (SMVS), and violet (M3). Asparagine attachment sites of the autopolysialylated N-glycans are shown as green spheres and Leu^{151} is marked as cyan sphere. This model was made using SWISS-MODEL server (238–241).

It is important to note that previous results showed that ST8Sia-IV and ST8Sia-II autopolysialylation is not required for their ability to polysialylate NCAM (135, 137). Nevertheless, it can be imagined that a negatively charged polySia chain on a polyST could interact with a substrate directly or their growing polySia chains, or even the surface of a polyST to control its interactions with substrate or the substrate's growing polySia chain. To determine whether autopolysialylation of ST8Sia-IV is altered for any of the PBR mutants, I assessed their autopolysialylation. I individually expressed myc-tagged polyST PBR mutants in COS-1 cells, immunoprecipitated them using an anti-myc antibody, and assessed their autopolysialylation by immunoblotting with an anti-polySia antibody (Fig. 53).

The PBR mutations did not eliminate autopolysialylation, but the R82A and K99A mutants exhibited reduced autopolysialylation at 47 ± 13% (S.D.) and 24 ± 11% (S.D.) of the wild type enzyme, respectively. We have previously used autopolysialylation as a measure of catalytic activity and in this respect our data would suggest that Arg^{82} and Lys^{99} mutations reduce the catalytic activity of the enzyme. However, we see no evidence of a reduced catalytic activity for the K99A mutant that efficiently polysialylates NCAM (Figs. 47 and 53). In addition, results from competition experiments in this chapter and previous publications (200) and direct binding experiments (236), indicate that Arg^{82} indeed participates in binding to NCAM FN1, as well as NRP-2. Interestingly, molecular mass of the residual autopolysialylated K99A mutant is confined to the high molecular mass range, indicating that a small number of chains on the enzyme are fully elongated. These observations raise the following questions: (1) what is the mechanism of autopolysialylation-is it truly a "self" polysialylation or does it require monomer-monomer recognition for "cross" polysialylation? (2) Is the hypothetical positively charged surface of ST8Sia-IV important for polySia chain elongation on the enzyme as well as the substrate? (3) Could the requirements for autopolysialylation of ST8Sia-IV differ for NCAM and NRP-2? I directly address questions 1 and 3 below.

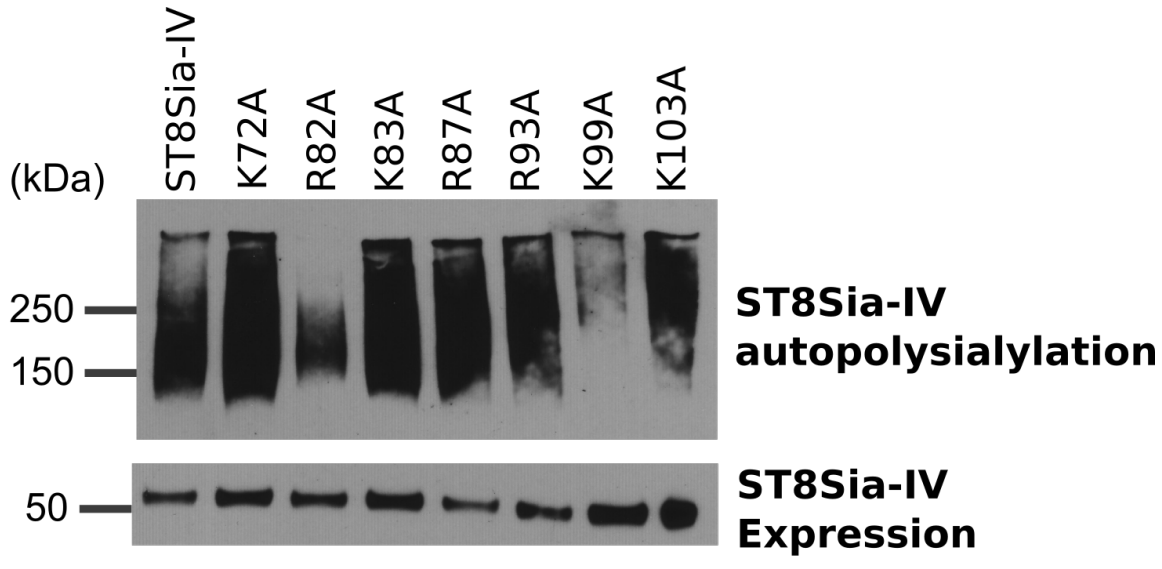
ST8Sia-IV
K72A
R82A
K83A
R87A
R93A
K99A
K103A
(kDa)
250
150
50
ST8Sia-IV
autopolysialylation
ST8Sia-IV
Expression

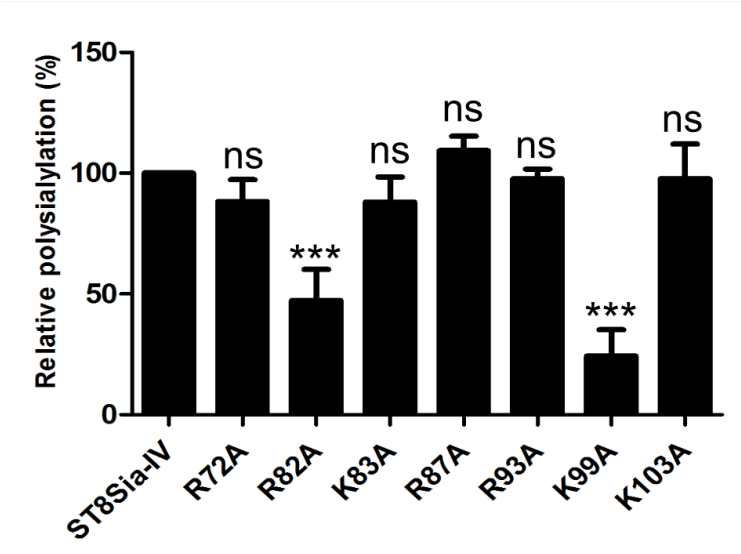
Relative polysialylation (%)
150
100
50
0
ns
ns
ns
ns
***
***
ST8Sia-IV
R72A
R82A
K83A
R87A
R93A
K99A
K103A

Figure 53: Replacing Arg^{82} and Lys^{99} reduces the autopolysialylation of ST8Sia-IV. Myc-tagged ST8Sia-IV PBR mutants were expressed in COS-1 cells and their autopolysialylation was evaluated by immunoblotting of the immunoprecipitated enzymes using an anti-polySia antibody. An aliquot of cell lysate was boiled with Laemmli sample buffer to remove polySia and immunoblotted with an anti-myc antibody. Quantification of the experimental results was performed as described under "Materials and Methods" with data from three different experiments and with error bars representing S.D. Data is reported as % polysialylation with respect to wild type ST8Sia-IV, which is normalized to 100%. Statistical analysis was performed using a one-way ANOVA test with a Dunnett's post-hoc test, where ***, $0.0001<p<0.001$; *ns*, $p>0.05$.

D. PolyST autopolysialylation appears to be a self-polysialylation process.

Previous work by Mühlenhoff et al. proposed that while NCAM polysialylation requires prior addition of terminal α2,3 or α2,6 sialic acid residue (245), polySTs can add the sialic acid residue to terminal galactose residue for autopolysialylation (135). However, it was not known whether a single polyST molecule can polysialylate itself or is polysialylated by a neighboring molecule. I reasoned that if an inactive polyST was polysialylated by an active polyST, then this would be evidence for a "cross" polysialylation process, while the inability of an inactive polyST to be polysialylated by an active polyST would suggest a "self" polysialylation process. With this in mind, I co-expressed V5-tagged ST8Sia-IV with myc-tagged ST8Sia-IV H331K (catalytically inactive mutant). I found that the active ST8Sia-IV co-immunoprecipitated with the inactive H331K mutant, making it impossible to determine whether the polySia I detected was on the inactive mutant or the active enzyme. To address this problem, I used two non-autopolysialylated, catalytically active ST8Sia-IV mutants, mut2.3 and L151A. ST8Sia-IV mut2.3 is a mutant in which the two autopolysialylated glycan attachment sites are mutated (N74S and N119Q), and as a result the enzyme is not autopolysialylated but can still polysialylate NCAM (137). The ST8Sia-IV L151A mutation lies in the SML region. This mutant is localized properly in the Golgi, did not autopolysialylate, but could polysialylate NCAM (Dr. Brett Close, personal communication). Upon co-expressing these two mutants with ST8Sia-IV H331K, I observed that the non-autopolysialylated ST8Sia-IV mutants that polysialylated NCAM were not capable of polysialylating ST8Sia-IV H331K (Fig. 54). These results suggest that ST8Sia-IV autopolysialylation is self- and not cross-polysialylation process, and that the decreases in autopolysialylation observed in the R82A and K99A mutants were not likely the result of a loss of protein-protein interaction between two enzyme monomers.

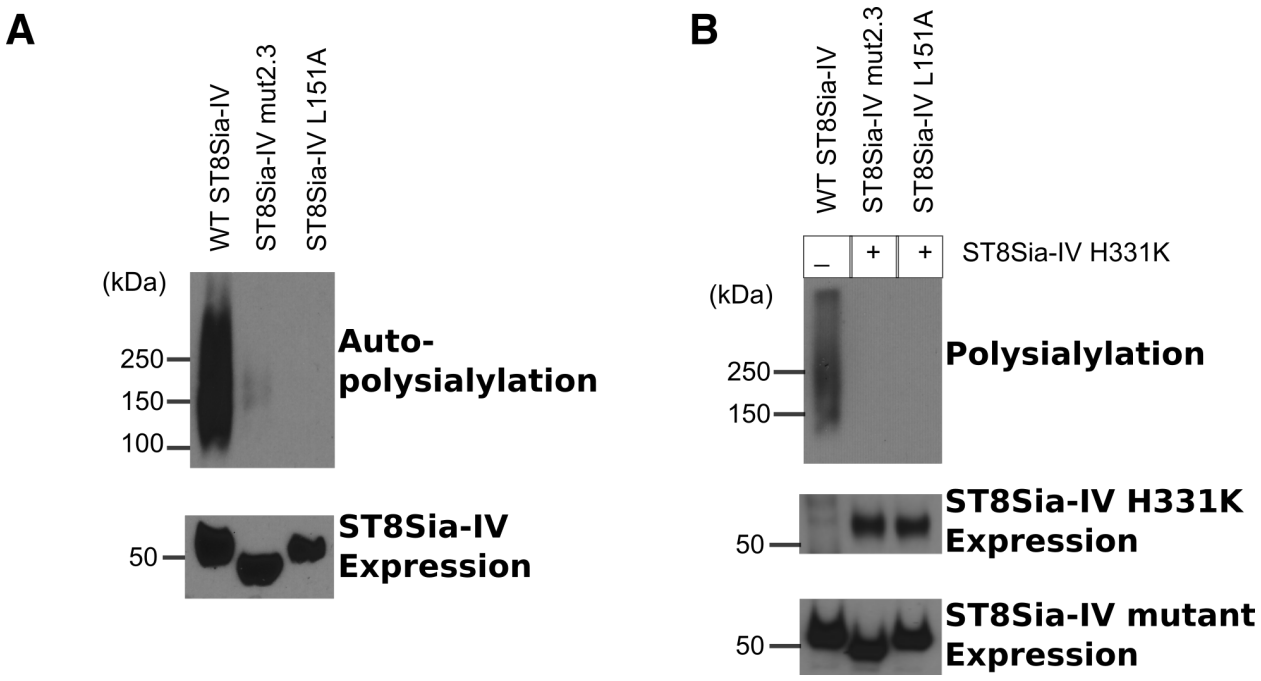

Figure 54: ST8Sia-IV autopolysialylation appears to be a self-polysialylation process. A, Autopolysialylation of ST8Sia-IV mut2.3 and L151A mutants. V5-tagged ST8Sia-IV mut2.3 or L151A mutants were expressed in COS-1 cells and immunoprecipitated from the cell lysates using anti-V5 antibody. Their polysialylation was assessed by immunoblotting with anti-polySia antibody. B, Myc-tagged ST8Sia-IV H331K was co-expressed with the V5-tagged mut2.3 or L151A catalytically active, but non-autopolysialylated enzyme mutants in COS-1 cells. Myc-tagged wild-type (WT) ST8Sia-IV was expressed alone as an autopolysialylation control. Wild-type ST8Sia-IV (control) or the H331K mutant were immunoprecipitated from the cell lysates using an anti-myc antibody and immunoblotted using an anti-polySia antibody. To determine expression levels of proteins, an aliquot of cell lysate was boiled in Laemmli sample buffer to remove polySia and immunoblotted using anti-V5 and anti-myc antibodies.

E. ST8Sia-IV autopolysialylation is required for NRP-2, but not NCAM, polysialylation.

To examine the relationship between ST8Sia-IV autopolysialylation and polysialylation of NCAM and NRP-2, V5-tagged mut2.3 and L151A ST8Sia-IV mutants were co-expressed with myc-tagged NCAM or NRP-2. Following immunoprecipitation using an anti-V5 antibody, substrate polysialylation was detected by immunoblotting with an anti-polySia antibody (Fig. 55). Protein expression was determined as described earlier. I observed that NCAM was polysialylated by both the mut2.3 and L151A mutants, while NRP-2 was not. This indicated that NRP-2 polysialylation was influenced by autopolysialylation status of ST8Sia-IV. Why this may be the case will be addressed in the Discussion section of this chapter.

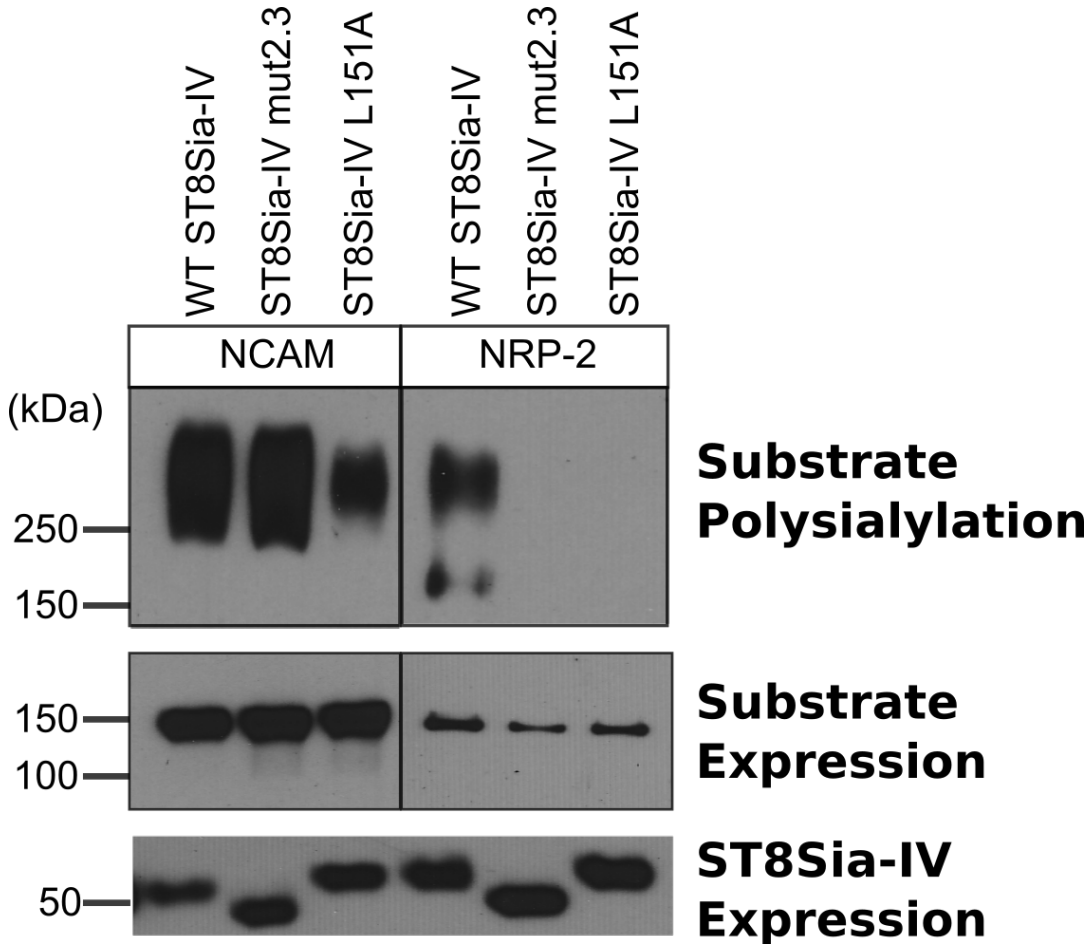

Figure 55: Catalytically active, non-autopolysialylated ST8Sia-IV mutants polysialylate NCAM but not NRP-2. V5-tagged wild-type ST8Sia-IV and its non-autopolysialylated mutants mut2.3 and L151A were co-expressed in COS-1 cells with myc-tagged NCAM or NRP-2. Substrates were immunoprecipitated using an anti-V5 antibody and their polysialylation was assessed by immunoblotting with an anti-polySia antibody. An aliquot of cell lysate was boiled with Laemmli sample buffer to remove polySia and immunoblotted with anti-myc and anti-V5 antibodies to evaluate relative expression levels of substrates and enzyme mutants, respectively.

F. Polysialylation of NCAM and SynCAM 1 by ST8Sia-II requires the contribution of an expanded set of PBR residues.

ST8Sia-II polysialylates both NCAM and SynCAM 1 *in vivo* (111, 162). ST8Sia-II plays important roles during embryonic development (163) and in late stage cancers (187), but the biochemical mechanism of its substrate recognition is largely unknown. In order to determine which ST8Sia-II PBR residues are involved in NCAM and SynCAM 1 polysialylation, we made ST8Sia-II constructs with PBR arginines or lysines mutated individually to alanines. We then assessed intracellular localization of these mutants using indirect immunofluorescence microscopy and found that they co-localized with the GM130 Golgi marker indicating that the mutants are Golgi-localized and correctly folded. We then co-expressed membrane-anchored substrates with wild-type ST8Sia-II and its PBR mutants to determine effect of PBR mutations on substrate polysialylation. These experiments rendered inconclusive and inconsistent results. Upon further investigation, I observed that ST8Sia-II co-immunoprecipitates with substrates and the presence of the autopolysialylated enzyme confounded our results. This was likely exacerbated by the unusually high expression levels we uniquely observe for ST8Sia-II in in the pcDNA3.1 transient expression system. Similar co-immunoprecipitation was not observed with membrane-anchored forms of NCAM or NRP-2 when co-expressed with ST8Sia-IV in the same expression system.

To circumvent this problem, I expressed V5-tagged ST8Sia-II in the pCAG expression system, which expressed more moderate levels of the enzyme, and used Fc-tagged soluble forms of the NCAM and SynCAM 1 substrates (NCAM-Fc and SynCAM-Fc) that traverse the secretory pathway and are secreted into the cell medium. The Fc-tagged substrates were precipitated from the cell medium using protein A-Sepharose beads and their polysialylation was evaluated by immunoblotting with an anti-polySia antibody (Figs. 56 and 57, *upper panels*). Substrate protein expression levels (Figs. 56 and 57, *middle panels*) and ST8Sia-II protein expression levels (Figs. 56 and 57, *lower panels*) were determined as described in the figure legends. We also confirmed the absence of any co-precipitated ST8Sia-II-V5 following substrate precipitation by immunoblotting proteins released from the protein A-Sepharose beads using an anti-V5 antibody (data not shown).

When NCAM-Fc was co-expressed with wild type ST8Sia-II and its PBR mutants in COS-1 cells, mutation of residues analogous to Arg^{82} and Arg^{93} in ST8Sia-IV, namely Arg^{97} and Lys^{108}, led to a significant reduction in NCAM-Fc polysialylation to 33 ± 13% (S.D.) and 23 ± 12% (S.D) of that observed with the wild type enzyme, respectively. I also observed that replacing Lys^{114} and Lys^{118} with alanine also significantly reduced NCAM polysialylation to 42 ± 18% (S.D.) and 31 ± 11% (S.D.) of that observed with the wild type enzyme, respectively (Fig. 56, *top panel*).

For SynCAM-Fc polysialylation by ST8Sia-II, I saw that replacing Arg^{97}, Lys^{102}, Lys^{108}, Lys^{114} and Lys^{118} with alanines led to a substantial reduction or near elimination of SynCAM-Fc polysialylation (51 +/- 16% (S.D.), 21 +/- 20% (S. D.), 59 +/- 20% (S. D.), 3 +/- 5% (S. D.) and 2 +/- 3% (S. D.)) of that observed with wild type enzyme, respectively). Notably, the contribution of Lys^{102} appears to be uniquely important for SynCAM 1 polysialylation (Fig. 57, *top panel*).

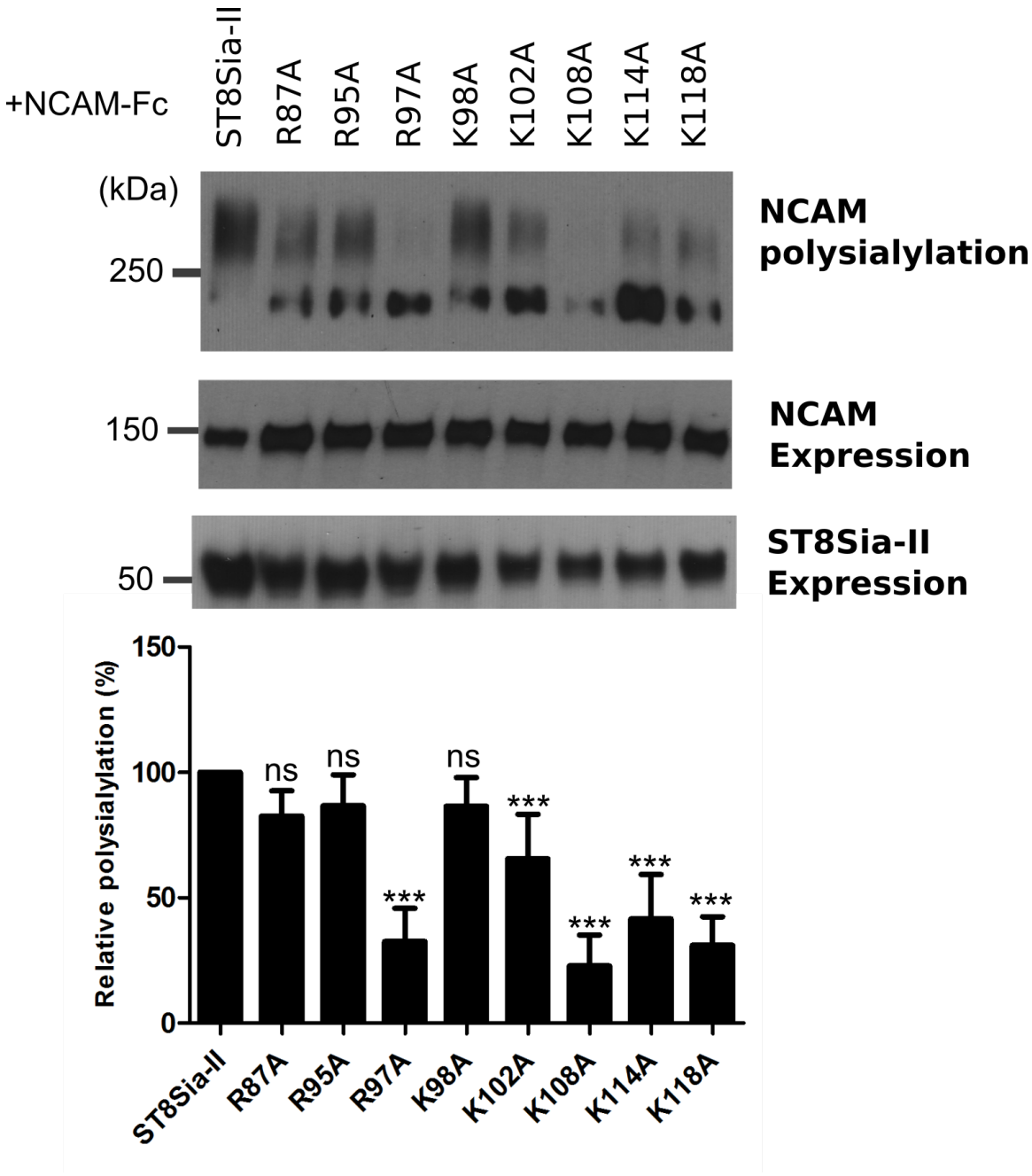
+NCAM-Fc
ST8Sia-II
R87A
R95A
R97A
K98A
K102A
K108A
K114A
K118A
(kDa)
250
150
50
NCAM polysialylation
NCAM Expression
ST8Sia-II Expression
Relative polysialylation (%)
150
100
50
0
ns
ns
ns
***
***
***
***
***
ST8Sia-II
R87A
R95A
R97A
K98A
K102A
K108A
K114A
K118A

Figure 56: A larger set of PBR residues is important for NCAM polysialylation by ST8Sia-II. NCAM-Fc and its PBR mutants were co-expressed with V5-tagged ST8Sia-II in COS-1 cells. NCAM-Fc proteins were precipitated from the cell medium using protein A-Sepharose beads, released from these beads, and their polysialylation assessed by immunoblotting using an anti-polySia antibody. Twenty-five percent of the NCAM-Fc bound beads were boiled in Laemmli sample buffer and immunoblotted using an HRP-conjugated anti-human IgG to evaluate NCAM-Fc expression levels. An aliquot of cell lysate was boiled in Laemmli sample buffer and immunoblotted with an anti-V5 antibody to determine expression levels of the ST8Sia-II mutants. Quantification of the experimental results was performed as described under "Materials and Methods" with data from six different experiments with error bars representing S.D. Data is reported as % polysialylation with respect to the polysialylation of NCAM-Fc by wild type ST8Sia-II, which is normalized to 100%. Statistical analysis was performed using a one-way ANOVA test with a Dunnett's post-hoc test, where ***, $0.0001<p<0.001$; *ns*, $p>0.05$.

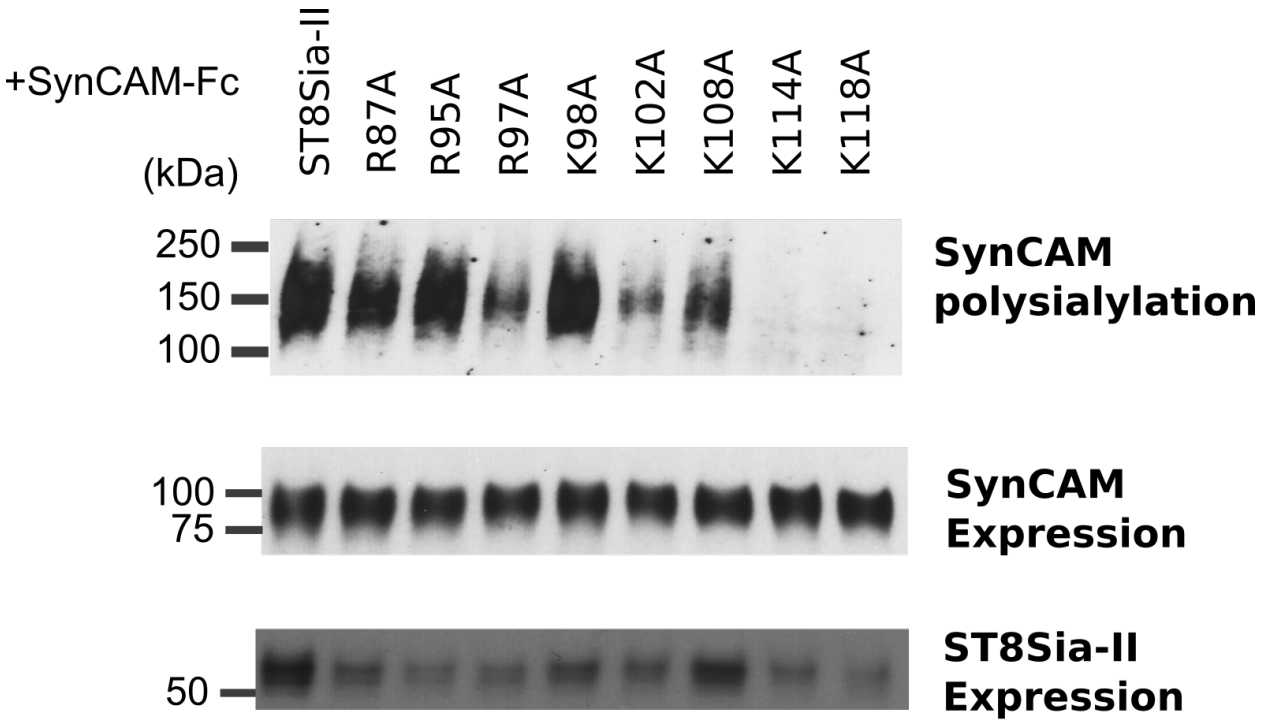
+SynCAM-Fc
ST8Sia-II
R87A
R95A
R97A
K98A
K102A
K108A
K114A
K118A
(kDa)
250
150
100
SynCAM polysialylation
100
75
SynCAM Expression
50
ST8Sia-II Expression

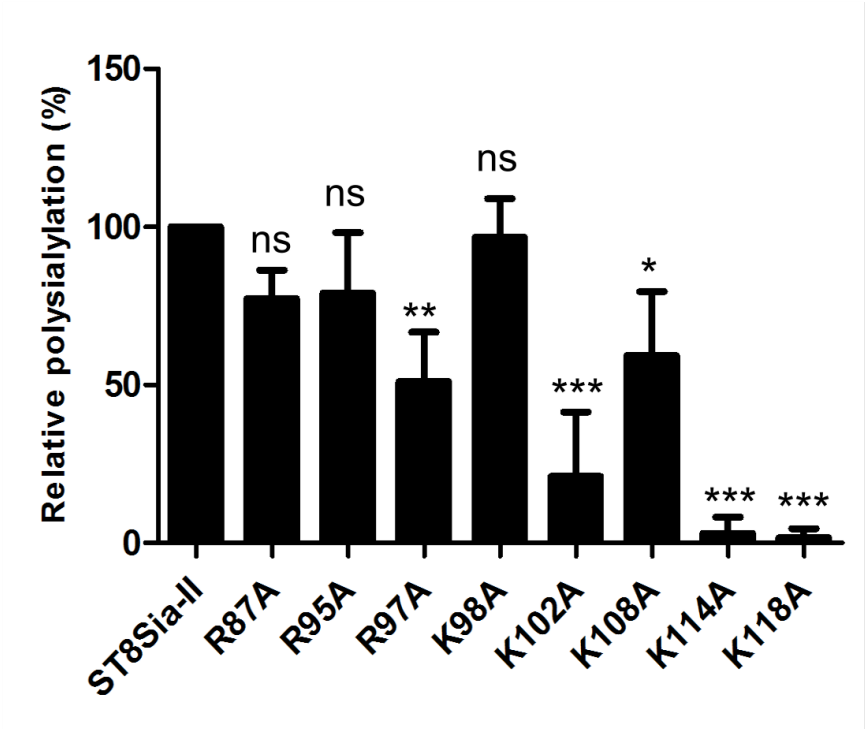
Relative polysialylation (%)
150
100
50
0
ns
ns
ns
**
***
*
***
***
ST8Sia-II
R87A
R95A
R97A
K98A
K102A
K108A
K114A
K118A

Figure 57: SynCAM polysialylation by ST8Sia-II requires contributions from multiple PBR residues. SynCAM-Fc and its PBR mutants were co-expressed with V5-tagged ST8Sia-II in COS-1 cells. SynCAM-Fc proteins were precipitated from the cell medium using protein A-Sepharose beads and immunoblotted to evaluate its polysialylation using an anti-polySia antibody. Twenty-five percent of the SynCAM-Fc bound protein A-Sepharose beads was boiled with Laemmli sample buffer to remove polySia and immunoblotted using HRP-conjugated anti-human IgG to evaluate expression levels of SynCAM-Fc. An aliquot of cell lysate was boiled in Laemmli sample buffer to remove polySia and immunoblotted with an anti-V5 antibody to determine expression levels of the ST8Sia-II PBR mutants. Quantification of the experimental results was performed as described under "Materials and Methods" with data from three different experiments and with error bars representing S.D. Data is reported as % polysialylation with respect to the polysialylation of NCAM-Fc by wild type ST8Sia-II, which is normalized to 100%. Statistical analysis was performed using a one-way ANOVA test with a Dunnett's post-hoc test, where *, $0.01<p<0.05$; **, $0.001<p<0.01$; ***, $0.0001<p<0.001$; *ns*, $p>0.05$.

G. The role of ST8Sia-II PBR residues in NCAM and SynCAM 1 recognition.

In order to determine whether the ST8Sia-II PBR residues that reduce substrate polysialylation are also required for substrate recognition, we mutated the ST8Sia-II PBR residues in the catalytically inactive ST8Sia-II H346K mutant and performed the same competition assay we used to evaluate ST8Sia-IV substrate binding requirements. We verified proper folding and Golgi localization of these mutants by indirect immunofluorescence microscopy, co-localizing them with Golgi marker GM130 (data not shown). I co-expressed NCAM-Fc or SynCAM-Fc with V5-tagged wild-type ST8Sia-II, and myc-tagged ST8Sia-II H346K and its PBR mutants in a 1:1:6 ratio (substrate: ST8Sia-II:ST8Sia-II wild type or PBR mutant). Fc-tagged substrates were recovered and their polysialylation was evaluated by immunoblotting with anti-polySia antibody (Figs. 58 and 59, *upper panels*). Substrate polysialylation observed in the presence of ST8Sia-II H346K and its PBR mutants, relative to expression level of respective substrates, was quantified and reported as fold recovery from the competition with ST8Sia-II H346K.

In the case of NCAM, the ST8Sia-II H346K R97A and K108A mutants showed maximum recovery from the competition (11.48 ± 2.54 fold (S.D.) and 9.54 ± 1.95 fold (S.D.), respectively). Notably, these residues are analogous to Arg^{82} and Arg^{93} in ST8Sia-IV, which are also crucial for recognition and polysialylation of NCAM. Other ST8Sia-II PBR basic residues that reduced polysialylation to intermediate levels showed commensurate recovery in competition assays (Fig. 58). Specifically, the K114A and K118A led to 6.79 ± 1.4 fold (S.D.) and 5.9 ± 1.32 fold (S.D.) recovery of polysialylation, respectively. In addition, the K102A mutant that led to a decrease in NCAM polysialylation to 66% that seen in the presence of the wild type enzyme, also led to a 5.83 +/- 1.53 (S. D.) fold recovery in polysialylation in the competition assay. For SynCAM 1, Lys^{102} stood out as the key contributor for ST8Sia-II recognition followed by Lys^{114}. Replacing these residues in the ST8Sia-II H346K mutant led to 3.64 ± 0.44 fold (S.D.) and 2.19 ± 0.21 fold (S.D.) recovery of polysialylation, respectively (Fig. 59). On the other hand, Arg^{97} and Lys^{108}, which modestly reduced SynCAM 1 polysialylation, did not produce commensurate competition recovery and hence, these residues could be more important for elongation of polySia chains, as discussed previously.

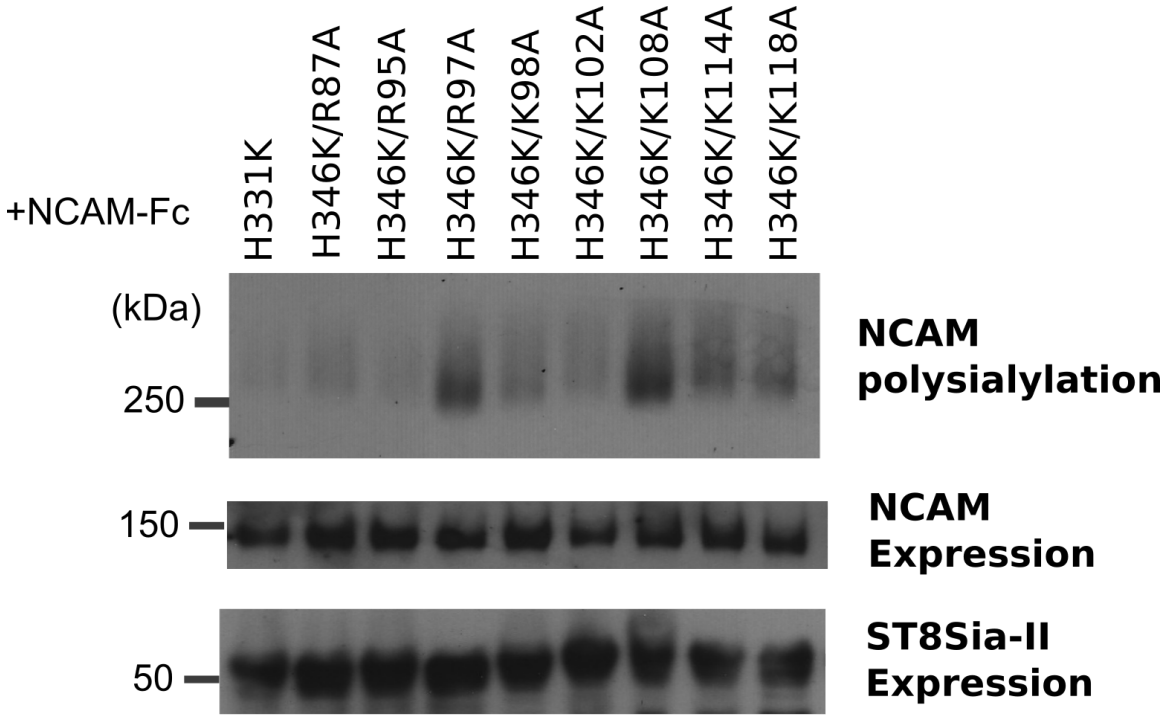
+NCAM-Fc
H331K
H346K/R87A
H346K/R95A
H346K/R97A
H346K/K98A
H346K/K102A
H346K/K108A
H346K/K114A
H346K/K118A
(kDa)
250
150
50
NCAM polysialylation
NCAM Expression
ST8Sia-II Expression

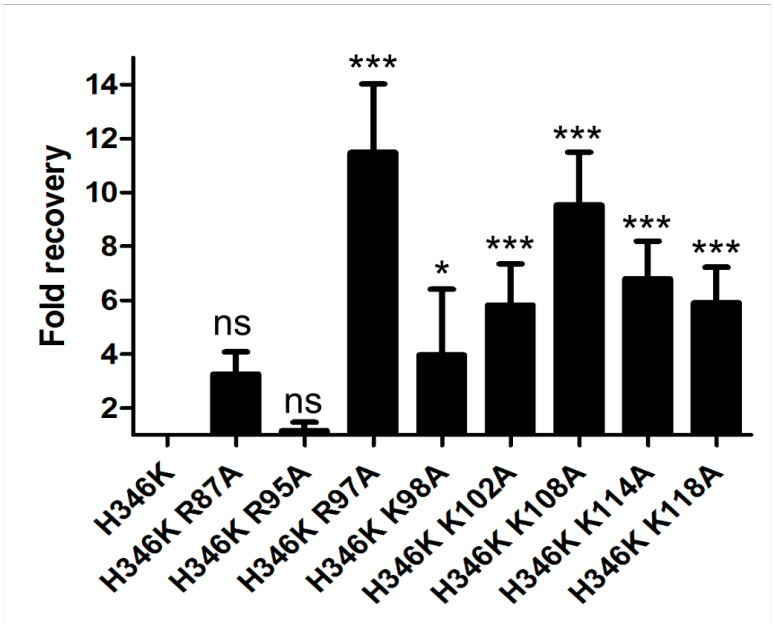
Fold recovery
14
12
10
8
6
4
2
ns
ns
***
*
***
***
***
***
H346K
H346K R87A
H346K R95A
H346K R97A
H346K K98A
H346K K102A
H346K K108A
H346K K114A
H346K K118A

Figure 58. Competition experiments demonstrate that ST8Sia-II recognition of NCAM-Fc requires a larger set of PBR residues relative to its recognition by ST8Sia-IV. NCAM-Fc was co-expressed with untagged wild-type ST8Sia-II, and myc-tagged ST8Sia-II H346K or its PBR mutants in a 1:1:6 ratio in COS-1 cells. NCAM-Fc was recovered from the cell medium using protein A-Sepharose beads. Polysialylation of NCAM-Fc was assessed by immunoblotting using anti-polySia antibody. Twenty-five percent of the NCAM-Fc bound protein A-Sepharose beads were boiled with Laemmli sample buffer to remove polySia and blotted with an HRP-conjugated anti-human IgG to evaluate NCAM-Fc expression. An aliquot of cell lysate was boiled with Laemmli sample buffer and immunoblotted with anti-V5 antibody to evaluate the relative expression levels of ST8Sia-II H346K and its PBR mutants. Quantification of the experimental results was performed as described under "Materials and Methods" with data from five different experiments and with error bars representing S.D. Data was reported as fold recovery with respect to the polysialylation of NCAM-Fc with wild type ST8Sia-II in the presence of ST8Sia-IV H346K as a competitor, which is normalized to 1. Statistical analysis was performed using a one-way ANOVA test with a Dunnett's post-hoc test, where *, $0.01<p<0.05$; ***, $0.0001<p<0.001$; *ns*, $p>0.05$.

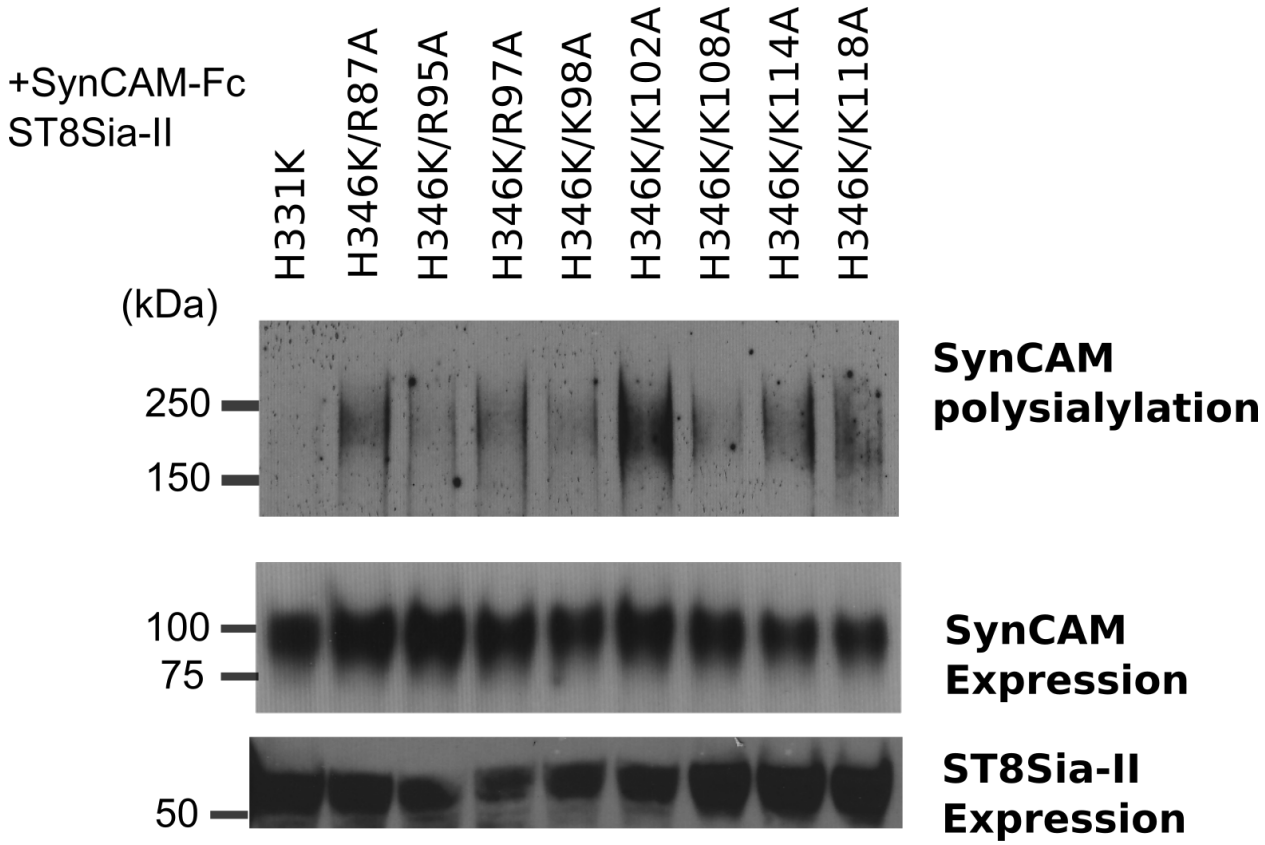
+SynCAM-Fc
ST8Sia-II
H331K
H346K/R87A
H346K/R95A
H346K/R97A
H346K/K98A
H346K/K102A
H346K/K108A
H346K/K114A
H346K/K118A
(kDa)
250
150
SynCAM polysialylation
100
75
SynCAM Expression
50
ST8Sia-II Expression

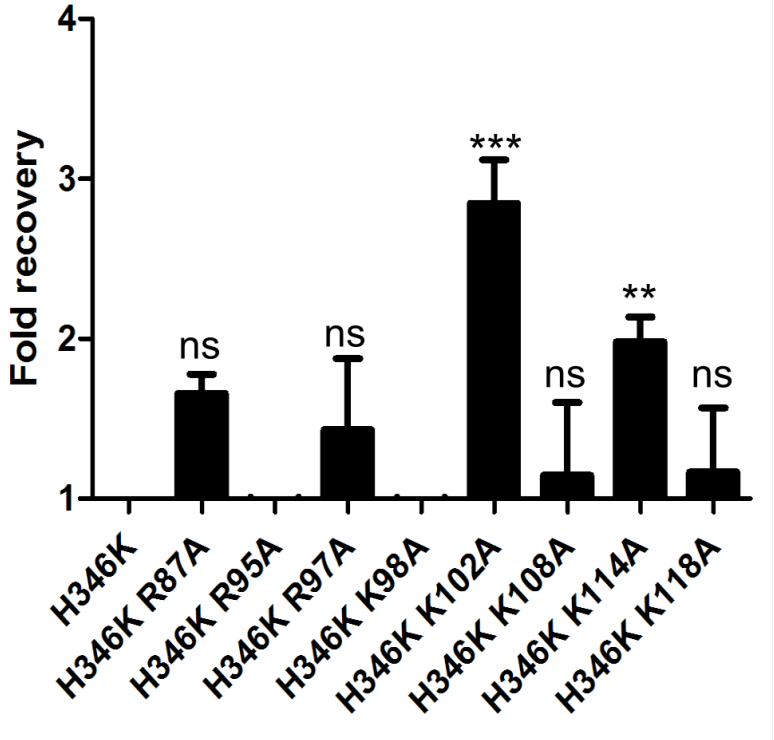
Fold recovery
4
3
2
1
ns
ns
***
ns
**
ns
H346K
H346K R87A
H346K R95A
H346K R97A
H346K K98A
H346K K102A
H346K K108A
H346K K114A
H346K K118A

Figure 59. Competition experiments demonstrate that SynCAM-Fc recognition by ST8Sia-II primarily involves Lys^{102} and Lys^{114}. SynCAM-Fc was co-expressed with untagged wild-type ST8Sia-II, and myc-tagged ST8Sia-II H346K or its PBR mutants in a 1:1:6 ratio in COS-1 cells. SynCAM-Fc was recovered from the cell medium using protein A-Sepharose beads. Polysialylation of SynCAM-Fc was assessed by immunoblotting using anti-polySia antibody. Twenty-five percent of the SynCAM-Fc bound protein A-Sepharose beads were boiled with Laemmli sample buffer to remove polySia and blotted with an HRP-conjugated anti-human IgG to evaluate SynCAM-Fc expression. An aliquot of cell lysate was boiled with Laemmli sample buffer and immunoblotted with anti-V5 antibody to evaluate relative expression levels of ST8Sia-II H346K and its PBR mutants. Quantification of the experimental results was performed as described under "Materials and Methods" with data from five different experiments and with error bars representing S.D. Data was reported as fold recovery with respect to the polysialylation of SynCAM-Fc with wild type ST8Sia-II in the presence of ST8Sia-IV H346K as a competitor, which is normalized to 1. Statistical analysis was performed using a one-way ANOVA test with a Dunnett's post-hoc test, where **, $0.001<p<0.01$; ***, $0.0001<p<0.001$; *ns*, $p>0.05$.

Similar to the ST8Sia-IV K99A mutant in NRP-2 polysialylation, the ST8Sia-II K118A mutant was not capable of polysialylating SynCAM-Fc and had no effect in the competition assay. However, the two mutants differed in their ability to polysialylate NCAM. ST8Sia-IV K99A was able to polysialylate NCAM demonstrating that it was not catalytically inactive. However, ST8Sia-II K118A also reduced NCAM polysialylation, although not to the extent it inhibited SynCAM-Fc polysialylation (31% versus 2% of that observed with the wild type enzyme).

H. Autopolysialylation of ST8Sia-II is reduced when Lys^{114} or Lys^{118} are replaced.

I wondered whether the K118A mutant in ST8Sia-II like the K99A mutant in ST8Sia-IV might exhibit reduced autopolysialylation and whether ST8Sia-II autopolysialylation was also required for SynCAM 1 polysialylation. To evaluate the role of PBR residues in ST8Sia-II autopolysialylation, I expressed myc-tagged ST8Sia-II PBR mutants in COS-1 cells, immunoprecipitated these proteins from cell medium using an anti-myc antibody and immunoblotted with an anti-polySia antibody to evaluate their autopolysialylation. A comparison of ST8Sia-II and ST8Sia-IV autopolysialylation requirements showed that both enzymes required Lys^{99}/ Lys^{114} for efficient autopolysialylation, however other required PBR residues differed. The K114A and K118A mutants showed the most severe impact on ST8Sia-II autopolysialylation with decreases to 32 ± 9% (S.D.) and 15 ± 7% (S.D.) of wild type autopolysialylation levels. For ST8Sia-IV, the R82A (analogous to R97A in ST8Sia-II) decreased autopolysialylation to ~45% of the wild type enzyme and K99A (analogous to K114A in ST8Sia-II) showed decreased autopolysialylation to ~25% of the wild type enzyme. (Figs. 53 and 60). Notably, the correlation between the reduction in K118A autopolysialylation and NCAM-Fc and SynCAM-Fc polysialylation, may suggest that the K118A mutant is impacting ST8Sia-II catalytic activity or a common requirement for polySia chain elongation. As for the K114A mutant, it not only impacts NCAM-Fc and SynCAM-Fc polysialylation, but also relieves the ST8Sia-II H346K competition for both NCAM-Fc and SynCAM-Fc, suggesting it plays a role in substrate recognition. This is not the case for the analogous Lys^{99} in ST8Sia-IV, which when replaced with alanine decreases NRP-2 polysialylation and enzyme autopolysialylation without a substantial impact on the competition assay/substrate recognition.

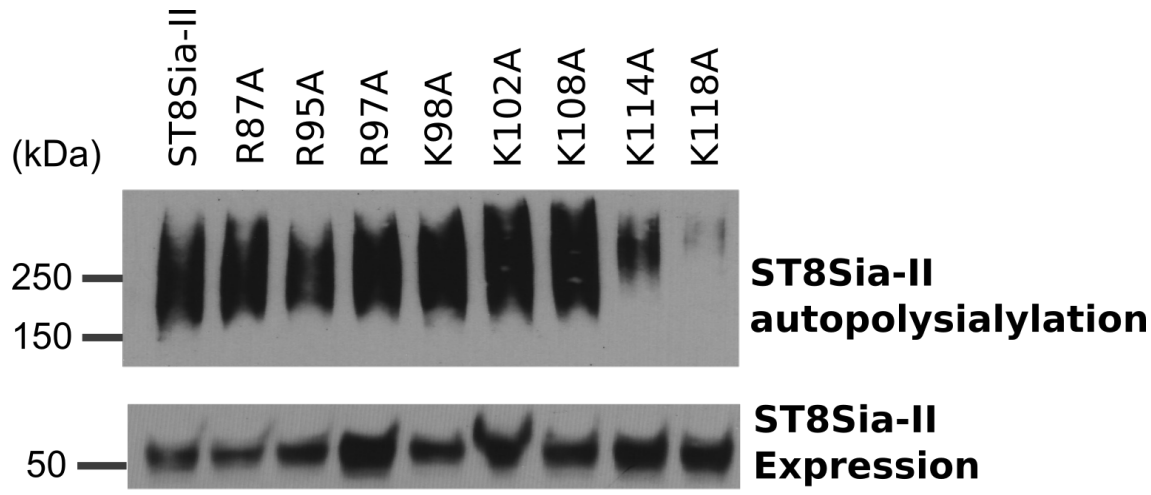
(kDa)
ST8Sia-II
R87A
R95A
R97A
K98A
K102A
K108A
K114A
K118A
250
150
50
ST8Sia-II
autopolysialylation
ST8Sia-II
Expression

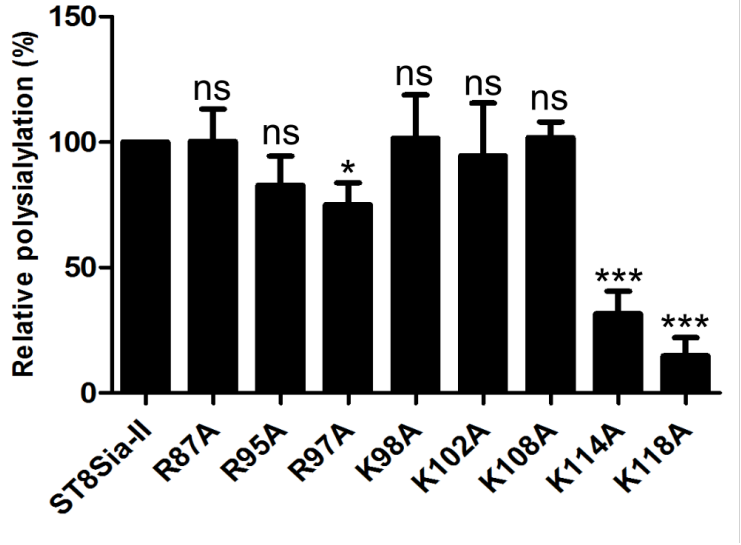
Relative polysialylation (%)
150
100
50
0
ns
ns
*
ns
ns
ns
***
***
ST8Sia-II
R87A
R95A
R97A
K98A
K102A
K108A
K114A
K118A

Figure 60: Replacing Lys^{114} and Lys^{118} substantially reduce the autopolysialylation of ST8Sia-II. Myc-tagged ST8Sia-IV and its PBR mutants were expressed in COS-1 cells and their autopolysialylation was evaluated by immunoblotting of immunoprecipitated proteins using an anti-polySia antibody. An aliquot of cell lysate was boiled with Laemmli sample buffer to remove polySia and immunoblotted with an anti-myc antibody to evaluate protein expression level. Quantification of the experimental results was performed as described under "Materials and Methods" with data from four different experiments with error bars representing S.D. Data was reported as % of wild type enzyme autopolysialylation. Statistical analysis was performed using a one-way ANOVA test with a Dunnett's post-hoc test, where ***, $0.0001<p<0.001$; *ns*, $p>0.05$.

Despite the functional differences between Lys^{114} in ST8Sia-II and Lys^{99} in ST8Sia-IV, both appear to play a role in autopolysialylation. I wondered whether the impact that the K114A mutant has on SynCAM polysialylation may be not only related to decreased recognition/binding but also a lower ST8Sia-II autopolysialylation. Or in other words, is ST8Sia-II autopolysialylation required for SynCAM-Fc polysialylation? Using a catalytically active, non-autopolysialylated ST8Sia-II mutant (mut2.4.5) (136), I found that enzyme autopolysialylation was not required for NCAM polysialylation, as seen before (136), and was also not required for SynCAM 1 polysialylation (Fig. 61), indicating that the requirement for polyST autopolysialylation is unique for NRP-2 polysialylation by ST8Sia-IV.

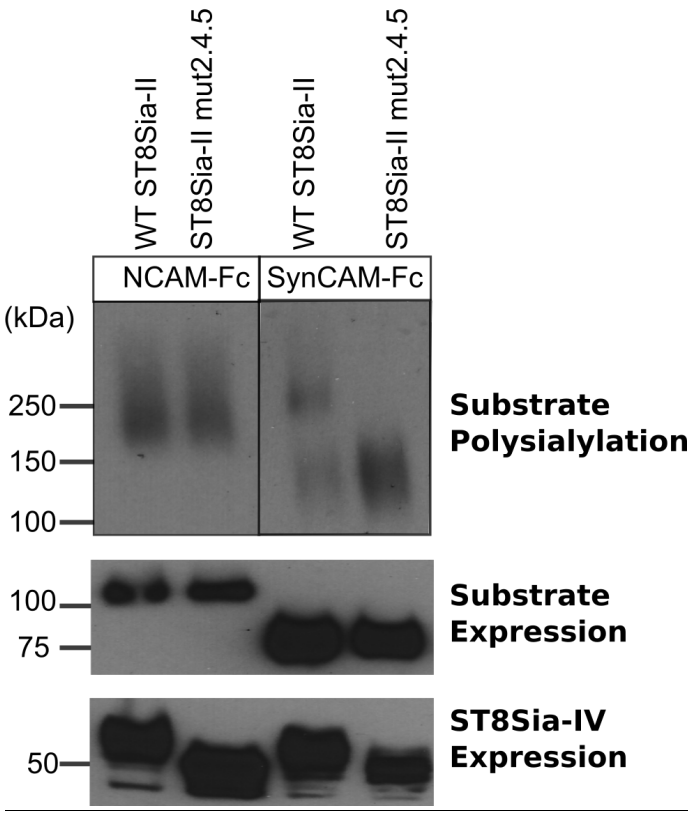

Figure 61: Effect of the polyST autopolysialylation on polysialylation of NCAM and SynCAM 1. Fc-tagged NCAM and SynCAM 1 were co-expressed separately with V5-tagged ST8Sia-II or its non-autopolysialylated mutant (ST8Sia-II mut2.4.5) in COS-1 cells. The substrates were recovered from the cell media using protein A-Sepharose beads. Polysialylation of substrates was assessed by immunoblotting using anti-polySia antibody. Twenty-five percent of the protein A-Sepharose beads loaded with Fc-tagged proteins were boiled with Laemmli sample buffer to remove polySia and blotted with an HRP-conjugated anti-human IgG to evaluate protein expression. An aliquot of cell lysate was boiled with Laemmli sample buffer and immunoblotted with anti-V5 antibody to evaluate the relative expression levels of polySTs and their non-autopolysialylated mutants.

DISCUSSION

In this chapter, I have described my work defining the role of basic sequences in the polySTs for recognition and polysialylation of NCAM, NRP-2, and SynCAM 1. Earlier work by others has shown that glycosylation or glycan modification events can be protein-specific. For example, the first step in the biosynthesis of mannose-6-phosphate on the N-glycans of lysosomal enzymes required for their targeting to the lysosomes (87), and the addition of terminal GalNAc to N-glycan chains of pituitary glycoprotein hormones as the first step in the biosynthesis of the GalNAc-4-SO_4 structure required for their clearance from the circulation (246). Notably, in both of these cases, basic patches play a role in initial substrate recognition (87, 88, 246, 247). The importance of the NCAM FN1 acidic patch for its polysialylation (192, 194), led to the hypothesis that basic regions in polySTs may function as complementary binding sites for acidic residues in substrates, and this would mediate substrate recognition. In addition, a basic surface or groove on the polySTs was also proposed as a way of tethering and stabilizing the growing polySia chains on substrates. Without the latter interaction, chain polymerization may halt prematurely and a substrate may appear unpolysialylated if the chain length had not reached a length recognized by the anti-polySia antibodies (usually 8 units or longer). Two unique basic regions were identified in the polySTs, the PBR and the PSTD that were envisioned to function in substrate recognition and polySia chain elongation.

Dr. Frederick Troy's group first identified and analyzed the polyST PSTD sequences. They showed that mutating Lys^{276} and Arg^{277} in the ST8Sia-IV PSTD had a significant impact on NCAM polysialylation (198). They also showed that heparin serves as a competitive inhibitor of NCAM polysialylation, suggesting that polySia chain elongation may require anchoring to a basic region on the surface of a polyST (198). Dr. Deirdre Foley in our lab later mutated basic residues in the second basic region, the PBR, and observed that Arg^{82} and Arg^{93} also reduce NCAM polysialylation (199). When she analyzed autopolysialylation of the PBR and PSTD mutants, however, PSTD mutants resulted in a more substantial decrease in, or even elimination of, enzyme autopolysialylation, unlike the PBR mutants. She therefore reasoned that the PSTD mutants likely impaired overall catalytic activity of ST8Sia-IV, which is

conceivable considering proximity of the PSTD region to the catalytic sialylmotif SMS (199). Consequently, the idea emerged that the PBR residues play a role in substrate recognition, whereas the PSTD residues form the basic surface that is important for polySia chain elongation. The first part of this concept was also supported by later results in the laboratory that showed that a ST8Sia-IV fragment consisting of amino acids 1-140 and including the PBR, but not the PSTD, acted as a competitive inhibitor of polysialylation (200).

More recently, Volkers et al (125) modeled ST8Sia-IV on the crystal structure of ST8Sia-III (shown in Figure 51). This model suggested that PBR and PSTD are close together in the three dimensional structure (124, 125), and that the PBR and PSTD residues form a basic surface that might bind growing polySia chain (Fig. 52). These investigators also docked the Ig5-FN1 structure identified solved by our lab and using our previous data (125, 207). This model predicts that Glu^{521} in the FN1 domain interacts with Arg^{93} in the ST8Sia-IV PBR region whereas Glu^{523} interacts with the basic residues in the PSTD. In addition, Arg^{93} makes contacts with residues in the PSTD (125). Interestingly, this model predicts that Arg82 may make contacts in the Ig5 region. Taken together, these studies indicate that any mutation in PBR or PSTD basic residues should be viewed with regards to its effect on (1) substrate recognition, (2) polySia chain elongation, or (3) catalytic activity. In my study, I have focused on all of the PBR basic residues in ST8Sia-II and –IV to determine their importance for NCAM, NRP-2, and SynCAM-1 polysialylation and enzyme autopolysialylation.

In these studies I have identified three different groups of polyST PBR residues based on the impact of replacing them on substrate polysialylation and inactive enzyme competition. **Group 1** polyST PBR residues (Fig. 62, green) are those that when replaced significantly decreased both substrate polysialylation and the ability of the inactive enzyme to compete with the active enzyme, suggesting that they are involved in substrate recognition and binding. For ST8Sia-IV these include Arg^{82} for both NCAM and NRP-2, and Arg^{93} for NCAM. For ST8Sia-II, these include Arg^{97} (analogous to Arg^{82} in ST8Sia-IV), Lys^{108} (analogous to Arg93 in ST8Sia-IV), Lys^{114} and Lys^{118} for NCAM, and Lys^{102} and

Lys^{114} for SynCAM 1. I have verified the role of Arg^{82} and Arg^{93} in NCAM FN1 recognition and binding using biophysical methods (236). The correlation between the competition assay results and my direct binding studies indicates that the competition approach is a good indicator of which residues are required for substrate binding. What is apparent from these results is that more PBR residues are required for ST8Sia-II to recognize substrates, and while there are similarities in NCAM recognition by ST8Sia-IV (Arg^{82}/Arg^{93}) and ST8Sia-II (Arg^{97}/Lys^{108}), the recognition requirements for non-NCAM substrates may overlap with those of NCAM, but are not identical.

ST8Sia-IV PBR/NCAM WKI**N**SSLVLEI**RK**NILRFLDAE**R**DVSVV**K**SSFKPG

ST8Sia-IV PBR/NRP-2 WKI**N**SSLVLEI**RK**NIL**R**FLDAERDVSVV**K**SSFKPG

Autopolysialylation * *

ST8Sia-II PBR/NCAM WRH**N**QTLSLRI**R**KQIL**K**FLDAE**K**DISVL**K**GTL**K**PG

ST8Sia-II PBR/SynCAM WRH**N**QTLSLRIRKQIL**K**FLDAEKDISVL**K**GTL**K**PG

Autopolysialylation * *

Figure 62. Summary of the impact of ST8Sia-IV and ST8Sia-II PBR mutants on substrate polysialylation, substrate recognition (Competition Assays), and enzyme autopolysialylation. To make comparisons between competition assays that varied in their fold recovery of polysialylation, I set the highest fold recovery to 10 for each enzyme/substrate pair and adjusted the other numbers to that scale. I then grouped residues impacting polysialylation and/or competition into three groups:

Green indicates those residues that when replaced led to substrate polysialylation of between 0-50% that seen with the wild type enzyme AND rated between 5-10 on the loss of competition/recovery of polysialylation scale. Loss of polysialylation matches the loss of substrate recognition.

Red indicates those residues that when replaced led to substrate polysialylation of between 51% and 100% of that seen with the wild type enzyme AND rated between 5-10 on the loss of competition/recovery of polysialylation scale. Loss of recognition/competition was greater than observed loss in polysialylation.

Blue indicates those residues that when replaced led to substrate polysialylation of between 0-50% that seen with the wild type enzyme AND rated between 0-4 on the loss of competition/recovery of polysialylation scale. Loss of polysialylation was greater than the observed loss of recognition/competition.

Those residues that impact autopolysialylation when replaced with alanines are indicated by a *. The three helical sections of the PBR are underlined in the top ST8Sia-IV PBR sequence (125, 203). Autopolysialylated N-glycan is found on Asn^{74} in ST8Sia-IV and Asn^{89} in ST8Sia-II and is marked in bold.

Group 2 polyST PBR residues (Fig. 62, red) are those that when replaced did not impact or only led to modest decreases in substrate polysialylation, but when replaced in the inactive enzyme did significantly decrease its ability to act as a competitive inhibitor. These residues include ST8Sia-IV Lys^{83} for NCAM and NRP-2 polysialylation and Arg^{87} for NRP-2, and ST8Sia-II Lys^{102} for NCAM. I speculate that mutating these residues leads to a local change in folding that potentially shifts substrate binding. For example, Lys^{83} is adjacent to Arg^{82}, a residue crucial for recognition and polysialylation of NCAM and NRP-2. Replacing Lys^{83} with alanine could alter positioning of Arg^{82}, shifting substrate recognition to other basic residues that allow polysialylation, in the case of NCAM, possibly Arg^{93} alone. However, in a competition scenario when the active enzyme is able to bind using the full recognition site (Arg^{82} and Arg^{93}), the competitor with the weaker binding site loses out.

Group 3 polyST PBR residues (Fig. 62, blue) are those that when replaced decreased substrate polysialylation, but did not significantly impact the ability of the inactive enzyme to compete with the active enzyme. Residues that fall into this category include ST8Sia-IV Lys^{99} for NRP-2 polysialylation and ST8Sia-II Lys^{118} for SynCAM 1 polysialylation (Fig. 61, blue). How could a PBR mutation reduce polysialylation without affecting binding to the substrate? One possibility is that the polyST mutant is catalytically inactive. This possibility has been ruled out for ST8Sia-IV K99A because it robustly polysialylates NCAM (Fig. 47). However, this is a distinct possibility for the ST8Sia-II K118A mutant that substantially reduced polysialylation of NCAM and SynCAM 1 and led to a dramatic reduction in enzyme autopolysialylation. However, replacing this residue in the ST8Sia-II H346K protein did compromise its ability to act as a competitive inhibitor of NCAM polysialylation, but not SynCAM 1 polysialylation, suggesting it plays a role in NCAM recognition but not SynCAM 1 recognition, and making catalytic inactivity less likely.

Polysialylation is believed to consist of following steps: (1) an initial polyST-substrate protein-protein interaction that would lead to (2) initiation of polySia synthesis on appropriate acceptor glycans, and (3) elongation of polySia chains. My observations suggest that Lys^{99} could be involved in polySia

chain elongation on NRP-2. Direct analysis of this possibility is complicated. However, I reasoned that understanding the contributions of the PBR residues to the autopolysialylation of ST8Sia-IV would tell me whether all steps in the polysialylation process are common to substrate polysialylation and autopolysialylation, and if not, the way the PBR mutants impact autopolysialylation might help me better understand the role of PBR residues in Groups 2 and 3.

Based on my results shown in Figure 53, autopolysialylation appears to be a self-polysialylation process because active ST8Sia-IV mutants that cannot be polysialylated themselves (mut2.3 and L151A), could polysialylate NCAM but could not polysialylate an inactive ST8Sia-IV mutant. Thus, a negative impact of a PBR mutant on autopolysialylation is not likely due to an inhibition of monomer-monomer binding and cross-polysialylation. It is conceivable, however, that both substrate polysialylation and enzyme autopolysialylation would employ interactions with a basic surface of the enzyme for polySia chain elongation.

Evaluation of which PBR basic residues are key for enzyme autopolysialylation revealed that mutating Arg^{82} and Lys^{99} in ST8Sia-IV reduced enzyme autopolysialylation to ~45% and ~25% of wild type levels, while mutating Lys^{114} and Lys^{118} in ST8Sia-II reduced enzyme polysialylation to 32% and 15% of wild type levels (Figs. 53 and 60). For ST8Sia-IV, two things were notable. First, that mutating Arg^{82} not only had an impact on substrate recognition/binding and polysialylation, but that it also had an impact on the process of autopolysialylation, which from my other experiment suggests does not require a monomer-monomer interaction. Did this mean that Arg^{82} might participate in both substrate binding and polySia chain elongation? Second, that mutating Lys^{99} impacted NRP-2 polysialylation (but not recognition) and enzyme autopolysialylation, but not NCAM recognition or polysialylation was curious, and implied the possibility that polySia chain elongation might be substrate specific in the sense that the positioning of different substrates might lead to different sets of basic residues on the surface of the polyST being used to support polySia chain elongation.

An alternate possibility that I tested was that enzyme autopolysialylation is required for non-NCAM substrate polysialylation. En-bloc transfer of previously synthesized polySia chains from polyST glycans to substrates had been previously been ruled out as non-autopolysialylated polySTs are able to polysialylate NCAM (135, 136, 138). However, as shown in Figure 55, NRP-2 polysialylated did require ST8Sia-IV autopolysialylation, as the two non-autopolysialylated mutant enzymes were not able to polysialylate NRP-2. It is very important to note here that in the past the lab used enzyme autopolysialylation as a measure of the overall catalytic activity of a mutant enzyme. However, my results suggest that the lack of autopolysialylation may not always reflect a lack of activity. Instead, mutants unable to autopolysialylate may have defects in chain elongation because of a disruption of a basic surface that engages the growing polySia chain and this would be expected to impact the polysialylation of some or all substrates if they use the same surface.

It is conceivable that the mechanism of polySia chain elongation may differ for the various substrates due to significant differences in the structures of substrate recognition domains that are involved in polysialylation and the types of glycans that are polysialylated. For instance, the NRP-2 MAM domain-linker region tandem is structurally very different from NCAM Ig5-FN1 tandem (207, 224), and my work shows that non-NCAM substrates have both overlapping and distinct sets of required basic residues for enzyme recognition suggesting that substrates engage the enzyme is somewhat different ways. In addition, NCAM and SynCAM 1 are polysialylated on N-glycans while NRP-2 is polysialylated on O-glycans. The N-glycans of NCAM or SynCAM 1 are larger than the core-1 or core-2 O-glycans reported to be polysialylated on NRP-2 (229). While ST8Sia-IV autopolysialylation and NRP-2 polysialylation by this enzyme both seem to require Lys^{99}, possibly due to its role in polySia chain elongation, why enzyme autopolysialylation is essential for NRP-2 polysialylation is difficult to decipher. Further experiments will be needed to determine whether ST8Sia-IV autopolysialylation generates a specific conformation that is required for polysialylation of NRP-2 and if the fact that O-glycans are being polysialylated has something to do with this requirement. It seems unlikely that an en bloc transfer of

polySia chains to the NRP-2 O-glycans would occur, as that would suggest that the enzyme employs unique catalytic mechanisms for different substrates.

CHAPTER VI

Concluding Remarks

PolySia with its unique electrostatic, steric, and hydrodynamic properties has substantial influence on the structure and function of its carrier proteins by lowering their interactions, the interactions of cells that express them, and in turn this also impacts signaling downstream of these carriers. The charge properties of polySia also make it an attractive field for positively charged neurotransmitters, ions, and growth factors and this modulates their signaling through corresponding receptors (reviewed in (96, 97, 134)). Consequently, polySia plays important roles in nervous system development, learning, memory, maintenance of circadian rhythm, nerve and liver regeneration (reviewed in (96, 134)). Deregulation of polySia expression is implicated in neurological disorders, cancers, and potentially even immune disorders (reviewed in (96, 186)). Understanding the molecular mechanism of polysialylation is key for the design of approaches to enhance or block polysialylation for therapeutic benefits.

Previous work by our laboratory and others has provided ample evidence that the process of polysialylation is restricted to a limited number of proteins. This selectivity is a consequence of specific recognition domains within substrates such as NCAM. Elimination of the NCAM FN1 domain led to loss of polysialylation and binding of ST8Sia-IV despite the presence of glycans in the Ig5 domain that are usually polysialylated (192, 193). Furthermore, an acidic patch in the FN1 domain and the polybasic region (PBR) in ST8Sia-IV were individually shown to be important for NCAM polysialylation using mutational analysis (192, 199). Structural characterization of the NCAM Ig5-FN1 tandem also revealed sequences governing the relationship between the two domains as well as sequences important for positioning of the polySTs. Both of these factors are important for the robust polysialylation of NCAM.

The goal of this work was to delineate the role of specific sequences in the protein-specific polysialylation of NCAM utilizing direct biophysical methods as well as biochemical analysis. I also

sought to extend understanding of this mechanism beyond the NCAM-ST8Sia-IV interaction to other important polySia carrier proteins, NRP-2 and SynCAM 1 and the other polyST, ST8Sia-II. My work also provides the first clues for the role and mechanism of polyST autopolysialylation. I have accomplished these goals by using mutational analysis, design of chimeric proteins, structural modeling, and biophysical methods such as ITC and NMR. In this chapter, I summarize findings of my study, report my progress on design of a polyST-substrate interaction inhibitor, and present potential models for protein-specific polysialylation suggested by my work.

Biophysical characterization of the interaction interface between the NCAM FN1 domain and ST8Sia-IV PBR.

In chapter III, I have demonstrated that the acidic patch on the FN1 domain of NCAM and select residues of the ST8Sia-IV PBR directly and specifically interact with each other, providing support for our working model that acidic patch recognition by polyST PBR serves as initial docking step in protein specific polysialylation. Earlier work identified other sequences in the FN1 domain that potentially provide a surface for additional contacts between ST8Sia-IV and the FN1 domain to position this polyST for polysialylation of Ig5 N-glycans. For example, mutation of the proline residues in the PSSP sequence in the FN1 domain led to loss of polysialylation as well as ST8Sia-IV binding (193). On the other hand, replacing the FN1 α-helix or QVQ sequences shifted NCAM polysialylation from Ig5 N-glycans to FN1 O-glycans (195). Results of my HSQC NMR analysis reported in chapter III (Figs. 20 and 21) allowed me to map the interaction interface of ST8Sia-IV PBR on to the FN1 domain, and I was able to dissect effects mediated by the PBR region only vis-à-vis those resulting from other sequences in ST8Sia-IV. Remarkably, this interaction region extended beyond previously characterized acidic residues to include nearby Asp^{506} in the acidic patch.

In addition to the acidic patch, NMR analysis revealed perturbations in the Ig5-FN1 linker region and the GGVPI loop implying that the PBR peptide binds at these sites or relays a conformational change to these sequences upon binding to the acidic patch. I favor the latter possibility as the lab has shown earlier that the GGVPI and NGKG loops are not involved in binding to the ST8Sia-IV by co-

immunoprecipitation studies (193). Furthermore, in the crystal structure of the Ig5-FN1 tandem, N-glycan sites that are polysialylated are on the opposite face of that of the acidic patch. If a slight conformational change is induced in these loop regions as well as the Ig5-FN1 linker region, it could serve to reorient the glycan sites while preserving the hydrogen bond structure observed between the loop regions and Ig5-FN1 linker region. This repositioning could then allow for interactions with the other Ig5 and FN1 sequences for proper positioning of polySTs for optimum polysialylation of NCAM (Fig. 63).

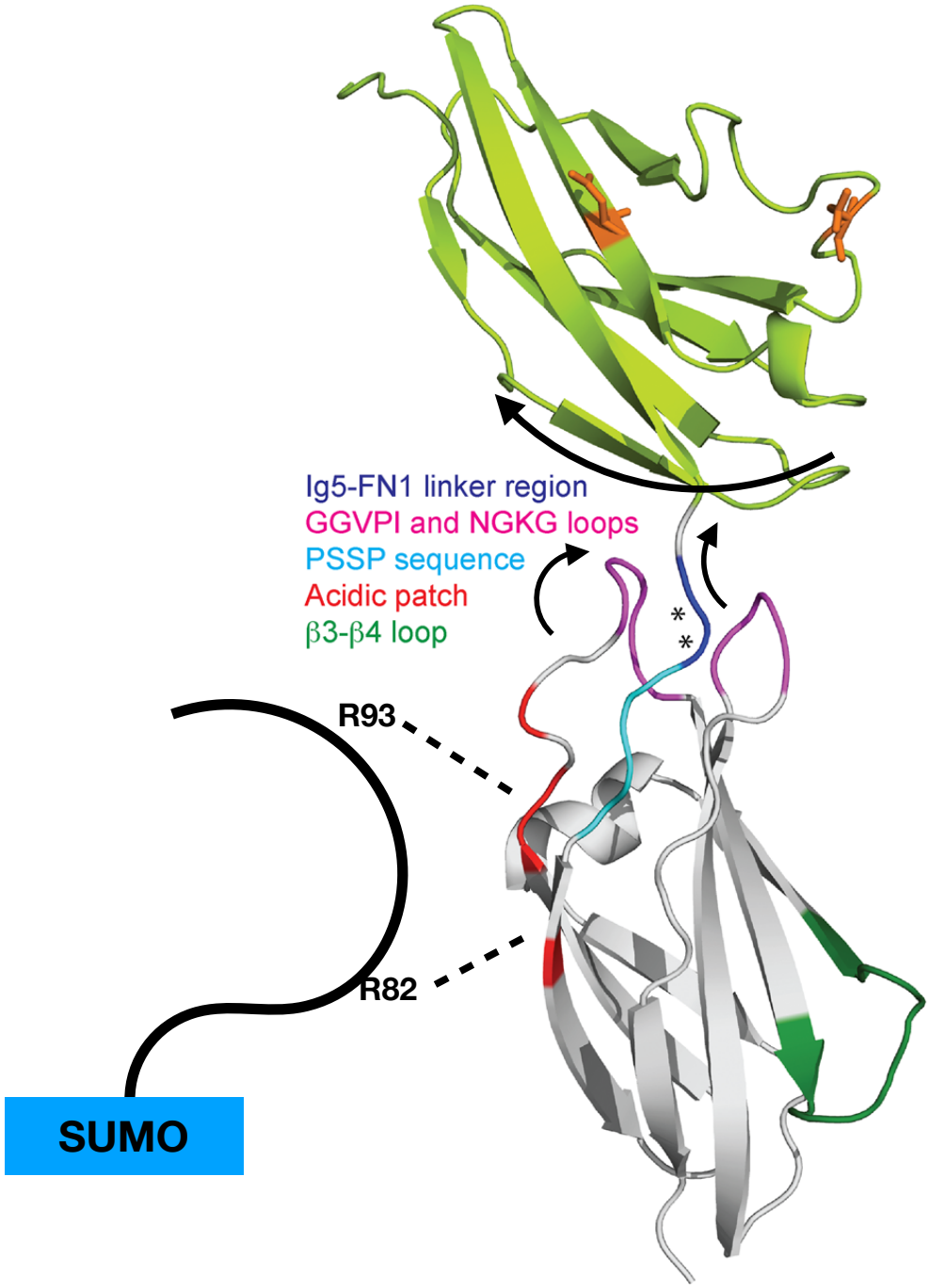

Figure 63: Model showing relayed conformational changes upon binding of PBR peptide to the FN1 acidic patch.

Design of the PBR peptide for inhibition of polysialylation in cells.

As the ST8Sia-IV PBR peptide binds directly to the NCAM FN1 domain, it can be used as a specific competitive inhibitor of the NCAM-polyST interaction, which may be useful as a therapeutic approach to block cancer metastasis. Attempts to inhibit polysialylation have thus far relied on non-specific chemical agents. 3F-NeuAc was recently shown to act as a global inhibitor of sialylation (248). Zanghi et al. (249, 250) showed that ammonia interferes with nucleotide-sugar pools and inhibits polysialylation. CMP was show to inhibit polySia-mediated tumor cell migration (251); however, all of the above treatments are expected to block sialyltransferases in general and are likely to have a a negative impact on a number of important processes.

In order to inhibit the polyST-substrate interaction, the inhibitor must be delivered to the Golgi. An approach I decided to pursue for Golgi delivery of the PBR peptide involves its fusion to the B-subunit of *E.coli* shiga toxin 2 (Stx2B). Shiga toxin is comprised of an A-subunit, which inhibits transcription and a B-subunit, which controls trafficking of the cytotoxic subunit. The B-subunit forms a pentamer to bind monomer of A-subunit (252). Stx binds glycans on the Gb3 glycolipid on the cell surface and is subsequently endocytosed (253). Stx then translocates from the trans-Golgi network (TGN) to the nucleus via the ER (252). Shiga toxin fused peptides have previously been used to inhibit MHC Class I receptors in the ER (254).

As the C-terminus of Stx2b is involved in binding to the glycans of the Gb3 glycolipid, I fused the PBR peptide, composed of residues 74-100 of ST8Sia-IV to the N-terminus of Stx2b. Using microscale thermophoresis, I was able to observe binding between the recombinant NCAM FN1 domain and Stx2b-linked PBR peptide (Fig. 64). Future experiments will focus on delivery of this peptide to the polySia expressing cells as a proof-of-concept. Peptidomimetics can then be used for the design of

optimized therapeutic agents.

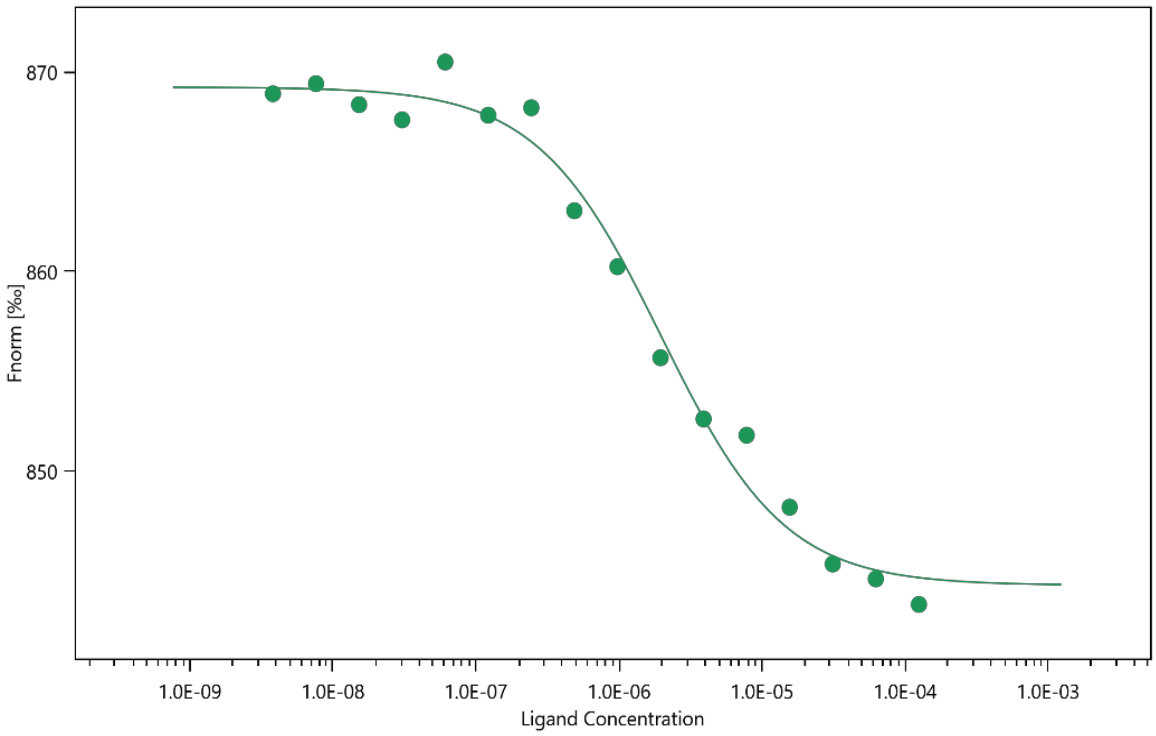

Figure 64: Interaction between NCAM FN1 and Stx2b-PBR using microscale thermophoresis. His-tagged Stx2b was labeled with Red-Tris-NTA fluorescent dye and maintained at 20 nM. Concentration of non-labeled NCAM FN1 was varied between 125 μM to 4 nM. After 15 min incubation, samples were subjected to microscale thermophoresis.

Investigation of mechanism of polysialylation of NRP-2.

In chapter IV, I have shown that NRP-2 polysialylation also follows a two-domain paradigm. The NRP-2 MAM domain and the adjacent O-glycan containing linker region were necessary and sufficient for NRP-2 polysialylation as (1) a NRP2 ΔCF protein lacking the CUB and FV/VIII domains was capable of getting polysialylated (Fig. 33), and (2) achieving polysialylation of NRP-1-Fc to the level of NRP-2 necessitated replacement of its MAM domain-linker region tandem with that of NRP-2 (Fig. 37).

The importance of the MAM domain as recognition domain was highlighted by MAM domain deletion experiments. Removing the MAM domain from NRP-2 resulted in lack of polysialylation, as well as binding to ST8Sia-IV (Fig. 40). These results are in accordance with previous observations that the FN1 domain is critical for NCAM polysialylation as well as recognition/binding by ST8Sia-IV (192, 193). However, the structural folds as well as size of these two domains differ significantly. It is remarkable however, that these recognition domains have similar acidic pI values- 4.59 for NCAM FN1 domain and 4.96 for NRP-2 MAM domain as calculated using ProtParam server (255). These values are in stark contrast with pI values of the related domains that have been shown to be suboptimum replacements for these domains as exemplified by NRP-1 MAM domain (pI = 6.66), OCAM FN1 domain (pI= 6.88) or NCAM FN2 domain (pI= 6.34). It therefore appears a unifying theme that the acidic domains adjacent to the glycan-carrying regions are important for polysialylation. Having said that, the placement of glycans with regards to the acidic patch or the presence of secondary interaction sites in the glycan carrying domains could also play a role in driving robust polysialylation.

An unexpected result of my work was the observation that NRP-1 is capable of being polysialylated by ST8Sia-IV (Fig. 35). My studies revealed a unique molecular mechanism for NRP-1 polysialylation that involves its well-documented recycling via endosomal compartments. My data support that the repeated encounter of NRP-1 with overexpressed ST8Sia-IV in the late Golgi or endosomal compartments is responsible for its polysialylation, despite a weaker recognition of its MAM domain by ST8Sia-IV and a suboptimal linker region with different locations of Ser/Thr residues carrying

O-glycans (Fig. 65). The role of recycling endocytosis in polysialylation is novel and can be relevant in diseases such as cancer where polySTs and NRP-1 have both been reported to be upregulated (96, 186, 210, 256).

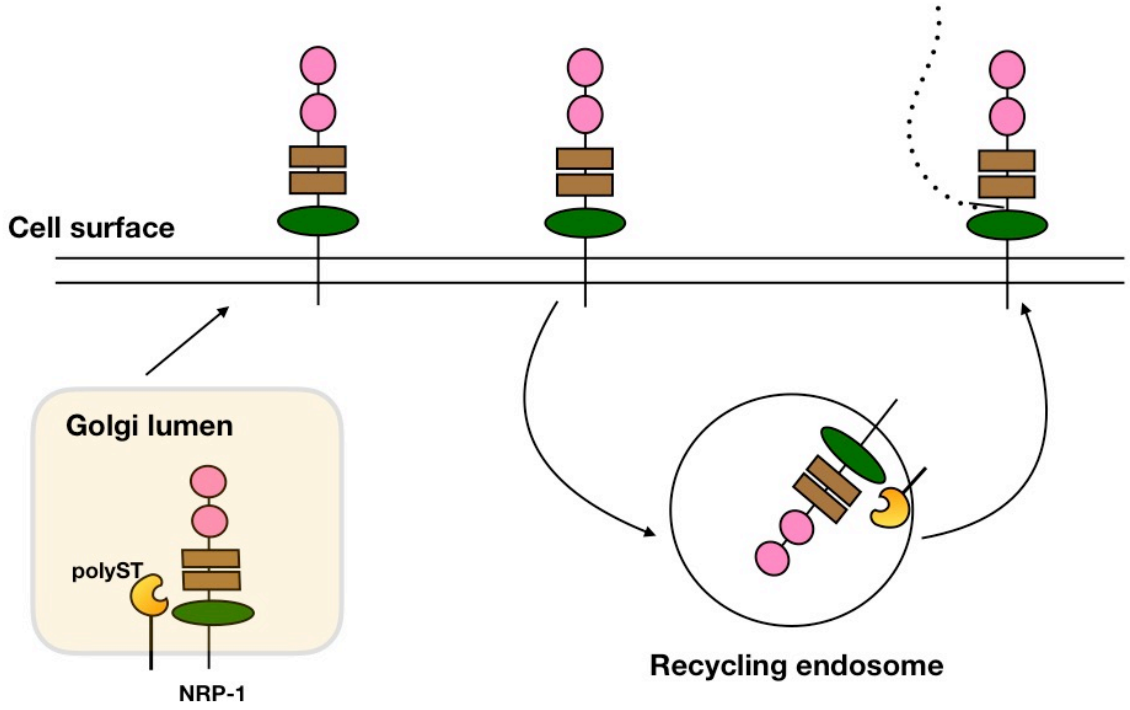

Figure 65: Model for NRP-1 polysialylation. NRP-1 is as such not an optimum polyST substrate. Single pass through the Golgi likely does not lead to NRP-1 polysialylation. Membrane-anchored NRP-1; however, undergoes constant recycling to the intracellular polyST-positive compartments which results in its polysialylation due to repeated exposure to the polyST residing in these compartments.

Why then are the NRPs not observed to be frequently polysialylated? Even the cells, such as A549 lung cancer cells, that endogenously express ST8Sia-IV, will polysialylate exogenously expressed NCAM, but not NRP-2. However, I observed when additional exogenous ST8Sia-IV is co-expressed with NRP-2 in these cells, then NRP-2 polysialylation is detected. One possibility is that NRP-2 is a weaker polyST substrate and hence, much higher enzyme concentrations are required for NRP-2 recognition and polysialylation. A second interesting possibility comes from my results in chapter V, is that the mechanism of O-glycan polysialylation is inherently different than that of N-glycan polysialylation and autopolysialylation of polySTs might be required for this process (Figs. 54 and 61). Further studies may be required to determine what is required for polySTs to be polysialylated, whether an enzyme conformation capable of autopolysialylation is required to initiate polySia synthesis on O-glycans, or whether the presence of polySia on polyST *per se* plays a more direct role in NRP-2 O-glycan polysialylation. In attempts to gain further insights into the process of NRP-2 O-glycan polysialylation, I have compared the properties of polysialylated N- and O-linked glycans the precise O-glycan structures that serve as acceptors for NRP-2 polysialylation have not been characterized; however, sialylated O-glycan structures are frequently much smaller than the sialylated N-glycan structures that serve as acceptors for polysialylation (Figs. 3 and 5). One possibility is that the initial shorter polySia chains synthesized on NRP-2 may remain tethered to adjacent NRP-2 domains blocking further elongation unless stearic repulsion is provided by large polySia chains present on autopolysialylated ST8Sia-IV. In line with this idea, the NRP-2 FV/VIII domains adjacent to the polysialylated linker are more basic than the NCAM Ig4 domain adjacent to the polysialylated Ig5 domain (pI = 8.31 vs pI = 5.2, respectively). On the other hand, the polySia chains on ST8Sia-IV could repel the growing polySia chain on NRP-2 by charge-charge repulsion blocking its binding to the FV/VIII domains. Once the length of growing polySia chain increases beyond a certain size, further elongation most likely occurs farther away from the protein. This model may partially explain requirement of autopolysialylation for NRP-2 polysialylation (Fig. 66).

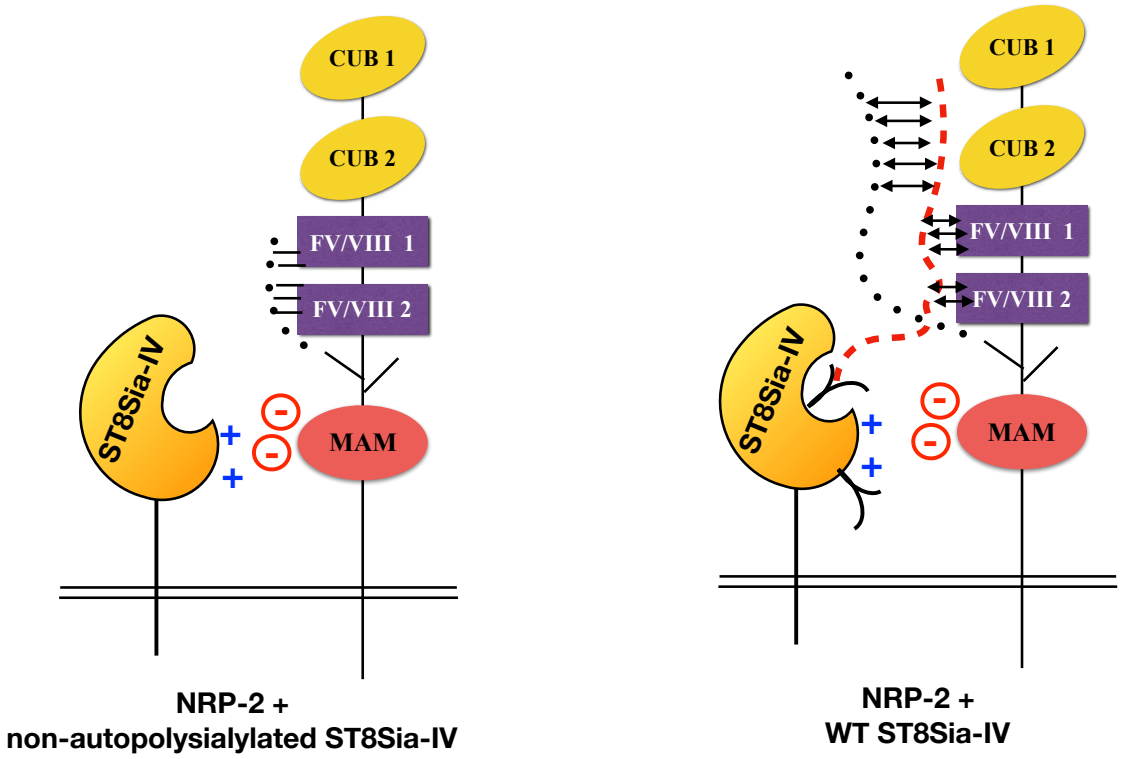

Figure 66: Model for NRP-2 polysialylation with emphasis on ST8Sia-IV autopolysialylation. Left panel shows synthesis of shorter polySia chains by non-autopolysialylated ST8Sia-IV, that remain tethered to NRP-2 FV/FVIII domains. Right panel shows the elongation of polySia on NRP-2. PolySia chains on ST8Sia-IV are shown in red and polySia chains on NRP-2 are shown in black. Repulsive interactions between the two polySia chains and polyST polySia chain and NRP-2 FV/FVIII domains are represented by two-headed arrows.

The role of polySia in NRP-2 function is not clear. Recently, Kiermaier et al. (110) have shown that polysialylated NRP-2 on mature dendritic cells is dispensable for migratory responses in response to CCL21 chemokine, which is in contrast with the previous studies (106, 108, 109). They showed that in fact, polySia on CCR7 is responsible for these functions (110). It is not clear; however, whether polySia plays a role in signaling downstream of NRP-2 coreceptors, the plexins and VEGFRs. Interestingly, a fraction of NRP-1 is modified by the glycosaminoglycans (GAGs), heparan sulfate or chondroitin sulfate, and these GAG chains were shown to modulate VEGFR2 signaling because of their binding to VEGF (230). PolySia has remarkably similar properties to that of heparan sulfate or chondroitin sulfate owing to its size and negative charge. It is therefore possible that polySia on NRP-2 plays a similar role as the GAG chains on NRP-1 in VEGFR signaling.

The role of polyST PBR residues in polysialylation of various substrates.

In chapter V, I have described my work towards determining the residues important for recognition and polysialylation of NCAM, NRP-2 and SynCAM 1, and to assess whether substrate polysialylation by ST8Sia-II follows the same rules as ST8Sia-IV. These experiments revealed that ST8Sia-II has a larger interaction interface for NCAM, as well as SynCAM 1 polysialylation, relative to that used by ST8Sia-IV for NCAM and NRP-2 polysialylation (Compare Figs. 50 and 51 to Figs. 56 and 57). Residues that corresponded to Arg^{82} and Arg^{93} in ST8Sia-IV, namely Arg^{97} and Lys^{108} in ST8Sia-II, were key residues for NCAM recognition and polysialylation by ST8Sia-II. However, mutations in Lys^{114} and Lys^{118} also reduced NCAM polysialylation and partially eliminated competition by the H346K ST8Sia-II mutant. For SynCAM 1, replacing Lys^{102}, Lys^{114} and Lys^{118} reduced polysialylation (Fig. 57), but only mutations in Lys^{102} and Lys^{114} recovered competition exhibited by ST8Sia-II H346K (Fig. 59).

ST8Sia-II is the major polyST during development and it is the more efficient of the two polySTs. These differences in efficiency were identified when Galuska and colleagues (167) evaluated the polysialylation of brain glycoconjugates in mice with different allelic combinations of the two polySTs. Elimination of ST8Sia-II had a greater impact on total polySia than elimination of ST8Sia-IV.

Seidenfaden et al. (257) showed that treatment of SHSY-5Y neuroblastoma cells with retinoic acid reduced ST8Sia-II mRNA expression and induced ST8Sia-IV mRNA expression, which led to rapid increase in polysialylation without increasing total polySia levels. It is tempting to speculate that higher efficiency of ST8Sia-II is due to its expanded residue requirement for polysialylation. This would make its interactions with substrates stronger and lessen the possibility of dissociation and aborted polysialylation, thus increasing its efficiency.

Results of competition studies to determine residues important for NCAM polysialylation by ST8Sia-IV were in accordance with the results of ITC and NMR studies described in chapter III (Arg^{82} and Arg^{93}) (236). Arg^{82} was a residue common for recognition of NCAM as well as NRP-2. Additionally, Arg^{87} appeared to be playing a secondary role in NRP-2 recognition. Interestingly, for NCAM, as well as NRP-2, Lys^{83} did not influence polysialylation but showed recovery from competition. We hypothesize that as this residue is adjacent to Arg^{82}, it is likely important for positioning of this residue. Mutating Lys^{83} potentially alters the binding interface. For the polysialylation experiments the "new" binding interface is sufficient for recognition and polysialylation, while in the competition experiments, the wild type active enzyme with its optimal recognition interface binds more strongly than the Lys^{83} mutant resulting in a decrease in competition and increase in polysialylation.

Evaluating autopolysialylation of polyST PBR mutants allowed us to determine whether the effects of these mutations in polysialylation and competition experiments were due to defective substrate recognition, or possibly chain elongation or decreased catalytic activity. ST8Sia-IV K99A mutant likely represented effects on the polySia chain elongation, as roles in substrate recognition and catalytic activity were ruled out by my experiments. Mutating Lys^{99} to alanine results in lower autopolysialylation as well as NRP-2 polysialylation. Compromised catalytic activity of this mutant can be ruled out as the K99A mutant effectively polysialylates NCAM, and changes in substrate recognition were not apparent in NRP-2 competition experiments. On the other hand, the ST8Sia-II K118A mutant was defective in NCAM and SynCAM 1 polysialylation, as well as autopolysialylation. When this mutant was made in ST8Sia-II

H346K, a modest recovery from competitive inhibition was observed for NCAM but not SynCAM 1. As a result, I cannot completely rule out that ST8Sia-II Lys^{118} could exhibit impaired catalytic activity, but it seems to contribute to recognition of NCAM.

Notably, for ST8Sia-II as well as ST8Sia-IV, some of the residues that are of common importance for the recognition of respective substrates (Arg^{82} in ST8Sia-IV and Lys^{114} in ST8Sia-II) exhibit lower autopolysialylation (Figs. 53 and 60). It is possible that these residues may have a dual role in substrate recognition and polySia chain elongation, which would lead to a model in which there is a switch from enzyme-substrate protein-protein interaction to enzyme-substrate polySia chain protein-carbohydrate interaction, and these residues are involved in both types of interaction. Or in other words, the polyST PBR first interacts with the acidic patch on the substrate recognition domain and then with the substrate's growing polySia chain, as shown in Figure 67. In this model, the role of polySia chains on the polySTs is difficult to predict. Nevertheless, it can be imagined that repulsive forces established by the negatively charged polySia chains on polySTs and growing polySia chains on the substrates could drive the elongation process similar to the model described in Figure 67. Furthermore, analysis of structural models of ST8Sia-IV reveals an alternative elongation surface constituted by residues Lys^{135}-Lys^{140} in ST8Sia-IV and Arg^{145}-Lys^{153}. These stretches each have three basic residues and are in similar, but not identical, locations in the two enzymes. Remarkably, the side chains of ST8Sia-IV Arg^{82} and Arg^{138} are in proximity (2.6 Å) and the side chains of ST8Sia-II Lys^{114} and Arg^{145} are in close proximity (5.4 Å) providing support for the role of these residues in elongation.

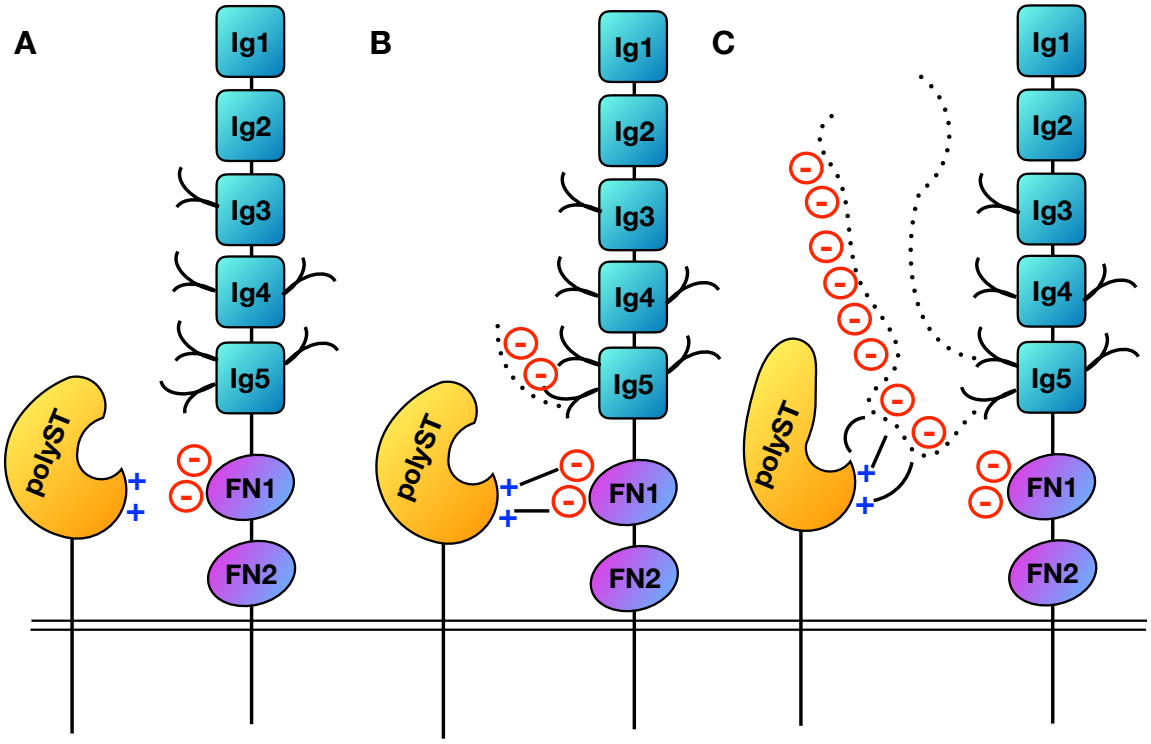

Figure 67: Model for changing interactions of polyST as the process of polysialylation continues. A, polyST basic sequences recognize FN1 acidic sequences as an initial step. B, docking of a polyST at the NCAM FN1 domain leads to initiation of polySia chain synthesis. C, as the polySia chains continue to grow, increasing steric hindrance repels the polyST from interacting with the substrate and basic sequences in the polySTs switch from a protein-protein interaction to a protein-carbohydrate interaction.

Preliminary investigation into the mechanism of autopolysialylation.

Having observed changes in autopolysialylation upon mutating the polyST PBR residues, I wondered whether these mutations impede recognition by the neighboring polyST molecule for "cross" polysialylation or whether making these mutations prevented the elongation of polySia chains on the enzymes. In order to address these possibilities, understanding of the mechanism of autopolysialylation was necessary. My work suggests that autopolysialylation is a "self" (a polyST molecule polysialylates itself) and not catalyzed by a nearby molecule or "cross" polysialylation (Fig. 54). "Self" polysialylation would necessitate a dynamic structure. Work by Mühlenhoff et al. (135) has suggested that ST8Sia-IV has a unique ability to transfer a Sia residue on to a Gal residue on its own N-glycans but not those of NCAM, which further supports the idea of "self" polysialylation.

Evidence for the presence of autopolysialylated enzymes *in vivo* is limited to some reports showing the presence of a few polySTs fragments in the liquid chromatography-mass spectrometry (LC-MS) analysis performed after immunoprecipitation with an anti-polySia antibody (110). Some cell lines, such as A549 adenocarcinoma cell line or MCF-7 breast cancer cell line, that can polysialylate exogenous NCAM owing to the presence of the endogenous polySTs do not otherwise show detectable levels of polySia (Dr. Helena Palka-Hamblin, personal communication) or polysialylation of exogenous NRP-2 (discussed above). The precise mechanism driving autopolysialylation is not clear; however, the autopolysialylated form of ST8Sia-IV is active toward a broader range of substrates. Such a mechanism of autocatalysis is not unusual. Poly(ADP-ribose) polymerase-1 (PARP-1) has been shown to modify itself with poly(ADP-ribose) chains (258). Recent structural characterization of this protein revealed that this protein always exists in monomeric form and exhibits auto- as well as DNA poly(ADP-ribosylation) activities (259). Moreover, this automodification modulates its activity on free DNA vs. chromatin and is sensitive to NAD^+ and nicked DNA concentrations (260). It is therefore conceivable that availability of substrates or ligands i.e. NCAM or CMP-Sia can drive the autocatalytic process. Confirmation of this hypothesis would necessitate *in vitro* biochemical analysis as well as extensive biophysical characterization of mutants.

Final conclusions

In this thesis work, biochemical and biophysical determinants of protein-specific polysialylation of various substrates was investigated. I have demonstrated a direct interaction between the NCAM FN1 acidic patch and the ST8Sia-IV PBR region, which likely serves as an initial step for protein-specific polysialylation. Biophysical characterization of this interaction has led to more refined understanding of the relationship between the NCAM FN1 domain and the adjacent Ig5 domain that carries polysialylated N-glycans. I have also defined sequence requirements for NRP-2 polysialylation and have shown that it follows the 'two-domain paradigm'. I have further shown that NRP-1 can be a novel polyST substrate because of its recycling to the polyST-expressing compartments, despite containing a suboptimum recognition domain. I have extended my study to include the other polyST, ST8Sia-II, to understand the biochemical basis governing its polysialylation of NCAM and SynCAM 1. Finally, my work sheds light on the role and mechanism of autopolysialylation in substrate polysialylation.

It is my belief that this work has contributed to the understanding of the molecular mechanism of polysialylation, a glycosylation event that is of crucial importance during development, tissue regeneration, and various pathological conditions including cancer. Results of this study can provide insights into novel approaches to control polySia expression for therapeutic benefits.

CITED LITERATURE

1. Moremen, K. W., Tiemeyer, M., and Nairn, A. V. (2012) Vertebrate protein glycosylation: diversity, synthesis and function. *Nat. Rev. Mol. Cell Biol.* **13**, 448–462

2. Shrimal, S., Cherepanova, N. A., and Gilmore, R. (2015) Cotranslational and posttranslocational N-glycosylation of proteins in the endoplasmic reticulum. *Semin. Cell Dev. Biol.* **41**, 71–78

3. Steentoft, C., Vakhrushev, S. Y., Joshi, H. J., Kong, Y., Vester-Christensen, M. B., Schjoldager, K. T.-B. G., Lavrsen, K., Dabelsteen, S., Pedersen, N. B., Marcos-Silva, L., Gupta, R., Paul Bennett, E., Mandel, U., Brunak, S., Wandall, H. H., Levery, S. B., and Clausen, H. (2013) Precision mapping of the human O-GalNAc glycoproteome through SimpleCell technology. *EMBO J.* **32**, 1478–1488

4. Steentoft, C., Vakhrushev, S. Y., Vester-Christensen, M. B., Schjoldager, K. T.-B. G., Kong, Y., Bennett, E. P., Mandel, U., Wandall, H., Levery, S. B., and Clausen, H. (2011) Mining the O-glycoproteome using zinc-finger nuclease–glycoengineered SimpleCell lines. *Nat. Methods*. **8**, 977–982

5. Van Der Wel, H., Ercan, A., and West, C. M. (2005) The Skp1 prolyl hydroxylase from Dictyostelium is related to the hypoxia-inducible factor-?? class of animal prolyl 4-hydroxylases. *J. Biol. Chem.* **280**, 14645–14655

6. Furmanek, A., and Hofsteenge, J. (2000) Protein C-mannosylation: Facts and questions. *Acta Biochim. Pol.* **47**, 781–789

7. Maynard, J. C., Burlingame, A. L., and Medzihradszky, K. F. (2016) Cysteine S-linked *N* -acetylglucosamine (S-GlcNAcylation), A New Post-translational Modification in Mammals. *Mol. Cell. Proteomics*. **15**, 3405–3411

8. De Leon, C. A., Levine, P. M., Craven, T. W., and Pratt, M. R. (2017) The sulfur-linked analog of O-GlcNAc (S-GlcNAc) is an enzymatically stable and a reasonable structural-surrogate for O-GlcNAc at the peptide and protein levels. *Biochemistry*. 10.1021/acs.biochem.7b00268

9. Xiao, H., and Wu, R. (2017) Global and Site-Specific Analysis Reveals Unexpected and Extensive Protein S-GlcNAcylation in Human Cells. *Anal. Chem.* 10.1021/acs.analchem.6b05064

10. Haltiwanger, R. S., and Lowe, J. B. (2004) Role of Glycosylation in Development. *Annu. Rev. Biochem.* **73**, 491–537

11. Varki, A. (2017) Biological roles of glycans. *Glycobiology*. **27**, 3–49

12. Nairn, A. V., Aoki, K., Dela Rosa, M., Porterfield, M., Lim, J. M., Kulik, M., Pierce, J. M., Wells, L., Dalton, S., Tiemeyer, M., and Moremen, K. W. (2012) Regulation of glycan structures in murine embryonic stem cells: Combined transcript profiling of glycan-related genes and glycan structural analysis. *J. Biol. Chem.* **287**, 37835–37856

13. Torres, C. R., and Hart, G. W. (1984) Topography and polypeptide distribution of terminal N-acetylglucosamine residues on the surfaces of intact lymphocytes. Evidence for O-linked GlcNAc. *J. Biol. Chem.* **259**, 3308–3317

14. Hart, G. W., Holt, G. D., and Haltiwanger, R. S. (1988) Nuclear and cytoplasmic glycosylation: novel saccharide linkages in unexpected places. *Trends Biochem. Sci.* **13**, 380–384

15. Wells, L. (2001) Glycosylation of Nucleocytoplasmic Proteins: Signal Transduction and O-GlcNAc. *Science (80-.).* **291**, 2376–2378

16. Comer, F. I., and Hart, G. W. (2001) Reciprocity between O-GlcNAc and O-phosphate on the carboxyl terminal domain of RNA polymerase II. *Biochemistry*. **40**, 7845–7852

17. Comer, F. I., and Hart, G. W. (2000) O-glycosylation of nuclear and cytosolic proteins. Dynamic interplay between O-GlcNAc and O-phosphate. *J. Biol. Chem.* **275**, 29179–29182

18. Hanover, J. A. (2017) Glycan-dependent signaling : O-linked. **15**, 1865–1876

19. Kornfeld, R. (1985) Assembly of Asparagine-Linked Oligosaccharides. *Annu. Rev. Biochem.* **54**, 631–664

20. Varki, A., Cummings, R. D., Aebi, M., Packer, N. H., Seeberger, P. H., Esko, J. D., Stanley, P., Hart, G., Darvill, A., Kinoshita, T., Prestegard, J. J., Schnaar, R. L., Freeze, H. H., Marth, J. D., Bertozzi, C. R., Etzler, M. E., Frank, M., Vliegenthart, J. F. G., L??tteke, T., Perez, S., Bolton, E., Rudd, P., Paulson, J., Kanehisa, M., Toukach, P., Aoki-Kinoshita, K. F., Dell, A., Narimatsu, H., York, W., Taniguchi, N., and Kornfeld, S. (2015) Symbol nomenclature for graphical representations of glycans. *Glycobiology*. **25**, 1323–1324

21. Cherepanova, N., Shrimal, S., and Gilmore, R. (2016) N-linked glycosylation and homeostasis of the endoplasmic reticulum. *Curr. Opin. Cell Biol.* **41**, 57–65

22. Lowenthal, M. S., Davis, K. S., Formolo, T., Kilpatrick, L. E., and Phinney, K. W. (2016) Identification of Novel N-Glycosylation Sites at Noncanonical Protein Consensus Motifs. *J. Proteome Res.* **15**, 2087–2101

23. Zielinska, D. F., Gnad, F., Schropp, K., Wi??niewski, J. R., and Mann, M. (2012) Mapping N-Glycosylation Sites across Seven Evolutionarily Distant Species Reveals a Divergent Substrate Proteome Despite a Common Core Machinery. *Mol. Cell*. **46**, 542–548

24. Zielinska, D. F., Gnad, F., Wiśniewski, J. R., and Mann, M. (2010) Precision mapping of an in vivo N-glycoproteome reveals rigid topological and sequence constraints. *Cell*. **141**, 897–907

25. Bause, E., and Legler, G. (1981) The role of the hydroxy amino acid in the triplet sequence Asn-Xaa-Thr(Ser) for the *N* -glycosylation step during glycoprotein biosynthesis. *Biochem. J.* **195**, 639–644

26. Lizak, C., Gerber, S., Numao, S., Aebi, M., and Locher, K. P. (2011) X-ray structure of a bacterial oligosaccharyltransferase. *Nature*. **474**, 350–355

27. Helenius, A., and Aebi, M. (2004) Roles of N-Linked Glycans in the Endoplasmic Reticulum. *Annu. Rev. Biochem.* **73**, 1019–1049

28. D'Alessio, C., and Dahms, N. M. (2015) Glucosidase II and MRH-domain containing proteins in the secretory pathway. *Curr. Protein Pept. Sci.* **16**, 31–48

29. Roth, J., and Zuber, C. (2017) Quality control of glycoprotein folding and ERAD: the role of N-glycan handling, EDEM1 and OS-9. *Histochem. Cell Biol.* **147**, 269–284

30. Stanley, P. (2011) Golgi glycosylation. *Cold Spring Harb. Perspect. Biol.* **3**, 1–13

31. Colley, K. J. (1997) Localization of Golgi glycosyltransferases. *Trends Glycosci. Glycotechnol.* **9**,

267–282

32. Colley, K. J. (1997) Golgi localization of glycosyltransferases: more questions than answers. *Glycobiology*. **7**, 1–13

33. Bhide, G. P., and Colley, K. J. (2017) Sialylation of N-glycans: mechanism, cellular compartmentalization and function. *Histochem. Cell Biol.* **147**, 149–174

34. Ioffe, E., and Stanley, P. (1994) Mice lacking N-acetylglucosaminyltransferase I activity die at mid-gestation, revealing an essential role for complex or hybrid N-linked carbohydrates. *Proc. Natl. Acad. Sci. U. S. A.* **91**, 728–32

35. Akama, T. O., Nakagawa, H., Wong, N. K., Sutton-Smith, M., Dell, A., Morris, H. R., Nakayama, J., Nishimura, S.-I., Pai, A., Moremen, K. W., Marth, J. D., and Fukuda, M. N. (2006) Essential and mutually compensatory roles of α-mannosidase II and α-mannosidase IIx in N-glycan processing in vivo in mice. *Proc. Natl. Acad. Sci.* **103**, 8983–8988

36. Stanley, P. (2016) What Have We Learned from Glycosyltransferase Knockouts in Mice? *J. Mol. Biol.* **428**, 3166–3182

37. Hennet, T., and Cabalzar, J. (2015) Congenital disorders of glycosylation: A concise chart of glycocalyx dysfunction. *Trends Biochem. Sci.* **40**, 377–384

38. Schachter, H., and Freeze, H. H. (2009) Glycosylation diseases: Quo vadis? *Biochim. Biophys. Acta - Mol. Basis Dis.* **1792**, 925–930

39. Freeze, H. H., Eklund, E. A., Ng, B. G., and Patterson, M. C. (2015) Neurological Aspects of Human Glycosylation Disorders. *Annu. Rev. Neurosci.* **38**, 105–125

40. Bennett, E. P., Mandel, U., Clausen, H., Gerken, T. A., Fritz, T. A., and Tabak, L. A. (2012) Control of mucin-type O-glycosylation: A classification of the polypeptide GalNAc-transferase gene family. *Glycobiology*. **22**, 736–756

41. Takeuchi, H., and Haltiwanger, R. S. (2014) Significance of glycosylation in Notch signaling. *Biochem. Biophys. Res. Commun.* **453**, 235–242

42. Praissman, J. L., and Wells, L. (2014) Mammalian O-mannosylation pathway: Glycan structures, enzymes, and protein Substrates. *Biochemistry*. **53**, 3066–3078

43. Tran, D. T., and Ten Hagen, K. G. (2013) Mucin-type o-glycosylation during development. *J. Biol. Chem.* **288**, 6921–6929

44. Corfield, A. (2017) Eukaryotic protein glycosylation: a primer for histochemists and cell biologists. *Histochem. Cell Biol.* **147**, 119–147

45. Revoredo, L., Wang, S., Bennett, E. P., Clausen, H., Moremen, K. W., Jarvis, D. L., Ten Hagen, K. G., Tabak, L. A., and Gerken, T. A. (2016) Mucin-type o-glycosylation is controlled by short- And long-range glycopeptide substrate recognition that varies among members of the polypeptide GalNAc transferase family. *Glycobiology*. **26**, 360–376

46. Hang, H. C., and Bertozzi, C. R. (2005) The chemistry and biology of mucin-type O-linked glycosylation. *Bioorganic Med. Chem.* **13**, 5021–5034

47. Kato, K., Jeanneau, C., Tarp, M. A., Benet-Pagès, A., Lorenz-Depiereux, B., Bennett, E. P.,

Mandel, U., Strom, T. M., and Clausen, H. (2006) Polypeptide GalNAc-transferase T3 and familial tumoral calcinosis: Secretion of fibroblast growth factor 23 requires O-glycosylation. *J. Biol. Chem.* **281**, 18370–18377

48. Tian, E., Hoffman, M. P., and Ten Hagen, K. G. (2012) O-glycosylation modulates integrin and FGF signalling by influencing the secretion of basement membrane components. *Nat. Commun.* **3**, 869

49. Takeuchi, H., Kantharia, J., Sethi, M. K., Bakker, H., and Haltiwanger, R. S. (2012) Site-specific O-glucosylation of the epidermal growth factor-like (EGF) repeats of notch: Efficiency of glycosylation is affected by proper folding and amino acid sequence of individual EGF repeats. *J. Biol. Chem.* **287**, 33934–33944

50. Vasudevan, D., and Haltiwanger, R. S. (2014) Novel roles for O-linked glycans in protein folding. *Glycoconj. J.* **31**, 417–426

51. Luca, V. C., Kim, B. C., Ge, C., Kakuda, S., Wu, D., Roein-Peikar, M., Haltiwanger, R. S., Zhu, C., Ha, T., and Garcia, K. C. (2017) Notch-Jagged complex structure implicates a catch bond in tuning ligand sensitivity. *Science (80-.).* **355**, 1320–1324

52. Shi, S., and Stanley, P. (2003) Protein O-fucosyltransferase 1 is an essential component of Notch signaling pathways. *Proc. Natl. Acad. Sci. U. S. A.* **100**, 5234–9

53. Praissman, J. L., Live, D. H., Wang, S., Ramiah, A., Chinoy, Z. S., Boons, G. J., Moremen, K. W., and Wells, L. (2014) B4GAT1 is the priming enzyme for the LARGE-dependent functional glycosylation of ??-dystroglycan. *Elife*. 10.7554/eLife.03943

54. Praissman, J. L., Willer, T., Osman Sheikh, M., Toi, A., Chitayat, D., Lin, Y. Y., Lee, H., Stalnaker, S. H., Wang, S., Prabhakar, P. K., Nelson, S. F., Stemple, D. L., Moore, S. A., Moremen, K. W., Campbell, K. P., and Wells, L. (2016) The functional O-mannose glycan on ??-dystroglycan contains a phospho-ribitol primed for matriglycan addition. *Elife*. 10.7554/eLife.14473

55. Yoshida-Moriguchi, T., and Campbell, K. P. (2014) Matriglycan: A novel polysaccharide that links dystroglycan to the basement membrane. *Glycobiology*. **25**, 702–713

56. Feizi, T. E. N., and Haltiwanger, R. S. (2015) Editorial overview: Carbohydrate-protein interactions and glycosylation: Glycan synthesis and recognition: Finding the perfect partner in a sugar-coated life. *Curr. Opin. Struct. Biol.* **34**, 7–9

57. Xu, D., and Esko, J. D. (2014) Demystifying Heparan Sulfate–Protein Interactions. *Annu. Rev. Biochem.* **83**, 129–157

58. Matsuo, I., and Kimura-Yoshida, C. (2013) Extracellular modulation of Fibroblast Growth Factor signaling through heparan sulfate proteoglycans in mammalian development. *Curr. Opin. Genet. Dev.* **23**, 399–407

59. Sparks, S. E., and Krasnewich, D. M. (2015) *PMM2-CDG (CDG-Ia)*

60. Climer, L. K., Dobretsov, M., and Lupashin, V. (2015) Defects in the COG complex and COG-related trafficking regulators affect neuronal Golgi function. *Front. Neurosci.* **9**, 1–9

61. Jaeken, J. (2011) Congenital disorders of glycosylation (CDG): It's (nearly) all in it! *J. Inherit. Metab. Dis.* **34**, 853–858

62. Li, M., Cheng, R., Liang, J., Yan, H., Zhang, H., Yang, L., Li, C., Jiao, Q., Lu, Z., He, J., Ji, J., Shen, Z., Li, C., Hao, F., Yu, H., and Yao, Z. (2013) Mutations in POFUT1, encoding protein O-fucosyltransferase 1, cause generalized Dowling-Degos disease. *Am. J. Hum. Genet.* **92**, 895–903

63. Thiel, C., Lübke, T., Matthijs, G., von Figura, K., and Körner, C. (2006) Targeted disruption of the mouse phosphomannomutase 2 gene causes early embryonic lethality. *Mol. Cell. Biol.* **26**, 5615–5620

64. Mohamed, M., Ashikov, A., Guillard, M., Robben, J. H., Schmidt, S., Van Den Heuvel, B., De Brouwer, A. P. M., Gerardy-Schahn, R., Deen, P. M. T., Wevers, R. A., Lefeber, D. J., and Morava, E. (2013) Intellectual disability and bleeding diathesis due to deficient CMP-sialic acid transport. *Neurology*. **81**, 681–687

65. Wu, X., Steet, R. A., Bohorov, O., Bakker, J., Newell, J., Krieger, M., Spaapen, L., Kornfeld, S., and Freeze, H. H. (2004) Mutation of the COG complex subunit gene COG7 causes a lethal congenital disorder. *Nat. Med.* **10**, 518–523

66. Stowell, S. R., Ju, T., and Cummings, R. D. (2015) Protein Glycosylation in Cancer. *Annu. Rev. Pathol. Mech. Dis.* **10**, 473–510

67. Pinho, S. S., and Reis, C. A. (2015) Glycosylation in cancer: mechanisms and clinical implications. *Nat. Rev. Cancer*. **15**, 540–555

68. Kannagi, R. (2004) Molecular mechanism for cancer-associated induction of sialyl Lewis X and sialyl Lewis A expression-The Warburg effect revisited. *Glycoconj. J.* **20**, 353–364

69. Samraj, A. N., Pearce, O. M. T., Läubli, H., Crittenden, A. N., Bergfeld, A. K., Banda, K., Gregg, C. J., Bingman, A. E., Secrest, P., Diaz, S. L., Varki, N. M., and Varki, A. (2015) A red meat-derived glycan promotes inflammation and cancer progression. *Proc. Natl. Acad. Sci.* **112**, 542–547

70. Britain, C. M., Dorsett, K. A., and Bellis, S. L. (2017) The glycosyltransferase ST6Gal-I protects tumor cells against serum growth factor withdrawal by enhancing survival signaling and proliferative potential. *J. Biol. Chem.* **292**, 4663–4673

71. Lu, J., Isaji, T., Im, S., Fukuda, T., Kameyama, A., and Gu, J. (2016) Expression of N-acetylglucosaminyltransferase III suppresses α2,3-sialylation, and its distinctive functions in cell migration are attributed to α2,6-sialylation levels. *J. Biol. Chem.* **291**, 5708–5720

72. Schultz, M. J., Swindall, A. F., and Bellis, S. L. (2012) Regulation of the metastatic cell phenotype by sialylated glycans. *Cancer Metastasis Rev.* **31**, 501–518

73. Hiraiwa, N., Yabuta, T., Yoritomi, K., Hiraiwa, M., Tanaka, Y., Suzuki, T., Yoshida, M., and Kannagi, R. (2003) Transactivation of the fucosyltransferase VII gene by human T-cell leukemia virus type 1 Tax through a variant cAMP-responsive element. *Blood*. **101**, 3615–3621

74. Schultz, M. J., Holdbrooks, A. T., Chakraborty, A., Grizzle, W. E., Landen, C. N., Buchsbaum, D. J., Conner, M. G., Arend, R. C., Yoon, K. J., Klug, C. A., Bullard, D. C., Kesterson, R. A., Oliver, P. G., O'Connor, A. K., Yoder, B. K., and Bellis, S. L. (2016) The tumor-associated glycosyltransferase ST6Gal-I regulates stem cell transcription factors and confers a cancer stem cell phenotype. *Cancer Res.* **76**, 3978–3988

75. Liu, Z., Swindall, A. F., Kesterson, R. A., Schoeb, T. R., Bullard, D. C., and Bellis, S. L. (2011)

ST6Gal-I regulates macrophage apoptosis via ??2-6 sialylation of the TNFR1 death receptor. *J. Biol. Chem.* **286**, 39654–39662

76. Kitajima, K., Varki, N., and Sato, C. (2015) Advanced Technologies in Sialic Acid and Sialoglycoconjugate Analysis. 10.1007/128

77. Harduin-lepers, A., Mollicone, R., Delannoy, P., and Oriol, R. (2005) The animal sialyltransferases and sialyltransferase-related genes : a phylogenetic approach. **15**, 805–817

78. Varki, A., and Schauer, R. (2009) Sialic Acids. *Essentials Glycobiol.*

79. Hinderlich, S., Weidemann, W., and Yardeni, T. (2015) UDP-GlcNAc 2-Epimerase / ManNAc Kinase (GNE): A Master Regulator of Sialic Acid Synthesis. 10.1007/128

80. Chou, H.-H., Takematsu, H., Diaz, S., Iber, J., Nickerson, E., Wright, K. L., Muchmore, E. A., Nelson, D. L., Warren, S. T., and Varki, A. (1998) A mutation in human CMP-sialic acid hydroxylase occurred after the Homo-Pan divergence. *Proc. Natl. Acad. Sci. U. S. A.* **95**, 11751–11756

81. Varki, N. M., Strobert, E., Jr, E. J. D., Benirschke, K., and Varki, A. Biomedical Differences Between Human and Nonhuman Hominids : Potential Roles for Uniquely Human Aspects of Sialic Acid Biology. 10.1146/annurev-pathol-011110-130315

82. Matrosovich, M., Herrler, G., and Klenk, H. D. (2015) Sialic Acid Receptors of Viruses. *Top Curr Chem*. **367**, 1–28

83. Crocker, P. R., Paulson, J. C., and Varki, A. (2007) Siglecs and their roles in the immune system. **7**, 255–266

84. McEver, R. P., and Zhu, C. (2010) Rolling Cell Adhesion. *Annu. Rev. Cell Dev. Biol.* **26**, 363–396

85. Mondal, N., Jr, A. B., Stolfa, G., Antonopoulos, A., Lau, J. T. Y., Haslam, S. M., Dell, A., and Neelamegham, S. (2016) Regular Article ST3Gal-4 is the primary sialyltransferase regulating the synthesis of. **125**, 687–697

86. Yang, W. H., Nussbaum, C., Grewal, P. K., Marth, J. D., and Sperandio, M. (2016) Coordinated roles of ST3Gal-VI and ST3Gal-IV sialyltransferases in the synthesis of selectin ligands. **120**, 1015–1027

87. Baranski, T. J., Koelsch, G., Hartsuck, J. a., and Kornfeld, S. (1991) Mapping and molecular modeling of a recognition domain for lysosomal enzyme targeting. *J. Biol. Chem.* **266**, 23365–23372

88. Steet, R., Lee, W. S., and Kornfeld, S. (2005) Identification of the minimal lysosomal enzyme recognition domain in cathepsin D. *J. Biol. Chem.* **280**, 33318–33323

89. Mengeling, B. J., Manzella, S. M., and Baenziger, J. U. (1995) A cluster of basic amino acids within an alpha-helix is essential for alpha-subunit recognition by the glycoprotein hormone N-acetylgalactosaminyltransferase. *Proc Natl Acad Sci U S A*. **92**, 502–506

90. Miller, E., Fiete, D., Blake, N. M. J., Beranek, M., Oates, E. L., Mi, Y., Roseman, D. S., and Baenziger, J. U. (2008) A necessary and sufficient determinant for protein-selective glycosylation in vivo. *J. Biol. Chem.* **283**, 1985–1991

91. Fiete, D., Srivastava, V., Hindsgaul, O., and Baenziger, J. U. (1991) A hepatic reticuloendothelial cell receptor specific for SO4-4GalNAc??1, 4GlcNAc??1,2Man?? that mediates rapid clearance of lutropin. *Cell*. **67**, 1103–1110

92. Baenziger, J. U., Kumar, S., Brodbeck, R. M., Smith, P. L., and Beranek, M. C. (1992) Circulatory half-life but not interaction with the lutropin/chorionic gonadotropin receptor is modulated by sulfation of bovine lutropin oligosaccharides. *Proc. Natl. Acad. Sci. U. S. A.* **89**, 334–8

93. Rampal, R., Li, A. S. Y., Moloney, D. J., Georgiou, S. A., Luther, K. B., Nita-Lazar, A., and Haltiwanger, R. S. (2005) Lunatic fringe, manic fringe, and radical fringe recognize similar specificity determinants in O-fucosylated epidermal growth factor-like repeats. *J. Biol. Chem.* **280**, 42454–42463

94. Halmo, S. M., Singh, D., Patel, S., Wang, S., Edlin, M., Boons, G. J., Moremen, K. W., Live, D., and Wells, L. (2017) Protein O-linked mannose ??-1,4-N-acetylglucosaminyltransferase 2 (POMGNT2) is a gatekeeper enzyme for functional glycosylation of ??-dystroglycan. *J. Biol. Chem.* **292**, 2101–2109

95. Sato, C., and Kitajima, K. (2013) Disialic, oligosialic and polysialic acids: Distribution, functions and related disease. *J. Biochem.* **154**, 115–136

96. Colley, K. J., Kitajima, K., and Sato, C. (2014) Polysialic acid: Biosynthesis, novel functions and applications. *Crit. Rev. Biochem. Mol. Biol.* **49**, 498–532

97. Rutishauser, U. (2008) Polysialic acid in the plasticity of the developing and adult vertebrate nervous system. *Nat. Rev. Neurosci.* **9**, 26–35

98. Rutishauser, U., Acheson, A., Hall, A. K., Mann, D. M., &, and Sunshine, J. (1988) Neural Cell as Adhesion Molecule a Regulator of cell-cell Interactions. *Science (80-.).* **240**, 53–57

99. Rutishauser, U., Watanabe, M., Silver, J., Troy, F. A., and Vimr, E. R. (1985) Specific Alteration of Ncam-Mediated Cell-Adhesion By an Endoneuraminidase. *J. Cell Biol.* **101**, 1842–1849

100. Johnson, C. P., Fujimoto, I., Rutishauser, U., and Leckband, D. E. (2005) Direct evidence that neural cell adhesion molecule (NCAM) polysialylation increases intermembrane repulsion and abrogates adhesion. *J. Biol. Chem.* **280**, 137–45

101. Sato, C., Kitajima, K., Tazawa, I., Inoue, Y., Inoue, S., and Troy, F. A. (1993) Structural diversity in the ??2???8-linked polysialic acid chains in salmonid fish egg glycoproteins. Occurrence of poly(Neu5Ac), poly(Neu5Gc), poly(Neu5Ac, Neu5Gc), poly(KDN), and their partially acetylated forms. *J. Biol. Chem.* **268**, 23675–23684

102. Miyata, S., Yamakawa, N., Toriyama, M., Sato, C., and Kitajima, K. (2011) Co-expression of two distinct polysialic acids, ??2,8-and ??2,9-linked polymers of N-acetylneuraminic acid, in distinct glycoproteins and glycolipids in sea urchin sperm. *Glycobiology*. **21**, 1596–1605

103. Bhattacharjee, A. K., Jennings, H. J., Kenny, C. P., Martin, A., and Smith, I. C. (1975) Structural determination of the sialic acid polysaccharide antigens of Neisseria meningitidis serogroups B and C with carbon 13 nuclear magnetic resonance. *J. Biol. Chem.* **250**, 1926–1932

104. Finne, J. (1982) Occurrence of unique polysialosyl carbohydrate units in glycoproteins of developing brain. *J. Biol. Chem.* **257**, 11966–11970

105. Finne, J., Finne, U., Deagostini-Bazin, H., and Goridis, C. (1983) Occurrence of ??2-8 linked

polysialosyl units in a neural cell adhesion molecule. *Biochem. Biophys. Res. Commun.* **112**, 482–487

106. Curreli, S., Arany, Z., Gerardy-Schahn, R., Mann, D., and Stamatos, N. M. (2007) Polysialylated neuropilin-2 is expressed on the surface of human dendritic cells and modulates dendritic cell-T lymphocyte interactions. *J. Biol. Chem.* **282**, 30346–30356

107. Werneburg, S., Mühlenhoff, M., Stangel, M., and Hildebrandt, H. (2015) Polysialic acid on SynCAM 1 in NG2 cells and on neuropilin-2 in microglia is confined to intracellular pools that are rapidly depleted upon stimulation. *Glia*. **63**, 1240–1255

108. Bax, M., van Vliet, S. J., Litjens, M., García-Vallejo, J. J., and van Kooyk, Y. (2009) Interaction of polysialic acid with CCL21 regulates the migratory capacity of human dendritic cells. *PLoS.One.* **4**, e6987

109. Rey-Gallardo, A., Delgado-Martín, C., Gerardy-Schahn, R., Rodríguez-Fernández, J. L., and Vega, M. A. (2011) Polysialic acid is required for neuropilin-2a/b-mediated control of CCL21-driven chemotaxis of mature dendritic cells and for their migration in vivo. *Glycobiology*. **21**, 655–62

110. Kiermaier, E., Moussion, C., Veldkamp, C. T., Gerardy-Schahn, R., de Vries, I., Williams, L. G., Chaffee, G. R., Phillips, A. J., Freiberger, F., Imre, R., Taleski, D., Payne, R. J., Braun, A., Förster, R., Mechtler, K., Mühlenhoff, M., Volkman, B. F., and Sixt, M. (2016) Polysialylation controls dendritic cell trafficking by regulating chemokine recognition. *Science (80-.).* **351**, 186–191

111. Galuska, S. P., Rollenhagen, M., Kaup, M., Eggers, K., Oltmann-Norden, I., Schiff, M., Hartmann, M., Weinhold, B., Hildebrandt, H., Geyer, R., Muhlenhoff, M., and Geyer, H. (2010) Synaptic cell adhesion molecule SynCAM 1 is a target for polysialylation in postnatal mouse brain. *Proc. Natl. Acad. Sci.* **107**, 10250–10255

112. Werneburg, S., Buettner, F. F. R., M??hlenhoff, M., and Hildebrandt, H. (2015) Polysialic acid modification of the synaptic cell adhesion molecule SynCAM 1 in human embryonic stem cell-derived oligodendrocyte precursor cells. *Stem Cell Res.* **14**, 339–346

113. Werneburg, S., Buettner, F. F. R., Erben, L., Mathews, M., Neumann, H., Mühlenhoff, M., and Hildebrandt, H. (2016) Polysialylation and lipopolysaccharide-induced shedding of E-selectin ligand-1 and neuropilin-2 by microglia and THP-1 macrophages. *Glia*. **64**, 1314–1330

114. Yabe, U., Sato, C., Matsuda, T., and Kitajima, K. (2003) Polysialic acid in human milk. CD36 is a new member of mammalian polysialic acid-containing glycoprotein. *J. Biol. Chem.* **278**, 13875–80

115. Scheidegger, P., Papay, J., Zuber, C., Lackie, P. M., and Roth, J. (1994) Cellular Site of Synthesis and Dynamics of Cell Surface Re-Expression of Polysialic Acid of the Neural Cell Adhesion Molecule. *Eur. J. Biochem.* **225**, 1097–1103

116. Scheidegger, E. P., Sternberg, L. R., Roth, J., and Lowe, J. B. (1995) A human STX cDNA confers polysialic acid expression in mammalian cells. *J. Biol. Chem.* **270**, 22685–22688

117. Livingston, B. D., and Paulson, J. C. (1993) Polymerase chain reaction cloning of a developmentally regulated member of the sialyltransferase gene family. *J. Biol. Chem.* **268**, 11504–11507

118. Eckhardt, M., Mühlenhoff, M., Bethe, A., Koopman, J., Frosch, M., and Gerardy-Schahn, R. (1995) Molecular characterization of eukaryotic polysialyltransferase-1. *Nature*. **373**, 715–8

119. Datta, A. K., and Paulson, J. C. (1995) The sialyltransferase "sialylmotif" participates in binding the donor substrate CMP-NeuAc. *J. Biol. Chem.* **270**, 1497–1500

120. Datta, A. K., Sinha, A., and Paulson, J. C. (1998) Mutation of the sialyltransferase s-sialylmotif alters the kinetics of the donor and acceptor substrates. *J. Biol. Chem.* **273**, 9608–9614

121. Jeanneau, C., Chazalet, V., Augé, C., Soumpasis, D. M., Harduin-Lepers, A., Delannoy, P., Imberty, A., and Breton, C. (2004) Structure-function analysis of the human sialyltransferase ST3Gal I: Role of N-glycosylation and a novel conserved sialylmotif. *J. Biol. Chem.* **279**, 13461–13468

122. Audry, M., Jeanneau, C., Imberty, A., Harduin-Lepers, A., Delannoy, P., and Breton, C. (2011) Current trends in the structure-activity relationships of sialyltransferases. *Glycobiology*. **21**, 716–726

123. Datta, A. K., Chammas, R., and Paulson, J. C. (2001) Conserved Cysteines in the Sialyltransferase Sialylmotifs Form an Essential Disulfide Bond. *J. Biol. Chem.* **276**, 15200–15207

124. Angata, K., Yen, T. Y., El-Battari, A., Macher, B. A., and Fukuda, M. (2001) Unique Disulfide Bond Structures Found in ST8Sia IV Polysialyltransferase Are Required for Its Activity. *J. Biol. Chem.* **276**, 15369–15377

125. Volkers, G., Worrall, L. J., Kwan, D. H., Yu, C.-C., Baumann, L., Lameignere, E., Wasney, G. a, Scott, N. E., Wakarchuk, W., Foster, L. J., Withers, S. G., and Strynadka, N. C. J. (2015) Structure of human ST8SiaIII sialyltransferase provides insight into cell-surface polysialylation. *Nat. Struct. Mol. Biol.* **22**, 1–12

126. Angata, K., Chan, D., Thibault, J., and Fukuda, M. (2004) Molecular dissection of the ST8Sia IV polysialyltransferase: Distinct domains are required for neural cell adhesion molecule recognition and polysialylation. *J. Biol. Chem.* **279**, 25883–25890

127. Meng, L., Forouhar, F., Thieker, D., Gao, Z., Ramiah, A., Moniz, H., Xiang, Y., Seetharaman, J., Milaninia, S., Su, M., Bridger, R., Veillon, L., Azadi, P., Kornhaber, G., Wells, L., Montelione, G. T., Woods, R. J., Tong, L., and Moremen, K. W. (2013) Enzymatic basis for N-glycan sialylation: Structure of rat ??2,6-sialyltransferase (ST6GAL1) reveals conserved and unique features for glycan sialylation. *J. Biol. Chem.* **288**, 34680–34698

128. Kitazume-Kawaguchi, S., Kabata, S., and Arita, M. (2001) Differential Biosynthesis of Polysialic or Disialic Acid Structure by ST8Sia II and ST8Sia IV. *J. Biol. Chem.* **276**, 15696–15703

129. Rao, F. V, Rich, J. R., Rakić, B., Buddai, S., Schwartz, M. F., Johnson, K., Bowe, C., Wakarchuk, W. W., Defrees, S., Withers, S. G., and Strynadka, N. C. J. (2009) Structural insight into mammalian sialyltransferases. *Nat. Struct. Mol. Biol.* **16**, 1186–1188

130. Angata, K., Suzuki, M., McAuliffe, J., Ding, Y., Hindsgaul, O., and Fukuda, M. (2000) Differential biosynthesis of polysialic acid on neural cell adhesion molecule (NCAM) and oligosaccharide acceptors by three distinct alpha 2,8-sialyltransferases, ST8Sia IV (PST), ST8Sia II (STX), and ST8Sia III. *J. Biol. Chem.* **275**, 18594–601

131. von Der Ohe, M., Wheeler, S. F., Wuhrer, M., Harvey, D. J., Liedtke, S., Mühlenhoff, M.,

Gerardy-Schahn, R., Geyer, H., Dwek, R. a, Geyer, R., Wing, D. R., and Schachner, M. (2002) Localization and characterization of polysialic acid-containing N-linked glycans from bovine NCAM. *Glycobiology*. **12**, 47–63

132. Wuhrer, M., Geyer, H., Von Der Ohe, M., Gerardy-Schahn, R., Schachner, M., and Geyer, R. (2003) Localization of defined carbohydrates epitopes in bovine polysialylated NCAM. *Biochimie*. **85**, 207–218

133. Galuska, S. P., Geyer, R., Gerardy-Schahn, R., Mühlenhoff, M., and Geyer, H. (2008) Enzyme-dependent variations in the polysialylation of the neural cell adhesion molecule (NCAM) in vivo. *J. Biol. Chem.* **283**, 17–28

134. Schnaar, R. L., Gerardy-Schahn, R., and Hildebrandt, H. (2014) Sialic acids in the brain: gangliosides and polysialic acid in nervous system development, stability, disease, and regeneration. *Physiol. Rev.* **94**, 461–518

135. Mühlenhoff, M., Eckhardt, M., Bethe, a, Frosch, M., and Gerardy-Schahn, R. (1996) Autocatalytic polysialylation of polysialyltransferase-1. *EMBO J.* **15**, 6943–6950

136. Close, B. E., Wilkinson, J. M., Bohrer, T. J., Goodwin, C. P., Broom, L. J., and Colley, K. J. (2001) The polysialyltransferase ST8Sia II/STX: posttranslational processing and role of autopolysialylation in the polysialylation of neural cell adhesion molecule. *Glycobiology*. **11**, 997–1008

137. Close, B. E., and Colley, K. J. (1998) In vivo autopolysialylation and localization of the polysialyltransferases PST and STX. *J. Biol. Chem.* **273**, 34586–34593

138. Close, B. E., Tao, K., and Colley, K. J. (2000) Polysialyltransferase-1 autopolysialylation is not requisite for polysialylation of neural cell adhesion molecule. *J. Biol. Chem.* **275**, 4484–91

139. James, W. M., and Agnew, W. S. (1987) MULTIPLE OLIGOSACCHARIDE CHAINS IN THE VOLTAGE-SENSITIVE NA CHANNEL FROM ELECTROPHORUS ELECTRICUS: EVIDENCE FOR a-2,8-LINKED POLYSIALIC ACID. *Biochem. Biophys. Res. Commun.* **142**, 436–440

140. Zuber, C., Lackie, P. M., Catterall, W. A., and Roth, J. (1992) Polysialic acid is associated with sodium channels and the neural cell adhesion molecule N-CAM in adult rat brain. *J. Biol. Chem.* **267**, 9965–71

141. Kiselyov, V. V., Soroka, V., Berezin, V., and Bock, E. (2005) Structural biology of NCAM homophilic binding and activation of FGFR. *J. Neurochem.* **94**, 1169–1179

142. Kiselyov, V. V., Berezin, V., Maar, T. E., Soroka, V., Edvardsen, K., Schousboe, A., and Bock, E. (1997) The first immunoglobulin-like neural cell adhesion molecule (NCAM) domain is involved in double-reciprocal interaction with the second immunoglobulin-like NCAM domain and in heparin binding. *J. Biol. Chem.* **272**, 10125–10134

143. Kallapur, S. G., and Akeson, R. A. (1992) The neural cell adhesion molecule (NCAM) heparin binding domain binds to cell surface heparan sulfate proteoglycans. *J. Neurosci. Res.* **33**, 538–548

144. Ditlevsen, D. K., Povlsen, G. K., Berezin, V., and Bock, E. (2008) NCAM-induced intracellular signaling revisited. *J. Neurosci. Res.* **86**, 727–743

145. Kiselyov, V. V., Skladchikova, G., Hinsby, A. M., Jensen, P. H., Kulahin, N., Soroka, V.,

Pedersen, N., Tsetlin, V., Poulsen, F. M., Berezin, V., and Bock, E. (2003) Structural basis for a direct interaction between FGFR1 and NCAM and evidence for a regulatory role of ATP. *Structure*. **11**, 691–701

146. Francavilla, C., Cattaneo, P., Berezin, V., Bock, E., Ami, D., De Marco, A., Christofori, G., and Cavallaro, U. (2009) The binding of NCAM to FGFR1 induces a specific cellular response mediated by receptor trafficking. *J. Cell Biol.* **187**, 1101–1116

147. Seidenfaden, R., Krauter, A., Schertzinger, F., Gerardy-Schahn, R., and Hildebrandt, H. (2003) Polysialic acid directs tumor cell growth by controlling heterophilic neural cell adhesion molecule interactions. *Mol. Cell. Biol.* **23**, 5908–18

148. Seidenfaden, R., Krauter, A., and Hildebrandt, H. (2006) The neural cell adhesion molecule NCAM regulates neuritogenesis by multiple mechanisms of interaction. *Neurochem. Int.* **49**, 1–11

149. Röckle, I., Seidenfaden, R., Weinhold, B., Mühlenhoff, M., Gerardy-Schahn, R., and Hildebrandt, H. (2008) Polysialic acid controls NCAM-induced differentiation of neuronal precursors into calretinin-positive olfactory bulb interneurons. *Dev. Neurobiol.* **68**, 1170–1184

150. Ono, S., Hane, M., Kitajima, K., and Sato, C. (2012) Novel regulation of Fibroblast Growth Factor 2 (FGF2)-mediated cell growth by polysialic acid. *J. Biol. Chem.* **287**, 3710–3722

151. Beggs, H. E., Baragona, S. C., Hemperly, J. J., and Maness, P. F. (1997) NCAM140 interacts with the focal adhesion kinase p125(fak) and the SRC-related tyrosine kinase p59(fyn). *J. Biol. Chem.* **272**, 8310–9

152. Eggers, K., Werneburg, S., Schertzinger, A., Abeln, M., Schiff, M., Scharenberg, M. A., Burkhardt, H., Muhlenhoff, M., and Hildebrandt, H. (2011) Polysialic acid controls NCAM signals at cell-cell contacts to regulate focal adhesion independent from FGF receptor activity. *J. Cell Sci.* **124**, 3279–3291

153. Ong, E., Nakayama, J., Angata, K., Reyes, L., Katsuyama, T., Arai, Y., and Fukuda, M. (1998) Developmental regulation of polysialic acid synthesis in mouse directed by two polysialyltransferases, PST and STX. *Glycobiology*. **8**, 415–424

154. Hildebrandt, H., Mühlenhoff, M., Weinhold, B., and Gerardy-Schahn, R. (2007) Dissecting polysialic acid and NCAM functions in brain development. *J. Neurochem.* **103 Suppl**, 56–64

155. Hildebrandt, H., Becker, C., Mürau, M., Gerardy-Schahn, R., and Rahmann, H. (1998) Heterogeneous expression of the polysialyltransferases ST8Sia II and ST8Sia IV during postnatal rat brain development. *J. Neurochem.* **71**, 2339–48

156. Oltmann-norden, I., Galuska, S. P., Hildebrandt, H., Geyer, R., Gerardy-schahn, R., Geyer, H., and Mu, M. (2008) Impact of the Polysialyltransferases ST8SiaII and ST8SiaIV on Polysialic Acid Synthesis during Postnatal Mouse. *J Biol Chem*. **283**, 1463–1471

157. Lackie, P. M., Zuber, C., and Roth, J. (1990) Polysialic acid and N-CAM localisation in embryonic rat kidney: mesenchymal and epithelial elements show different patterns of expression. *Development*. **110**, 933–947

158. Lackie, P. M., Zuber, C., and Roth, J. (1994) Polysialic acid of the neural cell adhesion molecule (NCAM) is widely expressed during organogenesis in mesodermal and endodermal derivatives. *Differentiation*. **57**, 119–131

159. Galuska, C. E., Lütteke, T., and Galuska, S. P. (2017) Is Polysialylated NCAM Not Only a Regulator during Brain Development But also during the Formation of Other Organs ? 10.3390/biology6020027

160. Bonfanti, L., and Theodosis, D. T. (1994) Expression of polysialylated neural cell adhesion molecule by proliferating cells in the subependymal layer of the adult rat, in its rostral extension and in the olfactory bulb. *Neuroscience*. **62**, 291–305

161. Theodosis, D. T., Rougon, G., and Poulain, D. A. (1991) Retention of embryonic features by an adult neuronal system capable of plasticity: polysialylated neural cell adhesion molecule in the hypothalamo-neurohypophysial system. *Proc. Natl. Acad. Sci. U. S. A.* **88**, 5494–8

162. Angata, K., Nakayama, J., Fredette, B., Chong, K., Ranscht, B., and Fukuda, M. (1997) Human STX polysialyltransferase forms the embryonic form of the neural cell adhesion molecule. Tissue-specific expression, neurite outgrowth, and chromosomal localization in comparison with another polysialyltransferase, PST. *J. Biol. Chem.* **272**, 7182–7190

163. Mühlenhoff, M., Oltmann-Norden, I., Weinhold, B., Hildebrandt, H., and Gerardy-Schahn, R. (2009) Brain development needs sugar: the role of polysialic acid in controlling NCAM functions. *Biol. Chem.* **390**, 567–74

164. Angata, K., Long, J. M., Bukalo, O., Lee, W., Dityatev, A., Wynshaw-Boris, A., Schachner, M., Fukuda, M., and Marth, J. D. (2004) Sialyltransferase ST8Sia-II assembles a subset of polysialic acid that directs hippocampal axonal targeting and promotes fear behavior. *J. Biol. Chem.* **279**, 32603–32613

165. Eckhardt, M., Bukalo, O., Chazal, G., Wang, L., Goridis, C., Schachner, M., Gerardy-Schahn, R., Cremer, H., and Dityatev, a (2000) Mice deficient in the polysialyltransferase ST8SiaIV/PST-1 allow discrimination of the roles of neural cell adhesion molecule protein and polysialic acid in neural development and synaptic plasticity. *J. Neurosci.* **20**, 5234–5244

166. Cremer, H., Lange, R., Christoph, A., Plomann, M., Vopper, G., Roes, J., Brown, R., Baldwin, S., Kraemer, P., Scheff, S., Barthels, D., Rajewsky, K., and Wille, W. (1994) Inactivation of the N-CAM gene in mice results in size reduction of the olfactory bulb and deficits in spatial learning. *Nature*. **367**, 455–459

167. Galuska, S. P., Oltmann-Norden, I., Geyer, H., Weinhold, B., Kuchelmeister, K., Hildebrandt, H., Gerardy-Schahn, R., Geyer, R., and Mühlenhoff, M. (2006) Polysialic acid profiles of mice expressing variant allelic combinations of the polysialyltransferases ST8SiaII and ST8SiaIV. *J. Biol. Chem.* **281**, 31605–31615

168. Weinhold, B., Seidenfaden, R., Röckle, I., Mühlenhoff, M., Schertzinger, F., Conzelmann, S., Marth, J. D., Gerardy-Schahn, R., and Hildebrandt, H. (2005) Genetic ablation of polysialic acid causes severe neurodevelopmental defects rescued by deletion of the neural cell adhesion molecule. *J. Biol. Chem.* **280**, 42971–42977

169. Prosser, R. a, Rutishauser, U., Ungers, G., Fedorkova, L., and Glass, J. D. (2003) Intrinsic role of polysialylated neural cell adhesion molecule in photic phase resetting of the Mammalian circadian clock. *J. Neurosci.* **23**, 652–8

170. Fedorkova, L., Rutishauser, U., Prosser, R., Shen, H., and Glass, J. D. (2002) Removal of polysialic acid from the SCN potentiates nonphotic circadian phase resetting. *Physiol. Behav.* **77**, 361–369

171. Brenachot, X., Gautier, T., Nédélec, E., Deckert, V., Laderrière, A., Nuzzaci, D., Rigault, C., Lemoine, A., Pénicaud, L., Lagrost, L., and Benani, A. (2017) Brain Control of Plasma Cholesterol Involves Polysialic Acid Molecules in the Hypothalamus. *Front. Neurosci.* **11**, 1–9

172. Stamatos, N. M., Zhang, L., Jokilammi, A., Finne, J., Chen, W. H., El-Maarouf, A., Cross, A. S., and Hankey, K. G. (2014) Changes in polysialic acid expression on myeloid cells during differentiation and recruitment to sites of inflammation: role in phagocytosis. *Glycobiology*. **24**, 864–879

173. Drake, P. M., Stock, C. M., Nathan, J. K., Gip, P., Golden, K. P. K., Weinhold, B., Gerardy-Schahn, R., and Bertozzi, C. R. (2009) Polysialic acid governs T-cell development by regulating progenitor access to the thymus. *Proc. Natl. Acad. Sci. U. S. A.* **106**, 11995–2000

174. Drake, P. M., Nathan, J. K., Stock, C. M., Chang, P. V., Muench, M. O., Nakata, D., Reader, J. R., Gip, P., Golden, K. P. K., Weinhold, B., Gerardy-Schahn, R., Troy, F. A., and Bertozzi, C. R. (2008) Polysialic Acid, a Glycan with Highly Restricted Expression, Is Found on Human and Murine Leukocytes and Modulates Immune Responses. *J. Immunol.* **181**, 6850–6858

175. Ulm, C., Saffarzadeh, M., Mahavadi, P., Müller, S., Prem, G., Saboor, F., Simon, P., Middendorff, R., Geyer, H., Henneke, I., Bayer, N., Rinné, S., Lütteke, T., Böttcher-Friebertshäuser, E., Gerardy-Schahn, R., Schwarzer, D., Mühlenhoff, M., Preissner, K. T., Günther, A., Geyer, R., and Galuska, S. P. (2013) Soluble polysialylated NCAM: A novel player of the innate immune system in the lung. *Cell. Mol. Life Sci.* **70**, 3695–3708

176. Mishra, B., von der Ohe, M., Schulze, C., Bian, S., Makhina, T., Loers, G., Kleene, R., and Schachner, M. (2010) Functional Role of the Interaction between Polysialic Acid and Extracellular Histone H1. *J. Neurosci.* **30**, 12400–12413

177. Hänsch, M., Simon, P., Schön, J., Kaese, M., Braun, B. C., Jewgenow, K., Göritz, F., Küpper, J., Ahmadvand, N., Geyer, R., Middendorff, R., Müller, K., and Galuska, S. P. (2014) Polysialylation of NCAM correlates with onset and termination of seasonal spermatogenesis in roe deer. *Glycobiology*. **24**, 488–493

178. Hromatka, B. S., Drake, P. M., Kapidzic, M., Stolp, H., Goldfien, G. A., Shih Ie, M., and Fisher, S. J. (2013) Polysialic acid enhances the migration and invasion of human cytotrophoblasts. *Glycobiology*. **23**, 593–602

179. El Maarouf, A., Petridis, A. K., and Rutishauser, U. (2006) Use of polysialic acid in repair of the central nervous system. *Proc. Natl. Acad. Sci. U. S. A.* **103**, 16989–94

180. Zhang, Y., Zhang, X., Wu, D., Verhaagen, J., Richardson, P. M., Yeh, J., and Bo, X. (2007) Lentiviral-mediated expression of polysialic acid in spinal cord and conditioning lesion promote regeneration of sensory axons into spinal cord. *Mol. Ther.* **15**, 1796–804

181. Zhang, Y., Ghadiri-Sani, M., Zhang, X., Richardson, P. M., Yeh, J., and Bo, X. (2007) Induced expression of polysialic acid in the spinal cord promotes regeneration of sensory axons. *Mol. Cell. Neurosci.* **35**, 109–119

182. Tsuchiya, A., Lu, W. Y., Weinhold, B., Boulter, L., Stutchfield, B. M., Williams, M. J., Guest, R. V., Minnis-Lyons, S. E., Mackinnon, A. C., Schwarzer, D., Ichida, T., Nomoto, M., Aoyagi, Y., Gerardy-Schahn, R., and Forbes, S. J. (2014) Polysialic acid/neural cell adhesion molecule modulates the formation of ductular reactions in liver injury. *Hepatology*. **60**, 1727–1740

183. Sato, C., Hane, M., and Kitajima, K. (2016) Relationship between ST8SIA2, polysialic acid and its binding molecules, and psychiatric disorders. *Biochim. Biophys. Acta - Gen. Subj.* **1860**, 1739–1752

184. Krocher, T., Malinovskaja, K., Jorgenson, M., Aonurm-Helm, A., Zharkovskaya, T., Kalda, A., Rockle, I., Schiff, M., Weinhold, B., Gerardy-Schahn, R., Hildebrandt, H., and Zharkovsky, A. (2013) Schizophrenia-like phenotype of polysialyltransferase ST8SIA2-deficient mice. *Brain Struct. Funct.* **220**, 71–83

185. Szewczyk, L. M., Brozko, N., Nagalski, A., Röckle, I., Werneburg, S., Hildebrandt, H., Wisniewska, M. B., and Kuznicki, J. (2017) ST8SIA2 promotes oligodendrocyte differentiation and the integrity of myelin and axons. *Glia*. **65**, 34–49

186. Falconer, R. A., Errington, R. J., Shnyder, S. D., Smith, P. J., and Patterson, L. H. (2012) Polysialyltransferase: a new target in metastatic cancer. *Curr. Cancer Drug Targets*. **12**, 925–39

187. Tanaka, F., Otake, Y., Nakagawa, T., Kawano, Y., Miyahara, R., Li, M., Yanagihara, K., Nakayama, J., Fujimoto, I., Ikenaka, K., and Wada, H. (2000) Expression of polysialic acid and STX, a human polysialyltransferase, is correlated with tumor progression in non-small cell lung cancer. *Cancer Res.* **60**, 3072–3080

188. Tanaka, F., Otake, Y., Nakagawa, T., Kawano, Y., Miyahara, R., Li, M., Yanagihara, K., Inui, K., Oyanagi, H., Yamada, T., Nakayama, J., Fujimoto, I., Ikenaka, K., and Wada, H. (2001) Prognostic significance of polysialic acid expression in resected non-small cell lung cancer. *Cancer Res.* **61**, 1666–1670

189. Scheidegger, E. P., Lackie, P. M., Papay, J., and Roth, J. (1994) In vitro and in vivo growth of clonal sublines of human small cell lung carcinoma is modulated by polysialic acid of the neural cell adhesion molecule. *Lab. Invest.* **70**, 95–106

190. Nelson, R. W., Bates, P. A., and Rutishauser, U. (1995) Protein determinants for specific polysialylation of the neural cell adhesion molecule. *J. Biol. Chem.* **270**, 17171–17179

191. Close, B. E., Mendiratta, S. S., Geiger, K. M., Broom, L. J., Ho, L.-L., and Colley, K. J. (2003) The minimal structural domains required for neural cell adhesion molecule polysialylation by PST/ST8Sia IV and STX/ST8Sia II. *J. Biol. Chem.* **278**, 30796–805

192. Mendiratta, S. S., Sekulic, N., Lavie, A., and Colley, K. J. (2005) Specific amino acids in the first fibronectin type III repeat of the neural cell adhesion molecule play a role in its recognition and polysialylation by the polysialyltransferase ST8Sia IV/PST. *J. Biol. Chem.* **280**, 32340–8

193. Thompson, M. G., Foley, D. a, Swartzentruber, K. G., and Colley, K. J. (2011) Sequences at the interface of the fifth immunoglobulin domain and first fibronectin type III repeat of the neural cell adhesion molecule are critical for its polysialylation. *J. Biol. Chem.* **286**, 4525–34

194. Mendiratta, S. S., Sekulic, N., Hernandez-Guzman, F. G., Close, B. E., Lavie, A., and Colley, K. J. (2006) A novel alpha-helix in the first fibronectin type III repeat of the neural cell adhesion molecule is critical for N-glycan polysialylation. *J. Biol. Chem.* **281**, 36052–9

195. Foley, D. a, Swartzentruber, K. G., Thompson, M. G., Mendiratta, S. S., and Colley, K. J. (2010) Sequences from the first fibronectin type III repeat of the neural cell adhesion molecule allow O-glycan polysialylation of an adhesion molecule chimera. *J. Biol. Chem.* **285**, 35056–67

196. Kulahin, N., Kristensen, O., Rasmussen, K. K., Olsen, L., Rydberg, P., Vestergaard, B., Kastrup, J. S., Berezin, V., Bock, E., Walmod, P. S., and Gajhede, M. (2011) Structural model and trans-interaction of the entire ectodomain of the olfactory cell adhesion molecule. *Structure*. **19**, 203–211

197. Thompson, M. G., Foley, D. a, and Colley, K. J. (2013) The polysialyltransferases interact with sequences in two domains of the neural cell adhesion molecule to allow its polysialylation. *J. Biol. Chem.* **288**, 7282–93

198. Nakata, D., Zhang, L., and Troy, F. a. (2006) Molecular basis for polysialylation: A novel polybasic polysialyltransferase domain (PSTD) of 32 amino acids unique to the ??2,8-polysialyltransferases is essential for polysialylation. *Glycoconj. J.* **23**, 423–436

199. Foley, D. A., Swartzentruber, K. G., and Colley, K. J. (2009) Identification of Sequences in the Polysialyltransferases ST8Sia II and ST8Sia IV That Are Required for the Protein-specific Polysialylation of the Neural Cell Adhesion Molecule, NCAM. *J. Biol. Chem.* **284**, 15505–15516

200. Zapater, J. L., and Colley, K. J. (2012) Sequences prior to conserved catalytic motifs of polysialyltransferase ST8Sia IV are required for substrate recognition. *J. Biol. Chem.* **287**, 6441–53

201. Shen, Y., Delaglio, F., Cornilescu, G., and Bax, A. (2009) TALOS+: A hybrid method for predicting protein backbone torsion angles from NMR chemical shifts. *J. Biomol. NMR*. **44**, 213–223

202. Delaglio, F., Grzesiek, S., Vuister, G. W., Zhu, G., Pfeifer, J., and Bax, A. (1995) NMRPipe: A multidimensional spectral processing system based on UNIX pipes. *J. Biomol. NMR*. **6**, 277–293

203. Zhou, G.-P., Huang, R.-B., and Troy, F. A. (2015) 3D Structural Conformation and Functional Domains of Polysialyltransferase ST8Sia IV Required for Polysialylation of Neural Cell Adhesion Molecules. *Protein Pept. Lett.* **22**, 137–148

204. MacRaild, C. A., Daranas, A. H., Bronowska, A., and Homans, S. W. (2007) Global Changes in Local Protein Dynamics Reduce the Entropic Cost of Carbohydrate Binding in the Arabinose-binding Protein. *J. Mol. Biol.* **368**, 822–832

205. Sattler, M., Schleucher, J., and Griesinger, C. (1999) Heteronuclear multidimensional NMR experiments for the structure determination of proteins in solution employing pulsed field gradients. *Prog. Nucl. Magn. Reson. Spectrosc.* **34**, 93–158

206. Baker, N. A., Sept, D., Joseph, S., Holst, M. J., and Mccammon, J. A. (2001) Electrostatics of nanosystems : Application to microtubules and the ribosome. **98**, 10037–10041

207. Foley, D. A., Swartzentruber, K. G., Lavie, A., and Colley, K. J. (2010) Structure and Mutagenesis of Neural Cell Adhesion Molecule Domains: EVIDENCE FOR FLEXIBILITY IN THE PLACEMENT OF POLYSIALIC ACID ATTACHMENT SITES. *J. Biol. Chem.* **285**, 27360–27371

208. Robert, X., and Gouet, P. (2014) Deciphering key features in protein structures with the new ENDscript server. *Nucleic Acids Res.* 10.1093/nar/gku316

209. Prud'homme, G. J., and Glinka, Y. (2012) Neuropilins are multifunctional coreceptors involved in tumor initiation, growth, metastasis and immunity. *Oncotarget*. **3**, 921–39

210. Pellet-Many, C., Frankel, P., Jia, H., and Zachary, I. (2008) Neuropilins: structure, function and role in disease. *Biochem. J.* **411**, 211–226

211. Kawasaki, T., Kitsukawa, T., Bekku, Y., Matsuda, Y., Sanbo, M., Yagi, T., and Fujisawa, H. (1999) A requirement for neuropilin-1 in embryonic vessel formation. *Development*. **126**, 4895–4902

212. Kitsukawa, T., Shimizu, M., Sanbo, M., Hirata, T., Taniguchi, M., Bekku, Y., Yagi, T., and Fujisawa, H. (1997) Neuropilin–Semaphorin III/D-Mediated Chemorepulsive Signals Play a Crucial Role in Peripheral Nerve Projection in Mice. *Neuron*. **19**, 995–1005

213. Yuan, L., Moyon, D., Pardanaud, L., Bréant, C., Karkkainen, M. J., Alitalo, K., and Eichmann, A. (2002) Abnormal lymphatic vessel development in neuropilin 2 mutant mice. *Development*. **129**, 4797–4806

214. Chen, H., Bagri, A., Zupicich, J. A., Zou, Y., Stoeckli, E., Pleasure, S. J., Lowenstein, D. H., Skarnes, W. C., Chédotal, A., and Tessier-Lavigne, M. (2000) Neuropilin-2 Regulates the Development of Select Cranial and Sensory Nerves and Hippocampal Mossy Fiber Projections. *Neuron*. **25**, 43–56

215. Nakamura, F., Tanaka, M., Takahashi, T., Kalb, R. G., and Strittmatter, S. M. (1998) Neuropilin-1 extracellular domains mediate semaphorin D/III-induced growth cone collapse. *Neuron*. **21**, 1093–1100

216. Gu, C., Rodriguez, E. R., Reimert, D. V., Shu, T., Fritzsch, B., Richards, L. J., Kolodkin, A. L., and Ginty, D. D. (2003) Neuropilin-1 conveys semaphorin and VEGF signaling during neural and cardiovascular development. *Dev. Cell*. **5**, 45–57

217. Zachary, I. C. (2011) How neuropilin-1 regulates receptor tyrosine kinase signalling: the knowns and known unknowns. *Biochem. Soc. Trans.* **39**, 1583–91

218. Gluzman-Poltorak, Z., Cohen, T., Herzog, Y., and Neufeld, G. (2000) Neuropilin-2 is a receptor for the vascular endothelial growth factor (VEGF) forms VEGF-145 and VEGF-165. *J. Biol. Chem.* **275**, 18040–18045

219. Giger, R. J., Urquhart, E. R., Gillespie, S. K. H., Levengood, D. V., Ginty, D. D., and Kolodkin, A. L. (1998) Neuropilin-2 is a receptor for semaphorin IV: Insight into the structural basis of receptor function and specificity. *Neuron*. **21**, 1079–1092

220. Mamluk, R., Gechtman, Z., Kutcher, M. E., Gasiunas, N., Gallagher, J., and Klagsbrun, M. (2002) Neuropilin-1 binds vascular endothelial growth factor 165, placenta growth factor-2, and heparin via its b1b2 domain. *J. Biol. Chem.* **277**, 24818–24825

221. Appleton, B. A., Wu, P., Maloney, J., Yin, J., Liang, W.-C., Stawicki, S., Mortara, K., Bowman, K. K., Elliott, J. M., Desmarais, W., Bazan, J. F., Bagri, A., Tessier-Lavigne, M., Koch, A. W., Wu, Y., Watts, R. J., and Wiesmann, C. (2007) Structural studies of neuropilin/antibody complexes provide insights into semaphorin and VEGF binding. *EMBO J.* **26**, 4902–4912

222. Vander Kooi, C. W., Jusino, M. a, Perman, B., Neau, D. B., Bellamy, H. D., and Leahy, D. J. (2007) Structural basis for ligand and heparin binding to neuropilin B domains. *Proc. Natl. Acad. Sci. U. S. A.* **104**, 6152–6157

223. Bhide, G. P., Fernandes, N. R., and Colley, K. J. (2016) Sequence Requirements for Neuropilin-2

Recognition by ST8SiaIV and Polysialylation of Its O -Glycans *. *J. Biol. Chem.* **291**, 9444–9457

224. Yelland, T., and Djordjevic, S. (2016) Crystal Structure of the Neuropilin-1 MAM Domain: Completing the Neuropilin-1 Ectodomain Picture. *Structure*. **24**, 2008–2015

225. Ballmer-Hofer, K., Andersson, A. E., Ratcliffe, L. E., and Berger, P. (2011) Neuropilin-1 promotes VEGFR-2 trafficking through Rab11 vesicles thereby specifying signal output. *Blood*. **118**, 816–826

226. Grandclement, C., and Borg, C. (2011) Neuropilins: a new target for cancer therapy. *Cancers (Basel)*. **3**, 1899–928

227. Neufeld, G. (2002) The Neuropilins Multifunctional Semaphorin and VEGF Receptors that Modulate Axon Guidance and Angiogenesis. *Trends Cardiovasc. Med.* **12**, 13–19

228. Werneburg, S., Buettner, F. F. R., Erben, L., Mathews, M., Hildebrandt, H., Neumann, H., and Martina, M. (2016) Polysialylation and Lipopolysaccharide- Induced Shedding of E-Selectin Ligand-1 and Neuropilin-2 by Microglia and. *Glia*. 10.1002/glia.23004

229. Rollenhagen, M., Buettner, F. F. R., Reismann, M., Jirmo, A. C., Grove, M., Behrens, G. M. N., Gerardy-Schahn, R., Hanisch, F.-G., and Mühlenhoff, M. (2013) Polysialic acid on neuropilin-2 is exclusively synthesized by the polysialyltransferase ST8SiaIV and attached to mucin-type o-glycans located between the b2 and c domain. *J. Biol. Chem.* **288**, 22880–92

230. Shintani, Y., Takashima, S., Asano, Y., Kato, H., Liao, Y., Yamazaki, S., Tsukamoto, O., Seguchi, O., Yamamoto, H., Fukushima, T., Sugahara, K., Kitakaze, M., and Hori, M. (2006) Glycosaminoglycan modification of neuropilin-1 modulates VEGFR2 signaling. *EMBO J.* **25**, 3045–3055

231. Pellet-Many, C., Frankel, P., Evans, I. M., Herzog, B., Jünemann-Ramírez, M., and Zachary, I. C. (2011) Neuropilin-1 mediates PDGF stimulation of vascular smooth muscle cell migration and signalling via p130 ^{Cas}. *Biochem. J.* **435**, 609–618

232. Berger, P., and Ballmer-Hofer, K. (2011) The reception and the party after: How vascular endothelial growth factor receptor 2 explores cytoplasmic space. *Swiss Med. Wkly.* **141**, 2–9

233. De Vries, L., Lou, X., Zhao, G., Zheng, B., and Farquhar, M. G. (1998) GIPC, a PDZ domain containing protein, interacts specifically with the C terminus of RGS-GAIP. *Proc Natl Acad Sci U S A*. **95**, 12340–12345

234. Okon, I. S., Coughlan, K. A., Zhang, C., Moriasi, C., Ding, Y., Song, P., Zhang, W., Li, G., and Zou, M. H. (2014) Protein kinase LKB1 promotes RAB7-mediated neuropilin-1 degradation to inhibit angiogenesis. *J Clin Invest*. **124**, 4590–4602

235. Bae, D., Lu, S., Taglienti, C. A., and Mercurio, A. M. (2008) Metabolic stress induces the lysosomal degradation of neuropilin-1 but not neuropilin-2. *J. Biol. Chem.* **283**, 28074–28080

236. Bhide, G. P., Prehna, G., Ramirez, B. E., and Colley, K. J. (2017) The Polybasic Region of the Polysialyltransferase ST8Sia-IV Binds Directly to the Neural Cell Adhesion Molecule, NCAM. *Biochemistry*. **56**, 1504–1517

237. Arolas, J. L., Broder, C., Jefferson, T., Guevara, T., Sterchi, E. E., Bode, W., Stocker, W., Becker-Pauly, C., and Gomis-Ruth, F. X. (2012) Structural basis for the sheddase function of human meprin metalloproteinase at the plasma membrane. *Proc. Natl. Acad. Sci.* **109**, 16131–16136

238. Kiefer, F., Arnold, K., Kunzli, M., Bordoli, L., and Schwede, T. (2009) The SWISS-MODEL Repository and associated resources. *Nucleic Acids Res.* **37**, D387–D392

239. Guex, N., Peitsch, M. C., and Schwede, T. (2009) Automated comparative protein structure modeling with SWISS-MODEL and Swiss-PdbViewer: A historical perspective. *Electrophoresis*. **30**, S162–S173

240. Arnold, K., Bordoli, L., Kopp, J., and Schwede, T. (2006) The SWISS-MODEL workspace: a web-based environment for protein structure homology modelling. *Bioinformatics*. **22**, 195–201

241. Biasini, M., Bienert, S., Waterhouse, A., Arnold, K., Studer, G., Schmidt, T., Kiefer, F., Cassarino, T. G., Bertoni, M., Bordoli, L., and Schwede, T. (2014) SWISS-MODEL: Modelling protein tertiary and quaternary structure using evolutionary information. *Nucleic Acids Res.* **42**, 252–258

242. Duncan, J. R., and Kornfeld, S. (1988) Intracellular movement of two mannose 6-phosphate receptors: Return to the Golgi apparatus. *J. Cell Biol.* **106**, 617–628

243. Colley, K. J. (2010) Structure and Function of the Neural Cell Adhesion Molecule NCAM. **663**, 111–126

244. Yoshida, Y., Kurosawa, N., Kanematsu, T., Taguchi, A., Arita, M., Kojima, N., and Tsuji, S. (1996) Unique genomic structure and expression of the mouse α2,8-sialyltransferase (ST8Sia III) gene. *Glycobiology*. **6**, 573–580

245. Nakayama, J., and Fukuda, M. (1996) A human polysialyltransferase directs in vitro synthesis of polysialic acid. *J. Biol. Chem.* **271**, 1829–1832

246. Smith, P. L., and Baenziger, J. U. (1988) A pituitary N-acetylgalactosamine transferase that specifically recognizes glycoprotein hormones. *Science*. **242**, 930–933

247. Nishikawa, A., Gregory, W., Frenz, J., Cacia, J., and Kornfeld, S. (1997) The phosphorylation of bovine DNase I Asn-linked oligosaccharides is dependent on specific lysine and arginine residues. *J. Biol. Chem.* **272**, 19408–19412

248. Macauley, M. S., Arlian, B. M., Rillahan, C. D., Pang, P. C., Bortell, N., Marcondes, M. C. G., Haslam, S. M., Dell, A., and Paulson, J. C. (2014) Systemic blockade of sialylation in mice with a global inhibitor of sialyltransferases. *J. Biol. Chem.* **289**, 35149–35158

249. Zanghi, J. A., Mendoza, T. P., Schmelzer, A. E., Knop, R. H., and Miller, W. M. (1998) Role of nucleotide sugar pools in the inhibition of NCAM polysialylation by ammonia. *Biotechnol. Prog.* **14**, 834–844

250. Zanghi, J. a, Mendoza, T. P., Knop, R. H., and Miller, W. M. (1998) Ammonia inhibits neural cell adhesion molecule polysialylation in Chinese hamster ovary and small cell lung cancer cells. *J. Cell. Physiol.* **177**, 248–63

251. Al-Saraireh, Y. M. J., Sutherland, M., Springett, B. R., Freiberger, F., Ribeiro Morais, G., Loadman, P. M., Errington, R. J., Smith, P. J., Fukuda, M., Gerardy-Schahn, R., Patterson, L. H., Shnyder, S. D., and Falconer, R. A. (2013) Pharmacological Inhibition of polysialyltransferase ST8SiaII Modulates Tumour Cell Migration. *PLoS One*. **8**, 1–12

252. Johannes, L., and Römer, W. (2010) Shiga toxins — from cell biology to biomedical applications. *Nat. Rev. Microbiol.* **8**, 105–116

253. Karve, S. S., and Weiss, A. A. (2014) Glycolipid binding preferences of shiga toxin variants. *PLoS One*. 10.1371/journal.pone.0101173

254. Haicheur, N., Bismuth, E., Bosset, S., Adotevi, O., Warnier, G., Lacabanne, V., Regnault, A., Desaymard, C., Amigorena, S., Ricciardi-Castagnoli, P., Goud, B., Fridman, W. H., Johannes, L., and Tartour, E. (2000) The B subunit of Shiga toxin fused to a tumor antigen elicits CTL and targets dendritic cells to allow MHC class I-restricted presentation of peptides derived from exogenous antigens. *J Immunol*. **165**, 3301–3308

255. Gasteiger, E., Hoogland, C., Gattiker, A., Duvaud, S., Wilkins, M. R., Appel, R. D., and Bairoch, A. (2005) Protein Identification and Analysis Tools on the ExPASy Server. in *The Proteomics Protocols Handbook*, pp. 571–607, 10.1385/1592598900

256. Bagri, A., Tessier-Lavigne, M., and Watts, R. J. (2009) Neuropilins in tumor biology. *Clin. Cancer Res.* **15**, 1860–1864

257. Seidenfaden, R., Krauter, A., Schertzinger, F., Gerardy-schahn, R., and Hildebrandt, H. (2003) Polysialic Acid Directs Tumor Cell Growth by Controlling Heterophilic Neural Cell Adhesion Molecule Interactions Polysialic Acid Directs Tumor Cell Growth by Controlling Heterophilic Neural Cell Adhesion Molecule Interactions. *Mol. Cell. Biol.* **23**, 5908–5918

258. Lindahl, T., Satoh, M. S., Poirier, G. G., and Klungland, A. (1995) Post-translational modification of poly(ADP-ribose) polymerase induced by DNA strand breaks. *Trends Biochem. Sci.* **20**, 405–411

259. Langelier, M.-F., Planck, J., Roy, S., and Pascal, J. (2012) Structural basis for DNA-dependent poly(ADP-ribosyl)ation by human PARP-1. *Science (80-.).* **336**, 728–732

260. Muthurajan, U. M., Hepler, M. R. D., Hieb, A. R., Clark, N. J., Kramer, M., Yao, T., and Luger, K. (2014) Automodification switches PARP-1 function from chromatin architectural protein to histone chaperone. *Proc. Natl. Acad. Sci.* **111**, 12752–12757

VITA

NAME: Gaurang Bhide

EDUCATION:

University of Illinois at Chicago 2012-present
PhD, Biochemistry and Molecular Genetics (Advisor: Dr. Karen J. Colley)

University of Mumbai, India 2006-2010
B.Pharm., Pharmaceutical Sciences

Goethe Institut, Mumbai 2007-2009
Certificate courses in German language (A1 through B2.1)

RESEARCH EXPERIENCE:
University of Illinois at Chicago, Department of Biochemistry and Molecular Genetics
(Advisor: Dr. Karen Colley) 2013-present

Protein-specific polysialylation: biophysical and biochemical determinants of substrate recognition.

University of Georgia Complex Carbohydrate Research Center, Athens, GA 2016
Separation and characterization of glycoprotein and glycolipid oligosaccharides laboratory course

PUBLICATIONS JOURNAL

1. **Bhide G.P.**, Fernandes N.R., Colley K.J. (2016) Sequence requirements for Neuropilin-2 Recognition by ST8SiaIV and Polysialylation of its O-glycans, J Biol Chem. **291**(18), 9444-57.

2. **Bhide G.P.**, Colley K.J. (2017) Sialylation of N-glycans: mechanism, cellular compartmentalization and function, Histochem Cell Biol, **147**(2), 149-174, invited review.

3. **Bhide G.P.**, Prehna G., Ramirez B.E., Colley K.J. (2017) The polybasic region of the polysialyltransferase ST8SiaIV binds directly to the Neural Cell Adhesion Molecule, Biochemistry, **56**(10), 1504-1517.

4. **Bhide G.P.**, Zapater J.L., Colley K.J., Overlapping Sets of Basic Residues in the Polysialyltransferases are Required for Substrate Recognition and Polysialylation, *in preparation*.

5. Hsu H.J., Palka-Hamblin H.L., **Bhide G.P.**, Myung J.H., Cheong M., Colley K.J., Hong S., Non-Catalytic Endosialidase Enables Surface Capture of Small-cell Lung Cancer Cells Utilizing Strong Dendrimer-Mediated Enzyme-Glycoprotein Interactions, *in preparation*.

6. Palka-Hamblin H.L., **Bhide G.P.**, Colley K.J., *in preparation.*

PUBLICATIONS ABSTRACT

1. Bhide G.P., Prehna G., Ramirez B.E., Colley K.J. (2015), Biophysical Investigation of NCAM-Polysialyltransferase Interaction, Glycobiology, **25**(11), 1568.

2. Bhide G.P., Prehna G., Fernandes N.R.J., Zapater J.L., Ramirez B.E., Colley K.J. (2016) Protein-specific Polysialylation: Bringing a Biophysical Dimension to the Biochemical Evidence, Glycobiology, **26**(12), 1435-36.

TEACHING EXPERIENCE

Univeristy of Illinois at Chicago

GCLS 502 Molecular Biology	2014-2016
BIOS 454 Metabolic Biochemistry	2012
PHAR 331 Medicinal Biochemistry	2011

INTERNSHIP EXPERIENCE

GlaxoSmithKline Pvt. Ltd., Nashik, India 2009

AWARDS AND HONORS

UIC Graduate Student Council travel award for the oral presentation at the Gordon Glycobiology Research Seminars, Ventura, CA, 2017.

Dean's Scholar Fellowship, University of Illinois at Chicago, 2016.

Society for Glycobiology (SFG) travel award for the poster presentation at the SFG annual meeting, New Orleans, LA, 2016.

Gesellschaft der Freunde der Medizinischen Hochschule, Hannover, Germany travel award for the poster presentation at the Frontiers of Sialic acid Research Conference, Bad Lauterberg, Germany, Organizer: Dr. Rita Gerardy-Schahn, 2016.

UIC Clinical Center for Translational Science Predoctoral Education for Clinical and Translational Scientist (CCTS PECTS) Fellowship, 2015.

Society for Glycobiology (SFG) travel award for the poster presentation at the SFG annual meeting, San Francisco, CA, 2015.

PRESENTATIONS

Oral presentation, Gordon Glycobiology Research Seminars, Ventura, CA, Protein-specific Polysialylation: Determinants of Substrate Recognition, 2017.

Poster, Society for Glycobiology Annual Meeting, New Orleans, LA, Protein-specific polysialylation: bringing a biophysical dimension to the biochemical evidence, 2016.

Poster, Frontiers in Sialic Acid Research: From structural diversity to functional glycobiology conference, Bad Lauterberg, Germany, Biophysical Investigation of NCAM-Polysialyltransferase Interaction, Organizer: Dr. Rita Gerardy-Schahn, 2016.

Poster, Society for Glycobiology Annual Meeting, San Francisco, CA, Biophysical Investigation of NCAM-Polysialyltransferase Interaction, 2015.

Poster, Midwest Protein Folding Conference, University of Notre Dame, South Bend, IN, Biophysical Characterization of NCAM- Polysialyltransferase Interaction, 2015.

Professional memberships

2015- present Society for Glycobiology

2015- present American Association for Advancement of Sciences (AAAS)

APPENDICES

1. Journal of Biological Chemistry copyright agreement
2. ACS Biochemistry copyright agreement
3. iThenticate report

Copyright Permission Policy

These guidelines apply to the reuse of articles, figures, charts and photos in the ***Journal of Biological Chemistry***, ***Molecular & Cellular Proteomics*** and the ***Journal of Lipid Research***.

For authors reusing their own material:

Authors need **NOT** contact the journal to obtain rights to reuse their own material. They are automatically granted permission to do the following:

- Reuse the article in print collections of their own writing.
- Present a work orally in its entirety.
- Use an article in a thesis and/or dissertation.
- Reproduce an article for use in the author's courses. (If the author is employed by an academic institution, that institution also may reproduce the article for teaching purposes.)
- Reuse a figure, photo and/or table in future commercial and noncommercial works.
- Post a copy of the paper in PDF that you submitted via BenchPress.
- Link to the journal site containing the final edited PDFs created by the publisher.
- Authors who published their papers under the "Author's Choice" option may post the final edited PDFs created by the publisher to their own/departmental/university Web sites immediately upon publication. All other authors may do so 12 months after publication.

EXCEPTION: If authors select the Author's Choice publishing option:

- The final version of the manuscript will be covered under the Creative Commons Attribution license (CC BY), the most accommodating of licenses offered. Click here for details.
- The final version of the manuscript will be released immediately on the publisher's website and PubMed Central.

Please note that authors must include the following citation when using material that appeared in an ASBMB journal:

"This research was originally published in Journal Name. Author(s). Title. *Journal Name*. Year; Vol:pp-pp. © the American Society for Biochemistry and Molecular Biology."

For other parties using material for noncommercial use:

Other parties are welcome to copy, distribute, transmit and adapt the work — at no cost and without permission — for noncommercial use as long as they attribute the work to the original source using the citation above.

Examples of noncommercial use include:

- Reproducing a figure for educational purposes, such as schoolwork or lecture presentations, with attribution.
- Appending a reprinted article to a Ph.D. dissertation, with attribution.

For other parties using material for commercial use:

Navigate to the article of interest and click the "Request Permissions" button on the middle navigation bar. (See diagram at right.) It will walk you through the steps for obtaining permission for reuse.

Examples of commercial use by parties other than authors include:

- Reproducing a figure in a book published by a commercial publisher.
- Reproducing a figure in a journal article published by a commercial publisher.

Personal and Institutional Repositories:

- The "paper-in-press", ie, manuscript version of the article can be deposited at any time. The final, copyedited version of the article may not be deposited until 12 months after publication, unless the article is an Author's Choice article. Author's Choice articles may be deposited upon publication.
- An institution may deposit only articles published by individuals employed by or students attending the institution. The normal procedure is for the author to make the deposit.
- A link back to the article on the journal website should be provided.

Updated December 14, 2016

Title: The Polybasic Region of the Polysialyltransferase ST8Sia-IV Binds Directly to the Neural Cell Adhesion Molecule, NCAM

Author: Gaurang P. Bhide, Gerd Prehna, Benjamin E. Ramirez, et al

Publication: Biochemistry

Publisher: American Chemical Society

Date: Mar 1, 2017

PERMISSION/LICENSE IS GRANTED FOR YOUR ORDER AT NO CHARGE

This type of permission/license, instead of the standard Terms & Conditions, is sent to you because no fee is being charged for your order. Please note the following:

- Permission is granted for your request in both print and electronic formats, and translations.
- If figures and/or tables were requested, they may be adapted or used in part.
- Please print this page for your records and send a copy of it to your publisher/graduate school.
- Appropriate credit for the requested material should be given as follows: "Reprinted (adapted) with permission from (COMPLETE REFERENCE CITATION). Copyright (YEAR) American Chemical Society." Insert appropriate information in place of the capitalized words.
- One-time permission is granted only for the use specified in your request. No additional uses are granted (such as derivative works or other editions). For any other uses, please submit a new request.

If credit is given to another source for the material you requested, permission must be obtained from that source.

BACK CLOSE WINDOW

iThenticate Report Form

Information should be typed and then saved as a pdf. The completed form must be submitted to the defense committee with your thesis/dissertation. This form will also be submitted to the Graduate College with the final thesis/dissertation document and after successful defense.

The student is the sole author of their thesis or dissertation, and it is the student's responsibility to ensure that all information in their document is correctly cited and attributed, and that proper copyright permissions have been obtained. The *iThenticate* screening process should be only one part of their effort towards this end. For example, *iThenticate* cannot detect images and figures taken from other sources, texts in languages other than English, and user error (e.g. inappropriate exclusions).

Student Name (Last, First M.): **Bhide, Gaurang P.**
Student UIN: **662949606**
Student Email Address: gbhide2@uic.edu
Graduate Program Name (e.g., Biological Sciences): Biochemistry
Degree Sought: **Doctor of Philosophy**
Program Code (see http://catalog.uic.edu/gcat/degree-programs/grad-prof-degree-programs/): 20FS4050PHD
Thesis/Dissertation Title (must match title as submitted on the *Committee Recommendation Form* and the title page of the thesis/dissertation – use mixed case):

- Percent overlap in the initial *iThenticate* report -- before any review (e.g., 50%): **2%**
- Percent overlap in the *iThenticate* report -- after manual review to exclude trivial phrase overlaps and quoting/paraphrasing with proper citation (this is before editing your manuscript by adding citations, quote marks, correctly paraphrasing, etc.): 0%

If actual edits to the manuscript are required (such as adding citations, quote marks, rephrasing, etc.), the new version of the manuscript is uploaded to *iThenticate*.

- Percent overlap in the *iThenticate* report -- after manual review, and after trivial overlaps were excluded, following edits to exclude overlaps of concern, i.e. adding citations, quote marks, correctly paraphrasing, etc. (if no edits to the manuscript were required, type "not applicable"): N/A
- Have you included your own previously published work (Yes/No)? **Yes**
- If you have included your own previously published work, have you referenced it correctly according to the publisher's guidelines (Yes/No/Not Applicable)? **Yes**
- If you have included your own previously published work, did you include the publisher's copyright permission statement or written permission as an appendix (Yes/No/Not Applicable)? **Yes**
- Have you included collaborative work in your thesis/dissertation (Yes/No)? **Yes**
- If you have included collaborative work in your thesis/dissertation, have you included a "Contribution of Authors" paragraph as described in the *Introduction to Screening Your Thesis or Dissertation* (Yes/No/Not Applicable)? **Yes**

- Provide a brief statement to indicate what was changed in the editing of your manuscript including what you added to clarify contributions, previous publication and what you did to ensure proper citation and attribution (if no edits to the manuscript were required, type "not applicable"): **N/A**

General notes on *iThenticate* screening:

1. See the *iThenticate Review Procedures* at http://grad.uic.edu/ithenticate-review-procedures for complete information on using *iThenticate*.
2. The initial overlap % is not usually cause for major concern as:
    a. There will be instances in that first report that can be excluded, such as correctly cited material, or common phrases, etc.
    b. The point is to correct any actual deficiencies before the defense, and to achieve a document that has correct

citations and attributions.

3. The percent overlap in the sequence of *iThenticate* reports, and summary of changes statement you provide above, are to show the defense committee how any initial overlap problems were resolved. Many initial overlaps may be items that are actually fine, and you will exclude them during your review. The overlaps that are significant (if applicable), and that you should not exclude, would require corrections to your manuscript, such as adding citations, quote marks, and/or re-paraphrasing.
4. The goal is to achieve a final 0% overlap; however:
    a. You must be careful to exclude only instances that are trivial overlaps and not instances where corrections are necessary.
    b. A 0% similarity does not necessarily mean that everything is resolved. The zero may be rounded, so 0% may still have a number of instances that need to be addressed. You will be able to see this while doing your analysis.